UNIVERSITÀ
DEGLI STUDI
FIRENZE

DOTTORATO DI RICERCA IN
SCIENZE BIOMEDICHE

INDIRIZZO IN BIOCHIMICA E BIOLOGIA APPLICATA

CICLO XXVI

COORDINATORE Prof. Dello Sbarba Persio

THE TUMOR MICROENVIRONMENT: INSIGHT INTO FIBROBLASTS PATHOPHYSIOLOGICAL FUNCTIONS

Settore Scientifico Disciplinare BIO/10

Dottoranda
Dott.ssa Santi Alice

Tutore
Prof. Cirri Paolo

Coordinatore
Prof. Dello Sbarba Persio

Anni 2011/2013

TABLE OF CONTENTS

ABBREVIATIONS

2DE, 2D electrophoresis

AEs, anion exchangers

APCs, antigen-presenting cells

ARF6, ADP-ribosylation factor 6

ASCs, adipose tissue-derived stem cells

ATP, adenosine triphosphate

BCA, bicinchoninic acid

b-FGF, basic fibroblasts growth factor

BTs, bicarbonate transporters

CAFs, cancer-associated fibroblasts

CAs, carbonic anhydrases

CCL, CC chemokine ligand

CFDA-SE, Carboxyfluorescein diacetate succinimidyl ester

CFPs, circulating population of fibroblasts precursors

CPM, counts per minute

CSCs, cancer stem cells

CXCL, chemokine (C-X-C motif) ligand

DCs, dendritic cells

DMEM or **DME**, Dulbecco's Modified Eagle's Medium

DTT, dithiothreitol

ECM, extracellular matrix

ECs, endothelial cells

ED-A, extra-domain A

EGF, epidermal growth factor

EMM-PRIN, extracellular matrix metalloproteinases inducer

EMT, epithelial-mesenchymal transition

EMVs, extracellular membrane vesicles

EndMT, endothelial-mesenchymal transition

ERK, extracellular signal regulated kinase

ESCRT, endosomal sorting complex required for transport

FAP, fibroblasts activation protein

FBS, fetal bovine serum

FGF, fibroblasts growth factor

FSP1, fibroblasts specific protein 1

GAPDH, glyceraldehyde-3-phosphate dehydrogenase

GLUT, glucose transporters

HDFs, human dermic fibroblasts

HGF, hepatocyte growth factor

HIF-1, hypoxia-inducible factor 1

HPFs, human prostatic fibroblasts

HSCs, hematopoietic stem cells

ICAM, intercellular cell adhesion molecule

IFN, interferon

IGF, insulin growth factor

IL, interleukin

ILVs, intraluminal vesicles

IMG, intussusceptive microvascular growth

LFA-1, lymphocyte function-associated antigen 1

LOX, lysyl oxidase

LPS, lipopolysaccharide

MCP-1, monocyte chemoattractant protein 1

MCTs, monocarboxylate transporters

MDCs, myeloid dendritic cells

MDSCs, myeloid-derived suppressor cells

MFs, myofibroblasts

MHC, major histocompatibility complex

MLCK, myosin light-chain kinase

MMPs, matrix metalloproteinases

MMT, mesenchymal-mesenchymal transition

MSCs, bone marrow-derived mesenchymal stem cells

MVBs, multivesicular bodies

MVs, microvesicles

NBCs, Na^+/HCO_3^- cotransporters

NDCBE, electroneutral Na^+-driven Cl^-/HCO_3^- exchanger

NHE, Na^+/H^+ exchanger

NK, natural killer

NSF, N-ethylmaleimide-sensitive factor

PARs, protease-activated receptors

PBS, phosphate-buffered saline

PC3-GFP, green fluorescent protein (GFP)-expressing PC3 cells

PCP, planar cell polarity

PDCs, plasmacytoid dendritic cells

PDGF, platelet-derived growth factor

PG, proteoglycan

pHe, extracellular pH

pHi, intracellular pH

PI3K, phosphatidylinositol 3-kinase

PKM1, pyruvate kinase M1 isoform

PKM2, pyruvate kinase M2 isoform

PLD, phospholipase D

pO_2, oxygen pressure

PVDF, polyvinylidene difluoride

ROS, reactive oxygen species

SDF-1, stromal cells-derived factor 1

SNAP, soluble NSF-attachment protein

SOD-2, superoxide dismutase 2 (mitochondrial isoform)

SP, signal peptide

SSC, squamous cell carcinoma

TAMs, tumor-associated macrophages

TF, tissue factor

TGF-β, transforming growth factor-β

TNF, tumor necrosis factor

T_{reg}, regulatory T cells

uPA, urokinase-type plasminogen activator

V, relative spot volume

V-ATPase, vacuolar proton pump ATPase

VEGF, vascular endothelial growth factor

α-SMA, α-smooth muscle actin

INTRODUCTION

TUMOR INITIATION AND PROGRESSION

Tumors are genetic diseases that arise through a multi-step process in which the accumulation of mutations occurs mainly in genes involved in cell proliferation and differentiation or in cell death. To date, there are two different theories whose aim is to explain how a cell can collect the number of genetic changes needed to convert its normal phenotype into malignant.

The first hypothesis, initially move by Loeb *et al.* in 1974, originated from the observation that some tumors had multiple alterations compared to non-transformed tissues both in the karyotype (aneuploidy, translocations or rearrangements of chromosomes) and in nucleotide composition (deletions, insertions and substitutions of single nucleotides), which, it was thought, can not be explained by the normal mutation frequency. Therefore, Loeb *et al.* proposed the mutator phenotype theory, according to which genetic alterations in cancer cells occur more frequently than in normal ones [1, 2]. The difference in mutation rate was associated with cancer genetic instability due to alterations in genes encoding proteins responsible for the control of DNA replication and/or repair, as well as involved in chromosome segregation, in checkpoints surveillance during cell cycle, in cellular balance between death and birth, and in maintenance of CpG-island methylation patterns [2, 3]. In this hypothesis, genetic instability is responsible for the genotypic heterogeneity, characteristic of the tumor mass and represents the driving force of carcinogenesis [4].

The theory of the mutator phenotype in cancer was first re-examine by Nowell in 1976, who added the concept of clonal evolution to that of genetic instability [5], and then argued by Bodmer and Tomlinson in mid-nineties, which suggest that natural selection has a more important role with respect to genetic instability in tumor initiation and progression. This hypothesis derives from the observation that chromosomal or nucleotide instability is not a common feature of all cancers and is not a *conditio sine qua non* in tumorigenesis [6, 7]. On the contrary, it is widely accepted that tumor growth is a form of evolutionary process: through the mechanism of natural selection, only the cell carrier of one or more advantageous mutations is able to evade anti-growth signals and the result is an uncontrolled proliferation; after that other random genetic changes occur, each followed by waves of selection and expansion of most suitable clones. This process, together with the high rate of cell turnover, could explain the multiple alterations characteristic of

some cancers. The expression in the malignant cells of a mutator phenotype can, however, promote tumor progression, making it faster [6, 7]. To date, it is not clear whether the genetic instability is cause or consequence of tumorigenesis. In contrast, the hypothesis of natural selection and clonal evolution is validated and it is thought that this process has an important role in establishing the behavioral and morphological heterogeneity of cancer cells [8, 9].

In the last 30-40 years, many studies have suggested that the high heterogeneity of tumor mass can also reflect the hierarchical organization of stem/progenitor cells system, without necessarily excluding the stochastic model of clonal evolution [10]. In cancer of hematopoietic system, brain, breast and prostate have been identified biologically distinct populations of "tumor initiating cells", which have a similar behavior to stem cells of normal tissue, and for this reason are also known as cancer stem cells (CSCs) [11-15].

The properties that characterize normal stem cells are an extended, often unlimited proliferative potential, the high telomerase activity and the self-renewal ability through both a symmetric cell division (*i.e.* both daughter cells maintain the properties of progenitor) and asymmetric one (*i.e.* a daughter cell retains stem cells properties, while the other one begins the differentiation process which leads to the formation of a progeny capable of expressing different functional mature phenotypes). According to these abilities, the role of the CSCs can be identified in three interconnected contexts: by symmetric and/or asymmetric division they produce the heterogeneous population of malignant cells within a primary tumor, form the drug-resistant stem cells niche responsible for relapses following chemotherapy-induced remission and generate metastasis. It was hypothesized that CSCs arise from genetic changes in normal stem cells, or from progenitors, that, for definition, are provided with a significant replicative capacity, but regain self-renewal property after mutations [16-19].

Therapeutic strategies specifically directed to CSCs are considered the only ones able to eradicate the disease by reducing the risk for relapse and metastasis [10].

Figure I shows an overview of cancer development, where none of the theories mentioned above is excluded.

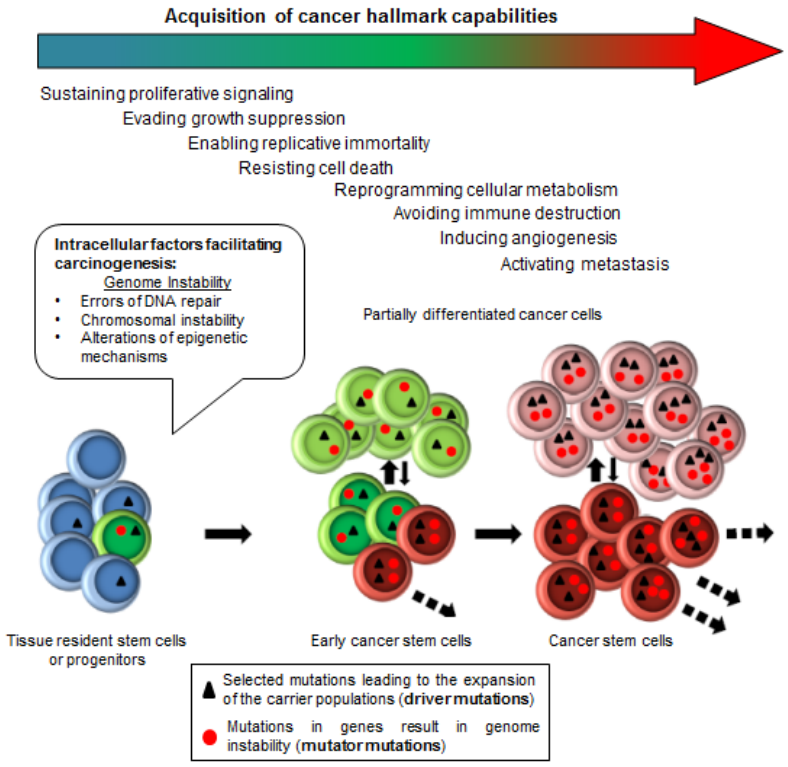

Figure I. Outline of cancer development. *Tumor evolves by a reiterative process of genetic diversification and clonal selection, in fact only the cells with advantageous alterations (driver mutations) undergo clonal expansions, thus producing a tumor mass and causing the phenotypic heterogeneity typical of its cells. In this context, genome instability can promote tumor development. During this multistep process, cancer cells acquire distinct biological capabilities (or hallmarks), thereby increasing their aggressiveness and malignancy. Cells with the stemness properties have a relevant role in the development and perpetuation of various tumors.*

The hallmarks of cancer cells

Cancers expand as clones from individual transformed cells and are diseases in continuous evolution due to the process of tumor progression, which generates subpopulations with increasing aggressiveness [20]. Tumor progression, in fact, consists in the progressive loss of differentiation due to morphological and metabolic alterations of tumor cells and is the result of several mechanisms (such as changes in gene expression, inactivation of tumor suppressor genes or activation of oncogenes) caused by chromosomal abnormalities, point mutations and an aberrant status of DNA methylation [20-22].

The accumulation of multiple alterations leads transformed cells to acquire characteristics and properties typical of malignancy by providing a competitive advantage compared with their normal counterpart. The new functional capabilities showed by most (if not all) cancer cells include: growth factor-independent proliferation, evasion of anti-growth signals, resistance to apoptosis, unlimited

proliferative potential, induction of neoangiogenesis, tissue invasion and metastasis [23-24] *(Figure I)*.

In normal tissue, cell proliferation is a controlled event, strictly balanced through anti-proliferative signals, or induction of programmed cell death in order to ensure the cell number required to maintain the correct tissue architecture and thus its function. Cell proliferation is promoted by an exogenous paracrine signal (growth factor), that binds and activates a specific cell surface receptor (mainly with intrinsic tyrosine kinase activity), which, in turn, triggers the intracellular signaling pathway. In contrast, anti-proliferative signals block cell growth by leading somatic cells to a quiescent state, thereby ensuring a homeostasis of cell number, or in a state of post-mitotic irreversible arrest corresponding to the acquisition of a functional phenotype [23]. The activation of apoptotic machinery, instead, occurs in detrimental or stress conditions, such as DNA damage, hypoxia, or survival factors shortage, thus preventing tumor initiation [25]. A further proliferative barrier typical of normal cells is the senescence [26], a process related to telomeres shortening due to the inability of DNA polymerase to replicate these chromosomal regions during S phase of the cell cycle and because of lack of telomerase gene expression, a specialized DNA polymerase able to perform this action. In fact, normal cells can replicate only a limited number of times and, when exhaust the telomeric region, enter into a non proliferative but viable condition until reaching crisis state and subsequent death by apoptosis [24].

Unlike their normal counterpart, tumor cells proliferation is mainly autonomous and decoupled from external mitogenic signals *(Figure I)*. This independence can be acquired through multiple ways: tumor cells become able to synthesize growth factors for which express specific receptors (autocrine stimulation) [27], overexpress a particular receptor becoming more responsive to the normal concentration of ligand [27], express constitutively activated surface receptors [27] or integrins (receptors that mediate cell-matrix and cell-cell contact) that promote cell survival and growth [28, 29], and have an aberrant regulation of Sos-Ras-Raf-MAPK cascade which continues to transmit an intracellular mitogenic signaling also in absence of normal upstream stimulatory signals [30]. The result is that tumor mass size increase depends on growing number of malignant cells that divides in a unit of time. They, in fact, besides acquiring the ability to sustain chronic proliferation, are capable to circumvent antigrowth signals *(Figure I)*, principally deregulating the two canonical suppressor of proliferation: RB protein (retinoblastoma-associated), which controls the entry into cell cycle especially depending on extracellular signals [31-33] and p53, which arrest the cell in G_1/S phase of the cell cycle if DNA is damaged,

if nucleotide pool are depleted, or if nutrient are suboptimal, and elicit apoptotic program when stress condition continues [24]. The mutations that impair p53 function [34, 35] together with the increased expression of apoptosis inhibitors (Bcl-2, Bcl-x_L), the down-regulation of pro-apoptotic factors (Bax, Bim and Puma) and the activation of phosphatidylinositol 3-kinase (PI3K)-Akt survival pathway belong also to the strategies that enable cancer cells to escape programmed cell death [24, 25].

In addition to uncontrolled growth and resistance to apoptosis, tumor cells show an unlimited replicative potential mainly (in 85-90% of cases) thanks to telomerase gene up-regulation [36] or in a smaller number of cases by a recombination-mediated mechanism, termed ALT (alternative lengthening of telomeres) [37] *(Figure I)*. The acquisition of these biological traits makes tumor cells capable of giving rise to macroscopic tumors, sometimes visible to the naked eye.

Similarly to what happens during embryogenesis, wound healing or female reproductive cycling, the formation of these cancer masses is accompanied by the growth of new blood vessels [38-40] *(Figure I)*. In fact, like normal tissue, tumors require nutrients and oxygen supplies as well as the elimination of metabolic waste and carbon dioxide [24].

The formation of new blood vessels (termed angiogenesis) is turned on by a process called “angiogenic switch”, which surprisingly occurs during the early stages of neoplastic progression when the balance between pro- and anti-angiogenic factors shifts towards a pro-angiogenic outcome [39] *(Figure II)*. Among the most common strategies used to move this balance there are the up-regulation of vascular endothelial growth factor-A (VEGF-A) [41-43] and/or fibroblasts growth factor (FGF) [44], which stimulate endothelial cells (quiescent in normal adult tissue) to continuously form new vessels, and the down-regulation of trombospondin 1 (TSP-1) [45] or β-interferon, whose role is to inhibit angiogenesis [46, 47]. The results are a vasculature convoluted and tortuous, and vessels enlarged, with an abnormal structure that cause disturbed blood flow [48, 49].

In addition to fulfill metabolic and proliferative needs of tumor cells, the new vessels represent one of the means by which such cells escape from primary tumor and colonize other parts of the body giving rise to metastasis *(Figure I)*. This multistep process begins with the detachment of transformed cells from the extracellular matrix at the site of the primary tumor, follows with the intravasation into nearby vessels, the dissemination into the bloodstream, both directly from the venous capillary and indirectly via lymphatic system, and with the passage through blood vessels wall into the parenchyma of the secondary site where metastasis will grow

[50, 51]. Invasion and metastasis are the typical characteristics of malignancy, in fact, colonization by tumor cells of distant tissues is the cause of 90% of human cancer deaths [52]. These properties are obtained by tumor cells thanks to the loss of expression or mutations of E-cadherin gene, a key factor of cell adhesion [53-55], or of gene encoding other mediators of cell-cell or cell-matrix contact and/or the up-regulation of genes encoding proteins involved in cell migration, such as N-cadherin [55]. During invasion and metastasis processes, epithelial transformed cells activate the epithelial-mesenchymal transition (EMT) program, which leads to assume a mesenchymal phenotype characterized by increased migratory capacity, by high resistance to apoptosis, by an elongated, spindle-shaped morphology, by the expression of matrix-degrading enzymes [56-60] and by the acquisition of stem cell-like capability of self-renewal [61]. Invasion and metastasis are complex processes completed only by transformed cells that present every hallmark described above [23].

THE TUMOR MICROENVIRONMENT

Solid tumors are complex tissues composed not only of highly heterogeneous cancer cells but also of abundance cellular and non-cellular components, also known as tumor microenvironment, that play an important role in cancer initiation, growth and progression *(Figure II)*. The cellular elements include both cells normally present in the parenchyma tissue or migrated as a result of tumorigenesis, such as fibroblasts, endothelial cells and pericytes, and a plethora of immune/inflammatory cells mostly recruited from circulation or bone marrow, in particular T- and B-cells, macrophages, neutrophils, mast cells and other bone marrow-derived cells [62] *(Figure II)*. These two groups of cells are responsible for the synthesis of the variety of molecules representing the non-cellular components of tumor-associated stroma, such as the extracellular matrix (ECM) proteins, proteases, cytokines and growth factors.

Other elements capable to affect the behavior of malignant cells are extracellular pH, oxygen (O_2) concentration, tissue pressure and fluid flow, also these physical and chemical parameters belong to the non-cellular components of tumor microenvironment [63] *(Figure II)*. The structure and the composition of TM are highly variable, with differences seen among various types of cancer, often in different areas of the same tumor and between patients [64]. Cancer cells can remodel the traits of microenvironment during disease progression, in turn, tumor-associated stroma not only functions as a supporting “scaffold” but also actively

participates to tumorigenesis contributing to the development and expression of certain hallmark capabilities [24, 65-67].

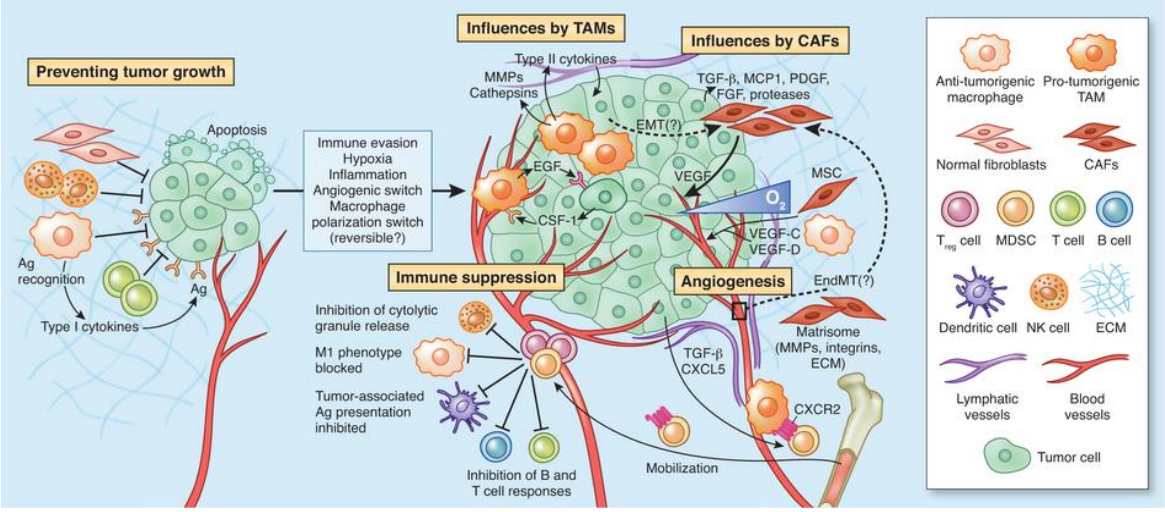

Figure II. The tumor microenvironment. *Tumor cells acquire the capabilities to resist cell death and to avoid immune destruction, but tumor growth is also promote by the other cellular components of tumor microenvironment. TAMs support growth, angiogenesis and invasion, by secreting numerous pro-tumorigenic proteases, cytokines and growth factors (such as EGF). MDSCs and T_{reg} cells, mobilized into the circulation by various cytokines (as TGF-β, and CXCL5-CXCR2), disrupt immune surveillance. CAFs, activated by tumor-derived factors (as TGF-β, FGF or PDGF), secrete ECM proteins and basement membrane components, modulate immune responses, support angiogenesis. Other extracellular elements contribute to tumor progression, including low O_2 tension, high interstitial fluid pressure and change in specific constituents of the ECM. EndMT, endothelial-mesenchymal transition; Ag, antigen; TAMs, tumor-associated macrophages; CAFs, cancer-associated fibroblasts; MDSCs, myeloid-derived suppressor cells; T_{reg}, regulatory T cells; EGF, epidermal growth factor; TGF-β, transforming growth factor; PDGF, platelet-derived growth factor [68].*

Fibroblasts

Activated fibroblasts

Fibroblasts are the most abundant cellular elements in connective tissue and with the fibrillar ECM, within they are embedded, form the structural scaffolding of organs. These cells are morphologically well described, they have an elongated shape and a typical fusiform or spindle-like profile; but not molecularly characterized, so are identified for what they are not: vascular, epithelial and inflammatory cells [69] *(Figure III)*.

Fibroblasts have multiple roles: they synthesize many of the constituents both of fibrillar ECM (such as type I, type III and type V collagen, and fibronectin) [70, 71] and of basal lamina (for example type IV collagen and laminin) [72]; are responsible for the remodeling and turnover of ECM by secreting matrix metalloproteinases (MMPs) [72, 73]; regulate differentiation and homeostasis of adjacent epithelia

through the secretion of growth factor or other soluble molecules involved in mesenchymal-epithelial interactions [74]; are important participants in inflammatory response to tissue damage and in wound repair [70, 75].

When tissue injury occurs, healing fibroblasts invade the wound and proliferate faster than normal ones both in order to replace lost or damaged fibroblasts due the injury, and to increase its number facilitating tissue repair [76]. Moreover, fibroblasts secrete increased amounts of ECM constituents and MMPs, and generate larger contraction forces promoting wound closure [77]. Healing fibroblasts, also known as myofibroblasts (MFs), are characterized by an "activated" phenotype [78, 79]. They acquire contractile stress fibers, *de novo* express α-smooth muscle actin (α-SMA) and the alternatively spliced fibronectin isoform containing the extra-domain A (ED-A), and are connected to each other by gap junctions [70] *(Figure III)*. To support the intense production of ECM components, activated fibroblasts possess a dispersed chromatin form (euchromatin) with one or two nucleoli in the nucleus, rough endoplasmic reticulum and a well developed Golgi apparatus [69].

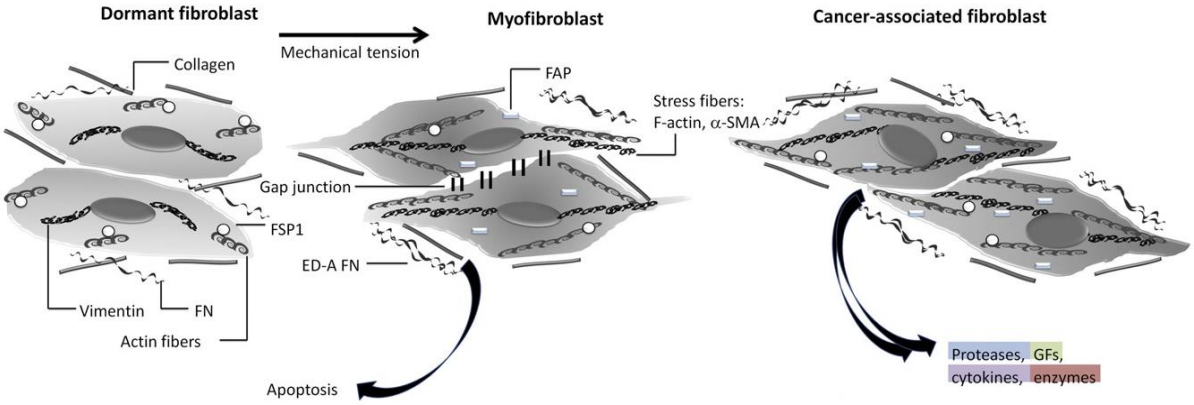

Figure III. Fibroblasts activation. *Normal fibroblasts are embedded within the fibrillar ECM of the connective tissue, have a fusiform shape, a prominent actin cytoskeleton and vimentin intermediate filaments. Activated fibroblasts (or MFs) differ morphologically and functionally from the quiescent ones. In response to mechanical tension, activated fibroblasts acquire stress fibers, express α-SMA and ED-A splice variant of fibronectin, in addition, form cell-cell contacts through gap junctions. Considering that "tumors are wound that do not heal", CAFs share several similarities with MFs. Once activated, CAFs produce proteases, growth factors, cytokines and enzymes. FN, fibronectin; FSP1, fibroblasts specific protein 1; FAP, fibroblasts activation protein [modified from ref. 149].*

Fibroblasts activation is induced by various stimuli derived from injured epithelia cells, which secrete transforming growth factor-β (TGF-β), epidermal growth factor (EGF) and basic-fibroblasts growth factor (b-FGF), otherwise they can be activated by direct cell-cell contact and communication with leukocytes [80, 81].

The transition from quiescent fibroblasts to activated ones is reversible, in fact, when the stimulus is turned off the number of MFs decreases and the site, now healed, is repopulated of resting fibroblasts with a normal phenotype [69, 77] *(Figure III)*.

Fibroblasts not only are the main cellular element of normal stroma, but also represent the most prominent cell type within reactive stroma of many solid tumors, as breast, prostate and pancreatic carcinoma [82, 83] *(Figure II)*. Peritumoral fibroblasts, also known as cancer-associated fibroblasts (CAFs) [84, 85], have a phenotype similar to healing fibroblasts (including the expression of α-SMA and of ED-A fibronectin), but, unlike them, persist in the activated state. For this reason, tumors are considered as "wounds that do not heal" [86] *(Figure III)*.

Cancer-associated fibroblasts

Heterogeneous subpopulations of fibroblasts has been observed in the margins and infiltrated in tumor mass. They are not always easy identified, because express several markers in common with other stromal cellular elements [82] and only partially share the expression of known markers of the activated state, as α-SMA, fibroblasts specific protein 1 (FSP1), platelet-derived growth factor (PDGF) receptor β and fibroblasts activation protein (FAP) [87, 88]. This heterogeneity may in part reflect the multiple origins of CAFs. At a glance, the predicted sources of CAFs are fibroblasts resident in the tumor site [89] *(Figure IV)*. In fact, within tumor microenvironment, cancer cells secrete numerous growth factors (TGF-β, PDGF and b-FGF), cytokines and chemokines that, through specific receptors present on local fibroblasts surface, trigger various tumor-promoting pathways. As result of this process, commonly called mesenchymal-mesenchymal transition (MMT), fibroblasts increase the production of ECM components, pro-angiogenic factors, chemokines and interleukins [90, 91].

Alternative sources of CAFs are bone marrow-derived mesenchymal stem cells (MSCs), hematopoietic stem cells (HSCs), and adipose tissue-derived stem cells (ASCs) *(Figure IV)*. MSCs are able to differentiate into mesenchymal tissue cells as bone, fat, cartilage, muscle and fibroblasts [92, 93], in fact, they are recruited to damaged sites during tissue repair, inflammation and to the tumor stroma in different cancer types, as breast, pancreatic and ovarian adenocarcinoma [94-98]. MSCs, recruited to the tumor site, thanks to growth factor (as VEGF, EGF, hepatocyte growth factor or HGF, b-FGF and PDGF) and cytokines (as monocyte chemoattractant protein 1, MCP-1, also known as CC chemokine ligand 2, CCL2)

secreted by cancer cells or by reactive stroma, differentiate into pericytes, MFs and endothelial cells contributing to the CAF populations [99-102].

HSCs, instead, are able to give rise to all functional blood cells and are precursors of osteoclasts and mast cells. Recent studies showed that a circulating population of fibroblasts precursors (CFPs) derived from HSCs are present in tumor mass. Their recruitment is mainly mediated by MCP-1 and by stromal cells-derived factor 1 (SDF-1), also known as chemokine (C-X-C motif) ligand 12 (CXCL12) [103]. The transition of HSCs-derived CFPs to the activated phenotype is mediated by TGF-β [104-106].

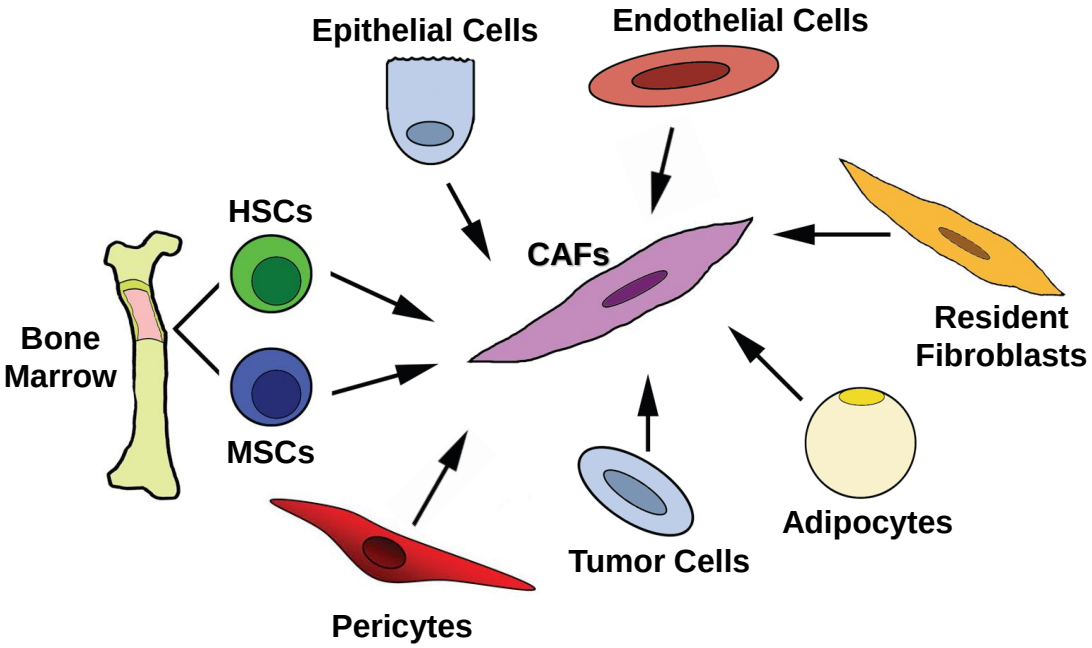

Figure IV. Multiple origins of CAFs within tumor microenvironment. *CAFs can derive from resident fibroblasts through MMT, from MSCs, HSCs, ASCs, and pericytes. Alternatively, CAFs can stem from epithelial and cancer cells through EMT, or from endothelial cells through EndMT [modified from ref. 115-116].*

The signaling pathway triggers by TGF-β has an important role also in the activation of ASCs, which are able to give rise to CAF-like cells when treated with conditioned media from breast cancer cell lines [107].

Another proposed sources of CAFs are cells of epithelial origin and endothelial cells, which, respectively through EMT [82, 108] and endothelial-mesenchymal transition (EndMT) [109], acquire fibroblasts morphology and express high levels of α-SMA [109, 110] *(Figure IV)*. Similarly, CAFs can stem directly from carcinoma cells through EMT, which enhances their migration and invasion ability [82, 108, 111] *(Figure IV)*. Finally, pericytes, *i.e.* cells present within the basement membrane of

capillaries and post-capillary venules often located closer to the tumor site, are another plausible source of CAFs [112, 113] *(Figure IV)*.

The precursors of CAFs pool of reactive stroma can vary with tumor type, during its progression and in the different areas of the same tumor. Considering the multiple origins suggested and the difficulty of identifying specific markers, Madar *et al.* had recently proposed a new definition for CAFs, as a cell "state" rather than a cell type. In other words, cells of different origins can exhibit CAFs state, which is a dynamic condition of fibroblasts-like cells acquired in the vicinity of tumor microenvironment, that actively promote cancer progression [114].

The role of CAFs in cancer initiation and progression

The activation of fibroblasts is mediated by numerous growth factors and cytokines secreted by cancer cells, such as TGF-β [117], PDGF-α/β [118, 119], b-FGF [120] and interleukin (IL) -6 [121] *(Figure V)*. In turns, altered fibroblasts are able to promote tumor initiation, its progression and metastasis.

The direct involvement of fibroblasts in cancer initiation was demonstrated by using mouse as xenograft model organism. In this context, Olumi *et al.* showed that immortalized epithelial cells, co-injected into mice with CAFs obtained from the primary tumor site, form cancerous masses, on the contrary, this effect does not occur in presence of normal fibroblasts [122]. Indeed, CAFs express high levels of epithelial mitogens, as HGF, EGF, b-FGF and cytokines, as SDF-1 and IL-6, which alone are sufficient to induce the transformation of adjacent epithelial cells and thus to favor tumor formation [123]. Modified fibroblasts can directly stimulate the proliferation of cancer cells by providing growth factors, or indirectly by helping these cells to evade apoptosis. They, in fact, secrete survival factors, as insulin growth factor (IGF)-1 and -2 [124, 125], and produce many ECM constituents (mainly various types of collagen), thereby promoting the ligation between integrin receptors and collagen fibers [126]. Both actions promote tumor cells survival via activation of the PI3K/Akt signaling pathway *(Figure V)*.

In addition to providing part of the ability of cancer cells to resist apoptosis, the CAFs-mediated ECM remodeling can also promote tumor invasion and metastasis. Activated fibroblasts, in fact, are able to cause qualitative and quantitative changes in ECM, which becomes stiffer [127, 128]. Part of this process can be attributed to an increased number of covalent cross-links between collagen fibers and other ECM components due to an excess activities of lysyl oxidase (LOX), which is expressed by fibroblasts in the early stage and also in carcinoma cells in the later one [126, 129]. Increase in mechanical force as a result of LOX activity facilitates metastatic

process [126] *(Figure V)*. Moreover, ECM anomalies, including rigidity, contribute, together with an altered vasculature, to increase interstitial fluid pressure supporting tumor drug resistance [130] *(Figure V)*.

CAFs are also a source of ECM-degrading enzymes, as MMPs and plasminogen activator *(Figure V)*. In particular, stromal cells from colon and breast carcinoma express the urokinase-type plasminogen activator (uPA) system, composed of uPA and uPA receptor (uPAR), which induces the turnover of ECM through the activation of plasminogen to the serine protease plasmin [131]. These proteases, through the degradation of ECM, create a physical path enabling tumor cells to penetrate basement membranes, by facilitating the invasion of surrounding tissue. Other functions of MMPs and plasmin include the ability to cleave and thus to activate latent growth factors, pro-inflammatory cytokines and their receptors, to release ECM-bound growth factors, or to cleave cell adhesion molecules, contributing to increase cancer cells proliferation, their motility, EMT and angiogenesis [132, 133]. These actions have been elucidated for MMP-1, MMP-3 (also known as stromelysin 1), MMP-13 and plasmin. The target of MMP-1 is the protease-activated receptor 1 (PAR1), a unique class of G protein-coupled receptors that, cleaved at the proper site, generate Ca^{2+}-dependent signals promoting cancer cells migration and invasion [134]. MMP-3 directly cleaves E-cadherin ectodomain at the cell surface, leading normal mammary epithelial cells to lose cell-cell adhesion and to activate EMT program [135]. MMP-13 releases VEGF from ECM promoting tumor angiogenesis and thus the invasive phenotype [136]. Plasmin, instead, can activate some MMPs, such as MMP-3 and MMP-13 [137-139].

In addition, CAFs are able to affect cancer cells motility by secreting soluble mediators, as TGF-β, HGF, VEGF, FGF and SDF-1 [66, 140] *(Figure V)*. Recently, Luga *et al.* showed a novel mechanism of communication between cancer and stromal cells. These last, in fact, are able to produce small membrane vesicles (in particular exosomes), which play a key role in promoting breast cancer cells protrusive activity and motility via Wnt-planar cell polarity (PCP) signaling [141] *(Figure V)*.

Further, there is evidence that stromal fibroblasts favor the dissemination of malignant cells through lymphatic and blood vessels, as well as are important in preparation of metastatic niche [142-144]. In keeping with this idea, cancer cells, endowed of self-renewal and tumor propagating capacity, function as “seeds”, instead the distant tissue together with fibroblasts derived from the primary tumor, represents the “soil” [145, 146]. In fact, CAFs co-traveling with metastatic tumor cells reach the secondary site, where participate in the formation of a

microenvironment permissive for the growth of metastatic colonies [147]. In this new location cancer cells induce the activation of resident normal fibroblasts [148].
Other important factors secreted by activated fibroblasts in tumor microenvironment are pro-inflammatory cytokines, as interleukins, interferon and member of the tumor necrosis factors (TNF) family [149] *(Figure V)*. In particular, expression of chemo-attractant cytokines and chemokines by intratumoral fibroblasts plays a key role in the recruitment of immune cells that, in turns, promote angiogenesis and metastasis [150]. Recent study showed that fibroblasts express a pro-inflammatory gene signature, which is already activated at initial hyperplastic stage in multistep skin tumorigenesis [151]. Therefore, fibroblasts are "educated" by cancer cells to express genes encoding several cytokines, including SDF-1, CXCL14 and CCL7 *(Figure V)*. The secretion of SDF-1 from CAFs enhances the mobilization of endothelial precursor cells from bone marrow and their recruitment into the tumor neovasculature [152]. Furthermore, SDF-1 increases the invasive capacity of pancreatic cancer cells and, together with CXCL8 produced by these malignant cells, promotes the complete angiogenic responses (*i.e.* proliferation, invasiveness and tube formation) of recruited endothelial cells [153]. CXCL14 expression in prostate cancer CAFs is up-regulated, too. This factor acts in autocrine fashion increasing both proliferation and migration rate of activated fibroblasts, which, in turns, promote tumor growth, angiogenesis and macrophage infiltration [154]. In a similar way, CCL7, up-regulated in fibroblasts associated to oral squamous cell carcinoma (SSC) by paracrine IL-1α secretion from these malignant cells, increases the invasiveness of oral SSC [155].
Another way used by altered fibroblasts to support tumor progression is by engaging a metabolic interplay with cancer cells. Stromal fibroblasts, in fact, are able to participate in the complex regulation of tumor metabolism, but there are opposite hypotheses about how this is done. In 2006, Koukourakis *et al.* proposed that cells within tumor microenvironment establish a harmonious metabolic collaboration, where CAFs express metabolic pathways complementary respect to cancer cells [156]. According to *Warburg* effect, tumor cells use glucose by aerobic glycolysis producing lactate [157-159], and to compensate the lower efficiency of adenosine triphosphate (ATP) production, due to incomplete glucose oxidation, increase the uptake of this sugar [160-162]. This behavior allows the diversion of glycolytic intermediates into various biosynthetic pathways in order to form macromolecules and organelles, and thus new cells [163, 164]. In this context, stromal cells buffer and recycle products of anaerobic metabolism of cancer cells sustaining their survival [156].

In 2009, instead, Pavlides *et al.* proposed a different model, whereby tumor cells induce a metabolic shift toward an aerobic glycolysis in stromal fibroblasts. The energy metabolites produced from aerobic glycolysis, *i.e.* lactate and pyruvate, are used by cancer cells in the mitochondrial tricarbossilic acids (TCA) cycle for ATP production via oxidative phosphorylation. This new theory is also known as "reverse *Warburg* effect" [165].

However, to better understand the metabolic interplay between tumor and stromal cells will be needed further confirmations.

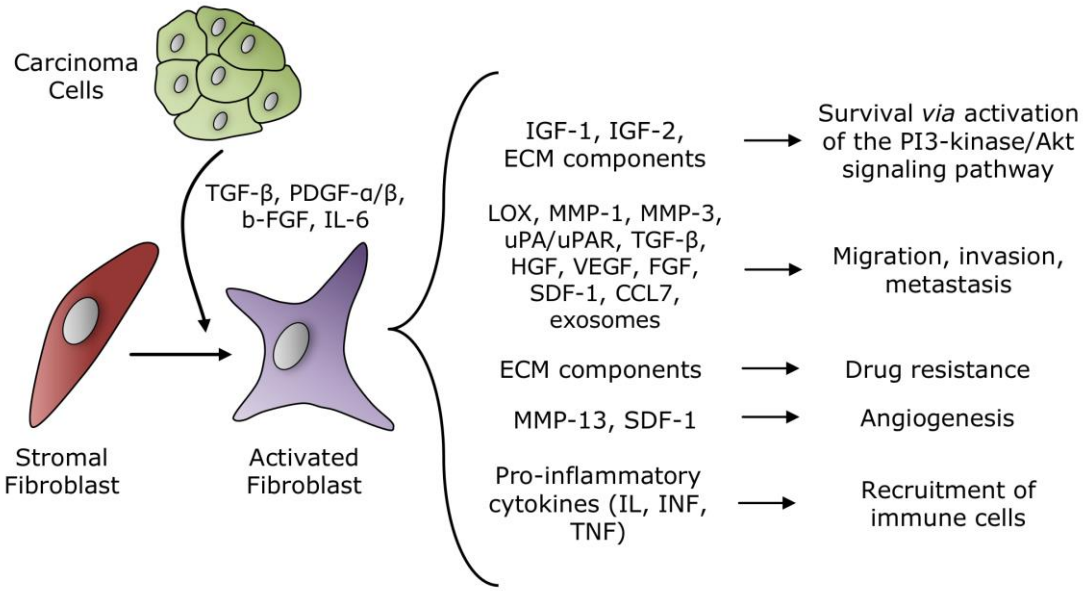

Figure V. Interactions between cancer cells and fibroblasts within tumor microenvironment. *Cancer cells produce growth factors, cytokines and other molecules, which induce and maintain the fibroblasts activated phenotype. Once activated, fibroblasts produce growth factors and cytokines that sustain tumor progression by promoting ECM remodelling, cell proliferation, angiogenesis and EMT. IL, interleukin; INF, interferon.*

Endothelial Cells

Other determinant cellular elements of stromal compartments are tumor-associated endothelial cells (ECs). ECs have a flattened shape and form a sheet (the endothelium) lining all blood vessels, which acts as cellular interface between the circulating blood and the vessel wall. ECs have an important role in tumor angiogenesis, in fact, angiogenic growth factors secreted by tumor cells or cells of the reactive stroma can directly activate receptors present on ECs promoting endothelial sprouting, branching, differentiation and survival [166, 167]. The formation of new blood network can occur by two mechanisms: vasculogenesis and angiogenesis. In the vasculogenesis, endothelial progenitor cells, present in the

vessel wall or recruited from the bone marrow, contribute to the formation of tumor vessels [168, 169].

Angiogenesis, instead, comprises two different mechanisms: endothelial sprouting and intussusceptive microvascular growth (IMG). The sprouting process is based on endothelial cells migration, proliferation and the budding of new tubes or the formation of bridges between existing ones. IMG is a phenomenon of splitting angiogenesis, where the existing vessels lumen is divides by the formation and insertion of tissue folds and columns of interstitial tissue [170, 171]. Besides the participation in tumor neovasculature, ECs serve as interface between circulating blood cells, tumor cells and the ECM, thereby playing a central role in controlling leukocyte recruitment, tumor cells behavior and metastasis formation [172].

Pericytes

Pericytes are contractile cells, related to vascular smooth muscle cells, which wrap around the endothelial cells, establishing with them a close physical contact in the outer surfaces of the finest branches of the vascular tree (the capillaries and sinusoids). Recent studies showed that pericytes are associated with the neovasculature of most, if not all, cancers. In this context, they can stabilize blood vessels, inhibit endothelial proliferation, maintain capillary diameter, regulate blood flow and provide endothelial survival signals via heterotypic contacts and soluble factors [173-175]. Their recruitment into tumor blood vessels is dependent on PDGF-B secreted by endothelial cells [176]. Other studies, instead, found that tumors with few pericytes density on their vasculature were associated with an increase in the number of metastases [173, 177]. For these reasons, the role of pericytes in tumors is not completely understood and future research is needed.

Immune/inflammatory cells

Tumor infiltrating cells of immune/inflammatory system include populations with a different phenotype and thus functionally heterogeneous, mainly macrophages, dendritic cells (DCs), myeloid-derived suppressor cells (MDSCs) and neutrophils *(Figure II)*. These cellular effectors can act in opposite ways both antagonizing or promoting tumor development, therefore the frequency of infiltrating inflammatory cells, their specific subset, as well as their maturation stage and spatial location within tumor microenvironment have determinant effects on clinical and immunologic outcomes [178, 179].

Macrophages are abundant components of tumor microenvironment, they originate from $CD34^+$ bone marrow progenitors, which, in the circulation system, differentiate into monocytes and, once recruited in peripheral tissue, mature into macrophages

and exert specific immunological functions [180]. In tissues, monocytes can differentiate in two different phenotypes classified as M1 and M2 responses [181, 182]. Their M1 polarization is mediated by inflammatory mediators, such as granulocyte macrophage-colony stimulating factor (GM-CSF), interferon-γ (IFN-γ) and lipopolysaccharide (LPS) [183]. Type 1 activated macrophages secrete pro-inflammatory cytokines and chemokines, including CXCL19 and CXCL10 leading helper T lymphocytes 1 (Th1), Th17 and natural killer (NK) cells development and differentiation [184].

M2 profile, instead, is induced in response to macrophage-colony stimulating factor (M-CSF), IL-4, IL-10, IL-13, IL-21, CC chemokine receptor 4 (CCR4), or to immunosuppressive agents as Activin A, corticosteroids, prostaglandins (PGs) and vitamin D3 [181, 185]. M2 macrophages express a different set of cytokines and chemokines, such as CCL17, CCL22 and CCL24 promoting regulatory T cells recruitment and development [172]. According to their phenotypic characteristic, M1 macrophages have high microbicidal activity, immunostimulatory function and are present in incipient tumors, where are capable to kill tumor cells; on the contrary, M2 macrophages encourage tissue repair and remodeling, neoangiogenesis process and tumor invasion and metastasis [184]. Tumor cells can regulate the function of tumor-associated macrophages (TAMs), "educating" them toward an M2 phenotype [186-188] *(Figure II)*.

Dendritic cells, another type of bone marrow-derived mononuclear cells, are the preeminent antigen-presenting cells (APCs) for T lymphocytes in lymphoid organs and in tissue. In human, two distinct subpopulations of DCs have been identified, myeloid DCs (MDCs) and plasmacytoid DCs (PDCs) [189, 190]. Although their role is not yet clear, both types of DCs are implicated in tumor development but with different functions. MDCs inhibit tumor neoangiogenesis by producing IL-12 [191], on the contrary, PDCs, attracted in tumor microenvironment and protected by CXCL12 secreted by tumor cells, induce not only the formation of new vessels by producing TNF-α and IL-8 [192, 193] but also tumor progression and metastasis by secreting proteases, like MMP-1, -2, -3, -9 and -19 and their inhibitors, as tissue inhibitor metalloproteinases (TIMP) -1 and -2 [194].

In addition to these "mature" infiltrating cells, also MDSCs, an immature population of myeloid cells precursors of DCs, macrophages and/or granulocytes, are present in tumors [195, 196]. In this context, they are induced by various factors produced by malignant cells and/or cells of tumor microenvironment [197, 198] and act as tumor-promoting cells by inhibiting innate and adaptive immunity, and by hindering immunotherapy [199].

Also neutrophils are a component of the immune microenvironment of solid tumors [200-203]. These cells are recruited by CXCL8, a chemoattractant expressed by both cancer and stromal cells of many types of human tumors [201, 204]. Neutrophils are able to promote angiogenesis process by directly secreting VEGF, or inducing its release, or that of b-FGF from ECM, by producing MMPs [205, 206], but like other inflammatory cells also possess antitumor activity. In fact, they can kill tumor cells by releasing proteases, membrane perforating molecules, reactive oxygen species (ROS) and cytokines, in particular TNF-α and IL-1β [207]; otherwise, according the signals within tumor microenvironment, can inhibit angiogenesis by producing elastase [208, 209].

Hypoxia in the tumor microenvironment

O_2 is one of the most important elements required to sustain aerobic life. In aerobic organisms, as humans, cellular respiration encompasses a set of redox metabolic reactions based on the oxidation of glucose to carbon dioxide (CO_2) and the reduction of O_2 to water in order to generate the energy (ATP) necessary for biological processes.

The air we breath contains about 21% O_2 at atmospheric pressure of 760 mmHg, *i.e.* a value of 159 mmHg, but, already in the pulmonary alveoli, O_2 pressure (pO_2) comes down to about 2/3 to the one present in the ambient (66% of 159 ~ 100 mmHg, that corresponds to a concentration of 14%). When the arterial blood reaches tissues peripheral capillaries, pO_2 is still 100 mmHg, whereas that of interstitial fluids is 30 mmHg. This generates a pressure gradient which favors the movement of O_2 from the blood into the adjacent tissue and thus its diffusion into the cellular mitochondria [210].

The intracellular pO_2 necessary to satisfy normal metabolic requirements is 1-3 mmHg. On the contrary, it is known, that in the context of cancer mass, among areas with normal O_2 concentration, are present microregions with very low (down to zero) O_2 partial pressures. In the tumor microenvironment, the impairment of O_2 delivery is related to the decrease of perfusion and diffusion. The first is associated to an inadequate blood flow caused by structural and functional abnormalities of tumor neovascularization. The latter is due to an increase of distance between vessels and cells present within cancer mass as a result of tumor expansion and often leads to cell death by necrosis [211, 212]. Studies concerning the oxygenated status of the tumor showed that: the median pO_2 is lower in cancers compared to their normal counterparts; tumor microregions with low pO_2 cannot be predicted by clinical size, stages, grade, histology and site; the oxygenation status of different

tumors is generally more variable than that of different areas of the same tumor; the oxygenation status of recurrent cancers is lower than that of the corresponding primary ones [213].

In solid tumors, the critical O_2 partial pressure required to maintain the biological functions is between 45-50 mmHg in end-capillary blood and 0.02 mmHg in cytochromes. In fact, in the one hand, tumor cells reduced O_2 consumption (*i.e.* respiration rates) when the pO_2 in the blood at the venus end of the capillaries drops below 45-50 mmHg [214, 215] *(Figure VI)*. On the other hand, cytochromes aa_3 and c require O_2 partial pressures greater than 0.02-0.07 mmHg to maintain respiration [216-218] *(Figure VI)*.

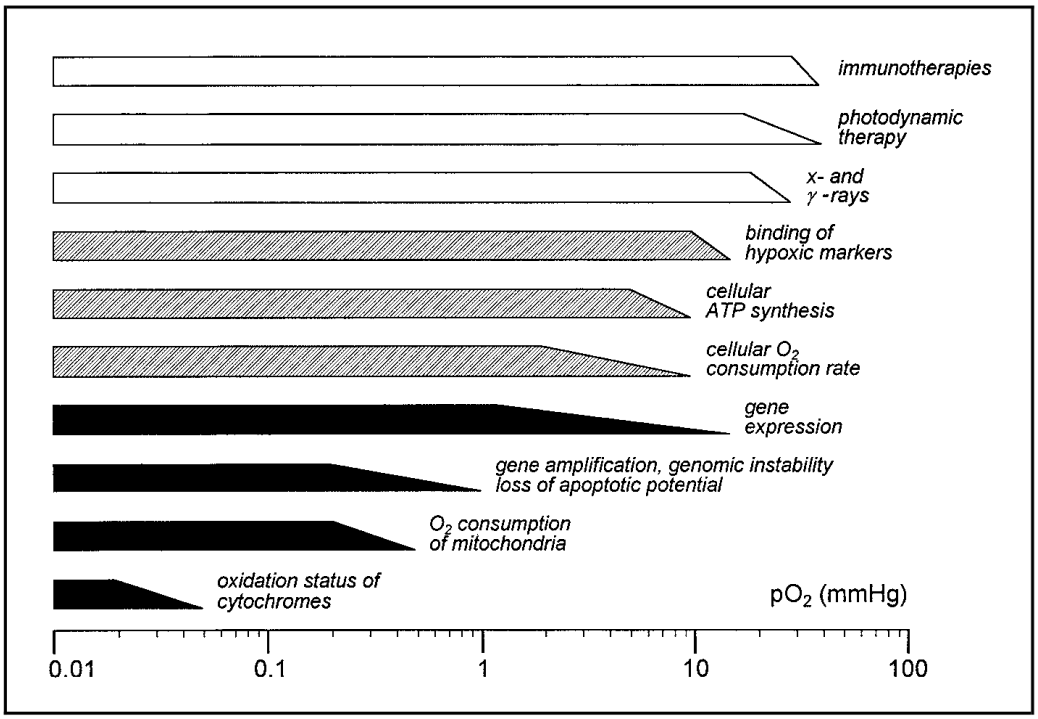

Figure VI. *Critical oxygen partial pressures that characterize the upper limit of the hypoxic range, below which activities or functions of tumor cells progressively change. Open bars: therapy form; hatched bars: cellular functions; solid bars: functions at the subcellular and molecular levels. The bars indicate the respective hypoxic ranges, with the lengths of the bevels showing the variation in threshold values as found by various authors for different end points [253].*

The hypoxic microenvironment is able to affects the behavior both of malignant and stromal cells (mainly fibroblasts and macrophages) and thus influences tumor propagation. In particular, hypoxia can induce a significant lengthening of G_1 phase or the arrest into it, differentiation, programmed cell death and necrosis [219-226]. The induction of these phenotypes may explain delayed relapses, quiescent micrometastasis [227, 228] and growth retardation in large tumor masses [229].

Into anoxic areas, instead, cells arrest their progression into cell cycle regardless of the phase in which they are.

Besides to the impairment of neoplastic growth, hypoxia can promote tumor development by enabling the cells to adapt to low pO_2 or to move from the original site to more suitable locations. Hypoxia induces the transcription of glycolytic enzymes (including hexokinase 2 and lactate dehydrogenase), glucose transporters (GLUT1 and GLUT3) *(Figure VII)*, angiogenic molecules, survival and growth factors (such as VEGF, PDGF-β, angiogenin, Cyr61, TGF-β, IGF-2 and IL-8), enzymes, proteins able to promote tumor invasiveness (as uPA), chaperones and other resistance-related proteins [230-244], as well as the inhibition of integrin gene expression, thus supporting cell detachment [245]. The hypoxia-induced phenotype is the result of many variables, including the degree of hypoxia and microenvironmental epigenetic factors. For example, hypoxia-inducible factor 1 (HIF-1), the master transcription factor induced in these stress conditions and the main responsible for the transcription of many genes encoding the proteins listed above, is able to exert opposite functions. Depending on the severity of hypoxia, HIF-1 can be in the dephosphorylated or phosphorylated status. The first form exerts pro-apoptotic effects, the other does not [246]. In addition, hypoxia can promote genomic instability (through point mutations and chromosomal aberrations) by increasing the number of genetic variants, and exerting a selective pressure can favor the expansion of the clone most suitable for this microenvironmental stress [232, 247-252] *(Figure VI)*. Despite these observation is not yet clear the level of O_2 at which hypoxia starts and causes biological problems.

Acidosis in the tumor microenvironment

The main effect due to tumor hypoxia is the decrease of mitochondrial functions (*i.e.* an impaired oxidative phosphorylation) and the shift to the glycolytic metabolism, which is a less energy-efficient process, but that does not rely on the presence of O_2 [254, 255]. This “glycolytic switch” is often permanent and persist after reoxygenation because the metabolic intermediates (lactate and pyruvate) can be used for anabolic reactions leading to the biosynthesis of amino acids, nucleotides and lipids, thus providing a selective advantage to highly proliferative tumor cells [254, 255]. In addition, Sonveaux *et al.* showed that the lactate produced by tumor cells within hypoxic areas is used by malignant cells located in the vicinity of blood vessels as substrate for oxidative phosphorylation. As result of this symbiotic relationship, the limited glucose available in the tumor mass is used in an effective way [256]. In fact, the switch to glycolysis requires an increased

consumption of glucose and leads to an excessive generation of acidic catabolites, such as CO_2, lactic acid, carbonic acid and protons (H^+) *(Figure VII)*. The release of these waste products in the extracellular space, together with the abnormal structure and function of tumor vasculature, is cause of the decline of extracellular pH (pHe), which usual is in the range of 6.5-7.0 [254, 257-260] *(Figure VII)*.

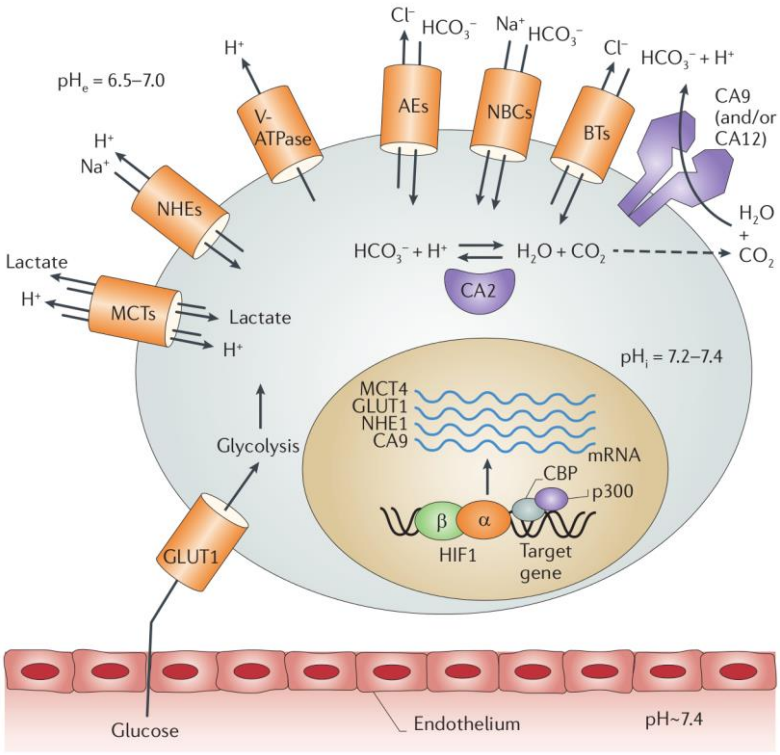

Figure VII. Proteins involved in pH regulation in cancer cells. *The pHi-regulating system that participates in cytoplasmic alkalinization of tumor cells includes NHE1, the plasma membrane V-ATPase and MCTs, whose function is to actively export acid, and AEs, NBCs, which, instead, import HCO_3^-. Also carbonic anhydrases (CA II, CA IX and CA XII) contribute to cellular alkalinization by catalyzing the reversible hydration of CO_2 to H^+ and HCO_3^-. Hence, the pHi is slightly alkaline (pH 7.2-7.4), whereas the pHe is slightly acidic (pH 6.5-7.0). The glucose transporter GLUT1 (which is up-regulated in most tumors) imports glucose into cancer cells. The expression of the genes encoding most of these proteins is under the transcriptional control of HIF-1. CBP, cyclic AMP-responsive element-binding (CREB) protein; p300, histone acetyltransferase p300 [255].*

Besides hypoxia, also the acidity of the extracellular milieu is a stress condition, since lowering of the pHe makes more difficult the control of the intracellular one. In fact minimal variations in intracellular pH (pHi), as low as 0.1 pH units, may affect several biochemical and/or biological processes, as energy production, enzyme function, membrane integrity, metabolism, proliferation, migration, invasion and metastasis, drug resistance and apoptosis [255, 257, 261-264]. pH homeostasis in any cell type is a critical process that involves complex molecular mechanisms (*i.e.* a variety of proteins and buffer systems) [265], but this get tangled

up for tumor cells, that prefer a more alkaline pHi (pH 7.4 o more) compared to their normal counterpart [256, 261, 265-268] *(Figure VII)*.

In cancer cells, the main players responsible for maintaining the alkaline pHi and the acidic pHe are: carbonic anhydrase (CA) II, CA IX and CA XII [269-271]; vacuolar proton pump ATPase (V-ATPase) [272]; the anion exchangers AE1 (also known as SLC4A1), AE2 (also known as SLC4A2) and AE3 (also known as SLC4A3) [273, 274]; Na^+/HCO_3^- cotransporters (NBCs) [275]; electroneutral Na^+-driven Cl^-/HCO_3^- exchanger (NDCBE; also known as SLC4A8) [275]; Na^+/H^+ exchanger 1 (NHE1; also known as SLC9A1) [275]; the monocarboxylate transporters MCT1, MCT2, MCT3 and MCT4 [276, 277] *(Figure VII)*. The expression of these proteins enables cells to develop defense mechanisms providing a selective advantage, and thus fostering the survival even in an extracellular microenvironment with an increased acid load [278].

Carbonic Anhydrases

The carbonic anhydrases (EC 4.2.1.1) are metalloenzymes whose major function is the catalysis of the reversible hydration of carbon dioxide to bicarbonate and protons ($CO_2 + H_2O \leftrightarrow HCO_3^- + H^+$), a reaction of critical importance in most organisms since the bicarbonate/carbonic acid system is the main buffer in all living cells. They are presents in Archaea, prokaryotes and eukaryotes and are encoded by members of three independent gene families: α-CAs (present in vertebrates, eubacteria, algae and cytoplasm of green plants), β-CAs (mainly in eubacteria, algae and chloroplasts of both mono- as well as dicotyledons) and γ-CAs (found in Archaea and some eubacteria) [279-281].

CAs perform their enzymatic function mainly in presence of zinc, but a cadmium-containing form was found to be expressed in marine diatoms during zinc limitation [282]. In mammals, 16 CA isoforms have been described (in human only 15 because CA XV in not present in primates). They differ in subcellular localization, tissue distribution, level of activity and susceptibility to different classes of inhibitors. There are cytosolic isoforms (CA I, CA II, CA III, CA VII and CA XIII), membrane bound ones (CA IV, CA IX, CA XII, CA XIV and CA XV), mitochondrial (CA VA and CA VB) and secreted isozymes (CA VI). In addition, there are three catalytic isoforms (CA VIII, CA X and CA XI), which are also known as CA-related proteins (CARP) [283, 284]. Among them all, CA IX and CA XII are overexpressed in many solid tumors, where they have an important role during the phase of progression, in metastases formation and in drug resistance [269-271, 285, 286].

CA IX

In 1992, Pastorekova and coworkers identified a cell density-regulated plasma membrane antigen in human HeLa cell line derived from cervical carcinoma using the monoclonal antibody M75 [287, 288]. Subsequently, cDNA sequence analysis of this antigen, named "MN protein", showed a 257 amino acid residues long polypeptide highly homologous to the mammalian CA catalytic domain [271, 289]. Thus, being the ninth CA identified, the "MN protein", was renamed CA IX [271, 289].

CA IX protein is composed from a N-terminal extracellular domain linked through a hydrophobic transmembrane region with a C-terminal intracellular tail. The extracellular part, which represents the 90% of the whole protein is formed by a signal peptide (SP), a proteoglycan domain (PG) similar to the keratan sulfate-binding domain of a large proteoglycan aggrecan, and by the CA catalytic domain [271, 289] *(Figure VIII)*.

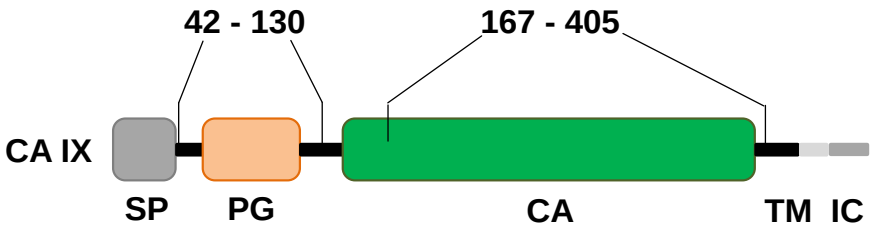

Figure VIII. Domains organization of the CA IX protein. *SP: signal peptide, PG: proteoglycan-like domain, CA: catalytic domain, TM: transmembrane segment, IC: intracellular, cytosolic tail [292].*

Unlike other CA, isoform IX has a dimeric nature resulting from a intermolecular disulfide bond between two adjacent monomers and stabilized through two hydrogen bonds and numerous van der Waals interactions [290, 291]. Each monomer contains a compact globular catalytic domain, where the active site is located in a large conical cavity, that from the surface of the protein goes down to its center [269, 291]. In the bottom of this cavity is located the zinc (II) ion. Alongside of the active site is positioned the PG-like region, whose role is to ensure a better catalytic efficiency at more acidic pH values [292, 293]. In fact, pKa value measured for CA IX catalytic domain alone is 7.01, on the contrary, whenever the protein construct contains also the PG region the optimal catalytic activity is at pH 6.49 [291]. PG domain function is probably mediated by its negatively charged amino acids. This region, by interacting with positively charged residues close to the active site, can both act as a cap controlling substrate accession and participate in the proton-transfer reaction [291].

Also the cytoplasmic tail can modulate CA IX catalytic activity both through the transmission of inside-out signaling to extracellular enzyme domain [294, 295] and increasing its activation [296, 297]. Similar to some cytosolic (CA I and CA II) and all extracellular CA isoforms, CA IX belongs to the highly active human α-CAs, as well as is susceptible to inhibition by anions and sulfonamides/sulfamates [269, 290, 298, 299].

In normal tissue, CA IX is mainly expressed on the basolateral surface of proliferating crypt enterocytes of the duodenum, jejunum and ileal mucosa [300], while a weak expression is present in the epithelia of male efferent ducts [301]. On the contrary, its expression is strongly increased in many type of tumor, including gliomas/ependymomas, mesotheliomas, papillary/follicular carcinomas, as well as carcinomas of the bladder, uterine cervix, kidneys, esophagus, lungs, head and neck, breast, brain and many other [302].

CA IX expressed in malignant cells has no mutations and its cDNA sequence is identical to that of normal cells. Hence, the association of this enzyme with tumors is exclusively related to its expression [303]. In tumor context, the increase of CA IX expression can occur in different conditions. In response to hypoxia, in increased cell density circumstances [304] and, for specific cell types, in acid microenvironment and during glucose deprivation [305-307], HIF-1 binds hypoxia responsive elements (HRE), which are localized in CA9 gene promoter just in front of the transcription start site at position -3/-10, and induces transcription of CA9 gene [304] *(Figure VII)*. In addition, functional inactivation of VHL (von Hippel Lindau) tumor suppressor gene, a member of E3 ubiquitin-ligase complex involved in the degradation of O_2-sensitive α-subunit of HIF-1, results in the hypoxia-independent expression of HIF-1 and thus of CA IX [308].

In solid tumors, CA IX overexpression is associated with poor prognosis [309-312].

CA IX *functions in tumor cells*

The prominent function of CA IX in the context of tumor microenvironment is the enzymatic catalysis. Isoform IX is one of the membrane bound CA isozymes whose catalytic domain is localized at the extracellular surface of the plasma membrane. This location of active site supports its role in controlling pH dynamics in solid tumors. CA IX is a peculiar member of CA family, in fact possesses several properties highly suitable for the tumor physiology. On the contrary to the other CA, isoform IX is insensitive to high lactate concentration found in the tumor [313], possesses the PG-like domain which enables it to function most efficiently at more acidic pH values typical of cancer mass [275, 292, 293], participates in the extracellular acidification [286] and regulates the intracellular pH [314].

Extracellular hydration of CO_2, indeed, results in the production of protons and bicarbonate. The first remains outside of the cells and increase the acidity of extracellular space, thus promoting tumorigenic transformation, chromosomal rearrangements, ECM breakdown, migration and invasion, protease activation and growth factor production [257, 315, 316]. In addition, acidic pHe can impair immune functions and influence the effect of conventional therapy on tumor cells, modulating the uptake of cancer drug [317].

The other product is transported inside the cells, where contributes to the production and the maintenance of alkaline pHi supporting cell survival and proliferation [317]. Vince and Reithmeier proposed that this transport could be mediated by a spatial and functional cooperation between bicarbonate transporter(s) and CA IX [318]. Subsequently, McMurtrie *et al.* showed that this cooperative complex (called "metabolon") is present in various cellular/tissue contexts and that can include different combinations of transporters and CA isozymes (AE1-3, NBC and CA II, CA IV and CA IX) [319]. It is also to note that CA IX is able to regulate pHi homeostasis both in presence and absence of the key pHi regulating protein NHE1 [320].

Besides the control of CO_2 metabolism, CA IX can directly participates to cell adhesion and migration both mediating the attachment of cells to solid support and competing with E-cadherin for the interaction with β-catenin, thus weakening cell-cell contact [321, 322]. Recent studies showed that also the PG-like N-terminal extension of CA IX extracellular domain can mediate cell adhesion [323]. This region, in fact, contains a sequence similar to that of aggrecan attachment domain and thus may be capable of binding ECM components [289, 323]. Moreover, tumor cells silenced for CA IX are less able to form cancer mass *in vivo*. Tumor growth is further reduced when the knock-down of CA IX is combined with that of CA XII, suggesting a functional complementarity between the two isoforms [320].

CA XII and CA II

Besides CA IX, other CA family members related to tumor biology are the isoforms XII and II. CA XII is a membrane-bound isozyme whose catalytic site is exposed at the cell surface; instead, CA II is a cytosolic isoform [283, 284]. CA XII is overexpressed in renal cancer cells [285, 324], breast cancer [325], and other many tumors [326]. This isozyme participates in the regulation of pHi and pHe and shows a complementary function compared to CA IX [320]. In fact, the knock-down of isoform IX results in up-regulation of XII one (at both mRNA and protein level) [257]. In breast cancer, CA XII has been shown to be a marker for good prognosis

[327], on the contrary, its spliced shorter variant seems to be a marker of poor prognosis in astrocytomas [328].

Unlike isoforms IX and XII, CA II is only weakly expressed in many tumors. Nevertheless, it is possible that, thanks to its high catalytic activity, is still able to participate in the maintenance of alkaline pHi and acidic pHe contributing to tumor growth and survival [257, 329]. Alternatively, it could perform its function at the level of tumor vasculature, where its expression is significantly higher than that of normal endothelium [330]. In the stomach, Pan *et al.* showed that knockout of CA IX leads to increase in CA II, and vice versa [331]. Although the reason why a membrane-bound isoform is compensated with a cytosolic one is intriguing, it is possible that both are able to interact with another protein by determining the formation of pH-regulating complex [257]. In order to clarify the function of both CA XII and CA II in the context of tumor microenvironment, further studies are required.

Membrane transporters

Other factors that contribute to pHi homeostasis in tumor cells are the isoform 1 of NHE [332, 333], MCTs and bicarbonate transporters (BTs), including NBCs, AEs and NDCBEs [334, 335]. NHE1 couples the export of H^+ across biological membranes to the import of Na^+, MCTs couple H^+ export with that of monocarboxylates (lactate and pyruvate), NBCs translocate Na^+ and HCO_3^- together in the same direction, AEs are responsible for Cl^--HCO_3^- exchange, and NDCBEs act as Na^+-dependent Cl^--HCO_3^- exchangers but are expressed by a limited number of cell types. NHE1, NBCs, NDCBEs perform their function using the energy stored in the inwardly directed electrochemical Na^+ gradient generated by Na^+-K^+ ATPase, the inward Cl^- gradient, instead, provides the driving force for AEs activity [336]. BTs [337], MCTs [338], but especially NHE1 [333, 339-341] are important proteins for cytoplasmic alkalinization and have a role in cell migration and invasion.

During migration and invasion processes, cancer cells change their morphology by acquiring the front-rear polarity and forming lamellipodia and invadopodia, respectively [342] *(Figure IX)*. The polarization of tumor cells along their longitudinal axis is fostered by NHE1, which is linked to actin filaments and controls the organization of the cytoskeleton [339, 343-345], as well as contributes to cytosolic alkalinization and extracellular acidification [346-349]. In fact, during cell migration NHE1 [343, 346, 347], together with NBC1 and AE2 [351-353], accumulates at the leading edge *(Figure IX)*. In this location, they mediate ions entry that, together with water influx across aquaporins (AQP1) [354], supports the outgrowth of the

lamellipodium [351-353]. In addition, they form the pH-regulating machinery which generates a pHi gradient from the front toward the rear part of cells. The neutral-alkaline pHi at the leading edge promotes cofilin activity which, by severing actin filament (F-actin), generate free barbed ends providing sites for further actin polymerization and thus driving membrane protrusion [355, 356] *(Figure IX)*.

Recent studies showed that the "metabolon" previously described [318, 319] is formed also at the lamellipodia present in the front of the cells, where NBCs and AE1, -2, -3 establish a functional cooperation with CA IX, whose role is to produce bicarbonate and to maximize the rate of its transport across the plasma membrane contributing to increase pHi [357-359].

At the rear end, instead, gelsolin, activated by acidic pHi and high Ca^{2+} concentration, controls the length of actin filaments by its severing and capping activities [360-362]. Gelsolin, in fact, helps to recycle actin promoting the retraction of the rear end of a migrating cell [363].

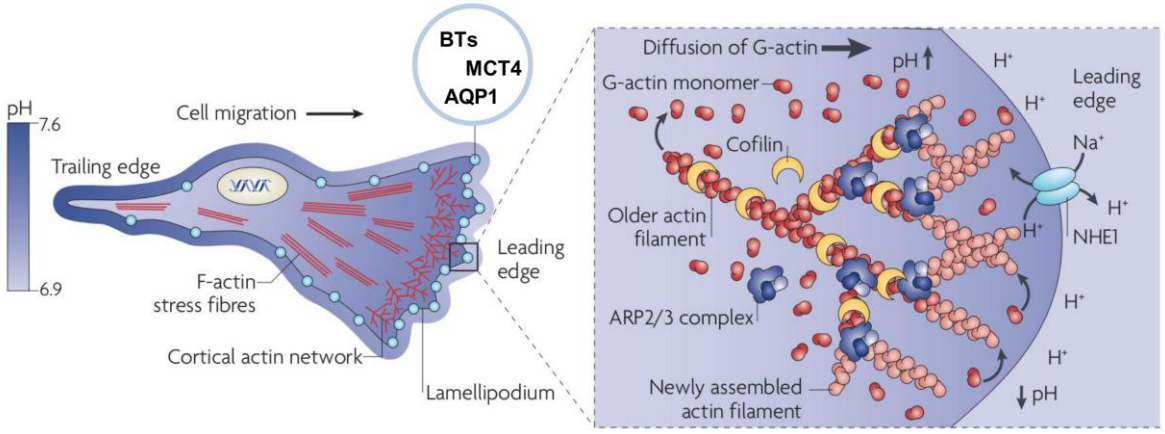

Figure IX. Role of protons in cell motility. *pH homeostasis is crucial for tumor cells migration and invasion. BTs (including NHE1, NBC1, AE2), MCT4, AQPs and CA IX, accumulate at leading edge membranes and promote the cytoplasmic alkalinization and pHe acidification. pHi alkalinization activates cofilin, an actin-binding protein capable of increasing the recycling of actin monomers (globular actin, or G-actin) at the rear of "older" actin filaments (filamentous actin, or F-actin), thereby inducing de novo localized actin assembly, cytoskeleton reorganization and membrane protrusion. pHe acidification results in the modulation of integrin-mediated cell-matrix adhesion, thus facilitating cell migration. At the trailing edge, instead, alkaline pHi and acid pHe drive the retraction of the rear part of migrating cells [modified from ref. 336].*

Oppositely to the pHi gradient, the pericellular proton concentration within the glycocalyx, generated by the pH-regulating complex described above, is up to twice as high at the leading edge than at the rear part of migrating cells [347-349] *(Figure IX)*. This pHe gradient coordinates the formation and release of focal adhesion contacts mediated by integrins with ECM or between cells.

Integrin-mediated interactions, indeed, are sensitive to proton concentration [347, 349, 364-366]. At the leading edge, the extracellular acidification mediated by NHE1 facilitates the formation of focal adhesion contacts, stabilizes the existent ones [348, 349] and fosters the exocytosis and function of MMPs by inducing both them protonation or that of their substrates, thus promoting proteases activity [367, 368]. The alkaline pH of the rear edge, instead, weakens the adhesion to ECM or to neighbored cells [363] and increases the entry of Ca^{2+} into cells through the proton-sensitive TRPM7 channel promoting gelsolin activity [369]. Like NHE1, NBC1 and AE2, also MCT4 accumulates at the leading edge, where export H^+ and monocarboxylates, contributing to lowering the pHe [370] *(Figure IX)*.

Besides H^+, the exported lactate may promote cell migration. It, in fact, up-regulates the synthesis of ECM components (such as hyaluronan and type I collagen) to which cells can adhere via a proton-sensitive mechanism, and thus migrate [371, 372]. Lastly, it is important to note that as NHE1 is one of the most prominent proteins regulating pHi, it has also an important role in supporting cancer cells survival and proliferation. It has been demonstrated that both its pharmacological inhibition [373-375] and its lacking activity [376, 377] in cancer cells results in a drastic reduction of tumor growth *in vivo*.

THE INTERCELLULAR COMMUNICATION

In pluricellular organisms, intercellular communication is instrumental for the survival and the function of cells and to ensure the integrity of tissues. Typically, the exchange of informations occurs through the transmission of electrical or chemical signals. The first allows the diffusion of nerve impulse across electrical synapses, formed of gap junctions or nexus, which enable the free flow of ions from one cell to another. The latter is mediated by extracellular molecules, such as nucleotides, lipids, short peptides or proteins released by cells. These molecules bind to specific receptors on other cells and activate intracellular pathways, thus modifying their physiological state. Alternatively, cells can communicate with each other after direct cell-cell contact through mechanisms of nibbling, trogocytosis and nanotubes. The mechanism of nibbling concerns the unique ability of DCs to capture antigen from live cells by physically stripping large membrane fragments without inducing death of the donor cells [378]. The trogocytosis, instead, describes the transfer of plasma membrane fragments from one cell to another, triggered by receptor signaling following cell-cell contact without cell death induction [378]. It is an active and, in some circumstances, bidirectional process that, compared to other transfer mechanisms, occurs very quickly (within minutes after cell-cell

conjugation) [379, 380]. This phenomenon was mainly observed in cells of the immune systems, including B cells, T cells, NK cells, monocytes [381] and DCs [382]. It was documented that both MHC (major histocompatibility complex) class I and class II proteins can transfer from APCs to T cells [383-388], and that many other cell-surface molecules can be transferred, not only to T cells, but also to B and NK cells enabling the coordination of the immune response [389].

Another mode of cell contact dependent protein trafficking is mediated by the formation of membranous channels of 50-200 nm in diameter, called nanotubes, that connect cells over long distances [378]. These nanotubular connections, first described in cultured rat pheochromocytoma PC12 cells [390], are formed by many different cell types, such as T, B, NK cells, macrophages [385, 391-393], and between different cancer cells (breast and ovarian cancer cell lines) and stromal cells (mesenchymal stem cells and ECs) [394]. These structures allow intercellular transfer of organelles (such as mitochondria) [394], of various plasma membrane components, of cytoplasmic molecules [395], as well as of calcium ions, MHC class I, pathogens, small organelles of the endosomal/lysosomal system and ATP-Binding Cassette transporter [396-401].

The intercellular communication mediated by the exchange of proteins can occurs also by trans-endocytosis, a biological process documented, for instances, in Notch-mediated signal between adjacent cells [402-404]. Notch is a transmembrane receptor involved in embryonic development and cell differentiation, and is formed by separable extracellular and intracellular domains linked together by non-covalent bonds [405, 406]. During the process of trans-endocytosis, the part of the receptor present on the outer surface of a cells is cleaved off and undergoes endocytosis into its neighboring cell, where is transferred into endosomes. Simultaneously, the intracellular domain is released in the cytoplasm, translocates to the nucleus, and activates gene transcription [405, 406].

In addition to these mechanisms, another form of intercellular communication involves the secretion by cells of small extracellular membrane vesicles (EMVs) characterized of an approximately spherical structure limited by a proteolipid bilayer and containing bioactive components, such as numerous proteins, lipids and nucleic acids [407-411] as well as, in the case of larger vesicles, mitochondria [412]. These vesicles were observed first in 1978 by Friend *et al.* in cultures of spleen nodules and lymph nodes from a patient with Hodgkin's disease [413], and then in 1980 by Poste and Nicolson, who found that vesicles secreted by highly metastatic B16 mouse melanoma cells enable the poorly metastatic ones to metastasize to the lung [414].

Subsequently, these vesicles were detected in the culture supernatant of different cell types both of hematopoietic origin (such as B cells [415], DCs [416, 417], mast cells [418], T cells [419] and platelets [421, 422]) and of non hematopoietic origin (as intestinal epithelial cells [423], tumor cells [424, 425], Schwann cells [426], neuronal cells [427, 428], astrocytes [429], ECs [430] and fibroblasts [141]). In addition, EMVs were found *in vivo* in diverse body fluids [431], including semen [432-434], blood [435], urine [436, 437], saliva [438], breast milk [439], amniotic fluid [440], ascites fluid [441-443], cerebrospinal fluid [444] and bile [445].
The identification of these numerous forms of intercellular communication supports the concept that "no cell is an island" [446]. All organisms, in fact, are composed by non-autonomous cells capable of interacting with each other thanks to a continuous horizontal exchange of informations.

Structure and biogenesis of extracellular membrane vesicles

Eukaryotic cells constitutively release heterogeneous populations of EMVs both *in vivo* and *in vitro*, which can be divided into two distinct subtypes, known as exosomes and microvesicles, characterized by different properties, including origin, size, morphology, buoyant density and protein composition.

Exosomes

Exosomes are membranous nanovesicles of 30-100 nm in diameter, with a rounded shaped morphology and a floating density of 1.10-1.21 g/mL in sucrose gradient [415, 447]. They arise as intraluminal vesicles (ILVs) in the endosomal compartments called multivesicular bodies (MVBs) by inward budding and pinching at the limiting membrane into the endosomal lumen [448], so they contain cytosolic components and expose the extracellular domains of transmembrane proteins, which thus maintain the same topological orientation as at the endosomal membrane [449, 450] *(Figures X-a and X-b)*. Thereof, MVBs not only represent a late step in the maturation of endosomes to lysosomes (degradative MVBs), but also participate in an alternative process. These compartments, in fact, can fuse with the plasma membrane and release their segregated vesicles into the extracellular space (exocytic MVBs), where upon ILVs are called exosomes [407] *(Figure X-a)*.
Exosomes can originate from multiple cell types, thus their cargo contains both type-specific and common molecules. Examples of cell-type specific proteins are transferrin receptor [451] and integrin α4β1 [452] in exosomes released by reticulocytes; CD3 [451], integrin β2 and the ubiquitin ligase c-CBL [419] in T cell derived exosomes; A33 antigen and the cell-surface peptidase IV/CD26 [423] in exosomes originate by enterocytes. The molecules ubiquitous in exosomes derived

from distinct source, instead, are cytoskeletal proteins (tubulin, actin and actin-binding proteins), molecules involved in the sorting of proteins/cargo, as ESCRT complex (endosomal sorting complex required for transport), chaperones (heat shock protein, as HSP70 and HSP90), proteins involved in signal transduction (protein kinase, 14-3-3 and heterotrimeric G proteins), clathrin, protein involved in transport and fusion (annexins and Rab proteins), several metabolic enzymes (such as peroxidases, pyruvate and lipids kinases and enolase-1), elongation factors and, perhaps, proteins that participate in some common exosomes functions not yet known [453, 454] *(Figure X-c)*.

According to their origin, exosomes do not contain any proteins derived from nucleus, mitochondria, endoplasmic-reticulum or Golgi-apparatus [455]. The process of protein sorting can be mediated by different mechanisms both ESCRT-dependent and -independent. ESCRT machinery is composed of four proteins complexes (known as ESCRT-0, -I, -II, -III) associate with accessory proteins (Alix, VPS4 and tsg101): the ESCRT-0, -I and -II complexes are able to recognize and sequester the mono-ubiquitinated proteins at the limiting membrane of endosomes, instead the ESCRT-III complex acts in the budding and scission phases [456, 457].

On the contrary, the ESCRT-independent mechanisms include: the non-specific engulfment of small portions of cytosol, the transient association of proteins with the transmembrane ones [458] and a process dependents on raft-based microdomains, where ceramide formed from sphingolipids by neutral sphingomyelinase can induce the coalescence of small microdomains into larger ones, promoting domain-induced budding [459]. Alternatively, proteins can be co-sorted in concert with other proteins, such as tetraspanins which are enriched in exosomes where cluster into membrane microdomains [460] *(Figure X-b)*, or flotillin, stomatin and lyn, that are raft-associated proteins [461]. Presence of several sorting mechanisms may induce the formation of heterogeneous subpopulations of ILVs.

The lipid composition of exosomes is similar to that of the plasma membrane of the producing cell [462], nevertheless in comparison to it, exosomes are highly enriched in cholesterol, sphingomyelin and hexosylceramides to the detriment of phosphatidylcholine and phosphatidylethanolamine [463-466]. In agreement with these observations cholesterol-rich MVBs secrete their vesicles cargo, on the contrary, the cholesterol-poor ones act as degradative MVBs [467].

Other components of exosomes are mitochondrial DNA (mtDNA) [468] small non-coding RNAs, as miRNAs (known to control gene expression by regulating mRNA turnover), and mRNAs, which can be translated into proteins by recipient cells, each one can be cell-type specific [410, 469, 470] *(Figure X-c)*. It is noteworthy that

not all mRNAs and miRNAs of a cell end up in exosomes. Their selective incorporation could be mediated by ESCRT-II, which acts also as RNA binding complex [471], by RISC (RNA-induced silencing complex) and its key components GW182 and AGO2 (argonaute), which are enriched in exosomes [472].

After that, ILVs were assembled, the secretory MVBs are transported toward the cell periphery, where fuse with the plasma membrane. Classically, intracellular trafficking and the fusion of compartments require the cytoskeleton (actin and microtubules), associated molecular motors (kinesins and myosins), molecular switches (small GTPase of the Rab family) and the fusion machinery [473].

The same effectors probably participate in the release of exosomes. Examples of Rab proteins involved in the mobilization event are: Rab11, engaged for Ca^{2+}-induced exosome secretion by the K562 erythroleukemia cell line [474] *(Figure X-a)*; Rab35, required for proteolipid protein (PLP)-enriched exosomes release by oligodendroglial cells [475]; Rab27a and Rab27b, which have a complementary role in spontaneous secretion of MHC class II-bearing exosomes by HeLa-CIITA cells [476], Rab27a, but not Rab27b, also acts in exosome secretion by different mouse mammary carcinoma [477]. In this contest, Rab proteins effect appears to be redundant and cell type dependent, alternatively, these proteins could act upstream of exosomes secretion. In fact, the selective inactivation of each of them only partially affects this process [475, 476].

Subsequently, the fusion of MVBs with the plasma membrane is probably driven by a specific protein machinery, which includes soluble factors (such as N-ethylmaleimide-sensitive factor, NSF, and soluble NSF-attachment protein, SNAP), membrane complexes (such as SNAP-attachment protein receptor) and synaptotagmin family members [478, 479].

Several events can regulate exosomes production, among them, the increase of cytosolic Ca^{2+} concentration is one of the most trigger [474] *(Figure X-a)*. In addition, DCs were stimulated to release exosomes as the result of the interaction with T cells, that recognize peptide-loaded MHC class II [480]; neuronal cells produce exosomes in response to plasma membrane depolarization; and cross-linking [427, 481] of CD3 in T cells stimulates exosomes release by T cells [419]. The intracellular mechanisms of exosomes biogenesis and secretion are not yet clearly defined and future works are needed. Process understanding, in fact, represents an essential step to further identify exosomes function and significance.

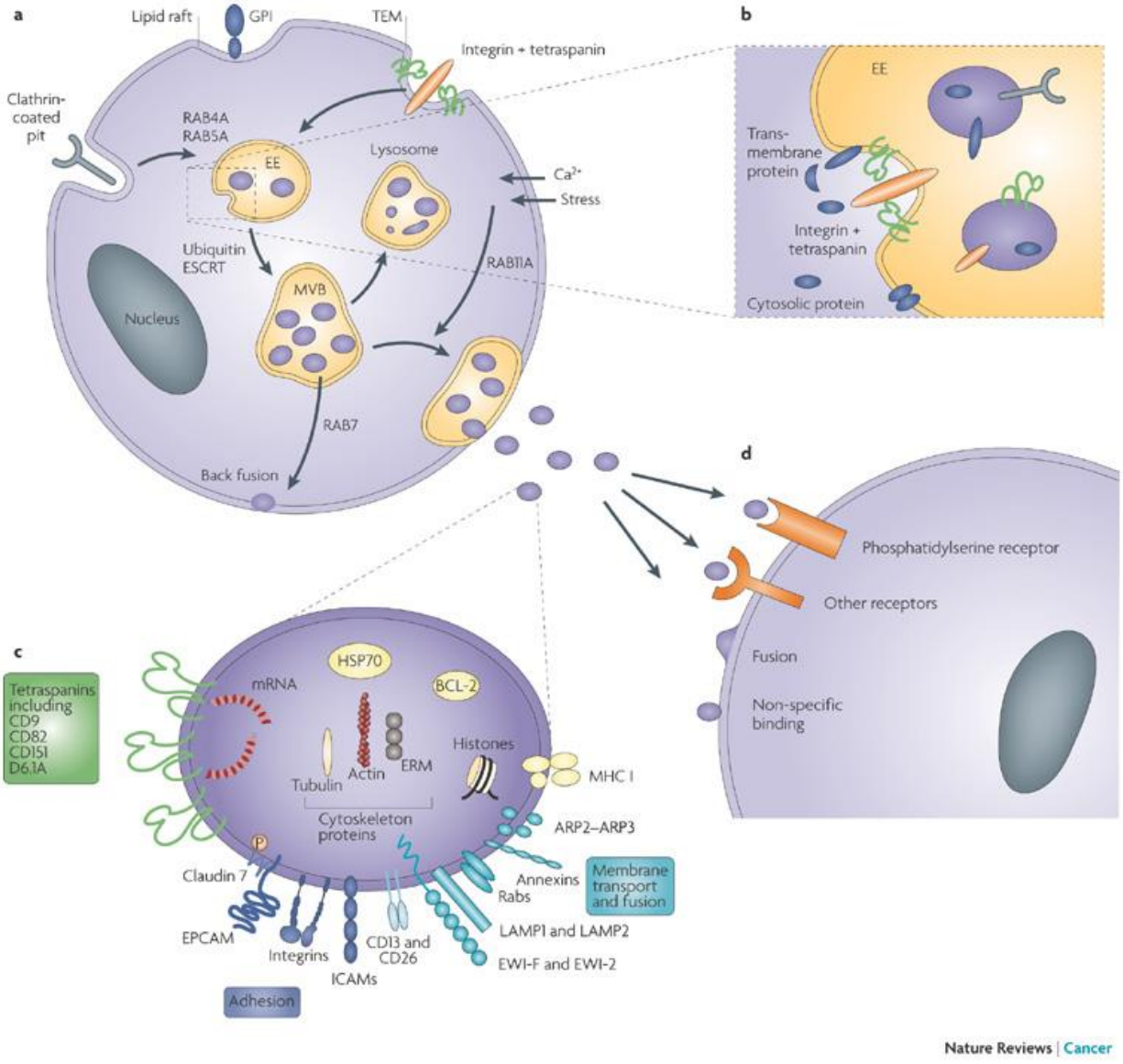

Figure X. The generation and composition of exosomes. *Membrane proteins are endocytosed via clathrin-coated pits, clustering of proteins in lipid rafts or tetraspanin-enriched membrane microdomains (TEMs). Then, they are addressed to early endosomes (EEs), those gradual maturation toward the late endosomes results in the increase of intraluminal vesicles number. These late endosomes are also known MVBs. The intracellular transport of these vesicles and their cargo selection are facilitated by ubiquitylation, Rab proteins and ESCRT machinery. MVBs can recycle proteins back to the membrane, evolve into lysosomes for degradation, or fuse their membrane with the plasma membrane thus releasing their intraluminal vesicles as exosomes. This last process is promoted by various stimuli, as Ca^{2+} flux and stress (**a, b**). The exosomes composition varies with the cell type, but includes some ubiquitous molecules, including Rab proteins, annexins and ARP2-ARP3, which are involved in membrane transport and fusion, adhesion proteins (as integrin and ICAMs), cytoskeleton proteins, tetraspanins and nucleic acids **(c)**. The uptake of exosomes by target cells occurs by different mechanisms: these vesicles can bind to specific receptors (mainly phosphatidylserine receptors), interact unspecifically or fuse with the recipient cells membrane **(d)**. ERM, ezrin-radixin-moesin; GPI, glycosylphosphatidylinositol; ICAM, intercellular adhesion molecule [420].*

Microvesicles

Microvesicles (MVs) are membranous particles with irregular shape and constitute a larger and more heterogeneous populations in size compared to exosomes, ranging from 50 to 1,000 nm in diameter [407, 482]. Their buoyant density is not yet been determined, but may overlap that of exosomes [378, 483]. MVs, as well as exosomes, arise through an unconventional mechanism (*i.e.* not based on the classic signal-peptide secretory transport pathway) [484] but in contrast to the exosomes endocytic origin, they are formed through direct outward budding from the plasma membrane and fission of their connecting membrane stalks [431, 485-487] *(Figures XII and XIII)*.

MVs formation is driven by the acquisition of membrane curvature which requires physical perturbations of the lipid bilayer [488]. These deformations seem to be mainly mediated by proteins and lipids, which can modify membrane shape through different mechanisms. First, cytosolic proteins recruited to the membrane can polymerize with an intrinsic curvature and thus impose it on the membrane [489-492] *(Figure XI-a)*. In this model, the constraints induced by proteins can be supported by lipid aggregation into microdomains, which leads to membrane bending by beginning the budding process [493]. Second, proteins can cause morphological changes in cell membrane according to the bilayer-couple hypothesis. This theory, initially popularized by Sheetz and Singer in 1974, proposes that through the physical insertion of amphipathic moieties into one face of the lipid bilayer, proteins can increase the surface area of this leaflet and thus induce the spontaneous curvature of the bilayer [494-496] *(Figure XI-b)*.

Third, contractile proteins can add or remove tensile forces, stretch only one face of the lipid matrix and thus create a structural asymmetry that would cause bending [497]. Fourth, proteins can contribute to regulate the lipid composition and distribution within the plasma membrane both due to asymmetric lipid synthesis and owing their relocation [498, 499]. Aminophospholipid translocases, in fact, are proteins that regulate the transfer of phospholipids from one leaflet to the other in an ATP-dependent manner. In particular, flippases are translocases that move phospholipids from the outer face to the inner one; on the contrary, floppases perform phospholipid transfer in the reverse direction [500-502]. In this respect, the movement of phosphatidylserine to the outer leaflet promotes membrane budding and vesicles formation [503, 504] *(Figure XI-c)*.

In addition, selective enrichment of cholesterol could decrease local membrane stiffness, alter the relative bilayer surface areas and promote the budding process [505-507] *(Figure XI-d)*. Hence, MVs shedding occurs at specific locations, where particular proteins and lipids accumulate [508].

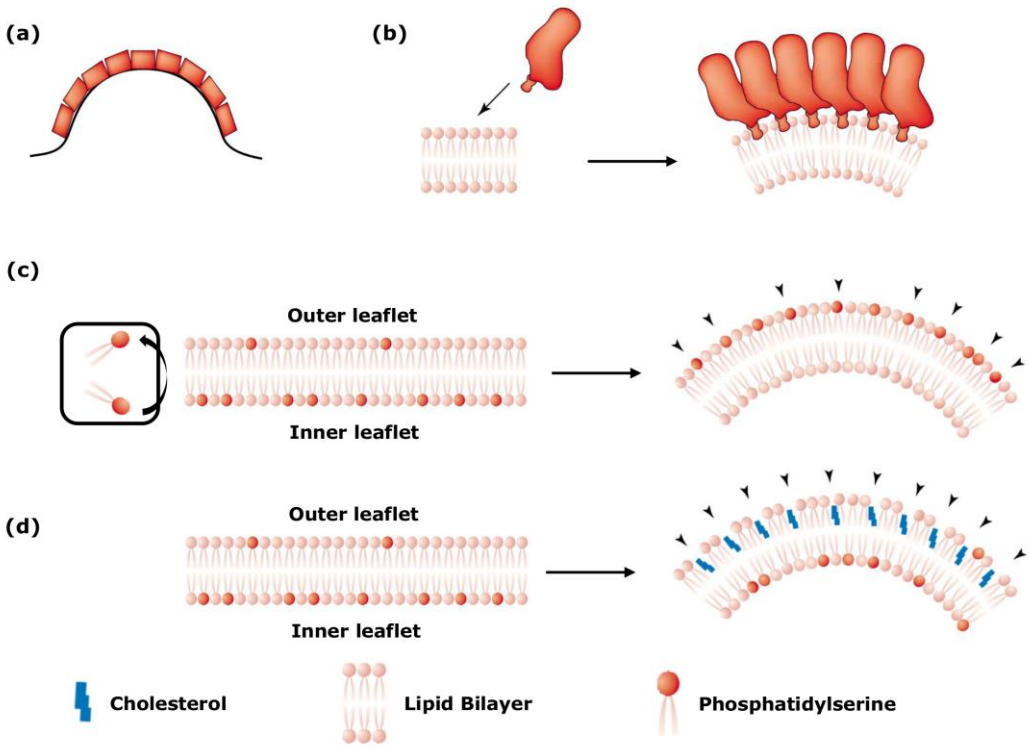

Figure XI. Mechanisms of membrane deformation mediated by proteins and lipids. *Proteins that assemble with an intrinsic curvature could drive membrane shape* ***(a)****. Membrane curvature according to the bilayer-couple hypothesis* ***(b)****. Transfer of lipids to one leaflet* ***(c)*** *and/or selective enrichment of cholesterol* ***(d)*** *result in membrane curvature owing to bilayer surface-area discrepancy between the two leaflets. Black arrowheads indicate the transferred lipids in* ***(c)*** *and cholesterol in* ***(d)*** *[modified from ref. 488].*

Once the bud is formed, it is physically separated from the plasma membrane of donor cells (the process known as fission) thanks to contraction of cytoskeletal structures by actin-myosin interactions [425, 509, 510]. In tumor cells, this phase starts with ADP-ribosylation factor 6 (ARF6), a small GTP-binding protein of Ras family expressed in all eukaryotes, which activates phospholipase D (PLD), that, in turn, recruits ERK (extracellular signal regulated kinase) to the plasma membrane. ERK is able to phosphorylate and activate MLCK (myosin light-chain kinase), a kinase that promotes myosin function, cytoskeleton contraction and thus the release of MVs [425] *(Figure XII)*. Vesicles contraction seems to be internally, at the necks of the bud, in this location contractile proteins complete the fission process

by acting like a drawstring [425, 508]. Besides translocases enzymes activity, also that of contractile proteins requires energetic input [508] *(Figure XII)*.

It is noteworthy that this signaling cascade does not affect exosomes release, supporting the concept that the biogenesis of these subtypes of vesicles involves distinct mechanisms [425].

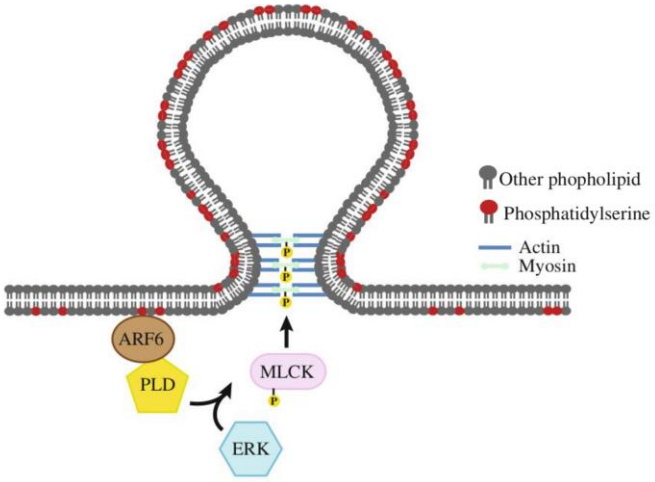

Figure XII. The signaling cascade that regulates outward budding and fission of MVs. *ARF6 activates PLD, which recruits ERK to the plasma membrane. ERK, in turn, activates by phosphorylation MLCK, which phosphorylates and activates myosin light chain, thereby triggering the release of MVs [529].*

MVs production is documented in resting cells, but the rate of this phenomenon becomes significantly higher in response to various stimulations, including increased in cytosolic Ca^{2+} concentration, cellular stress (such as DNA damage), cytokine exposure, anticancer drug treatment [511-515], and, for DCs, in response to LPS [417, 516] *(Figure XIII)*. Since the release of MVs causes the removal of small portions of membrane from the cell surface, they must be continuously replaced. In resting cells, the maintenance of an appropriate surface area is favor by the constitutive traffic of membrane enriched in vesicles-specific molecules. On the contrary, surface area homeostasis in high rate shedding cells requires a further compensation mechanism. In these activated cells, in fact, vesicles formation seems occur in conjunction with the discharge of non-secretory exocytic vesicles stored in the cytoplasm, which allow to insert “new portions” of membrane in the cell surface [517, 518] *(Figure XIII)*.

Like exosomes, MVs cargo is composed of bioactive components from cytosol, such as nucleic acids (in particular miRNAs) [519, 520], lipids, numerous proteins (including cytokines, oncogenes, growth factor receptors, integrin receptors, proteases and/or MHC class I molecules) [521], whole intact organelles, such as

mitochondria [412] and infectious particles (as HIV, human immunodeficiency virus, and prions) [522-525]. Transmembrane proteins incorporated into MVs conserve the same topological orientation of the parent cell [521]. Since MVs are released by different cell types, their composition depends on the cell from which they originate and the status in which it is [408]. Protein and lipid components of MVs are not random but selectively sorted at the cell surface, among them, there are also the proteins contained and trafficked via the ARF6-regulated endosomal recycling pathway, but compared to the mechanisms involved in exosomes biogenesis, these processes are less defined [526, 527]. However, the understanding about the structure and the biogenesis, not only of MVs but also exosomes, are not yet complete. In fact, despite the different origin, size, morphology, buoyant density and protein composition, MVs and exosomes derived from the cell cultures supernatant are not easy to separate because the size range overlap between the two different vesicles and also small vesicles (100 nm in diameter) may bud from the cell surface [528]. Finally, there is no general consensus as to the best method to isolate the two subpopulations.

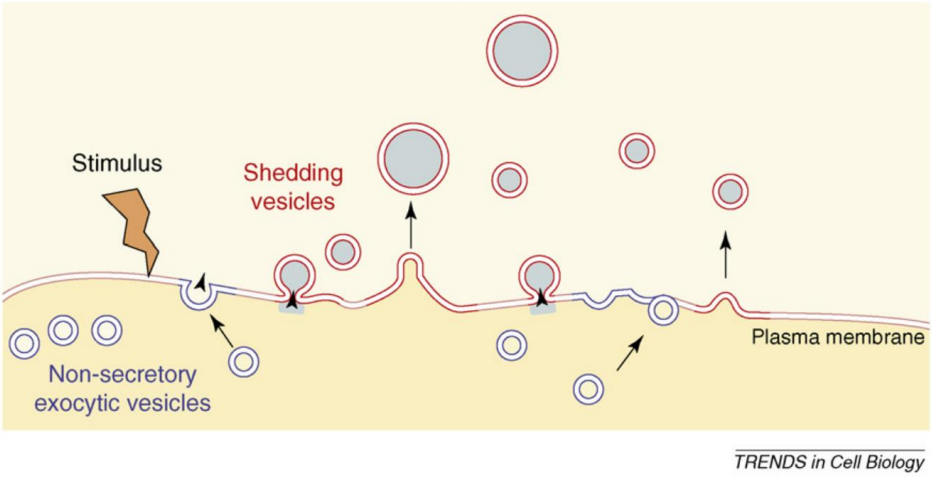

Figure XIII. Generation of MVs. *MVs (red membrane) directly shed from the plasma membrane of cells in the resting state or, with a higher rate, from cells activated in response to various stimuli (such as the increase of cytosolic Ca^{2+} concentration and cellular stress, represent as a thunderbolt in the extracellular space). The cargo of microvesicles (gray) is sorted out from the cytosol. MVs release, i.e. the removal of membrane fragment at the cell surface, is compensated by a concomitant input of membrane delivered through the non-secretory exocytic vesicles stored in the cytoplasm (blue membrane) [407].*

Functions of extracellular membrane vesicles

Initially it was thought that vesicles observed in the cell culture supernatant were cell debris formed during the processes of apoptosis or necrosis in response to damage, or merely membrane fragments artificially released upon *in vitro* cell

handling [530]. Nowadays, the identification of some molecular mediators of biogenesis processes, as well as of certain conditions capable of increasing the production of vesicles, in addition to the findings that EMVs do not contain a random array, but a specific set of proteins both in the membrane and in their inside, allowed to assert that EMVs are actively secreted by live cells and could represent a new type of intercellular messenger [531-535].

In fact, once in the extracellular environment, exosomes and MVs could participate in a wide variety of physiological as well as pathological processes. The functions of EMVs are the result of their interactions with recipient cells and are related to their cargo and to their structural and biochemical properties, which, in turn, depend on their source of origin [378, 536]. Several modes of interaction of EMVs with target cells have been proposed. EMVs may dock at the plasma membrane of recipient cells through lipids or ligands-receptor interactions [537] *(Figures X-d and XIV-a)*. For example, intracellular adhesion molecule 1 (ICAM1)-bearing exosomes secreted from mature DCs are captured by $CD8^+$ DCs with help of lymphocyte function-associated antigen 1 (LFA-1) [538] *(Figure X-c)*. Similarly, galectin-5 participates in the recruitment of reticulocyte exosomes by macrophages [539].

The binding is followed by different events. First, at this location MVs can establish a reaction platform, thus inducing the extracellular assembly of functional multimolecular complexes and the coordinate development of multi-signaling processes [540, 541]. Second, EMVs can directly fuse with the plasma membrane of target cells, resulting in the integration of their membrane proteins into the membrane of recipient cells and the release of their cargo into the cytoplasm *(Figures X-d and XIV-b)*. Third, vesicles can be internalized by endocytosis [378, 542] *(Figure XIV-c)*. This event can be followed by: the fusion of endocyted vesicles with the limiting membrane of the endosome, which causes the release of vesicles contents into the cytoplasm and the incorporation of the membrane proteins into the endosomal membrane, which, then, can be redirected to the cell surface *(Figure XIV-c-ii)*; the degradation of vesicles in the phagocytic pathway, which, for example, can lead to the production of antigenic peptides and their presentation onto MHC class II and I molecules at the cell surface [378, 407] *(Figure XIV-c-iii)*; transcytosis, in fact, it has been documented that, at least MVs, once segregated within endosomes, can be released intact back to the extracellular space [407] *(Figure XIV-c-i)*.

In addition, upon release from their cell of origin, vesicles could not remain intact for long, but broken down and release their contents in the extracellular environment, thus depositing paracrine signals.

For example, shedding vesicles derived from tumor cells release MMPs and their inducer (CD147 or EMM-PRIN, extracellular matrix metalloproteinases inducer), that, through the degradation of ECM, promote the motility of malignant cells, which become capable to invade tissues more quickly [543-545]. The vesicles shed from neurons, astrocytes, hepatocarcinoma and endothelia, instead, release FGF_2 [428, 429, 546]. Taraboletti *et al.* showed that EVMs derived from ovarian carcinoma cell lines burst is promote when the extracellular pH is acidic [547].
Further, this mechanism allows the regulated release by cells of proteins deprived of signal sequences, which, for this reason, can not enter the classical secretory pathway [407].
It also has been observed that vesicles secretion could be used to eliminate proteins resistant to lysosomal degradation. For example, during the process of red blood cell maturation, reticulocyte releases exosomes to remove membrane proteins no more necessary for its function, such as transferrin receptor [548].
Given that most of EMVs studies have been performed *in vitro* or from body fluids, their overall biological relevance remains unclear.

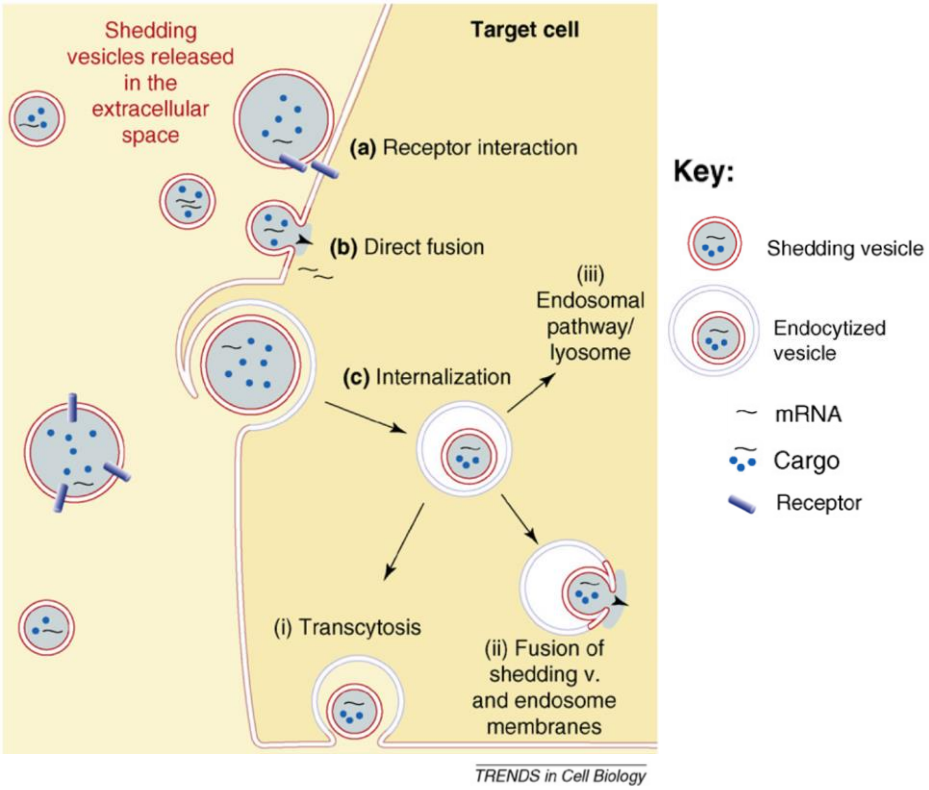

Figure XIV. Interactions of MVs with their recipient cells. *Once MVs are released by donor cells into the extracellular space they can: bind to the surface of the target cells by specific receptors* ***(a)****; fuse their membrane with that of recipient cells* ***(b)****; be internalized by endocytosis* ***(c)****. This last event can be followed by: transcytosis* ***(i)****; the fusion of MVs membrane with that of cell endosome* ***(ii)****; the targeting to lysosome for the degradation of their contents* ***(iii)****. The arrows indicate the direction of cargo discharge taking place upon vesicles membrane fusion [modified from ref. 407].*

EMVs in tumor diseases

Besides the direct cell-cell contact and the secretion of bioactive molecules [549], the communication and the exchange of informations between cancer cells and the activated stroma can be mediated by the release of EMVs [550]. These vesicles contribute to the mutual horizontal transfer of tumor suppressors, phosphoproteins, proteases, growth factors, nucleic acids and bioactive lipids [551], all of which can modulate several phases of tumor progression, such as immune surveillance, inflammation, angiogenesis, thrombosis, invasion, metastasis, chemoresistance and further important biological events [408, 552-561]. Tumor cells may release various forms of membrane vesicles, each one characterized by unique morphological traits and functions [562]. They include exosomes, microvesicles [563] and a particular form of larger particles (called large oncosomes, 1,000-10,000 nm in diameter) which shed from the plasma membrane of certain types of cancer cells during the amoeboid motility [564].

In the tumor microenvironment, tumor-derived vesicles can promote cancer cells survival, aiding the escape from apoptosis as well as from immune surveillance. MVs represent a protective mechanism from cell death because they serve as a means to remove the potentially dangerous caspase 3. In fact, MVs contain considerable amounts of this effector of apoptosis, which, for this reason, is not detectable within the cells [565, 566]. In addition, Shedden *et al.* showed that chemoresistant cancer cells express more membrane shedding-related genes compared with chemosensitive counterpart, suggesting a link between vesicles secretion and multidrug resistance [512]. The modulation of the immune system activities, instead, is mediated both through the mechanism of "complement resistance" [567] and by the suppression of the immune response. Shedding vesicles can contain the complement inhibitor membrane cofactor protein CD46, which inactivates the complement complex, hence avoiding cell lysis [568], as well as can express immune modulatory molecules. In particular, MVs from different types of cancer cells expose the ligand (FasL, CD95L) of the death receptor Fas (CD95), which induces apoptosis in activated T cells and diminishes their killer activity [569, 570]. Lymphoblastoma-derived microvesicles, instead, express latent membrane protein-I (LMP-I), which inhibits leucocyte proliferation [571]. Vesicles produced by human melanoma or colorectal carcinoma cells are also able to fuse with plasma membrane of monocytes, thus impairing their differentiation to APCs, but promoting the release of immunosuppressive cytokines, whose role is to block cytolytic T-cell activation and function [572].

Further, tumor-derived vesicles can support invasive growth and metastasis of cancer cells with different mechanisms. First, MVs contain and expose proteases, including MMP-2, MMP-9, MT1-MMP, their zymogens, uPA and EMM-PRIN, that, as reported above, degrade numerous components of the ECM, allowing malignant cells to cross the basement membranes [425, 547, 573-575].

Second, tumor cells, but maybe also endothelial cells, monocytes and platelets, can produce procoagulant tissue factor (TF)-bearing MVs [576-578], which perform their function through coagulation-dependent and -independent mechanisms. In the former, TF-bearing MVs begin the intravascular coagulation and lead to fibrin production, which, in turn, can coat tumor cells protecting them from immune detection and attacks, as well as provides the structural support necessary for angiogenesis [579-581]. In the last, TF expressed by vesicles induces the paracrine activation of ECs through a specific class of G-protein-coupled receptors, known as PARs (protease-activated receptors), causing the increased secretion of the pro-angiogenic heparin-binding EGF-like growth factor (HB-EGF) by these cells [582].

Third, tumor-derived vesicles can transfer mutant molecules to non-malignant and normal cells, thereby influencing their phenotype and biological behavior. It has been documented that the vesicles-mediated passage of oncogenic EGF receptor (EGFR or EGFRvIII) from aggressive glioma cells to indolent ones leads to morphological transformation of these recipient cells and increases their anchorage-independent growth capacity [583]. Similar findings were reported by Peinado *et al.*, who found that highly metastatic melanoma produces EMVs containing MET. This tyrosine kinase is able to increase the metastatic behavior of primary tumors by permanently re-educating the recipient bone marrow-derived cells (BMDCs) that, once activated, support the formation of pre-metastatic niches in distant organs [561].

Nucleic acids are also packaged in tumor-derived microvesicles and contribute to the transfer of genetic informations between cells. MVs contain: miRNAs, that may modify the transcriptome of recipient cells promoting tumor progression and metastases, but the mechanisms are not yet completely understood [469, 584-586]; noncoding RNAs (ncRNAs), that are involved in gene regulation at both transcriptional and post-transcriptional levels [587]; retrotransposon RNAs, such as LINE-1, HERV-K and Alu [411], that, by inserting themselves into the genome, can increase its plasticity [588]; cDNAs and genomic DNA derived from DNA replication, although their source is not fully clear [411]; mRNAs that promote tumor growth, invasion, immune repression [469] and angiogenesis [589].

For example, cancer cell-derived MVs can transfer mRNA encoding growth factor (including VEGF and HGF) to monocytes, which then produce these molecules [520, 590].

The protein, lipid and RNA contents of tumor-derived vesicles can be modified by different types of stressors typical of tumor microenvironment, such as hypoxia [591-593], acidosis [594], oxidative stress [595-597], thermal stress [596, 598, 599], radiation [591], shear stress [600] and cytotoxic drugs [601]. Accordingly, thermal and oxidative stresses induce leukaemia/lymphoma T and B to produce exosomes enriched in natural killer group 2, member D (NKGD2) ligands, which decrease the capacity of immune system to kill target cells [596]. Further, the treatment of aggressive B-cell lymphoma cells with chimeric anti-CD20 monoclonal antibody (rituximab) leads to the production of CD20-bearing exosomes, which act by protecting cells from antibody and complement-dependent cytolysis [602]. Melanoma cells cultured in acidic milieu, instead, generate exosomes enriched in ganglioside GM3 and sphingomyelin increasing the rigidity of their membrane. This alteration of lipid composition enables the exosomes to fuse more efficiently with the plasma membrane of recipient cells [594]. As for proteins and lipids, also RNA content seems to be stress-mediated. For example, exposure of breast cancer cells to hypoxia results in secretion of exosomes enriched in miR-210 [593]. However, further analysis will be necessary to elucidate how stress conditions modulate RNA content of tumor-derived vesicles. Intriguingly, alterations in the protein, lipid and RNA composition can cause change in the biological functions of vesicles, but their impact on tumor development needs to be clarified [603].

Besides cancer cells, the activated stroma (macrophages, fibroblasts and platelets) may release EMVs into the tumor microenvironment [551]. In particular, platelet-derived MVs stimulate mRNA expression of pro-angiogenic factors in cancer cells [598] and, as mentioned above, fibroblasts-derived exosomes induce breast cancer cell migration and invasiveness through the Wnt-PCP signaling [141].

EMVs released by both cancer and stromal cells can perform their function locally (in the tumor microenvironment), as well as at the systemic level owing to their dissemination through body fluids (such as blood and urine), suggesting that the detection of these vesicles could be used as circulating non-invasive biomarkers not only for the early diagnosis [437, 469], but also in the surveillance of disease progression, and thus for prognosis [605-607]. In addition, EMVs may have other multiple applications. Because the release of vesicles can promote tumor development, the production and secretion processes themselves could also be an interesting target of anti-cancer therapy [608].

Further, EMVs could be used as drug-delivery vehicles [609] or as adjuvant anti-cancer treatment. In fact, cancer cell-derived MVs may facilitate immune attacks by transferring tumor antigens to APCs, which in turns activate T cells [424], alternatively, autologous dendritic cells-derived MVs, which act by triggering cytotoxic T lymphocytes *in vivo*, may be used as autologous anti-cancer immunotherapy [454, 610-614]. Finally, because the anti-cancer therapy modulates the contents of vesicles, the effectiveness of this treatment can be assessed by analyzing vesicles themselves [615].

Other functions of EMVs

EMVs represent a new way of communication shared by an increasing number of cell types. In particular, APCs-derived exosomes express MHC-peptide complexes which are able to be directly recognized by their cognate T-cell receptor and activate primed $CD4^+$ and $CD8^+$ T cells [415, 616-618]; on the contrary, exosomes must be captured by DCs to induce the activation of naïve T lymphocytes [619]. This different behavior may depend on the activated conformation of LFA-1 integrin at the surface of DCs and primed (but not naïve) T lymphocytes, which efficiently bind to ICAM1-bearing exosomes [538, 617]. Alternatively, the activation of naïve T cells may require not only the TCR-dependent signal, but also the cytokines secreted by DCs [530]. As with APCs-derived exosomes, those released by B cells display MHC class I and class II, which activate specific T cell responses [451], and functional integrins, that mediate the anchorage to ECM components and to cytokine-activated fibroblasts. For example, exosomes adhesion to TNF-α-activated fibroblasts results in cytosolic calcium changes [620].

In addition, exosomes were secreted by epithelia both from the apical and the basolateral sides of the polarized cell monolayers. Exosomes released at the apical membrane contain specific molecules, such as syntaxin 3, microsomal dipeptidase CD26 and may be involved in a clearance process [451]. Basolateral exosomes, instead, are constitutively enriched in A33 antigen and MHC class II after activation by IFN-γ, and seem participate in antigen presentation [621].

Further, vesicles released from intraocular epithelia in response to inflammation contain the target antigen hr44 and CD63 and have a role in the maintenance of ocular immune privilege [622]. Further, cauda epididymal region produce exosomes [623], known as “epididymosomes”, that participate in sperm epididymal maturation by transferring P25b, a component of a family of sperm surface proteins necessary for the binding to the surface of the egg [451]. Recent reports showed that ECs produce exosomes enriched with miR143/145, which are transferred to

smooth muscle cells (SMCs), influencing gene expression of miRNA target and thus providing atheroprotective properties [624].

Although there are several evidences of the potential biological function of EMVs, to date, most of the studies were performed *in vitro* or from body fluids and the knowledge about their possible function *in vivo* is still very little. Furthermore, it is not clear if the amounts of EMVs used in *in vitro* experiments are comparable to those *in vivo*. In this regard, only one study was conducted. In 2006, Taylor *et al.* showed that the serum of women delivering the pregnancies at full term has higher concentration of placenta-derived exosomes compared to women delivering preterm, and that these vesicles express significantly higher levels of biologically active molecules, such as FasL and MHC class II. These vesicles are able to inhibit T cell responses in a CD95L-dependent manner and this inhibition is greater with vesicles obtained from the serum of women delivering at term, suggesting that the function of these vesicles is to prevent the maternal immune response against the fetus [625].

MATERIALS AND METHODS

Cell cultures

Human prostatic cancer cells (PC3 and DU145) and A375 human melanoma cell line were purchased from European Collection of Cell Culture (ECACC). Human dermic fibroblasts (HDFs) are from Invitrogen™ Life Technologies and NIH-3T3 mouse fibroblasts are from *Istituto Zooprofilattico Sperimentale della Lombardia e dell'Emilia-Romagna*. Healthy (HPFs) and transformed (CAFs) human prostatic fibroblasts were isolated from surgical explantation of patients who signed informed consent in accordance with the Ethics Committee of *Azienda Ospedaliera Universitaria Careggi by Prof. Serni of Dipartimento di Medicina Sperimentale e Clinica/Urology* (Firenze, Italy). Cells were routinely cultured in Dulbecco's Modified Eagle's Medium (DMEM) supplemented with 2 mM glutamine, with penicillin (100 U/mL) and streptomycin (100 µg/mL), and with 10% fetal bovine serum (FBS, Euroclone). Cells were incubated at 37°C in a humidified atmosphere of 5% CO_2-95% air.

Materials

Unless otherwise specified all reagents are from Sigma/Aldrich. Carboxyfluorescein diacetate succinimidyl ester (CFDA-SE), Opti-MEM and Lipofectamine® transfection reagent are from Invitrogen™ Life Technologies. Polyvinylidene difluoride (PVDF) membrane and Immobilon Western Chemiluminescent HRP Substrate are from Millipore. Boyden chambers were purchased from Euroclone. Cocultures separation was performed by MACS MicroBeads and MACS Column Technology patented by Miltenyi Biotec. Apoptosis test is performed by Annexin-V-Fluos staining kit from Roche. Sodium [^{14}C] bicarbonate, L-amino acids mixture [^{14}C] and the storage phosphor screen are from Perkin Elmer. 2D Quant kit, Ettan™ IPGphor™ system, IPGphor Cup Loading Strip Holders and the ECL plus immunodetection system were purchased from GE Healthcare, USA. ReadyStrip™ IPG strips were purchased from Bio-Rad. CA IX siRNA, anti-enolase and anti-actin antibodies were purchased from Santa Cruz Biotechnology. Anti-glyceraldheyde-3-phosphate dehydrogenase (GAPDH) and anti-superoxide dismutase 2 (SOD-2) antibodies were from Abcam, anti-β-tubulin was from Sigma/Aldrich, anti-pyruvate kinase M1 (PKM1) was from Proteintech, anti-pyruvate kinase M2 (PKM2) was from Cell Signaling Technology, anti-vimentin was from Thermo, anti-CA IX was from Bioscience Slovakia.

Proliferation assay

The proliferation was evaluated using CFDA-SE. Tumor or stromal cells were labeled with the dye at the concentration of 2.5 μM. Then PC3, DU145 or fibroblasts were cultured alone or in coculture for 40 hours. After that the cells were detached, fixed in 3% paraformaldehyde and analyzed by flow cytometry. The fluorescence value obtained was analyzed by ModFit software to estimate the proliferation index.

Fluorescence analysis of protein transfer

The transfer of proteins from donor cells to recipient cells was evaluated by using CFDA-SE. Donor cells were labeled with the dye at the concentration of 10 μM and then plated in coculture with recipient cells. For flow cytometry analysis the cells were detached after 24 or 40 hours, fixed in 3% paraformaldehyde and the ability of donor cells to transfer proteins was evaluated by measuring the value of fluorescence intensity increase of recipient cells, which is obtained from the ratio between the fluorescence value of the recipient cells measured after coculture with donor cells and the autofluorescence of recipient cells. In fact, once that CFDA-SE passively diffuses into the cytoplasm of donor cells, intracellular esterases cleave its acetate groups and the probe is converted to the fluorescent ester, called CFSE. CFSE reacts with intracellular amines (including that of proteins) and forms fluorescent conjugates that are retained within the cells. For this reason, when labeled donor cells transfer their proteins to recipient ones, the fluorescence intensity of recipient cells increases, on the contrary, if the passage of fluorescent proteins does not occur, their fluorescence intensity remains close to that of autofluorescence.

For confocal microscopy analysis the coculture was grown on glass coverslips. Immediately after plating and after 6 hours the cells were washed with phosphate-buffered saline (PBS) and fixed in 3% paraformaldehyde for 20 minutes at 4°C. After that, the cells were washed again in PBS, mounted with glycerol plastine and observed by confocal fluorescence microscopy (Leica TCS SP5).

Analysis of lipid transfer

The transfer of lipids from donor cells to recipient ones was evaluated by using CellVue®. Donor cells were labeled with the dye according to the manufacturer's protocol and then plated in coculture with recipient cells on glass coverslips. Immediately after plating and after 6 hours the cells were washed with PBS and fixed in 3% paraformaldehyde for 20 minutes at 4°C. After that, the cells were washed again in PBS, mounted with glycerol plastine and observed by confocal fluorescence microscopy (Leica TCS SP5).

Conditioned media preparation

Tumor cells were grown in starvation medium for 48 hours, after that the medium was recovered, centrifuged at 1,000 xg for 20 minutes to discard cell debris and used to culture fibroblasts for 24 hours. Soon after the activation, fibroblasts were used for the experiments.

Alternatively, CAFs were grown in starvation medium for 48 hours, after that the medium was recovered, centrifuged at 1,000 xg for 20 minutes to discard cell debris and used for the proliferation experiments of tumor cells.

Acidification assay

The pH of the external medium of tumor cells or fibroblasts either in single cultures ($2x10^5$ cells) or in cocultures (10^5 fibroblasts and 10^5 DU145 or PC3) was determined after 24 hours in DME supplemented with 1 mM sodium bicarbonate (pH 7.6) at atmospheric CO_2.

Cell death determination

10^5 DU145 or PC3 were plated in DME supplemented with 25 mM hepes and 10 mM sodium bicarbonate at pH 6.8, pH 7.4 and pH 8.0 for 40 hours at 5% CO_2. Cells were detached with Accutase and labeled with Annexin-V-Fluos staining kit. The probe was directly detected by flow cytometry analysis.

In vitro 2D tumor migration assay

DU145 cells were grown to confluence, starved overnight at pH 6.8 or pH 8.0 in DME supplemented with 25 mM hepes and 10 mM bicarbonate at 37°C and 5% CO_2. A wound was made with a sterile micropipette tip. Floating cells were removed by washing with PBS and then fresh DME at pH 6.8 and pH 8.0 + 10% FBS was added. Cells were photographed immediately after the wound initiation and after 18 hours using an inverted Nikon Eclipse TS100 microscope (X10 objective) with Nikon Digital Sight camera system.

In vitro 3D tumor migration assays

$5x10^4$ green fluorescent protein (GFP)-expressing PC3 cells (PC3-GFP) were seeded in the top of Boyden chamber (trans-well migration assay) in serum-free medium alone or in coculture with $5x10^4$ fibroblasts, while medium + 10% FBS was placed in the well below in 24-well tissue culture plates. After 18 hours, while the insert was still moist, the non-migratory cells were mechanically removed from the interior of the insert using a cotton swab. Migrated cells were photographed immediately by fluorescence microscopy (Leica TCS SP5).

In addition, PC3 migration was monitored by xCELLigence Real-Time Cell Analyzer (RTCA) DP instrument (Roche Applied Science). $5x10^4$ PC3 were plated in serum-free medium into the upper chamber of CIM (cellular invasion/migration)-Plate 16, while medium supplemented with 10% FBS was placed in the well below. As cells migrate from the upper chamber to the bottom one, they contact and adhere to the electronic sensors on the underside of the microporous PET membrane of the Boyden-like chamber, resulting in an increase in impedance. The impedance increase correlates to increasing numbers of migrated cells on the underside of the membrane and is continuously recorded by the RTCA DP instrument. The impedance is displayed as a dimensionless parameter termed "cell index".

Cocultures separation

DU145 or PC3 were labeled with CFDA-SE and then plated in coculture with fibroblasts. For the CA IX expression analysis, after 40 hours cells were detached with Accutase and separated according to the manufacturer's protocol of MACS Column Technology. A fraction of each cell sample was used to determine the separation efficiency by flow cytometry, which detects the percentage of CFDA-SE-labeled tumor cells in fibroblasts sample after separation, and vice versa. The other part of the sample, instead, was lysed with 2-fold concentrated Laemmli electrophoresis buffer [627] without β-mercaptoethanol and bromophenol blue.

For radiolabeling experiments the cells were detached, separated according to the manufacturer's protocol of MACS Column Technology and the two cell populations recovered were counted with Bürker chamber. After that a fraction of each cell sample was used to determine the separation efficiency by flow cytometry, another fraction was used to measure the radioactivity (CPM, counts per minute) by liquid scintillation counter (Perkin Elmer), and, only for the samples subjected to 2D electrophoresis (2DE), a part was lysed and the proteins were opportunely extracted. The percentage purity of donor and recipient cells after the coculture separation was higher than 98%. The CPM values measured for recipient cells were calculated subtracting the radioactive contamination due to donor cells, and vice versa.

Analysis of CA IX expression

Cells were lysed with 2-fold concentrated Laemmli electrophoresis buffer [627] without β-mercaptoethanol and bromophenol blue and protein concentration was evaluated by bicinchoninic acid (BCA) assay. After that, samples were precipitated according to methanol/chloroform protocol [626]. Briefly, for about 150-300 µg of proteins contained in 150 µL of sample were added 600 µL of methanol, 150 µL of

chloroform and 450 µL of water, after each addition the sample was mixed by vortexing. Then the sample was centrifuged at 13,500 xg for 10 minutes, discarded the upper phase, kept the white precipitation disc evident between the upper and lower phases, and then 450 µL of methanol was added to the sample. After 10 minutes of centrifugation at 13,500 xg the supernatant was discarded and the pellet was dried in a vacuum centrifuge for 20 minutes. Then, the sample was resuspended in Laemmli electrophoresis buffer [627]. The proteins (40 µg for each sample) were separated by SDS-PAGE, transferred on PVDF membrane by Western blot and probed with anti-CA IX antibody, and with anti-actin antibody as loading control. Immunoblots were incubated in PBS supplemented with 5% bovine serum albumin and 0.05% Tween for 1 hour at room temperature with primary antibody and then in PBS supplemented with 1% bovine serum albumin and 0.05% Tween for 45 minutes with secondary antibody conjugated with horseradish peroxidase (HRP). Development was performed with Immobilon Western Chemiluminescent HRP Substrate and chemiluminescence was detected by UVP (Ultra-Violet Products) Ltd Chemidoc-it 500 Imaging System. Quantitative analysis of the spots was carried out by Kodak MI software.

Purification of membrane vesicles secreted by CAFs

The culture supernatant recovered from radioactively labeled CAFs was centrifuged at 1,000 xg for 20 minutes to discard cell debris. The supernatant was then centrifuged at 10,000 xg for 40 minutes. The pellet was resuspended in PBS and centrifuged again at 10,000 xg for 40 minutes. The supernatant was recovered and centrifuged at 100,000 xg for 90 minutes. The pellet was resuspended in PBS and centrifuged again at 100,000 xg for 90 minutes.

Serum present in fibroblasts growth medium was previously deprived of exosomes by centrifugation at 100,000 xg for 90 minutes.

For proliferation experiments, “10,000 xg pellet” was resuspended in starvation medium and used to grow DU145. For electrophoresis and Western blot analysis, instead, both the “10,000 xg pellet” and the “100,000 xg pellet” were suspended in 100 µL of 2-fold concentrated Laemmli electrophoresis buffer [627] (without β-mercaptoethanol and bromophenol blue) and assayed for protein content by the BCA method. 40 µg aliquots from each sample were additioned with β-mercaptoethanol and separated by SDS-PAGE. Subsequently gels were electroblotted onto PVDF membranes for detection or stained with colloidal blue coomassie. The stained gels were dried on a Slab Gel Dryer (Hoefer, model CD

2000). Dried gels and a storage phosphor screen were inserted in an exposure cassette.

After a 15 days exposure time, the images were acquired on a Cyclone Storage Phosphor Scanner (Perkin Elmer). The blots were incubated with anti-enolase, anti-β-tubulin, anti-GAPDH, anti-PKM1, anti-PKM2, anti-vimentin, anti-SOD-2 and anti-actin. After incubation with secondary antibodies, the blotting was developed by using the ECL plus immunodetection system and visualized by autoradiography.

Dynamic Light Scattering analysis

Membrane vesicles secreted by fibroblasts were purified as previously described, and resuspended in 800 μL of sterile PBS, after that their size distributions were obtained using Zetasizer Nano S Dynamic Light Scattering device and analyzed by the DTS software (Malvern Instrument Ltd). The analysis was performed at 25°C.

Sodium [^{14}C] Bicarbonate incorporation

DU145 were plated in DME supplemented with 25 mM hepes, 10 mM sodium bicarbonate, 20 μM sodium [^{14}C] bicarbonate (50.8 mCi/mmol) and 10% FBS at pH 8.0 for 24, 48 and 72 hours. The medium was changed every day. The cells were lysed in 2-fold concentrated Laemmli electrophoresis buffer [627] without β-mercaptoethanol and bromophenol blue. Protein concentration was evaluated by BCA assay. CPM values were obtained by scintillation counter (Perkin Elmer).

[^{14}C] L-amino acids incorporation

Fibroblasts were cultured for 72 hours in exosomes-deprived complete medium supplemented with a mixture of [^{14}C] L-amino acids. After that cells were detached, washed twice in starvation medium by centrifugation at 1,000 xg for 10 minutes, and plated in coculture with tumor cells.

GC-MS measurements

DU145 were plated in single culture and in coculture with fibroblasts in a 1:2 ratio in DME supplemented with 25 mM hepes and 25 mM sodium carbonate-^{13}C (pH 8.0) at 5% CO_2. The medium was changed every day. After 40 hours DU145 cells of single culture and DU145 cells separated from CAFs with MACS Column Technology were lysed in 100% cold (-80°C) ethanol. Ethanol soluble fraction was dried in a vacuum centrifuge. Dried cell extracts were redissolved in 100 μL of ethanol containing 1% acetic acid. The solution was transferred in a microvial, taken to dryness under a gentle stream of nitrogen at room temperature and then derivatized with N-methyl-N-(*t*-butyldimethylsilyl)trifluoroacetamide in the presence of 1% *t*-butyldimethylchlorosilane for 2 hours at 80°C.

The samples were analyzed on an Agilent GC-MS system composed by a 7820A gas chromatograph coupled to a 5975B mass spectrometer operating in electron ionization (EI, 70 eV) mode (Agilent Technologies Italy, Cernusco sul Naviglio, Milan, Italy). The system was equipped with an automatic liquid sampler. The column was a DB 5 MS, 20 m, 0.18 mm, 0.18 μm film thickness (J&W, Agilent Technologies); helium was the carrier gas, at 0.7 ml/min constant flow rate. The oven temperature program was as follow: from 150°C to 220°C then at 5°C/min, then at 30°C/min to 310°C, maintained for 3 minutes. The injections were performed in split mode (4:1 split ratio); the injection volume was 1.5 μL. The injector port and transfer line temperatures were 260°C and 280°C, respectively. The ion source operated at 230°C, while the quadrupole temperature was 150°C. Data were acquired in SIM mode and alternating SIM/scan mode. In SIM the fragment ion at m/z (M-57) was recorded for the ^{12}C and mono ^{13}C species in a specific retention time window: for scan acquisition mass spectra were acquired in the range from 40 m/z to 680 m/z. Data were acquired and elaborated using the MSD ChemStation software (version E.01.01.335, Agilent Technologies). The peaks for malate and fumarate from GC-MS signals were integrated, and atom percent excess (^{13}C) values were calculated by comparison with control samples and unlabeled standard solutions. It was not possible to measure the percent enrichment in oxaloacetate because of the low concentration as well as the instability of this substance.

Sample preparation and 2D Electrophoresis

For 2DE, cocultured DU145 and CAFs from eight independent experiments, separated after 6 hours by MACS column technology, were harvested by centrifugation at room temperature. CAFs and DU145 pellets were washed twice in PBS and resuspended in 50 mM Tris-HCl pH 7.0, 1% NP-40, 150 mM NaCl, 2 mM ethylene glycol bis(2-aminoethyl ether)tetraacetic acid, 100 mM NaF] containing a cocktail of protease inhibitors. After sonicated briefly, protein extracts were clarified by centrifugation at 14,000 xg for 10 minutes. Proteins were then precipitated following the chloroform/methanol protocol previously described [626] and the pellet was resuspended in 8 M urea, 4% 3-[(3-cholamidopropyl)dimethylammonio] propanesulfonic acid (CHAPS), and 20 mM dithiothreitol (DTT). The protein content was determined by using the 2D Quant kit. For each cell lysate sample, four 2DE replicate gels were made for each sample, in order to assess biological and analytical variation. The first dimension (isoelectric focusing, IEF) was carried out on ReadyStrip™ IPG strips, pH 3-10 NL (Bio-Rad) and achieved using the Ettan™ IPGphor™ system. IPG-strips were rehydrated with 350 μL of lysis buffer and 2%

v/v carrier ampholyte, for 12 hours at room temperature. Sample load, 800 µg per strip, was successively performed by cup loading in the IPGphor Cup Loading Strip Holders, with the sample cup system at the anodic side of IPG strips. IEF was then achieved at 20°C according to the following voltage steps: 30 V for 30 minutes, 200 V for 2 hours, 500 V for 2 hours, from 500 to 3500 V in 30 minutes, 3500 V for 5 hours, from 3500 to 5000 V in 30 minutes, 5000 V for 4 hours, from 5000 to 8000 V in 30 minutes, 8000 V until a total of 95 000 V/h was reached. After focusing, prior to the second-dimension separation, IPG strips were equilibrated in equilibration buffer (6 M urea, 75 mM Tris-HCl pH 8.8, 29.3% glycerol, 2% SDS) containing 1% (w/v) DTT for 15 minutes and then in the same equilibration buffer containing 2.5% iodoacetamide for a further 15 minutes.

The second dimension was carried out on 9-16% polyacrylamide linear gradient gels (18 cm × 20 cm × 1.5 mm) at 40 mA/gel constant current and 10°C until the dye front reached the bottom of the gel. Protein spots were visualized by colloidal coomassie blue staining. The stained gels were scanned with the Epson Expression 1680 Pro image scanner. Gels containing proteins radiolabeled with ^{14}C-labeled amino acids (both CAFs and DU145 proteins) were dried on a Slab Gel Dryer (Hoefer, model CD 2000). Dried gels and a storage phosphor screen were inserted in an exposure cassette. After an appropriate exposure time (2 days for fibroblasts 2DE gel and 15 days for DU145 2DE gel) the images were acquired on a Cyclone Storage Phosphor Scanner (Perkin Elmer).

Densitometric analysis of radiolabeled protein spots

Scanned colloidal coomassie blue images and autoradiographic images relative to gels containing ^{14}C-radiolabeled proteins were analysed by the ImageMaster 2D Platinum software (GE Healthcare, USA). Only 10 protein spots present in all the replicates of both fibroblasts and DU145 gels were taken into consideration for subsequent analysis. The relative spot volume (V) was calculated as %V of the total volume of 10 selected spots in each gel, corresponding to ^{14}C-radiolabeled proteins. The normalized %V of the 10 spots on three replicate 2D gels was averaged and the standard deviation was calculated.

In-gel digestion and MALDI-TOF analysis

24 protein spots, corresponding to radiolabeled proteins transferred from CAFs to DU145 tumor cells, were manually excised from the 2DE gel in which were separated the proteins isolated from the cocultured DU145 cells. Samples were transferred to a 1.5-mL Eppendorf tube, washed, reduced, carbamidomethylated and treated with a trypsin solution (Trypsin Proteomics Sequencing Grade)

according a modified protocol from Shevchenko *et al* [628]. Briefly: protein spots were manually excised from gels, washed in 50 mM ammonium bicarbonate (NH_4HCO_3)/CH_3CN 1/1, de-hydrated in CH_3CN and dried. Prior to proteolytic digestion, cysteine residues in proteins were reduced in 10 mM DTT for 30 minutes at 56°C and then alkylated for 30 minutes in the dark with 55 mM iodoacetamide in 25 mM NH_4HCO_3. Gel particles were then washed, de-hydrated and dried. Each sample was finally incubated 1 hour at 37°C in 20 µL of 20 µg/ml trypsin solution (Trypsin Proteomics Sequencing Grade) in 40 mM NH_4HCO_3 with 10% CH_3CN. An additional 30 µL of 40 mM NH_4HCO_3 with 10% CH_3CN were added to each sample and incubated over night at 37°C. The reaction was stopped adding a final concentration of 0.1% trifluoroacetic acid. The supernatant was collected and the gel was further extracted with 0.1% trifluoracetic acid in 50% CH_3CN. The extracts were combined and then analysed on a MALDI-TOF/TOF mass spectrometer Ultraflex III (Bruker Daltonics, Bremen, Germany) by using Flex Control 3.0 as data acquisition software. A 0.75 µL volume of the sample was mixed to 0.75 µL of the matrix (saturated solution of α-cyano-4-hydroxycinnamic acid in 50% (v/v) CH_3CN and 0.5% (v/v) TFA) on the anchorchip target plate and allowed to dry. Spectra were acquired in reflectron mode over the m/z range 860-4000 for a total of 500 shots. The instrumental parameters were chosen by setting the ion source 1 at 25 kV, ion source 2 at 21.5 kV, the pulsed ion extraction at 20 ns and the detector gain at 7.7x. The instrument was externally calibrated prior to analysis using the Bruker Peptide Calibration standard kit. All the resulting mass lists were cleaned up from eventually present contaminant masses, such as those from matrix, autodigestion of trypsin and keratins. Mass fingerprinting searching was carried out in Swiss-Prot databases using MASCOT (Matrix Science Ltd., London, U.K., http://www.matrixscience.com) software. The taxonomy was restricted to *homo sapiens*, a mass tolerance of 50 ppm was allowed, and the number of accepted missed cleavage sites was set to one. Alkylation of cysteine by carbamidomethylation was assumed as fixed modification. The experimental mass values were monoisotopic. No restrictions on protein molecular weight and pI were applied. The criteria used to accept identifications included the extent of sequence coverage, number of matched peptides and probabilistic score sorted by the software.

Capillary-LC-μESI-MS/MS

Each peptide mixture was submitted to capillary-LC-μESI-MS/MS analysis on an Ultimate 3000 HPLC (Dionex, San Donato Milanese, Milano, Italy) coupled to a LTQ Orbitrap mass spectrometer (Thermo Fisher, Bremen, Germany).

Peptides were concentrated on a precolumn cartridge PepMap100 C18 (300 μm i.d. × 5 mm, 5 μm, 100Å, LC Packings Dionex) and then eluted on a homemade capillary column packed with Aeris Peptide XB-C18 phase (180 μm i.d. × 15 cm, 3.6 μm, 100Å, 1/min. The loading mobile (Phenomenex, Torrance, CA, USA) at 1 phases were: 0.1% TFA in H_2O (phase A) and 0.1% TFA in CH_3CN (phase B). The elution mobile phases composition was: H_2O 0.1% formic acid/CH_3CN 97/3 (phase A) and CH_3CN 0.1% formic acid/ H_2O 97/3 (phase B). The elution program was: 0 minute, 4% B; 10 minutes, 40% B; 30 minutes, 65% B; 35 minutes, 65% B; 36 minutes, 90% B; 40 minutes, 90% B; 41 minutes, 4%B; 60 minutes, 4% B. Mass spectra were acquired in positive ion mode, setting the spray voltage at 2 kV, the capillary voltage and temperature respectively at 45 V and 200°C, and the tube lens at 130 V. Data were acquired in data-dependent mode with dynamic exclusion enabled (repeat count 2, repeat duration 15 seconds, exclusion duration 30 seconds) survey MS scans were recorded in the Orbitrap analyzer in the mass range 300-2000 m/z at a 15,000 nominal resolution at m/z = 400; then up to three most intense ions in each full MS scan were fragmented (isolation width 3 m/z, normalized collision energy 30) and analyzed in the IT analyzer. Monocharged ions did not trigger MS/MS experiments. The acquired data were searched with Mascot 2.4 search engine (Matrix Science Ltd., London, UK) against the SwissProt database. The taxonomy was restricted to *homo sapiens*. The experimental mass values were monoisotopic. Searches were performed allowing: (i) up to one missed cleavage sites, (ii) 10 ppm of tolerance for the monoisotopic precursor ion and 0.8 mass units for monoisotopic fragment ions, (iii) carbamidomethylation of cysteine as fixed modification and oxidation of methionine as variable modification. The criteria used to accept identifications included the extent of sequence coverage, number of matched peptides and probabilistic score sorted by the software.

Cluster Analysis

The identified proteins were subjected to functional pathway analysis using DAVID database (http://david.abcc.ncifcrf.gov/home.jsp) for better understanding their biological context and hypothesize in which physiological processes they may be involved. UniProt accession numbers of the radiolabeled proteins transferred from CAFs to DU145 tumor cells identified in our study were uploaded and mapped

against the *homo sapiens* data set to extract and summarize functional annotation associated with individual or group of genes/proteins and to identify gene ontology terms, molecular function, biological process and important pathways for the dataset.

Small interfering RNA (siRNA) Transfection

siRNA transfection was performed with Lipofectamine and Opti-MEM to knock-down CA IX gene expression. CA IX siRNA is a pool of three target-specific 19-25 nt siRNAs; a scrambled siRNA was used as control. The cells were used for the experiments the day after the transfection.

Xenograft experiments

In vivo experiments were performed co-injecting PC3 and fibroblasts knocked down for CA IX gene or non-silenced fibroblasts in 6 to 8 week old male severe combined immunodeficient (SCID)-bg/bg mice (Charles River Laboratories International). Six animals were used *per* group, which were daily monitored. The tumor size was measured every two or three days by a caliper and the tumor volumes were determined by measuring the length (L) and the width (W) of the tumor and calculating the volume ($V=LW^2/2$). Animals experiments were conducted in accordance with national guidelines and approved by the ethical committee of *Animal Welfare Office of Italian Work Ministry* and conform to the legal mandates and Italian guidelines for the care and maintenance of laboratory animals.

THE EFFECT OF CA IX CATALYSIS PRODUCTS WITHIN TUMOR MICROENVIRONMENT

AIM OF THE STUDY

The microenvironment of solid tumors is a very complex tissue composed by both cellular and non-cellular components. The major cellular elements include fibroblasts, endothelial and immune cells, which exhibit an altered phenotype induced by cancer cells able to form a permissive and supportive environment for tumor progression [629-631]. In fact, these cells produce a range of molecules representing the non-cellular components that modify tumor stroma, *i.e.* ECM proteins, proteases, cytokines and growth factors. In particular, many ways in which activated fibroblasts of tumor stroma, known as CAFs [82], support tumor progression has been described: by secreting growth factors (HGF, EGF, b-FGF) and cytokines (SDF-1 and IL-6) leading to the infiltration of immune cells, which, in turns promote *de novo* angiogenesis helping metastatic spread [150]; by remodeling ECM and thus influencing proliferation, survival and migration of cancer cells [127]; by producing and secreting lactate that is then metabolized by oxygenated tumor cells [632].

In addition to this unusual composition and behavior of tumor stroma, other characteristics that distinguish the tumor microenvironment from the corresponding normal tissue are: high interstitial fluid pressure, low O_2 tension and low pHe. These alterations are due to a perturbation of the balance between pro- and anti-angiogenic factors (process known as “angiogenic switch”), which leads to the formation of disorganized vasculature with structural and functional abnormalities [633], and thus to a reduced perfusion [212]. Other important factors responsible for tumor hypoxia and acidity are the high metabolic rate of tumor cells, which leads to a massive production of acidic metabolites [254, 259, 260, 275, 320, 339], and the increased diffusion distances between microvessels and tumor cells as result of tumor mass expansion [211]. The hypoxic environment contributes to the metabolic shift of cancer cells metabolism towards glycolysis, with the additional release of lactic acid in the extracellular milieu [326]. The high protons concentration, instead, poses a stress on the cells in that the extracellular acidification can ultimately lead to a decrease in pHi. In this condition the control of pHi, necessary for cells survival [263], is mediated by different types of pHi regulating proteins such as: NHE1, AEs, NBCs, MCTs and CAs [336].

The mammalian CA family contains 16 different isoforms, 13 of which are enzymatically active. Their main function is the catalysis of the reversible hydration of carbon dioxide to bicarbonate and protons ($CO_2 + H_2O \leftrightarrow HCO_3^- + H^+$). Among them, CA IX is a membrane-bound isoform with the catalytic domain located extracellularly and thus is one of the most important proteins involved in tumor extracellular acidification. CA IX is overexpressed in hypoxic conditions (a very common characteristic in fast growing solid tumors) under tight regulation by HIF-1 and is associated with cancer progression and poor prognosis [634, 635].

The aim of our study was to investigate proliferation and migration of cancer cells in the tumor microenvironment context, in particular by analyzing the effect of stromal CA IX catalysis products in the modulation of these phenotypes. Our experimental model is based on prostatic tumor cells (DU145 and PC3) and prostatic primary fibroblasts (HPFs) that, following activation by cancer cells, acquire the typical CAFs phenotype [121].

RESULTS

Cancer cells proliferation within tumor microenvironment

First, we found that tumor cells kept in hypoxia acidify the extracellular medium more than normoxic cells *(Figure 1A-C)* and that, in coculture, the protons release in the extracellular medium is greater than the sum of single culture cell proton release *(Figure 1B-D)*. This suggests that the interplay between cancer and stromal cells affects important changes in normal and/or in tumor cells metabolism leading to an "extra" acidification of the medium.

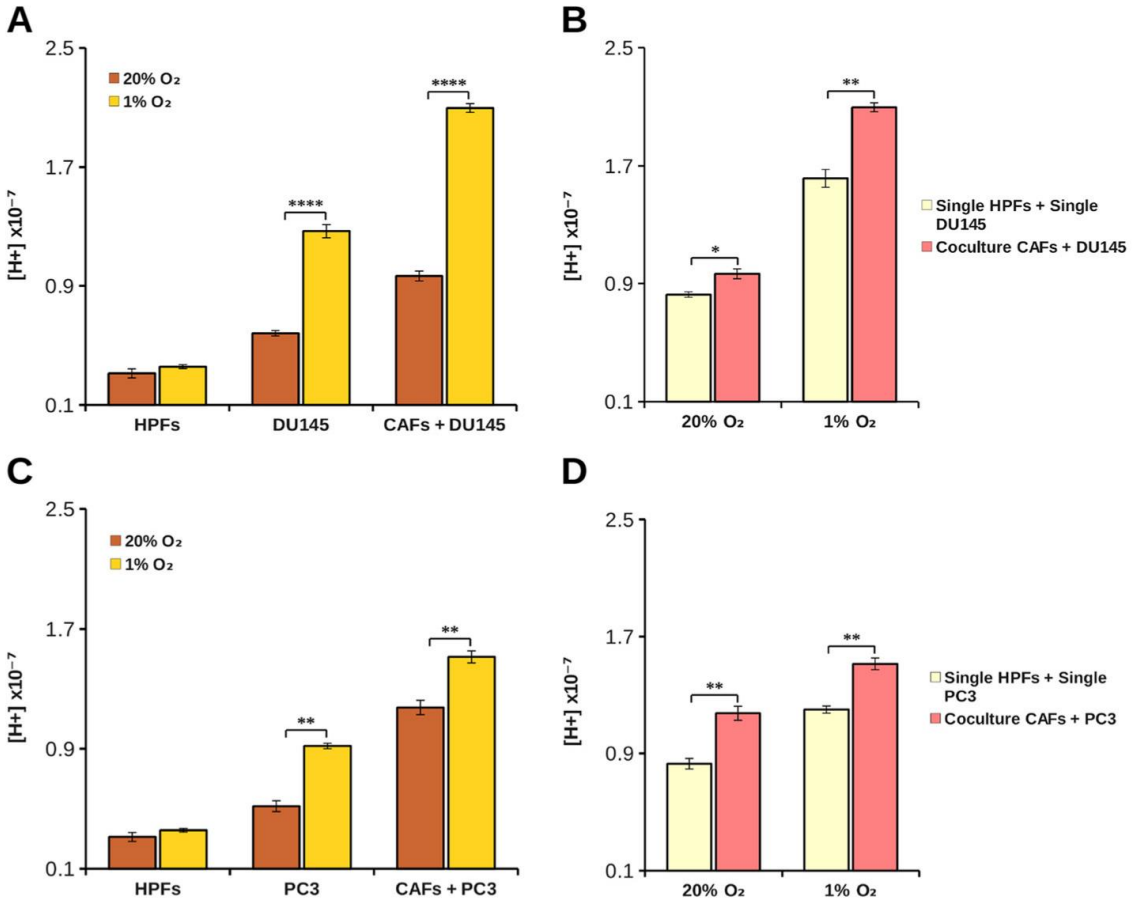

Figure 1. Effect of hypoxia and coculture on pHe. *Tumor and stromal cells were plated in single culture ($2x10^5$ for each cell type) and in coculture (10^5 DU145 or PC3 and 10^5 fibroblasts) at 37°C in unbuffered DME medium containing 1 mM bicarbonate in CO_2 free atmosphere either at 1% O_2 or 20% O_2. Results show protons concentration values measured in DU145 single and coculture* ***(A-B)*** *and in PC3 single and coculture* ***(C-D)*** *after 24 hours calculated as a means ± SD from five independent experiments (*, $p < 0.1$; **, $p < 0.05$; ****, $p < 0.005$).*

In order to evaluate the ability of CAFs to contribute to tumor growth at physiological (7.4) as well as acidic (6.8) or basic (8.0) pH, DU145 and PC3 were plated and grown for 40 hours in single or in coculture with CAFs at various pHe, using CFDA-SE cytofluorymetric assay to measure cell proliferation rate of a given

population in coculture conditions (see Methods). We found that single culture cell proliferation rate of both DU145 and PC3 was significantly decreased at acidic pHe *(Figure 2A-B)*, without notable presence of cell death in the pHe range considered *(Table I)*. In the presence of CAFs, tumor cells proliferation increases at every pHe value compared to the corresponding single culture *(Figure 2A-B)*. However, in coculture, CAFs attenuate the growth inhibition observed in single culture at pH 7.4 compared to pH 8.0, but the negative effect of the lowest pH 6.8 is only partially offset.

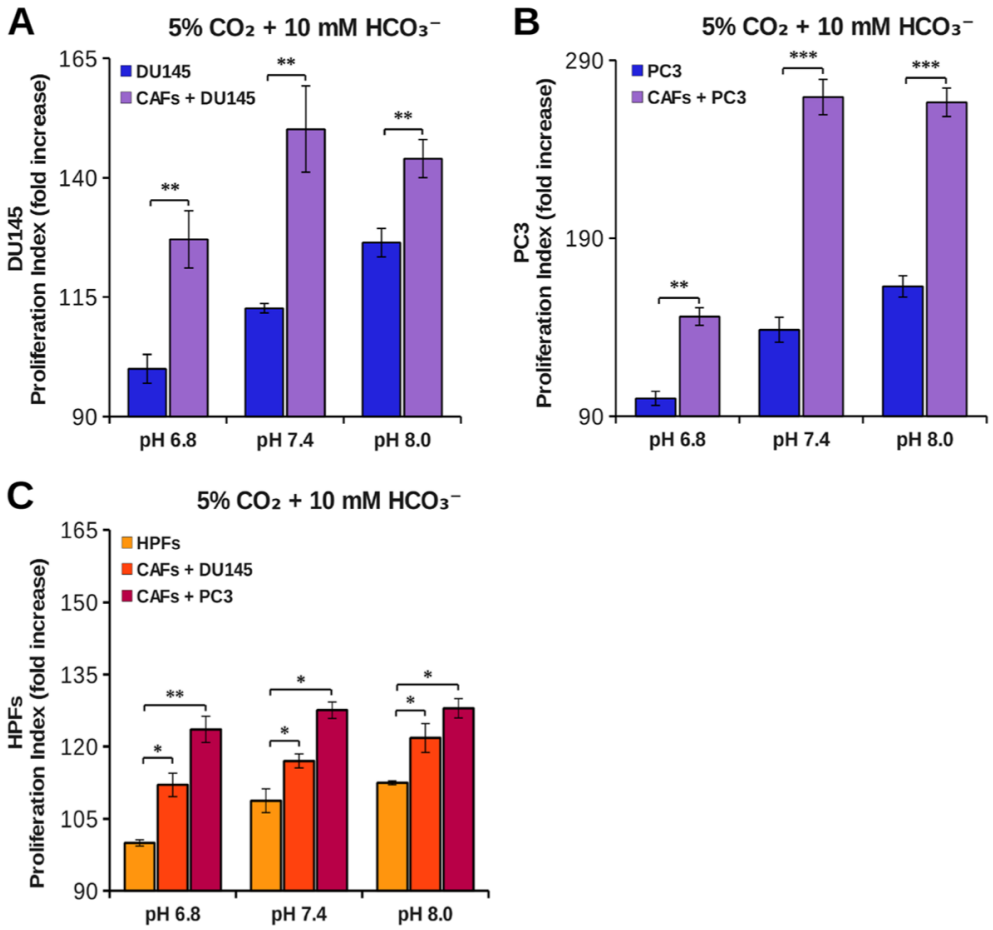

Figure 2. Effect of acidity on tumor cells growth. *DU145* ***(A)****, PC3* ***(B)*** *and HPFs* ***(C)*** *were labeled with CFDA-SE and then plated in single culture and in coculture. The cells were grown at various pHe in DME supplemented with 25 mM hepes and 10 mM bicarbonate at 37°C and 5% CO_2. After 40 hours cells were detached and analyzed by flow cytometry. The data show the fold increase of proliferation index calculated on an average of five experiments (*, $p < 0.1$; **, $p < 0.05$; ***, $p < 0.01$).*

In addition, the CAFs proliferation rate is significantly greater compared to HPFs one *(Figure 2C)*, although the difference is less extensive respect to the reciprocal effect of fibroblasts on cancer cells *(Figure 2A-B)*, suggesting that the interplay between cancer cells and fibroblasts is mainly devoted to promote tumor cells proliferation.

Table I. Cell death analysis of DU145 and PC3 cells.

DU145			
	Early Apoptosis (%)	Late Apoptosis (%)	Necrosis (%)
DMEM pH 8.0	4.3 ± 0.5	0.95 ± 0.1	0.65 ± 0.07
DME pH6.8	4.5 ± 1	0.5 ± 0.14	0.24 ± 0.05
DME pH 7.4	6.1 ± 0.9	1.2 ± 0.2	0.59 ± 0.05
DME pH 8.0	5.3 ± 0.7	1.6 ± 0.6	0.97 ± 0.1
PC3			
	Early Apoptosis (%)	Late Apoptosis (%)	Necrosis (%)
DMEM pH 8.0	3.5 ± 1	0.2 ± 0.09	0.53 ± 0.05
DME pH6.8	4.5 ± 1.4	0.3 ± 0.1	0.65 ± 0.04
DME pH 7.4	4.7 ± 1.4	0.9 ±0.3	2.4 ± 1
DME pH 8.0	4.3 ± 2	1 ± 0.4	2 ± 1

Tumor cells were were grown in DMEM (pH 8.0) and at various pHe in DME supplemented with 25 mM hepes and 10 mM bicarbonate at 37°C and 5% CO_2. After 40 hours cell death determination was performed by staining cells with Annexin-V-Fluos and flow cytometry analysis.

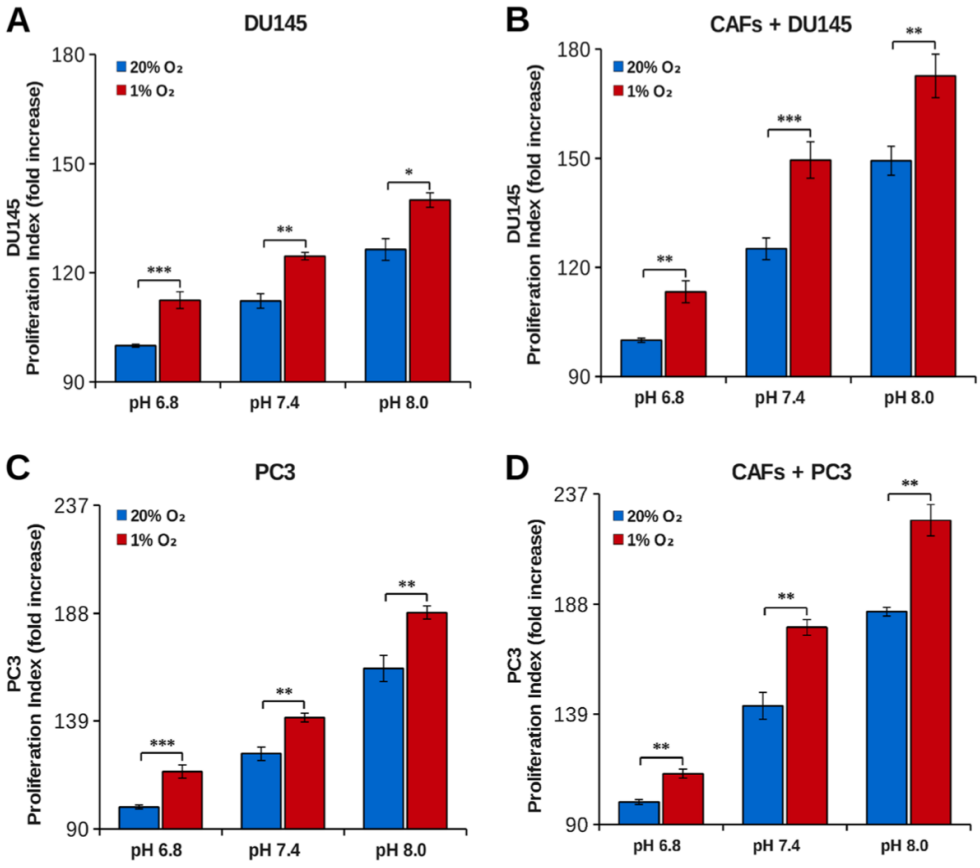

Figure 3. Effect of acidity on tumor cells growth in hypoxic condition. *DU145* ***(A-B)*** *or PC3* ***(C-D)*** *cells were labeled with CFDA-SE and then plated in single culture and in coculture with fibroblasts in a 1:2 ratio at 1% O_2 and at 20% O_2. The cells were grown at various pHe in DME supplemented with 25 mM hepes and 10 mM bicarbonate at 37°C and 5% CO_2. After 40 hours the cells were detached and analyzed by flow cytometry. The data show the proliferation index calculated on an average of six experiments (*, $p < 0.1$; **, $p < 0.05$; ***, $p < 0.01$).*

In order to assess the effect of extracellular acidity in environmental conditions more similar to *in vivo* condition, we compared the growth rate of both PC3 and DU145 cells kept at 1% O_2 at various pHe. Our results show that hypoxic conditions induce a significant increase in tumor cells growth rate compared to tumors kept at 20% O_2 *(Figure 3A-C)*. Nevertheless, in hypoxia we observed a pH dependence cell growth similar to the normoxic conditions, and the same, strong, pro-proliferative effect exerted by CAFs on cancer cells proliferation *(Figure 3B-D)*.

Bicarbonate ion contributes to cancer cells proliferation

The bicarbonate buffering system is essential to ensure the homeostasis of both pHi and pHe. The CO_2 reversible hydration is catalyzed by both intra- and extracellular CAs. In particular, extracellular CAs are involved in extracellular acidification as well as in bicarbonate production. As shown in *Figures 2* and *3*, a high concentration of H^+ ions has negative effects on cancer cells proliferation. Thus, we investigated the possible involvement of the other product of CO_2 hydration, *i.e.* bicarbonate, in tumor cells growth.

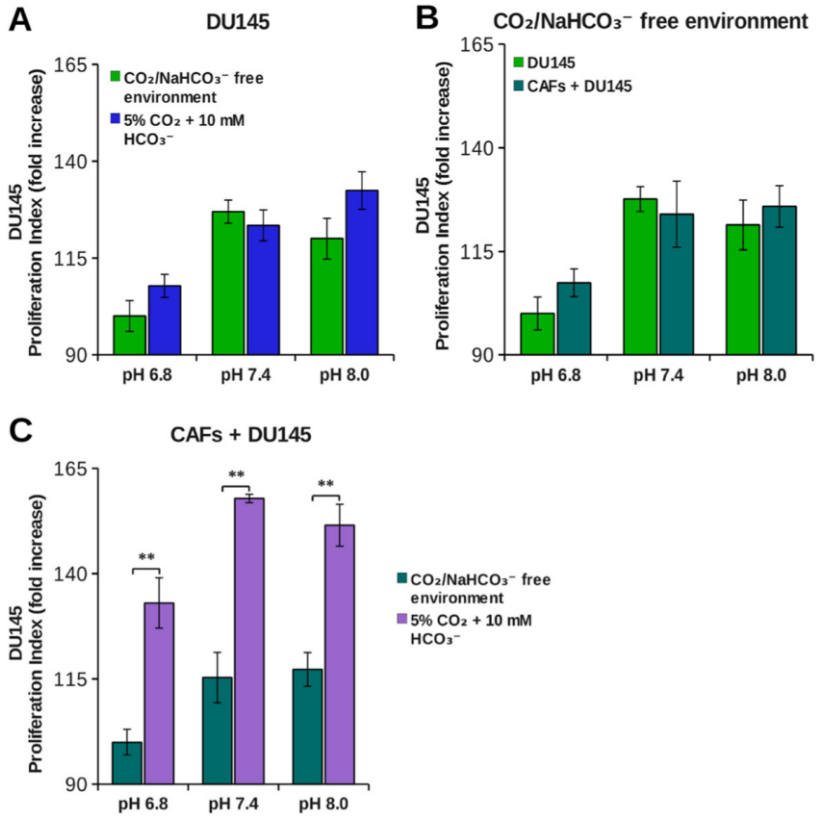

Figure 4. Effect of bicarbonate on DU145 tumor cells growth. *DU145 were labeled with CFDA-SE and then plated in single culture* ***(A)****, in coculture with fibroblasts in a 1:2 ratio* ***(C)*** *or both* ***(B)****. The cells were grown at various pHe in DME supplemented either with 25 mM hepes and 10 mM bicarbonate at 37°C and 5% CO_2 or in DME supplemented only with 25 mM hepes at 37°C in CO_2/bicarbonate free environment. After 40 hours cells were detached and analyzed by flow cytometry. The data show the proliferation index calculated on an average of four experiments (**, $p < 0.05$).*

Therefore we compared the growth rate of tumor cells at 5% CO_2 (which corresponds to CO_2 pressure present in peripheral tissues) in bicarbonate buffer, with that kept in CO_2-free environment (*i.e.* at atmospheric CO_2 concentration, 0.032% CO_2). Our results show that in single cultures the proliferation index of tumor cells (DU145 and PC3) is similar in both conditions, therefore bicarbonate does not influence cells growth rate *(Figures 4A-5A)*.

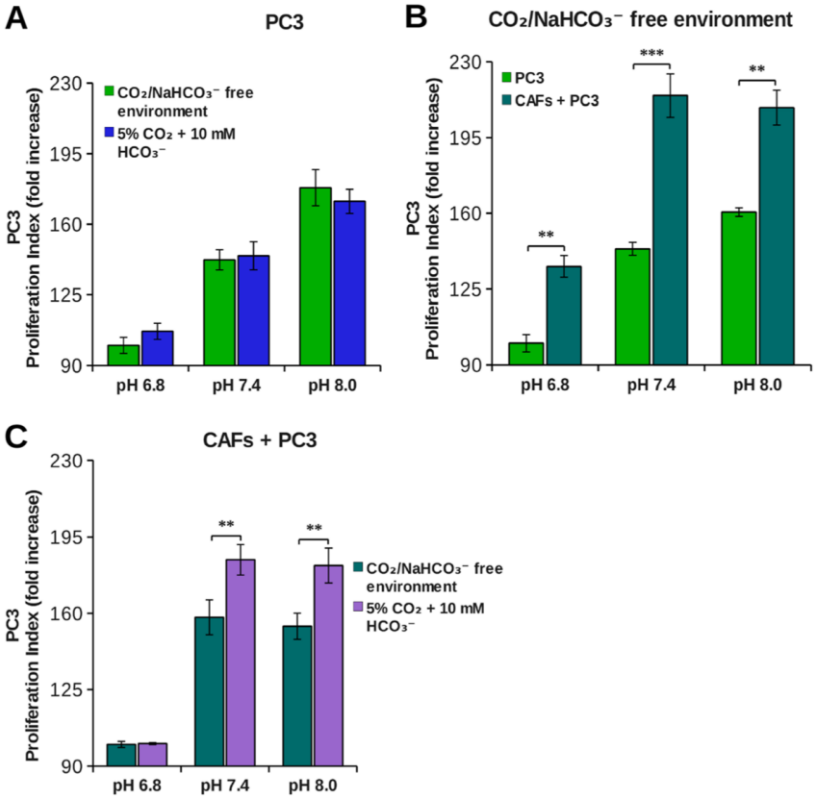

Figure 5. Effect of bicarbonate on PC3 tumor cells growth. *PC3 were labeled with CFDA-SE and then plated in single culture* ***(A)****, in coculture with fibroblasts in a 1:2 ratio* ***(C)*** *or both* ***(B)****. The cells were grown at various pHe in DME supplemented either with 25 mM hepes and 10 mM bicarbonate at 37°C and 5% CO_2 or in DME supplemented only with 25 mM hepes at 37°C in CO_2/bicarbonate free environment. After 40 hours cells were detached and analyzed by flow cytometry. The data show the proliferation index calculated on an average of four experiments (**, $p < 0.05$; ***, $p < 0.01$).*

In cocultures, instead, we found a different behavior in the two tumor cell lines. For DU145, we did not observe any difference in growth rate between single culture and coculture in CO_2-free environment *(Figure 4B)*, while CAFs exerted a powerful pro-proliferative effect in the presence of 5% CO_2 /bicarbonate buffer *(Figure 4C)*. In this condition about 90% of the increase in growth rate in the presence of CAFs is due to the presence of bicarbonate for each pHe value considered *(Table II)*. For PC3 cells, instead, the increase in growth rate due to the presence of CAFs occurs partly also in CO_2-free environment *(Figure 5B)*, bicarbonate being responsible only for about 30% of the overall growth rate increase in coculture *(Figure 5C and Table II)*.

Table II. Relative contribution of bicarbonate to DU145 and PC3 growth rate increase in coculture.

Relative contribution of bicarbonate in *DU145* growth rate increase in coculture (%)	
	5% CO_2 + 10 mM HCO_3^-
pH 6.8	82%
pH 7.4	100%
pH 8.0	89%
Relative contribution of bicarbonate in *PC3* growth rate increase in coculture (%)	
	5% CO_2 + 10 mM HCO_3^-
pH 6.8	1%
pH 7.4	25%
pH 8.0	38%

The relative contribution of CO_2/bicarbonate was calculated taking into account the relative DU145 and PC3 growth rate increase in the presence or in the absence of CO_2/bicarbonate in the same conditions.

Hence, whereas CAFs contribution to DU145 proliferation is essentially due to bicarbonate, PC3 cells largely depend on CAFs for their cell growth, but bicarbonate is not the main factor that contributes to this effect. In order to gain information on the use of bicarbonate by cancer cells we performed experiments with ^{14}C-bicarbonate that demonstrate the time-dependent organication of bicarbonate *(Figure 6)*. In addition, by using ^{13}C-bicarbonate and GC-MS, we found an increased steady state of DU145 intracellular ^{13}C-fumarate and ^{13}C-malate isotopes when they are grown in coculture with CAFs compared to single DU145 culture *(Table III)*. This evidence indicates an increase in the bicarbonate organication flux in highly proliferative conditions.

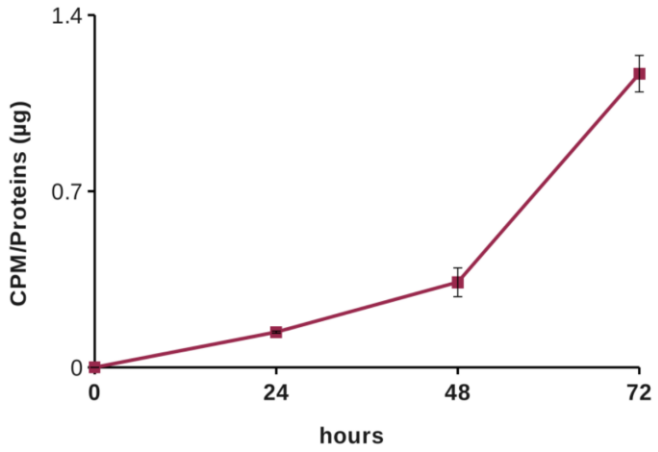

Figure 6. Bicarbonate organication. *DU145 were cultured in DME supplemented with 25 mM hepes, 10 mM sodium bicarbonate, 20 µM sodium bicarbonate [^{14}C] and 10% FBS at pH 8.0 for 24, 48 and 72 hours. The data show the CPM (counts per minute) value normalized on protein concentration of each sample, calculated on an average of three experiments.*

Table III. Isotopic analysis by GC-MS.

	$^{13}C/^{12}C$ (%)		
	DU145	DU145 after coculture	
MALATE	35.068 ± 0.518	36.341 ± 0.619	$p < 0.05$
FUMARATE	24.504 ± 0.239	25.258 ± 0.317	$p < 0.05$

Isotopic $^{13}C/^{12}C$ ratio of malate and fumarate extracted from DU145 single culture and from DU145 cells separated after being cocultured 40 hours with CAFs. Statistical analysis was performed on the basis of three independent experiments.

The role of stromal cells CA IX in promoting cancer cells growth

DU145 cells growth was significantly fostered in coculture condition exclusively in presence of bicarbonate/CO_2 buffering system, hence we determined the expression level of CA IX, the main responsible for extracellular bicarbonate production, in DU145 and in fibroblasts in single culture and after 40 hours of coculture at 1% and 20% O_2 followed by MACS separation of the two cellular populations.

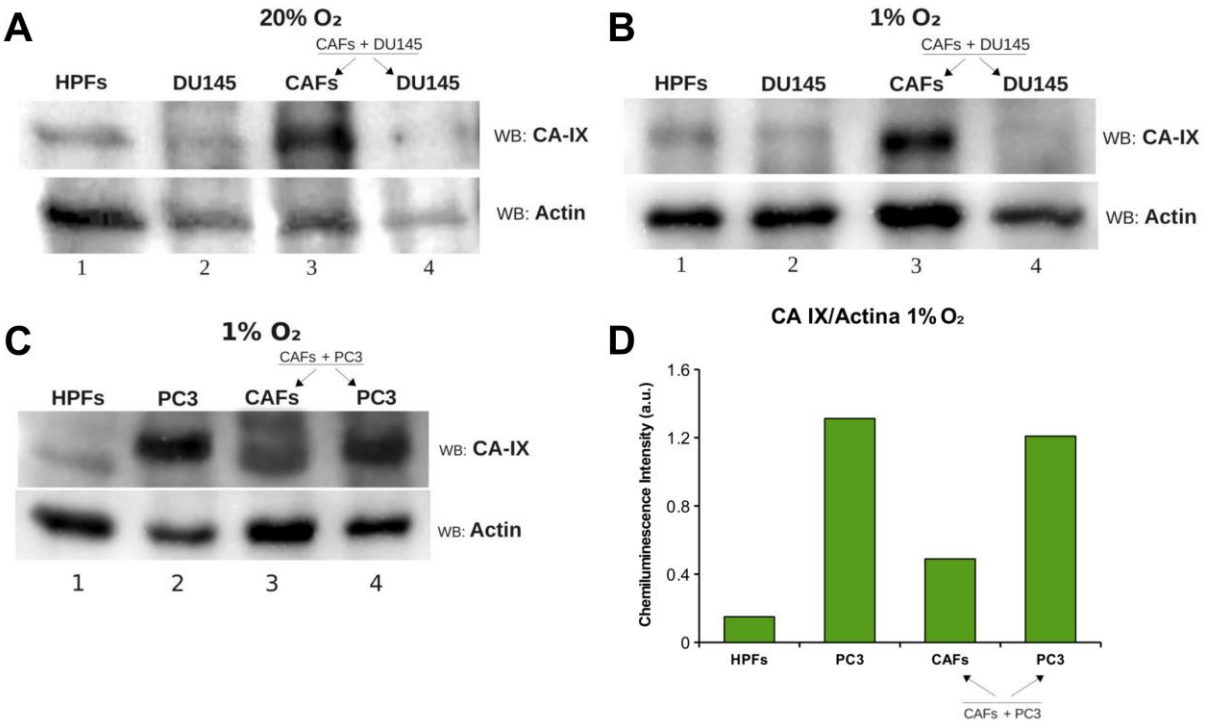

Figure 7. Analysis of CA IX expression in single culture and in coculture. *DU145 and fibroblasts were plated in single culture and in coculture in a 1:2 ratio for 40 hours at 20% O_2* ***(A)*** *and 1% O_2* ***(B)****. Similarly, PC3 and fibroblasts were plated in single culture and in coculture in a 1:2 ratio for 40 hours at 1% O_2* ***(C)****. After that, the cocultures were detached and separated by MACS Column Technology. The samples were lysed in Laemmli electrophoresis buffer and used for Western blot analysis. The membranes were treated with anti-CA IX and anti-actin antibodies. Lanes 1 and 2: HPFs and DU145 or PC3 in single culture. Lanes 3 and 4: CAFs and DU145 or PC3 after coculture and separation. The graph shows spots quantification* ***(D)****.*

We observed that CA IX expression in single culture is low both at 1% O_2 and 20% O_2, while it greatly increases only in CAFs after 40 hours of coculture with DU145 at both O_2 tensions *(Figure 7A-B)*. PC3 were less dependent on bicarbonate for their growth in coculture *(Figure 5C and Table I)*, accordingly we observed a reduced induction of stromal CA IX expression due to PC3 presence *(Figure 7C-D)* compared to that observed after activation of fibroblasts with DU145 *(Figure 7A-B)*.

In order to assess the role of CAFs CA IX in promoting cancer cells growth, we silenced stromal CA IX and measured DU145 growth rate in coculture conditions. Our results *(Figure 8A-B)* show that CAFs knocked down for CA IX are far less able to support cancer cells proliferation respect to non-silenced counterpart. In fact, the growth rate of DU145 in presence of CAFs knocked down for CA IX decreases both at 1% O_2 and at 20% O_2 and gets close to that of the single culture.

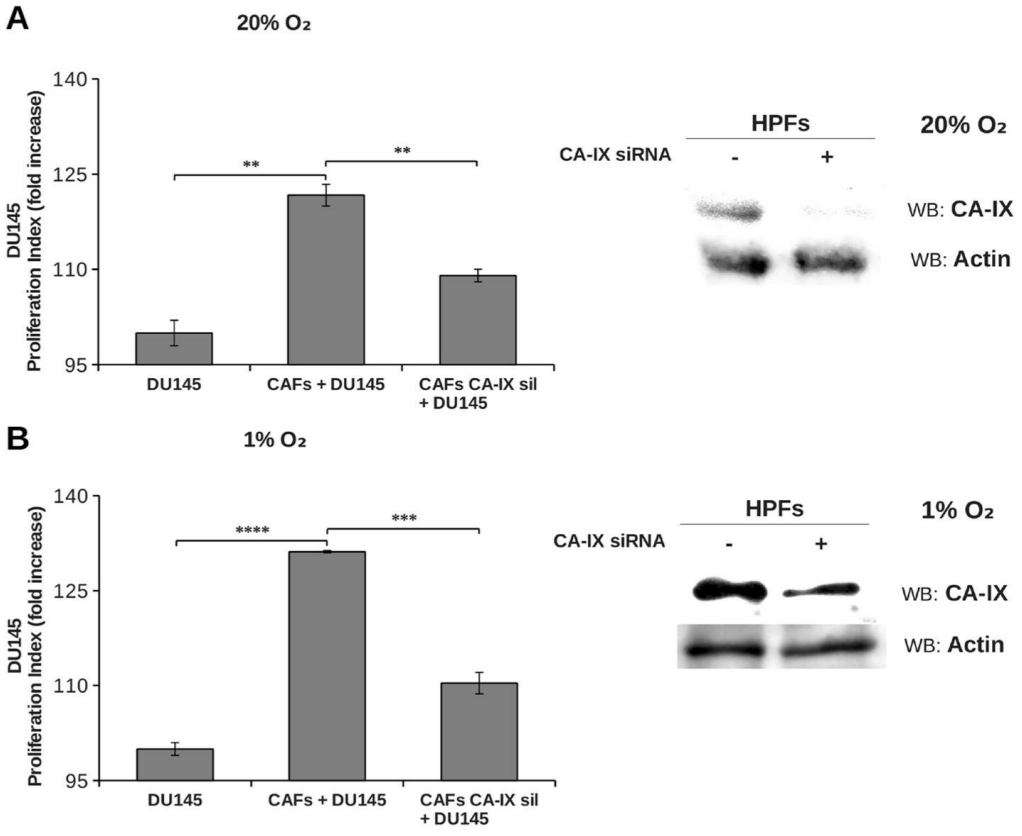

Figure 8. Effect of fibroblasts CA IX down-regulation on tumor cells proliferation. *DU145 were labeled with CFDA-SE and then plated in single culture and in coculture with fibroblasts knocked down for CA IX gene or non-silenced, in a 1:2 ratio at 20% O_2* ***(A)*** *and 1% O_2* ***(B)****. After 40 hours cells were detached and analyzed by flow cytometry. The data show the proliferation index calculated on an average of four experiments (**, $p < 0.05$, ***, $p < 0.01$; ****, $p < 0.005$). Western blot images show the analysis of CA IX expression in non-silenced or knocked down fibroblasts at 20% O_2* ***(A)*** *and 1% O_2* ***(B)****.*

Further, to assess the role of stromal CA IX in promoting *in vivo* tumor growth, we co-injected PC3 cells and CAFs (1:5 ratio) in the lateral flanks of SCID-bg/bg mice and we observed that fibroblasts knock-down for CA IX are less able to sustain tumor mass growth compared to control experiment with non-silenced fibroblasts *(Figure 9)*. Linear regression fitting on these data shows that tumor volume growth rate is about three times lower in presence of CAFs defective for CA IX expression compared to wild type ones.

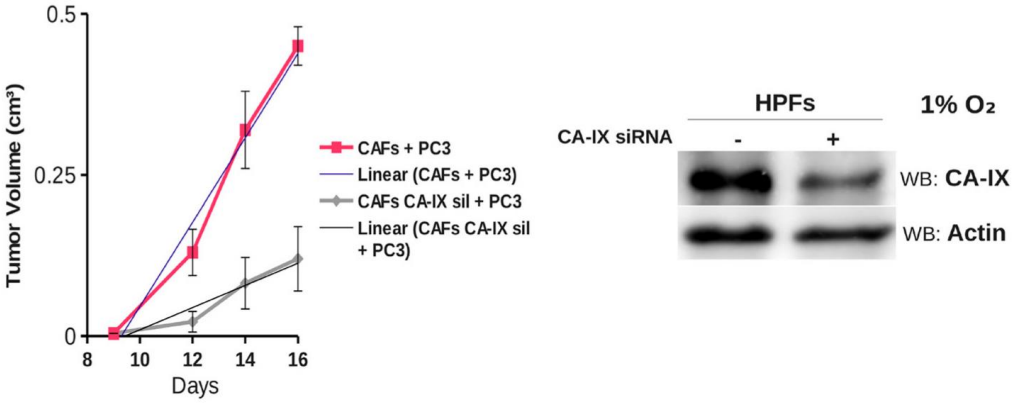

Figure 9. Silencing of CA IX in fibroblasts decreases tumor growth rate. *Xenograft growth in SCID bg/bg mice of wild-type (control) or CA IX-silenced CAFs injected s.c. with PC3 cells (CAFs:PC3 cells ratio 1:5). CA IX silencing by RNA interference in fibroblasts is shown (Timepoint 14 days: ***, $p < 0.01$; timepoint 16 days: ****, $p < 0.005$). Linear regression equation of "CAFs + PC3": $y=0.08065$ (± 0.01035) $x–0.82478$ (± 0.14473), $R^2=0.9676$; linear regression equation of "CAFs CA IX sil + PC3": $y=0.023219$ (± 0.003469) $x–0.249096$ (± 0.051038), $R^2=0.9563$.*

Cancer cells migration within tumor microenvironment

In order to evaluate the role of stromal CA IX in the modulation of cancer cells motility, PC3-GFP were plated in single culture or in coculture with CAFs silenced or not for CA IX *(Figure 10)*. The fluorescent migrated PC3 were observed by fluorescence microscopy. We found that CAFs increase PC3 motility and part of this effect is mediated by stromal CA IX expression. In fact, CAFs knocked down for CA IX are far less able to promote cancer cells migration with respect to non-silenced counterpart. Therefore, in coculture with CA IX-silenced fibroblasts, the number of migrating PC3 cells decrease and becomes similar to that of single culture *(Figure 10)*. This result reveal a correlation between stromal CA IX and migration of tumor cells, thus we analyzed the effect of CA IX catalysis products, protons and bicarbonate, in the regulation of tumor cells migratory phenotype. First, we investigated the effect of high protons concentration on cancer cells migration. In this regard, we evaluated migratory capacity of tumor cells at acidic (6.8) and basic pH (8.0). Remarkably, single culture cell migration capability of both PC3 *(Figure*

11) and DU145 *(Figure 12)* is greater at basic rather than at acidic pH, without notable presence of cell death in the pHe range considered *(Table I)*. In particular, real-time monitoring of PC3 migration shows that the number of migrated cells is quantitatively higher at basic rather than at acid pH *(Figure 11)*. Similarly, wound healing test performed with DU145 cell line shows that, although both pHe value lead to the acquisition of the migratory phenotype with an elongated shape, after 18 hours at pH 8.0 cells repaired the wound, instead, at pH 6.8 this action did not occur *(Figure 12)*.

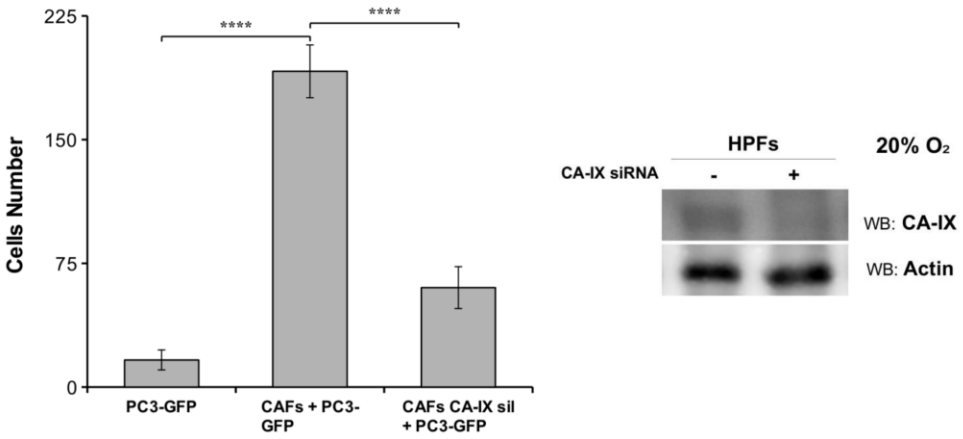

Figure 10. Effect of fibroblasts CA IX down-regulation on PC3 migration. *PC3-GFP were plated in the upper chamber in serum-free medium, while medium supplemented with 10% FBS was placed in the well below. Migration assay was performed in single culture and in coculture with fibroblasts knocked down for CA IX gene or non-silenced, in a 1:1 ratio. After 18 hours PC3-GFP migrated through the pores, to the other side of the membrane were observed by fluorescence microscopy and counted. The data show the number of migrated cells calculated on an average of three independent experiments (****, $p < 0.005$). Western blot image show the analysis of CA IX expression in non-silenced or knocked down fibroblasts.*

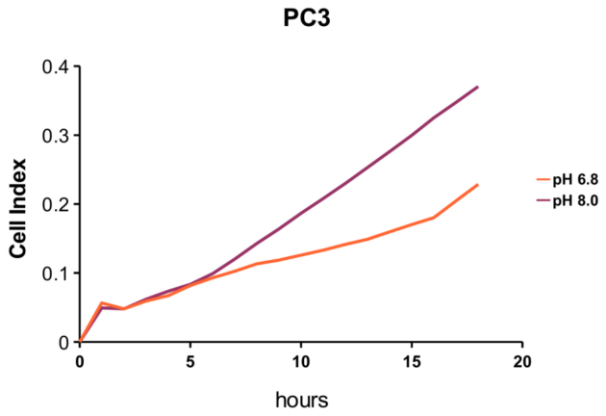

Figure 11. Effect of acidity on PC3 migration. *PC3 were plated in the upper chamber at pH 6.8 and pH 8.0 in serum-free DME supplemented either with 25 mM hepes and 10 mM bicarbonate at 37°C and 5% CO_2, while media at the same pHe supplemented with 10% FBS were placed in the well below. PC3 migration was monitored by xCELLigence Real-Time Cell Analyzer (RTCA) DP instrument.*

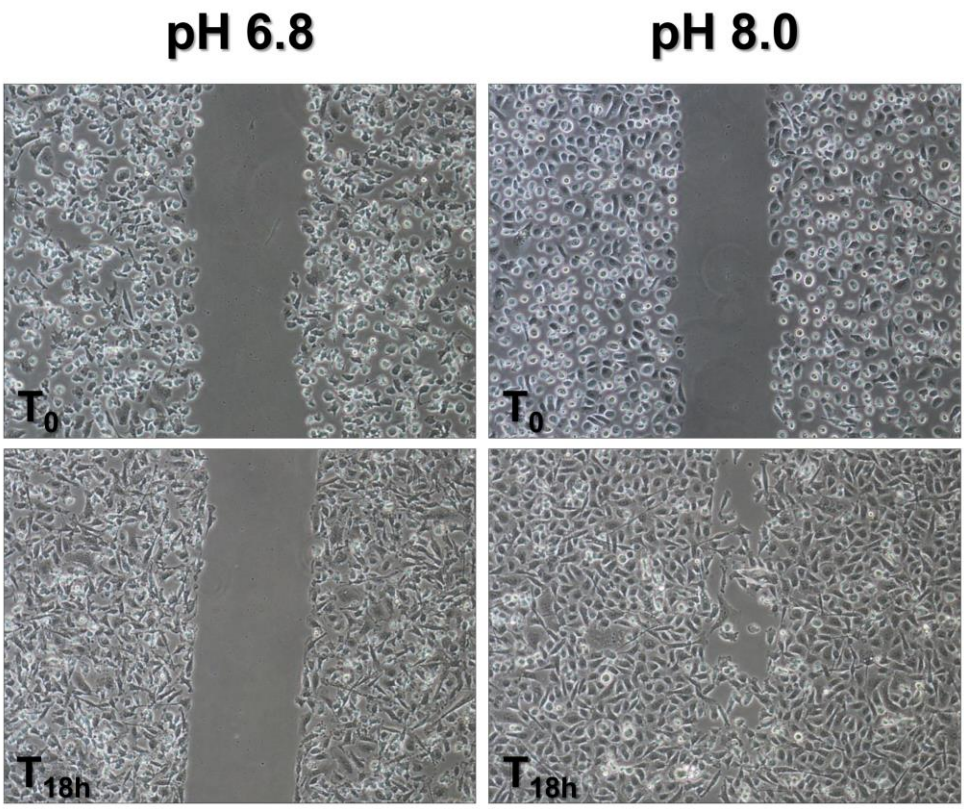

Figure 12. Effect of acidity on DU145 migration. *Confluent monolayers of DU145 cells were starved overnight with DME at pH 6.8 and pH 8.0 supplemented either with 25 mM hepes and 10 mM bicarbonate at 37°C and 5% CO_2. After that they were wounded and allowed to migrate. The wound was photographed at start and after 18 hours.*

In order to evaluate the ability of CAFs to support PC3 motility at acidic as well as at physiological (7.4) or basic pH, PC3-GFP were plated in single culture and in coculture with CAFs. We found that CAFs enhance PC3 migration rate compared to the corresponding single cultures *(Figure 13)*. However, the CAFs-mediated increase of PC3 migratory capacity at pH 7.4 and pH 8.0 is considerably higher than that observed at pH 6.8. Therefore, we observed a pH dependence cell migration both in single culture and in coculture. In both conditions, the acidity of the extracellular environment represents a disadvantageous element for the migration process.

Next, we investigated the possible involvement of bicarbonate (*i.e.* the other product of CO_2 hydration) in tumor cells migration. For this experiment, we compared PC3 migration capability at 5% CO_2 in bicarbonate buffer, with that of cells kept in CO_2-free environment. Our results show that single culture PC3 motility is similar in both conditions *(Figure 14)*. Also the migration rate of PC3 cocultured with CAFs increase in the same extent in CO_2-free environment and in CO_2/bicarbonate buffer, suggesting that bicarbonate produced by stromal CA IX is not involved in the regulation of cell migration *(Figure 14)*.

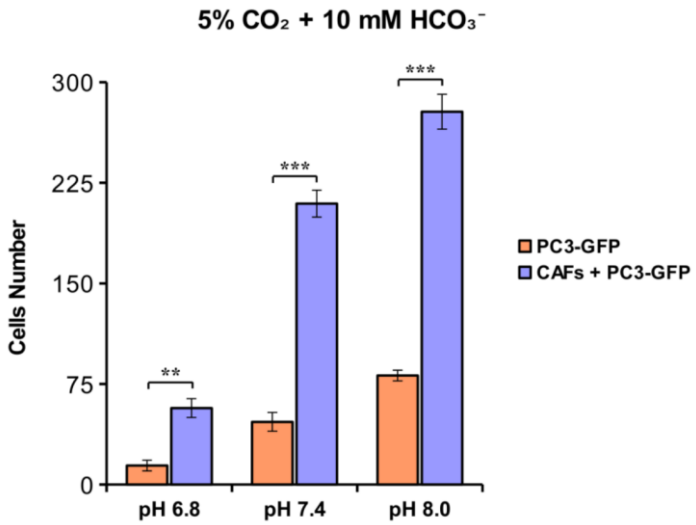

Figure 13. Effect of acidity on PC3 migration in single culture and coculture conditions. *PC3-GFP were plated in the upper chamber at various pHe in serum-free DME supplemented either with 25 mM hepes and 10 mM bicarbonate at 37°C and 5% CO_2; while media at the same pHe supplemented with 10% FBS were placed in the well below. Migration assay was performed both in single culture and in coculture with fibroblasts in 1:1 ratio. After 18 hours PC3-GFP cells migrated through the pores to the other side of the membrane were observed by fluorescence microscopy and counted. The data show the number of migrated cells calculated on an average of three independent experiments (**, $p < 0.05$; ***, $p < 0.01$).*

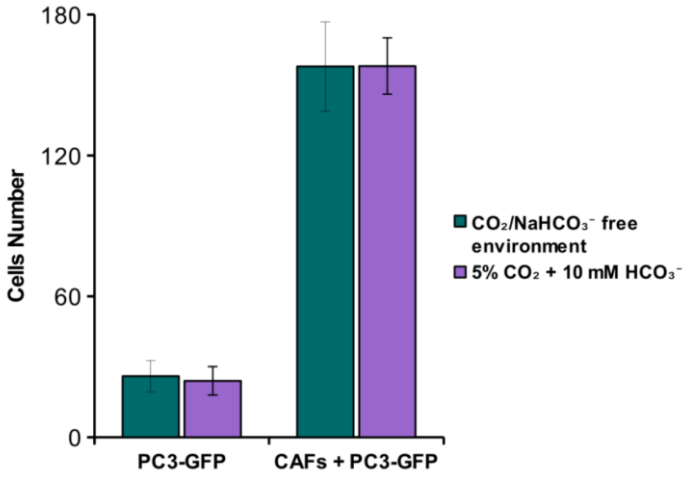

Figure 14. Effect of bicarbonate on PC3 migration. *PC3-GFP were plated in the upper chamber at pH 7.4 in serum-free DME supplemented either with 25 mM hepes and 10 mM bicarbonate at 37°C and 5% CO_2 or in DME supplemented only with 25 mM hepes at 37°C in CO_2/bicarbonate free environment; while medium at the same pHe supplemented with 10% FBS was placed in the well below. Migration assay was performed both in single culture and in coculture with fibroblasts in 1:1 ratio. After 18 hours PC3-GFP cells migrated through the pores to the other side of the membrane were observed by fluorescence microscopy and counted. The data show the number of migrated cells calculated on an average of three independent experiments.*

DISCUSSION

Solid tumors are composed of both highly genetically heterogeneous cancer cells and by numerous kinds of non transformed cells composing the so called tumor microenvironment. The main cellular component of tumor stroma is represented by an activated form of fibroblasts called CAFs. CAFs are widely recognized as key players in cancer progression [82, 636] mainly by sustaining tumor cells survival, proliferation and metastasis. According with these evidences, the emerging idea is that the possibility to counteract tumor progression depends on our understanding of cancer tissue physiology intended as a whole and not simply focusing on cancer cells behavior outside their physiological condition.

In this study we investigated the functional cooperation established between CAFs and tumor cells in the context of the tumor microenvironment, in particular by analyzing the effect of pHe acidification and of CA IX-mediated CO_2/bicarbonate fluxes in an *in vitro* coculture model of prostatic tumor. Single culture of HPFs produced less pHe acidification compared to cancer cells (PC3 or DU145) both at 1% O_2 and 20% O_2 *(Figures 1A and 1C)* according to the common notion that highly proliferating cells, intensifying the glycolytic flux, lead to a strong production and release of acidic equivalents to control their pHi. Surprisingly, PC3-CAFs coculture *(Figure 1D)*, as well as DU145-CAFs one *(Figure 1B)*, showed a synergistic increment of acidic equivalents production.

The proliferation index determined for each population in single and coculture system suggests: 1) PC3 or DU145 cells proliferation rate in single culture are highly sensitive to environmental pH. Acidic pHe is a stressful condition for tumor cells that leads to a notable reduction of proliferation *(Figure 2A-B)*, without presence of cell death *(Table I)*; 2) tumor cells, when cocultured with CAFs, show a significant increase in cell proliferation rate at every pHe considered. Nevertheless, the presence of CAFs is not sufficient to completely overcome the negative effect of acidic pHe *(Figure 2A-B)*; 3) the transdifferentiation of HPFs to CAFs, induced by their coculture with tumor cells, leads to an increase in fibroblasts proliferation rate *(Figure 2C)*, although at a lesser extent compared to that observed for cancer cells *(Figure 2A-B)*; 4) hypoxic conditions, commonly found in tumor microenvironment, further contribute to enhance tumor cells proliferation rate both in single culture and in coculture *(Figure 3A-D)*. In conclusion, coculture gives a proliferative advantage mainly to cancer cells, particularly in hypoxia, whereas pHe acidification constitutes a negative environmental condition.

One of the proteins responsible for pHe acidification in the context of tumor microenvironment is CA IX [255, 304], whose catalytic activity leads to extracellular production of protons and bicarbonate. Given that low pHe has a negative impact on both PC3 and DU145 proliferation, we have investigated the role of the other product of CO_2 hydration, bicarbonate, in cancer cells proliferation. Summary data reported in *Table II* show that CAFs-mediated DU145 cells proliferation rate enhancement relies almost totally on bicarbonate presence in the extracellular medium *(Figure 4B-C)*, while only 30% of PC3 cells proliferation increase due to the presence of CAFs is warranted by bicarbonate *(Figure 5B-C)*.

A key question is why bicarbonate does not influence cells proliferation rate in single DU145 and PC3 culture *(Figures 4A and 5A)*. We supposed that bicarbonate concentration sufficient for sustaining single culture cell proliferation can be obtained by atmospheric CO_2 or by cell respiration derived CO_2. On the contrary, when the growth rate of cancer cells is strongly increased, consequently to CAFs-mediated activation, bicarbonate concentration is the rate limiting ion both for DU145 and PC3 growth. Accordingly, in order to fulfill the demand of bicarbonate there is an up-regulation of stromal CA IX when CAFs are cocultured with cancer cells. Stromal CA IX up-regulation is linked to the extent of bicarbonate contribution to cancer cells proliferation. In fact, we observed a greater CA IX expression increase when CAFs were cultured with DU145 *(Figure 7A-B)* rather than with PC3 *(Figure 7C-D)*.

It has been shown that bicarbonate may serve as a shuttle to transport protons outside the cell. In this hypothesis, CO_2 hydration by extracellular CAs produces protons and bicarbonate, and then the latter is transported within the cell by bicarbonate transporters contributing to cytoplasm alkalinization [637, 638] and reforming CO_2. Our results, indeed, show that tumor cells also use bicarbonate as a mono carbonic fragment to build biosynthesis intermediates necessary for sustain their high proliferation rate *(Figure 6 and Table III)* and that this process is enhanced in tumor cells cocultured with activated fibroblasts compared to cancer cells alone as indicated by the increased steady state concentrations of the two Krebs cycle intermediates analyzed *(Table III)*.

The important role of stromal CA IX for sustaining cancer cells growth has been confirmed by siRNA mediated CA IX silencing in CAFs that leads to a remarkable decrease of DU145 proliferation compared to standard coculture conditions *(Figure 8A-B)*. The results of *in vitro* coculture model are also clearly confirmed by *in vivo* experiments in which we show that CAFs impaired in CA IX expression lead to a strong reduction of tumor growth *(Figure 9)*.

In summary, these data reveal a new effect of reciprocal interplay between CAFs and tumor cells in the context of the tumor microenvironment mediated by CA IX catalytic activity. In fact, the up-regulation of stromal CA IX induced by cancer cells leads both to the acidification of extracellular milieu and to the production of bicarbonate. While extracellular acidification is disadvantageous for cell proliferation, bicarbonate, through its organication, supplies cancer cells with intermediates useful to sustain their high proliferation rate. It is conceivable that in solid tumors the extracellular acidification could be maintained within acceptable limits by the dynamics of the extracellular fluid, while CA IX activity ensures the amount of bicarbonate sufficient for not constitute a limit to cancer cells growth rate.

Recent study showed that CA IX actively contribute also to cell adhesion and migration, two important steps of metastatic process, which enables tumor cells to escape the primary mass and colonize new body sites where, at least initially, nutrients and space are not limiting. Different ways in which CA IX participates in cell motility has been described: by competing with E-cadherin for the interaction with β-catenin [322]; by leading to disassemble focal adhesion, mainly through inactivation of Rho small GTPase [639]; by co-localizing and physically interacting at the leading edge with bicarbonate transporters NBCe1 and AE2, *i.e.* the pH regulating cell apparatus of moving cells [357].

Our results show that, not only CA IX expressed by cancer cells, but also that up-regulated in CAFs surface during coculture conditions *(Figure 7A-D)* promote cancer cells motility. In fact, the increase of cancer cell migration rate observed in coculture is remarkably reduced in presence of CA IX silenced CAFs *(Figure 10)*.

Surprisingly, none of the two CA IX catalysis products have beneficial effect on tumor cells migration either in single culture or in coculture. On one hand, the CO_2/bicarbonate fluxes do not interfere with PC3 migration *(Figure 14)*; on the other one, the extracellular acidity represents an unfavorable condition *(Figures 11-12)*. The negative effect of high protons concentration is not restored in presence of CAFs, and PC3 migration rate remain very low at pH 6.8, instead, significantly increase at pH 7.4 and pH 8.0 *(Figure 13)*.

The migration rate determined for tumor cells both in acidic environment and in the presence or absence of bicarbonate buffer system suggest: 1) the migrating cells of a tumor mass are present at the periphery (invasion front) of the cancer, where the acid/alkaline balance is keep by blood vessels, which remove CO_2 and lactic acid. Conversely, cells of the central tumor region, where acidic waste accumulates, are less able to migrate. This evidence was confirmed by Hlubek *et al.* [640] who found

that dedifferentiated human colorectal carcinoma cells accumulate the transcriptional activator β-catenin in the nucleus, in contrast to cells of the tumor center; 2) the contribution of stromal CA IX to cancer cells migration is not mediated by its catalysis products, indicating that this CA IX effect could be due to its non-catalytic related function. Besides its role at the cell surface, a very recent study place CA IX among the cell-surface signal transducers undergoing nuclear translocation [641]. Therefore, stromal CA IX could contribute to tumor cells migration by exhibiting a potential intracellular function. Nevertheless, functional aspects of CA IX in tumor cells migration and invasion are still unclear, so future investigations are required.

NEW CONCEPTS ABOUT FIBROBLASTS TROPHIC FUNCTION

AIM OF THE STUDY

Fibroblasts are mesenchymal cells with many vital functions both during fetal development and in adult organisms. Their main actions are the production and the continue remodeling of ECM components, which constitute the structural framework, *i.e.* the connective tissues, of most organs. However, they are also important producers of trophic factors. In fact, fibroblasts, mainly mouse embryonic fibroblasts or MEFs, have been long used as feeder cell layers for the culture and the maintenance of mouse and human embryonic stem cells. In this context, their role is to provide a complex mixture of nutrients, cytokines and growth factors for the long term survival and proliferation of undifferentiated pluripotent stem cells. Fibroblasts, in fact, release various essential growth factors, cytokines and ECM components, such as TGF-β, activin A, laminin-511, and vitronectin [642]. However, not all the secreted molecules are still known and inconsistencies in expression and secretion of these factors make it difficult to determine which components are indispensable [642, 643].

Besides these functions, fibroblasts are also involved in the regulation of epithelial differentiation, in inflammation processes as well as play major roles in wound healing. In fact, they are associated with many diseases, either because implicated in their inception/progression, or because the hyperactivity of these cells can result in excessive production and deposition of ECM components (a process known as fibrosis), determining adverse effect on tissues [72]. Fibroblasts play an essential role in tumor biology representing the major components of tumor associated stroma. These activated fibroblasts are known as CAFs [82]. The transition of a normal fibroblast into an activated one is mediated by growth factors and cytokines secreted by cancer cells. CAFs, in turns, promote neoplastic progression by secreting many cytokines [644, 645]; by releasing lactate that is ultimately uploaded by tumor cells [632]; by producing extracellular bicarbonate through the catalytic activity of their own CA IX [646]; by ECM remodeling; by stimulating inflammation, angiogenesis and lymphangiogenesis [151, 152, 647].

The aim of our study was to investigate the ancillary function of fibroblasts, in particular in the context of the tumor microenvironment. In our experimental model we used non transformed cells, HPFs obtained from surgical explantation of patients, human dermal fibroblasts (HDFs), NIH-3T3 murine fibroblasts, and

malignant cells, including two different human tumor cell lines of prostatic origin (DU145 and PC3) and a human melanoma cell line (A375). The acquisition of the typical CAFs phenotype was obtained by coculturing primary fibroblasts with tumor cells or with their conditioned medium [121].

Since the ability of these cells to secrete soluble signaling molecules has been the subject of various study, we analyzed whether the interplay between fibroblasts and tumor cells could occur through the horizontal transfer of material, in particular of cytoplasmic proteins and membrane lipids.

RESULTS

Fibroblasts transfer proteins and lipids to surrounding cells

In our experimental model, CAFs are able to promote tumor progression by increasing cancer cells proliferation. This analysis was performed by using CFDA-SE cytofluorymetric assay to measure tumor cells proliferation rate both in single culture and in coculture conditions (see Methods). Our results show that DU145 *(Figure 15A)* and PC3 *(Figure 15B)*, increase their growth rate of 30-40% when cocultured with CAFs and of 10-20% when cultured in their conditioned medium, indicating that less than 47% of fibroblasts pro-proliferative effect is mediated by the release of soluble factors or by other form of paracrine intercellular crosstalk.

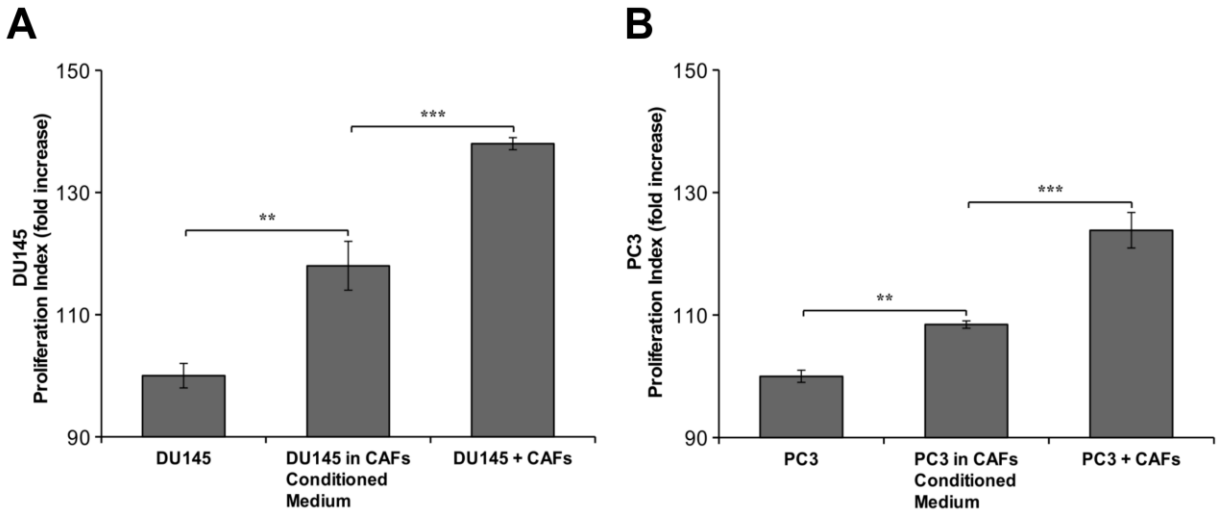

Figure 15. CAFs promote cancer cells growth. *DU145* ***(A)*** *and PC3* ***(B)*** *were labeled with CFDA-SE and then plated in single culture (both in starvation medium and in the medium conditioned by CAFs for 48 hours) and in coculture with fibroblasts in 1:2 ratio in starvation medium. After 40 hours cells were detached and analyzed by flow cytometry. The data show the fold increase of proliferation index calculated on an average of four independent experiments (**, $p < 0.05$; ***, $p < 0.01$).*

Always in the context of the tumor microenvironment, we observed that fibroblasts are able to horizontally transfer materials to tumor cells. Confocal microscopy of fibroblasts labeled with CFDA-SE (to follow the transfer of proteins) or with CellVue® (to monitoring the passage of lipids) cocultured with DU145 show that fibroblasts transfer both fluorescent proteins *(Figure 16A)* and lipids *(Figure 16B)* to tumor cells in time dependent manner. On the contrary, when DU145, labeled with CFDA-SE or CellVue®, were plated with unlabeled fibroblasts, we did not detect any of the two effects: either the passage of proteins *(Figure 16C)* or of lipids *(Figure 16D)*.

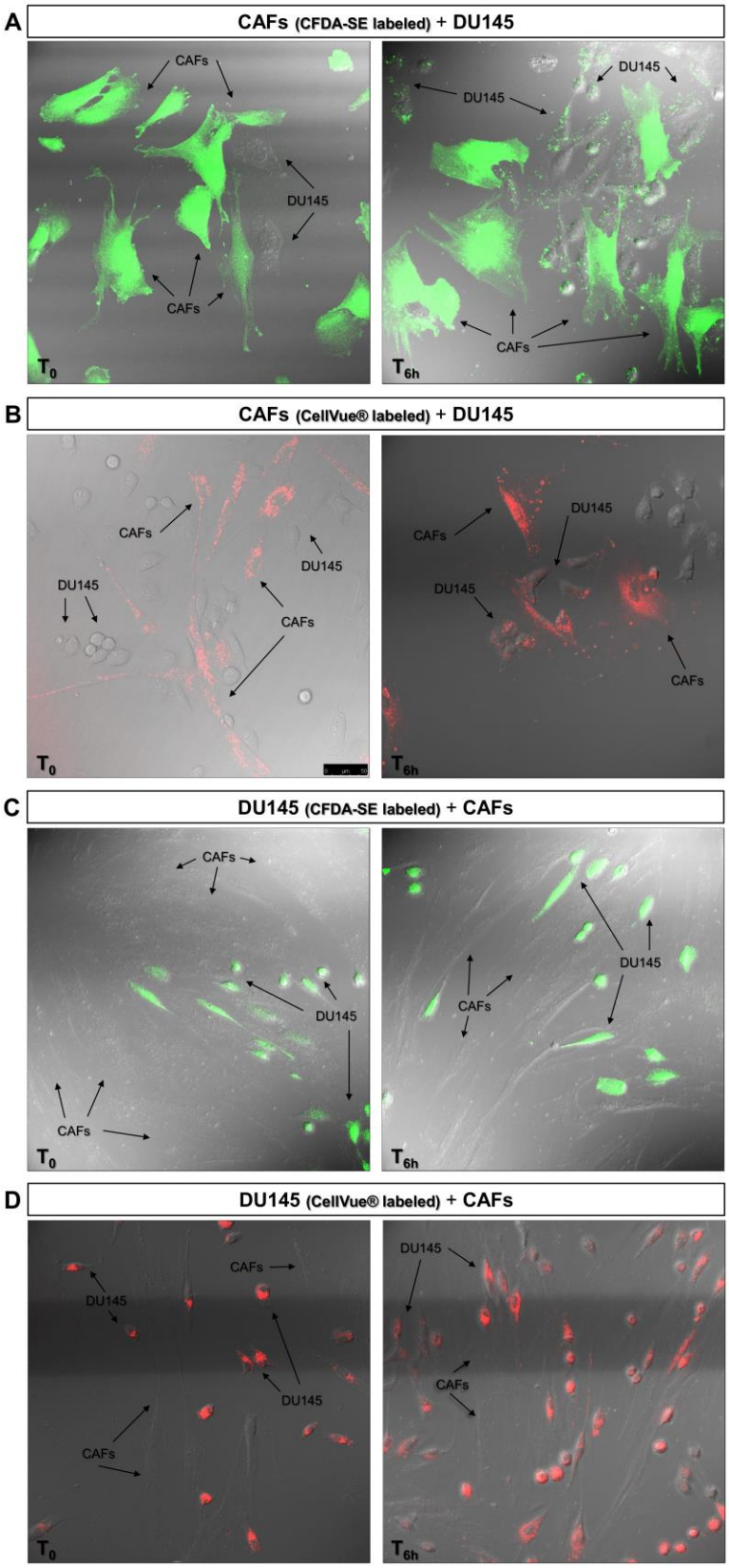

Figure 16. Confocal microscopy analysis of protein and lipid transfer. *Fibroblasts were labeled with CFDA-SE* ***(A)*** *or with CellVue®* ***(B)*** *and then plated in coculture with unlabeled DU145 tumor cells in 2:1 ratio on glass coverslips; in turns, DU145 tumor cells were labeled with CFDA-SE* ***(C)*** *or with CellVue®* ***(D)*** *and then plated in coculture with unlabeled fibroblasts in 2:1 ratio on glass coverslips. Immediately after plating and after 6 hours the cells were fixed in paraformaldehyde and observed by confocal fluorescence microscopy.*

Thus, the different capability of protein transfer between CAFs and cancer cells was quantified by a CFDA-SE cytofluorymetric assay in which we measured the fluorescence intensity increase of recipient cells after coculturing with labeled donor cells (see Methods). Our results show that CAFs of prostatic and dermal origin transfer their proteins to tumor prostatic cells (both DU145 and PC3) and to A375, respectively *(Figure 17A)*. On the contrary, the passage of proteins from tumor cells to fibroblasts is notably less *(Figure 17A)*. Besides CAFs, also healthy human fibroblasts derived from the same anatomical sites (HPFs and HDFs) and immortalized, but non transformed, NIH-3T3 murine fibroblasts are able to perform this action *(Figure 17B)*. In order to maintain fibroblasts in a non-activated state these experiments were carried out by using the same stromal cells as recipients. *Figure 17B* shows that all the types of the tested fibroblasts behave as donor as well as recipient cells, in fact, they transfer proteins to the unlabeled surrounding counterpart.

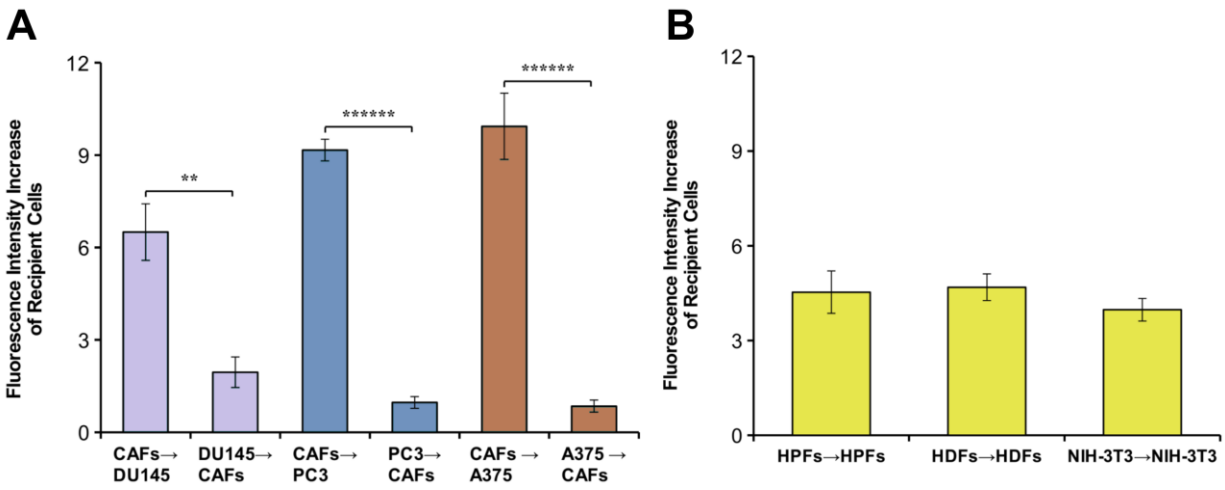

Figure 17. Flow cytometry analysis of protein transfer. *Fibroblasts of prostatic and dermal origin were labeled with CFDA-SE and then plated in coculture in 2:1 ratio with unlabeled prostatic cancer cells (both DU145 and PC3) and A375, respectively; in turns, cancer cells of prostatic origin (both DU145 and PC3) and A375 were labeled with CFDA-SE and then plated in coculture in 2:1 ratio with unlabeled fibroblasts of prostatic and dermal origin, respectively* ***(A)****. HPFs, HDFs and NIH-3T3 were labeled with CFDA-SE and then plated in coculture in a 2:1 ratio with their unlabeled counterpart* ***(B)****. After 40 hours* ***(A)*** *or 24 hours* ***(B)*** *cells were detached and analyzed by flow cytometry. The data represent the value of fluorescence intensity increase of recipient cells calculated on an average of three independent experiments (**, $p < 0.05$; *****, $p < 0.001$).*

Then, we characterized the kinetic aspect of protein transfer, both evaluating the dose- (*i.e.* the ratio between donor and recipient cells) and the time-dependence. We observed that the amount of transferred proteins increases when the ratio between recipient tumor cells and donor fibroblasts is in favor of the latter *(Figure 18A-B)*, and that the passage of proteins exhibit an increasing trend *(Table IV)*.

The quantitative analysis of the time-course of protein transfer was performed by plating fibroblasts, previously labeled with a mixture of ^{14}C amino acids, and prostatic cancer cells (DU145 or PC3) in coculture in 2:1 ratio for 6, 16 and 24 hours. After that, the two populations were separated and the respective radioactivity values were measured by liquid scintillation counter (see Methods). The measurement of the radioactivity bound to the proteins transferred from CAFs to tumor cells shows that after 24 hours each fibroblast has transferred about 4.0 % of its total protein mass to a DU145 cell and about 9.5% to a PC3 cell *(Table IV).*

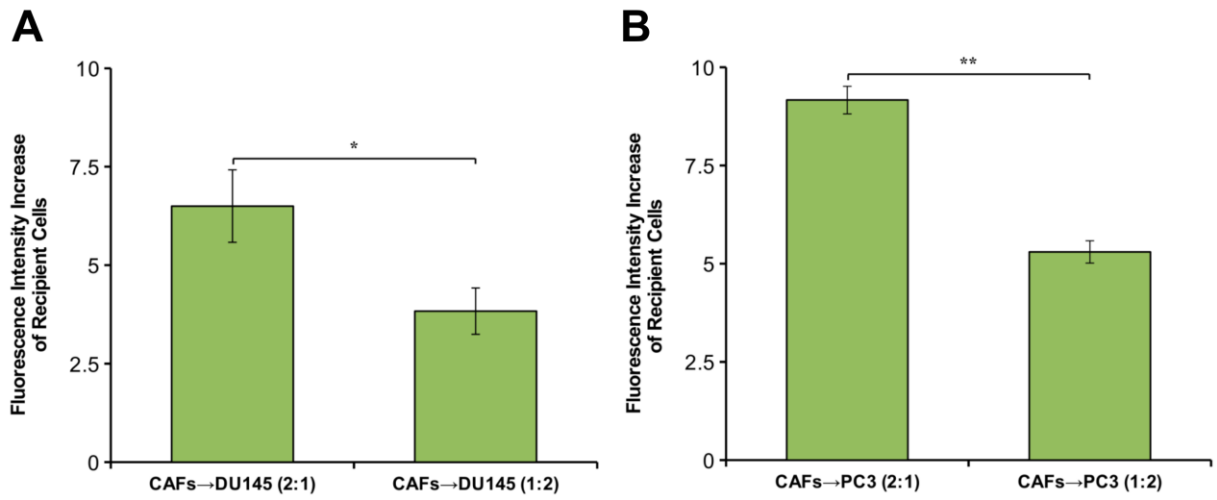

Figure 18. Kinetic analysis of protein transfer from CAFs to tumor cells. *Fibroblasts of prostatic origin were labeled with CFDA-SE and then plated with DU145* ***(A)*** *and PC3* ***(B)*** *both in 2:1 ratio and 1:2 ratio. After 40 hours cells were detached and analyzed by flow cytometry. The data represent the value of fluorescence intensity increase of recipient cells calculated on an average of three independent experiments (*, p < 0.1; **, p < 0.05).*

Table IV. Quantitative analysis of time-course of protein transfer from CAFs to tumor cells.

Percentage of CAFs protein mass transferred to DU145		
6 hours	**16 hours**	**24 hours**
0.5% ± 0.2	**1.9%** ± 0.4	**4.0%** ± 0.4
Percentage of CAFs protein mass transferred to PC3		
6 hours	**16 hours**	**24 hours**
0.9% ± 0.3	**2.7%** ± 0.4	**9.5%** ± 0.9

*The percentage of CAFs protein mass transferred to tumor cells was obtained from the ratio between CAFs radioactivity and that of cancer cell measured for single cell after coculture and separation (CAFs + DU145: "6 hours" vs "16 hours" **, p < 0.05; "16 hours" vs "24 hours" **, p < 0.05; CAFs + PC3: "6 hours" vs "16 hours" **, p < 0.01; "16 hours" vs "24 hours" **, p < 0.01).*

In order to test the relevance of this mechanism in the context of the tumor microenvironment, we compared the transfer capability of healthy fibroblasts with respect to CAFs, using healthy stromal cells as recipients. For these experiments, healthy prostatic and dermal fibroblasts were previously grown with the medium conditioned by their respective tumor cells, and thus converted into CAFs. We observed that, although the modulation of this phenomenon depends on the type of tumor cell used for fibroblasts activation, CAFs both of prostatic *(Figure 19A)* and dermal origin *(Figure 19B)* transfer a greater amount of proteins compared to their non-activated counterparts. In particular, fibroblasts activated by PC3 increase their potential for protein transfer of about 2.66 fold, instead those activated by DU145 and A375 show an increase of about 1.5 fold *(Figure 19A-B)*.

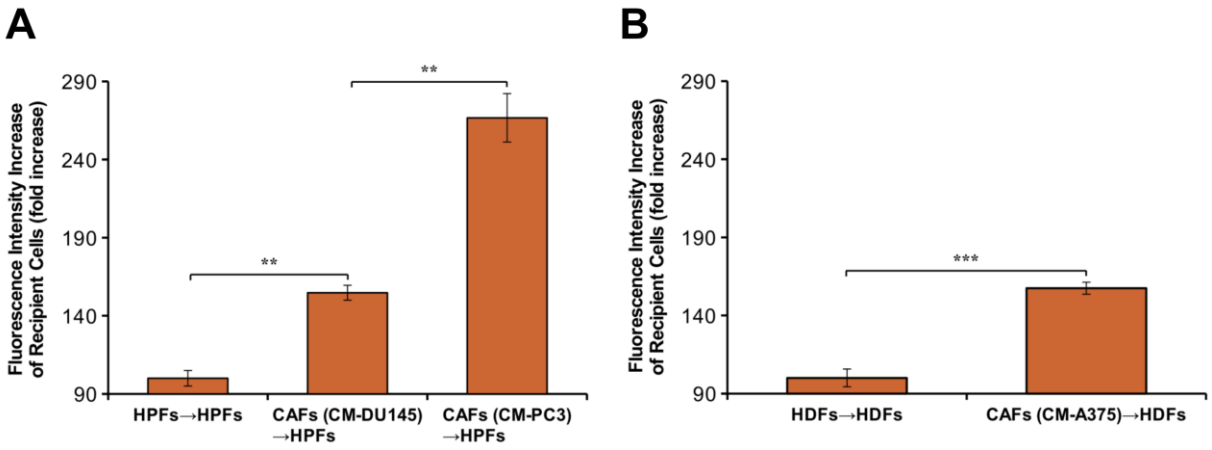

Figure 19. Quantitative analysis of protein transfer mediated by healthy fibroblasts and activated ones. *Healthy fibroblasts of prostatic origin (HPFs) and those activated (CAFs) with the medium conditioned by prostatic tumor cells, both DU145 and PC3, were labeled with CFDA-SE and then plated in coculture with unlabeled healthy fibroblasts in a 2:1 ratio in starvation medium* ***(A)****. Healthy fibroblasts of dermal origin (HDFs) and those activated (CAFs) with the medium conditioned by A375, are labeled with CFDA-SE and then plated in coculture with unlabeled healthy fibroblasts in a 2:1 ratio in starvation medium* ***(B)****. After 24 hours cells were detached and analyzed by flow cytometry. The data represent the fold increase of the value of fluorescence intensity increase of recipient cells calculated on an average of four independent experiments (**, $p < 0.05$; ***, $p < 0.01$). CM, medium conditioned by tumor cells.*

Identification of the proteins transferred from CAFs to tumor cells

Our next goal was to identify some of CAFs proteins transferred to tumor cells. The approach we have implemented for the comprehensive profiling and identification of the transferred proteins involves the preliminary radiolabeling of fibroblasts proteins. Stromal cells were cultured for 72 hours in a complete medium supplemented with a mixture of ^{14}C L-amino acids in order to induce their

incorporation into proteins. Therefore, radioactively labeled fibroblasts were plated in coculture with DU145. After 6 hours the two populations were separated, lysed and subjected to 2DE. The representative gels of their protein profile obtained after colloidal coomassie blue staining are displayed on *Figures 20A* and *20C*, instead, *Figures 20B* and *20D* show the corresponding images obtained from the autoradiographies of the same gels after being dried. *Figure 20B* displays the overall labeling of fibroblasts proteins, while the DU145 autoradiography *(Figure 20D)* shows limited radiolabeled-protein contents that are proteins derived from CAFs. The degree of purity of DU145 isolated after coculture (see Methods), in fact, is sufficiently high to exclude that the radioactive signal is due to fibroblasts contamination.

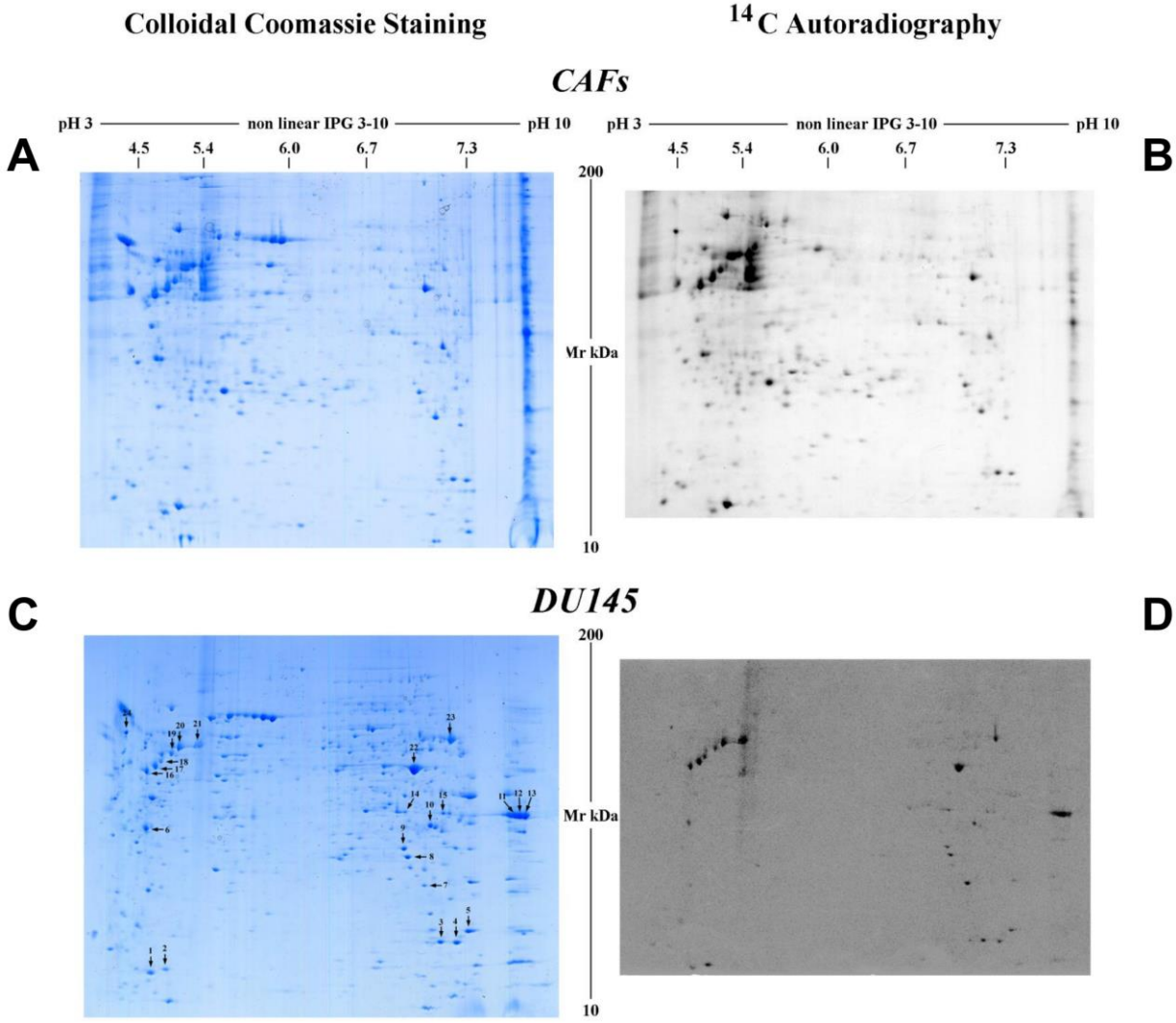

Figure 20. Proteomic analysis of CAFs and DU145 after coculture and separation. *Radioactively labeled CAFs were cocultured with DU145, after 6 hours the two populations were separated and subjected to 2DE. The figures show the representative gels of their protein profile after colloidal coomassie blue staining* ***(A-C)****, and display the corresponding images obtained from the autoradiographies of the same gels after being dried* ***(B-D)****.*

The image analysis and the determination of the specific radioactivity of some transferred proteins both in DU145 and in CAFs, further enabled to strengthen our hypothesis. We carried out the quantitative analysis of 10 protein spots selected among the radiolabeled proteins in DU145 by using the ImageMaster 2D Platinum software. These 10 spots were selected for their quality, in fact they are well separated from the surrounding ones, compact and non-saturated. The analysis was done on both the images related to the stained gels and on autoradiographies.
For each protein spot we determined the relative spot volume (V) calculated as %V with respect to the total volume of the 10 selected spots. The normalized %V of each spot on replicate 2D gels was averaged and the standard deviation was calculated *(Table V)*. The mean values obtained for the "Prot" (calculated on the spots of coomassie stained gels) and for the "^{14}C-Prot" (calculated on ^{14}C spots of the autoradiographies) were used to calculate the specific relative radioactivity of each spot, both in DU145 and in CAFs gels (%V "^{14}C-Prot"/%V "Prot"). *Table VI* shows the results. The specific enrichment calculated for the 10 spots highlights that a selective and specific protein transfer from CAFs to DU145 has occurred.

Table V. Quantitative analysis of ^{14}C labeled transferred proteins.

SPOT N°	Protein name	% V-DU145 (Prot) Mean ± sd	% V-DU145 (^{14}C-Prot) Mean ± sd	% V-CAFs (Prot) Mean ± sd	% V-CAFs (^{14}C-Prot) Mean ± sd
1	Thioredoxin	**6.48** ± 1.01	**9.21** ± 0.87	**9.48** ± 0.96	**6.28** ± 0.81
2	Galectin-1	**3.51** ± 0.05	**12.22** ± 0.07	**16.39** ± 0.14	**25.09** ± 0.09
7	Superoxide dismutase (mitochondrial)	**2.31** ± 0.05	**8.43** ± 0.08	**8.59** ± 1.04	**5.17** ± 0.98
8	Triosephosphate isomerase	**8.61** ± 0.96	**6.15** ± 0.88	**6.35** ± 0.31	**4.42** ± 0.27
9	Phosphoglycerate mutase 1	**7.09** ± 0.05	**4.75** ± 0.04	**1.80** ± 0.1	**1.9** ± 0.11
10	Glyceraldehyde-3-phosphate dehydrogenase	**6.91** ± 0.07	**4.55** ± 0.08	**8.83** ± 1.75	**6.39** ± 1.22
14	Malate dehydrogenase (cytoplasmic)	**2.77** ± 0.26	**4.23** ± 0.29	**4.85** ± 1.78	**1.76** ± 1.88
16	Vimentin	**9.79** ± 1.44	**15.79** ± 1.39	**18.70** ± 1.85	**30.24** ± 2.22
22	Alpha-enolase	**46.87** ± 1.02	**31.91** ± 0.95	**22.20** ± 2.41	**12.71** ± 1.67
24	Calreticulin	**5.63** ± 0.08	**2.71** ± 0.06	**2.76** ± 0.06	**5.99** ± 0.08

The relative spot volume (V) was calculated as %V of the total volume of 10 selected spots in each gel on both the images related to the stained gels (%V "Prot") and to the autoradiographies (%V "^{14}C-Prot"). The resulting values were used to calculate the specific relative radioactivity of each spot and thus the specific enrichment of the corresponding proteins.

Table VI. Specific enrichment of ^{14}C labeled transferred proteins.

SPOT N°	Protein name	Specific Radioactivity (DU145) % V-(^{14}C-Prot) / % V-(Prot)	Specific Radioactivity (CAFs) % V-(^{14}C-Prot) / % V-(Prot)	Specific Enrichment (DU145/CAFs)
1	Thioredoxin	**1.42** ± 0.25	**0.66** ± 0.08	**2.14** ± 0.47
2	Galectin-1	**3.48** ± 0.05	**1.53** ± 0.01	**2.27** ± 0.04
7	Superoxide dismutase (mitochondrial)	**3.65** ± 0.08	**0.60** ± 0.07	**6.06** ± 0.76
8	Triosephosphate isomerase	**0.71** ± 0.13	**0.69** ± 0.05	**1.02** ± 0.2
9	Phosphoglycerate mutase 1	**0.66** ± 0.007	**1.05** ± 0.08	**0.63** ± 0.052
10	Glyceraldehyde-3-phosphate dehydrogenase	**0.65** ± 0.014	**0.72** ± 0.16	**0.91** ± 0.21
14	Malate dehydrogenase (cytoplasmic)	**1.52** ± 0.18	**0.36** ± 0.07	**4.19** ± 0.95
16	Vimentin	**1.61** ± 0.27	**1.61** ± 0.19	**0.99** ± 0.21
22	Alpha-enolase	**0.68** ± 0.02	**0.57** ± 0.09	**1.18** ± 0.2
24	Calreticulin	**0.48** ± 0.01	**2.16** ± 0.06	**0.22** ± 0.008

The specific radioactivity was obtained taking into account the relative spot volume of each protein calculated with respect to the total volume of the 10 selected spots reported in Table V. In turn, the specific enrichment of each protein was obtained from the ratio between the values of specific radioactivity calculated in the two cell populations. ***Red****: lowered proteins compared to their contents in CAFs;* ***Green****: specifically enriched proteins compared to their contents in CAFs.*

We excised from DU145 gels the main 24 radiolabeled proteins and, after tryptic digestion, for each one was produced a peptide mass finger print by MALDI-TOF mass spectrometry analysis. Some spots were further analyzed by capillary-LC-μESI-MS/MS. The identification results were summarized in *Table VII*.

In order to gain insight into biological significance of the identified proteins, they were categorized according to the DAVID bioinformatics tool. Concerning biological processes, the identified proteins were distributed into two main categories. The major biological process, in which 50% of them are involved, is "generation of precursor metabolites and energy". Another large part (30%), instead, can be grouped in the "cellular component movement" class. The remaining five proteins are not associated with common biological processes, so we classified them as "other" *(Figure 21)*.

Table VII. Protein identification by MALDI-TOF mass spectrometry and capillary-LC-μESI-MS/MS analysis.

Spot N°	Accession N°	Protein name	Measured pI/Mr (kDa)	Theoretical pI/Mr (kDa)	MASCOT search results			
					N° of matched peptides	Sequence Coverage (%)	Score	
							MS Mix	MS/MS
1	P10599	Thioredoxin	4.76/13.25	4.82/12.01	21	83		695
2	P09382	Galectin-1	5.21/13.68	5.34/15.05	6	64	113	
3	Q9UC61	Peptidyl-prolyl cis-trans isomerase A	7.70/17.90	7.68 /18.23	9	62	128	
4	Q9UC61	Peptidyl-prolyl cis-trans isomerase A	7.88/17.79	7.68 /18.23	172	86		4150
5	P23528	Cofilin-1	8.01/19.92	8.22/18.72	11	65	152	
6	P06753	Tropomyosin alpha-3	4.66/33.25	4.68/32.86	58*	51*		1413*
	Q9UCS3	Tropomyosin alpha-4		4.67/28.62	44*	53*		1231*
7	Q9P2Z3	Superoxide dismutase (mitochondrial)	7.54/24.04	8.35/24.88	8	50	123	
8	P60174	Triosephosphate isomerase	7.37/27.99	5.65/31.06	10	45	120	
9	P18669	Phosphoglycerate mutase 1	7.33/29.43	6.67/28.90	124	83		3489
10	P04406	Glyceraldehyde-3-phosphate dehydrogenase	7.60/33.86	8.57/36.20	9	38	109	
11	P04406	Glyceraldehyde-3-phosphate dehydrogenase	8.57/35.77	8.57/36.20	7	38	97	
12	P04406	Glyceraldehyde-3-phosphate dehydrogenase	8.63/36.03	8.57/36.20	148	86		5004
	P40926	Malate dehydrogenase, mitochondrial		8.92/35.94	39	59		1702
	P22626	Heterogeneous nuclear ribonucleoproteins A2/B1		8.97/37.46	21	40		796
13	P04406	Glyceraldehyde-3-phosphate dehydrogenase	8.69/35.75	8.57/36.20	11	44	107	
	P22626	Heterogeneous nuclear ribonucleoproteins A2/B1		8.97/37.46	9	36	92	184
14	P40925	Malate dehydrogenase, cytoplasmic	7.34/36.90	6.91/36.63	7	27	83	
15	P07355	Annexin A2	7.73/36.57	7.57/38.81	17	50	210	
16	Q8N850	Vimentin	4.67/45.90	5.06/53.68	20	48	251	
17	Q8N850	Vimentin	4.90/46.99	5.06/53.68	22	51	239	
18	Q8N850	Vimentin	5.07/48.42	5.06/53.68	48	59		1433
19	Q8N850	Vimentin	5.10/50.48	5.06/53.68	82	78		2635
20	P06576	ATP synthase subunit beta, mitochondrial	5.21/51.42	5.26/56.52	19	74	238	
21	P68363	Tubulin beta chain	5.36/52.34	4.94/50.80	15	43	70	
	Q8N850	Vimentin		5.06/53.68	47	85	399	427
22	Q6GMP2	Alpha-enolase	7.43/46.13	7.01/47.48	18	48	177	
23	P14618	Pyruvate kinase M2	7.82/53.38	7.96/58.47	18	38	220	
24	P27797	Calreticulin	4.20/58.10	4.29/48.28	8	25	120	

* 2 missed cleavages

Mass lists were cleaned up from eventually present contaminant masses, such as those from matrix, autodigestion of trypsin and keratins. Mass fingerprinting or MS/MS searching were carried out in Swiss-Prot databases using MASCOT (Matrix Science Ltd., London, U.K., http://www.matrixscience.com) software. The taxonomy was restricted to human and the number of accepted missed cleavage sites was set to one. Alkylation of cysteine by carbamidomethylation was assumed as fixed modification. Oxidation of methionine was assumed as variable modification. The experimental mass values were monoisotopic. Mass lists were cleaned up from eventually present contaminant masses, such as those from matrix, autodigestion of trypsin and keratins and a mass tolerance of 50 ppm was allowed for mass fingerprinting searches. A peptide tolerance of 10 ppm and a MS/MS tolerance of 0.6 Da were allowed for MS/MS searches. No restrictions on protein molecular weight and pI were applied. The criteria used to accept identifications included the extent of sequence coverage, number of matched peptides and probabilistic score sorted by the software.

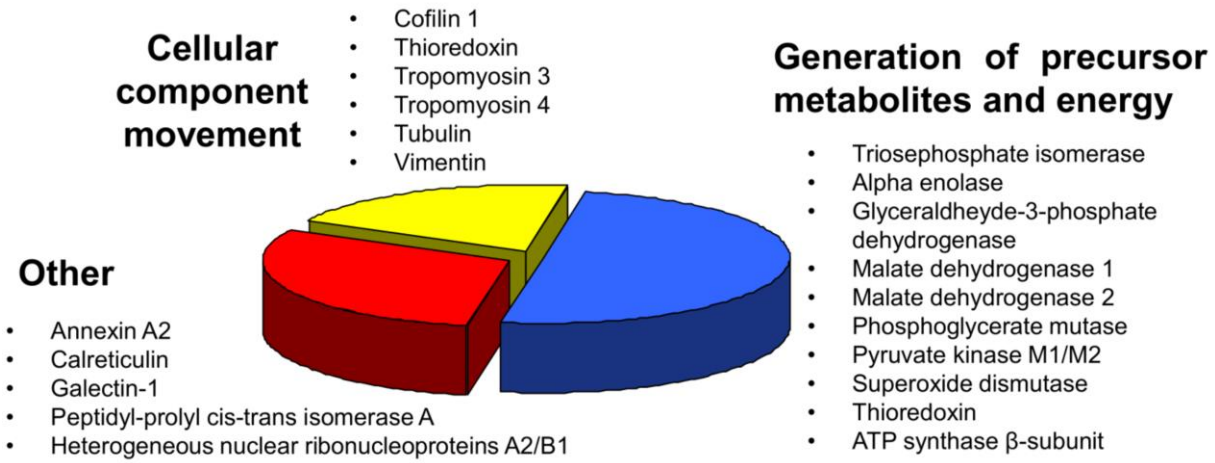

Figure 21. Functional clustering of the identified proteins. *Cluster analysis was performed by using DAVID database. The pie chart shows the resulting functional interpretation.*

The role of extracellular membrane vesicles in fibroblasts-tumor cells communication

Besides the networks of soluble molecules, it is known that cell-cell communication occurs also through membranous structures, called extracellular vesicles, that horizontally transfer biologically active mediators, including nucleic acids, receptors and enzymes [407-411]. We characterized the extracellular vesicles released by CAFs, and investigated their possible involvement as vehicles in protein transfer process to tumor cells. In this regard, the medium recovered from the culture supernatant of CAFs was centrifuged (see Methods) and two different fractions of vesicles were obtained. In particular, we separated vesicles within 10,000 xg pellet from that within 100,000 xg pellet, which were then examined for their size and content.

The size of these particles was revealed by Dynamic Light Scattering analysis. We found that the fraction within 10,000 xg pellet contains mainly only one population of vesicles with a diameter of about 1 μm *(Figure 22A-B)*, on the contrary, the prevalent population of vesicles within 100,000 xg pellet has a diameter of about 20 nm *(Figure 22C-D)*. Since a uniform nomenclature to define extracellular vesicles has not yet been adopted in the literature, in this study, fibroblasts-secreted vesicles will be classified exclusively in accordance to their size. Thus, for clarity, we will refer to vesicles with a diameter of about 1 μm as microvesicles (MVs), and to vesicles with a diameter of about 20 nm as exosomes like-vesicles.

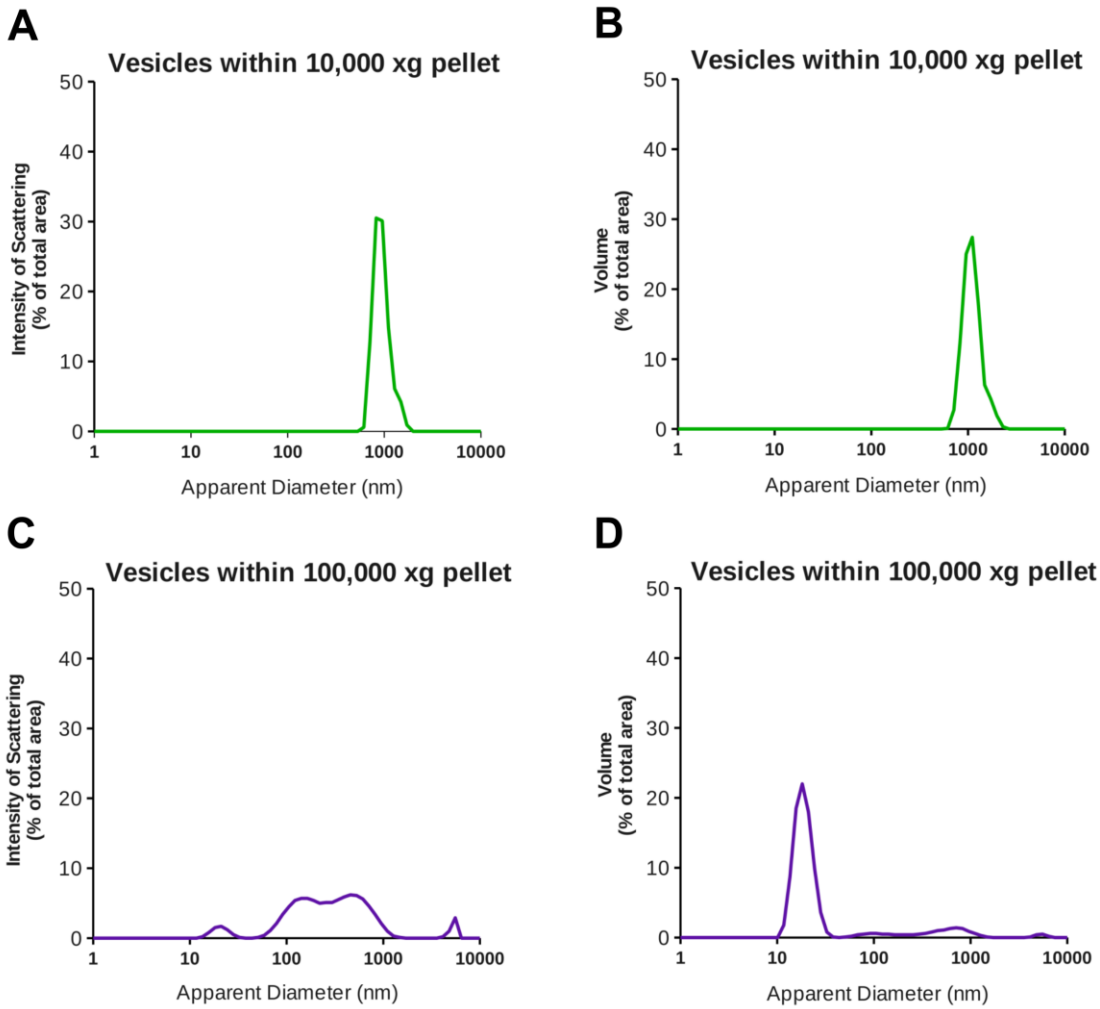

Figure 22. Size characterization of the vesicles released by CAFs. *The vesicles secreted by CAFs were isolated and their size distributions were obtained using Dynamic Light Scattering device. The average hydrodynamic diameter of vesicles within 10,000 xg pellet is 953.3 ± 168.8 nm* ***(A-B)****, on the contrary, the average hydrodynamic diameter of vesicles within 100,000 xg pellet is 20.75 ± 1.252 nm* ***(C-D)****.*

The composition of these distinct subtypes of vesicles was examined by SDS-PAGE. *Figure 23A* shows the representative gel of their protein profile obtained after colloidal coomassie blue staining, instead F*igure 23B* displays the corresponding image obtained from the autoradiography of the same gel after being dried. We found that both fractions contain radioactive proteins but with a different composition, in particular, MVs are rich in proteins with a molecular weight lower than 58 kDa, on the contrary, exosomes-like vesicles are rich in proteins with a molecular weight greater than about 40 kDa *(Figure 23A-B)*.

In order to determine which subtype of particles was responsible for the passage of the proteins previously identified, we performed the Western blot analysis.

We found that most of the transferred proteins are more abundant in vesicles with a diameter of about 1 μm *(Figure 23C)*, suggesting that MVs are one of the mediators that allow the passage of these biological molecules from CAFs to tumor cells.

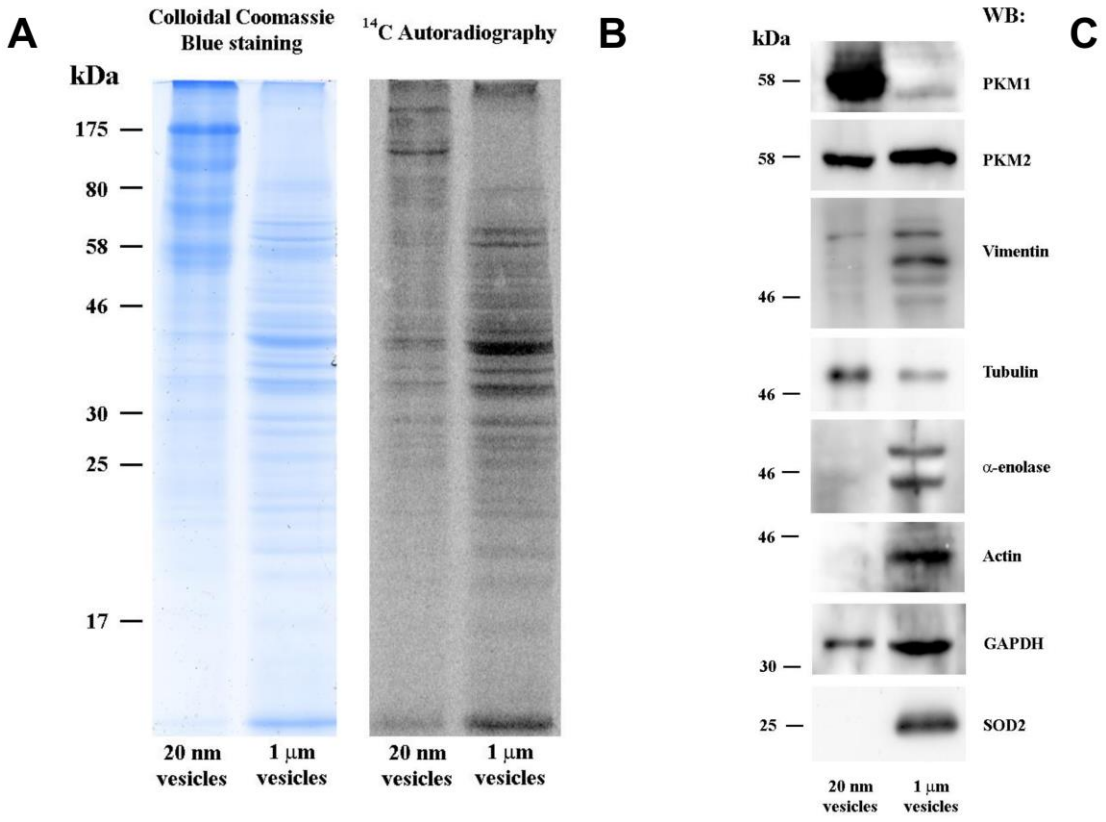

Figure 23. SDS-PAGE and Western blot analysis of the two subpopulations of vesicles obtained from the culture supernatant of CAFs. *The vesicles released by CAFs were lysed in Laemmli electrophoresis buffer and the samples were used for SDS-PAGE. The image shows the gel after colloidal coomassie blue staining* ***(A)****, and display the corresponding image obtained from the autoradiography of the same gel after being dried* ***(B)****. The vesicles recovered from the culture supernatant of CAFs were lysed in Laemmli electrophoresis buffer and used for Western blot analysis. The membrane were treated with anti-enolase, anti-β-tubulin, anti-glyceraldheide-3-phosphate dehydrogenase (GAPDH), anti-piruvate kinase M1 (PKM1), anti-piruvate kinase M2 (PKM2), anti-vimentin, anti-superoxide dismutase 2 (SOD-2) and anti-actin* ***(C)****.*

Finally, we investigated the possible biological roles of these proteins once they enter into the recipient cells. Considering the pro-proliferative effect mediated by CAFs conditioned medium *(Figure 15A-B)* and since the transferred proteins have a structural role as well as are mainly associated with the generation of precursor metabolites and energy *(Figure 21)*, we correlated protein transfer with fibroblasts trophic function. In this regard, we found that the proliferation index of DU145 grown with just MVs increases and gets close to that induced by CAFs conditioned medium *(Figure 24)*.

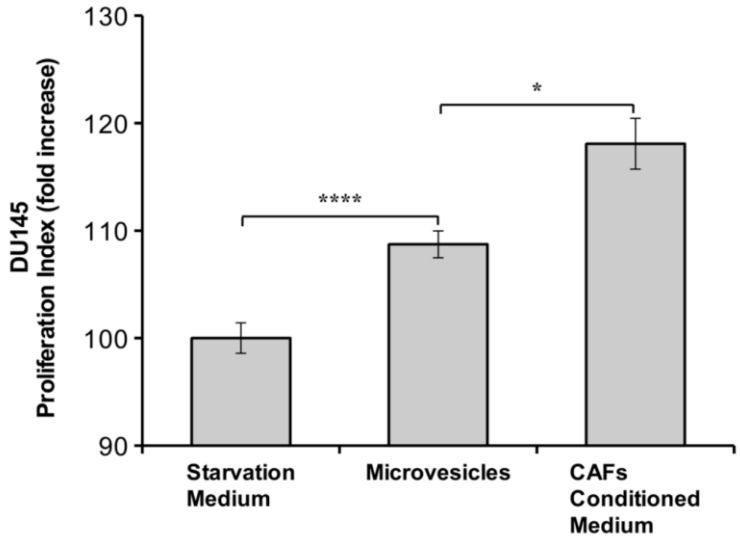

Figure 24. Effect of MVs on tumor cells growth. *DU145 were labeled with CFDA-SE and then grown in starvation medium, in starvation medium supplemented with MVs obtained from the culture supernatant of CAFs and in CAFs conditioned medium, respectively. After 40 hours cells were detached and analyzed by flow cytometry. The data show the proliferation index calculated on an average of four independent experiments (****, $p < 0.005$; *, $p < 0.1$).*

DISCUSSION

Fibroblasts in mammals comprise a class of highly heterogeneous cell types; in fact those isolated from different anatomical sites display distinct and characteristic gene-expression patterns, which make these cells poorly defined in molecular terms [72]. Despite these different transcriptional patterns, fibroblasts acquire a fine functional specialization, for all of them based on the secretion of growth factors and ECM components, as well as on the regulation of epithelial differentiation and of inflammation [70, 71, 74]. In this study, we add another function shared by human fibroblasts derived from different anatomical sites and by fibroblasts of murine origin. In particular, we found that healthy human fibroblasts of prostatic and dermal origin and non-transformed NIH-3T3 mouse fibroblasts are able to transfer cytoplasmic proteins to neighbouring cells *(Figure 17B)*.

Fibroblasts maintain this property also in pathological conditions, in particular in the context of the tumor microenvironment. Our results indicate that CAFs are able to horizontally transfer their proteins *(Figures 16A and 17A)* and lipids *(Figure 16B)* in time-dependent manner to their respective tumor cells. Intriguingly, the passage of material from tumor cells to fibroblasts is far less extensive or undetectable. In fact, although DU145 transfer proteins to CAFs in a very small extent detectable by flow cytometry *(Figure 17A)*, but not by confocal microscopy *(Figure 16C)*, PC3 and A375 are not able to perform this type of effect *(Figure 17A)*. Besides protein transfer, also the passage of lipids from DU145 to CAFs is very low and not visible by confocal microscopy *(Figure 16D)*. These evidences suggest that protein and lipid transfer represents an ancillary function of fibroblasts, that they execute both in physiological and in pathological conditions, and that, within our tumor microenvironment model, it is mainly unidirectional.

The monitoring of the kinetic aspect showed that the amount of transferred material boosts by increasing the ratio between donors and recipients *(Figure 18A-B)*, and that this passage is time-dependent *(Table IV)*. We quantified that tumor cells accumulate the proteins transferred from CAFs so quickly that after just 24 hours about 4.0% and 9.5% of CAFs total protein mass is transferred to DU145 and PC3, respectively *(Table IV)*. Notably, due to the higher mass of fibroblasts with respect to that of cancer cells, in real terms the proteins received by cancer cells represent a significant fraction of their own overall protein content.

It is known that activated fibroblasts of the tumor stroma are morphologically and functionally different from the quiescent ones, and produce proteases, growth factors, cytokines and enzymes [149]. The finding that CAFs, originated from

healthy prostatic and dermal fibroblasts, transfer a greater amount of proteins to neighbouring cells compared to their healthy counterparts *(Figure 19A-B)*, suggests that this differential effect could represent another hallmark of CAFs phenotype. All the lines of tumor cells analyzed are able to increase fibroblasts potential for horizontal protein transfer, but the modulation of this activation depends on the type of tumor cell. In fact, despite DU145 and PC3 cell lines are both models of prostate cancer, they regulate this phenomenon in different ways. In particular, while fibroblasts activated by DU145 increase their transfer ability of 1.54 fold, the amount of proteins transferred from PC3-activated fibroblasts is clearly much higher (the transfer increase is about 2.66 fold) *(Figure 19A)*. The A375-mediated modulation of fibroblasts potential transfer, instead, is similar to that of DU145 *(Figure 19B)*. Since the functional conversion of fibroblasts was performed with tumor cells conditioned medium, our hypothesis is that the different form of regulation could be due to a diverse tumor cells secretion profile both in qualitative and quantitative terms. The different degree of modulation mediated by prostatic cancer cells conditioned medium is consistent with data showed in *Table IV*, where CAFs transferred a greater amount of their total protein mass when cocultured with PC3 rather than DU145.

The 2DE analysis of radioactively labeled CAFs and DU145 separated after being cocultured *(Figure 20A-D)*, allowed us to identified the transferred proteins *(Table VII)* and to discover that this phenomenon is highly specific *(Tables V-VI)*. CAFs proteins transferred to DU145 are involved in the generation of precursor metabolites and energy, or are structural proteins associated with cellular movement *(Figure 21)*. The quantitative analysis of 10 protein spots selected among the transferred proteins shows that thioredoxin, galectin-1, SOD-2 (mitochondrial isoform) and malate dehydrogenase (cytoplasmic isoform) were specifically enriched, while phosphoglycerate mutase 1 and calreticulin were lowered compared to their relative content in CAFs, suggesting that protein transfer is a selective and not random event *(Tables V-VI)*.

Further, we reveal that CAFs-secreted MVs play a key role as vehicles in this particular form of communication. CAFs of prostatic origin are able to produce two subtypes of vesicles: the larger ones were prepared from the whole culture supernatant by centrifugation at 10,000 xg, have an average diameter of 953.3 ± 168.8 nm *(Figure 22A-B)*, and are rich in proteins with a molecular weight lower than 58 kDa *(Figure 23A-B)*. The smaller ones, obtained by centrifugation at 100,000 xg, include a population less homogeneous, where the prevailing fraction has a diameter of 20 ± 1.252 nm *(Figure 22C-D)*. Surprisingly, these vesicles are

richer in proteins with a molecular weight greater than about 40 kDa *(Figure 23A-B)*, which, given the small size of these vesicles, might correspond mainly to integral membrane proteins.

Our results show that, between the two subtypes of particles, MVs represent a means for the paracrine communication between fibroblasts and tumor cells. They, in fact, contain many proteins previously identified, including SOD-2 (mitochondrial isoform), GAPDH, α-enolase, tubulin, vimentin, M2 splice isoform of pyruvate kinase, and not the M1 isoform which, on the contrary, is more expressed in exosome-like vesicles, but is not present among the transferred proteins, thus strengthening our hypothesis *(Figure 23C and Table VII)*. Further evidence of MVs participation in protein transport from CAFs to DU145 comes from vimentin. In particular, we found that vimentin profile in DU145 autoradiography *(Figure 20D)* is similar to that observed in MVs by Western blot analysis *(Figure 23C)*. The various spots and bands displayed in both images may correspond to different glycosylated or phosphorylated forms of vimentin *(Figures 20D and 23C)*.

Since MVs shed directly from the plasma membrane, we hypothesized that the selective enrichment of some proteins compared to other depends on their uneven spatial distribution within cytoplasm. Therefore, the specific selection of certain proteins may be due to their prevalent localization close to the plasma membrane regions where vesicles bud. The inclusion of mitochondrial proteins inside the vesicles (such as SOD-2, malate dehydrogenase and ATP synthase β subunit), instead, may occur during their mitochondrial-targeting signal peptide-mediated transport.

The functional role of the passage of these proteins has been confirmed by cell proliferation experiments *(Figure 24)*. We found that DU145 increase their growth rate of about 8% when cultured in starvation medium supplemented only with MVs, suggesting that, besides to soluble factors-mediated cellular crosstalk, also membranous vesicles have a part in the pro-proliferative effect observed in tumor cells-CAFs coculture *(Figure 15A-B)*. It is noteworthy that this effect could be lower compared to what could be achieved in the presence of a continuous production of vesicles by fibroblasts in coculture condition *(Figure 15A-B)*.

In addition, recently Angelucci *et al.* showed that vimentin protein levels was clearly induced in the low-invasive MCF7 cell line cocultured with CAFs, and thus the epithelial mesenchymal transition is activated [648]. According to the observation that cells by capturing protein cargo contained within these vesicles can extend their transcriptome, it is possible that, besides the up-regulated gene-expression, fibroblasts-secreted MVs transfer vimentin to tumor cells by sustaining the increase

of its protein levels. Indeed, in DU145 autoradiography 5 of the 24 spots analyzed were identified as vimentin, which therefore is strongly represented *(Figure 20D and Table VII)*.

In summary, these data reveal a novel role of fibroblasts in the context of the tumor microenvironment, which could represent a general property related to the trophic function of connective tissue. In fact, in the simplest hypothesis, fibroblasts support the survival and proliferation of neighbouring cells (which may be not only tumor cells, but also healthy cells) by releasing soluble growth factors and, simultaneously, transfer them vesicles laden of proteins and lipids. On one hand, growth factors stimulate cell growth and proliferation; on the other hand, protein and lipid cargo present into vesicles could increase the rate of mass accumulation to the lower limit necessary for cell division.

REFERENCES

1. Loeb LA, Springgate CF and Battula N. Errors in DNA replication as a basis of malignant changes. 1974 Cancer Res **34**(9): 2311-2321;
2. Lengauer C, Kinzler KW and Vogelstein B. Genetic instabilities in human cancers. 1998 Nature **396**(6712): 643-649;
3. Cahill DP, Kinzler KW, Vogelstein B and Lengauer C. Genetic instability and darwinian selection in tumours. 1999 Trends Cell Biol **9**(12): M57-60;
4. Loeb LA. Mutator phenotype in cancer: origin and consequences. 2010 Semin Cancer Biol **20**(5): 279-280;
5. Nowell PC. The clonal evolution of tumor cell populations. 1976 Science **194**(4260): 23-28;
6. Tomlinson IP, Novelli MR and Bodmer WF. The mutation rate and cancer. 1996 Proc Natl Acad Sci USA **93**(25): 14800-14803;
7. Tomlinson I and Bodmer W. Selection, the mutation rate and cancer: ensuring that the tail does not wag the dog. 1999 Nat Med **5**(1): 11-12;
8. Fialkow PJ. Clonal origin of human tumors. 1976 Biochim Biophys Acta **458**(3): 283-321;
9. Fidler IJ and Kripke ML. Metastasis results from preexisting variant cells within a malignant tumor. 1977 Science **197**(4306): 893-895;
10. Jordan CT, Guzman ML and Noble M. Cancer stem cells. 2006 N Engl J Med **355**(12): 1253-1261;
11. Lapidot T, Sirard C, Vormoor J, Murdoch B, Hoang T, Caceres-Cortes J, Minden M, Paterson B, Caligiuri MA and Dick JE. A cell initiating human acute myeloid leukaemia after transplantation into SCID mice. 1994 Nature **367**(6464): 645-648;
12. Bonnet D and Dick JE. Human acute myeloid leukaemia is organized as a hierarchy that originates from a primitive hematopoietic cell. 1997 Nat Med **3**(7): 730-737;
13. Singh SK, Hawkins C, Clarke ID, Squire JA, Bayani J, Hide T, Henkelman RM, Cusimano MD and Dirks PB. Identification of human brain tumour initiating cells. 2004 Nature **432**(7015): 396-401;
14. Al-Hajj M, Wicha MS, Benito-Hernandez A, Morrison SJ and Clarke MF. Prospective identification of tumorigenic breast cancer cells. 2003 Proc Natl Acad Sci USA **100**(7): 3983-3988. [Erratum in, Proc Natl Acad Sci USA 2003; **100**(11):6890];
15. Chen X, Rycaj K, Liu X and Tang DG. New insight into prostate cancer stem cells. 2013 Cell Cycle **12**(4): 579-586;
16. Jamieson CH, Ailles LE, Dylla SJ, Muijtjens M, Jones C, Zehnder JL, Gotlib J, Li K, Manz MG, Keating A, Sawyers CL and Weissman IL. Granulocyte-macrophage progenitors as candidate leukemic stem cells in blast-crisis CML. 2004 N Engl J Med **351**(7): 657-667;
17. Cozzio A, Passegué E, Ayton PM, Karsunky H, Cleary ML and Weissman IL. Similar MLL-associated leukemias arising from self-renewing stem cells and short-lived myeloid progenitors. 2003 Genes Dev **17**(24): 3029-3035;
18. Huntly BJ, Shigematsu H, Deguchi K, Lee BH, Mizuno S, Duclos N, Rowan R, Amaral S, Curley D, Williams IR, Akashi K and Gilliland DG. MOZ-TIF2, but not BCR-ABL, confers properties of leukemic stem cells to committed murine hematopoietic progenitors. 2004 Cancer Cell **6**(6): 587-596;
19. Krivtsov AV, Twomey D, Feng Z, Stubbs MC, Wang Y, Faber J, Levine JE, Wang J, Hahn WC, Gilliland DG, Golub TR and Armstrong SA. Transformation from committed progenitor of leukaemia stem cell initiated by MLL-AF9. 2006 Nature **442**(7104): 818-22;
20. Nowell PC. Tumor progression: a brief historical perspective. 2002 Semin Cancer Biol **12**(4): 261-266;
21. Weinberg RA. The molecular basis of oncogenes and tumor suppressor genes. 1995 Ann NY Acad Sci **758**: 331-338;
22. Esteller M, Corn PG, Baylin SB and Herman JG. A gene hypermethylation profile of human cancer. 2001 Cancer Res **61**(8): 3225-3229;
23. Hanahan D and Weinberg RA. The hallmarks of cancer. 2000 Cell **100**(1): 57-70;
24. Hanahan D and Weinberg RA. Hallmarks of cancer: the next generation. 2011Cell **144**(5): 646-674;
25. Evan G and Littlewood T. A matter of life and cell death. 1998 Science **281**(5381): 1317-1322;
26. Hayflick L. Mortality and immortality at the cellular level. A review. 1992 Biochemistry (Mosc) **62**(11): 1180-1190;
27. Fedi P, Tronick SR and Aaronson SA, Growth factors. 1997 In cancer medicine, Holland JF, Bast RC, Morton DL, Frei E, Kufe DW and Weichselbaum RR, (eds) Williams and Wilkins: Baltimore, MD, pp 41-64;
28. Lukashev ME and Werb Z. ECM signaling: orchestrating cell behaviour and misbehaviour. 1998 Trends Cell Biol **8**(11): 437-441;
29. Giancotti FG and Ruoslahti E. Integrin signaling. 1999 Science **285**(5430): 1028-1032;

30. Medema RH and Bos JL. The role of p21ras in receptor tyrosine kinase signaling. 1993 Crit Rev Oncog **4**(6): 615-661;
31. Burkhart DL and Sage J. Cellular mechanisms of tumour suppression by the retinoblastoma gene. 2008 Nat Rev Cancer **8**(9): 671-682;
32. Deshpande A, Sicinski P and Hinds PW. Cyclins and cdks in development and cancer: a perspective. 2005 Oncogene **24**(17): 2909-2915;
33. Sherr CJ and McCormick F. The RB and p53 pathways in cancer. 2000 Cancer Cell **2**(2): 103-112;
34. Harris CC. p53 tumor suppressor gene: from the basic research laboratory to the clinic--an abridged historical perspective. 1996 Carcinogenesis **17**(6): 1187-1198;
35. Levine AJ. p53, the cellular gatekeeper for growth and division. 1997 Cell **88**(3): 323-331;
36. Bryan TM and Cech TR. Telomerase and the maintenance of chromosome ends. 1999 Curr Opin Cell Biol **11**(3): 318-324;
37. Bryan TM, Englezou A, Gupta J, Bacchetti S and Reddel RR. Telomere elongation in immortal human cells without detectable telomerase activity. 1995 EMBO J **14**(17): 4240-4248;
38. Bouck N, Stellmach V and Hsu SC. How tumors become angiogenic. 1996 Adv Cancer Res **69**: 135-174;
39. Hanahan D and Folkman J. Patterns and emerging mechanisms of the angiogenic switch during tumorigenesis. 1996 Cell **86**(3): 353-364;
40. Folkman J. Tumor angiogenesis. 1997 In cancer medicine, Holland JF, Bast RC, Morton DL, Frei E, Kufe DW and Weichselbaum RR, (eds) Williams and Wilkins: Baltimore, MD, pp 181-204;
41. Ferrara N. Vascular endothelial growth factor. 2009 Arterioscler Thromb Vasc Biol **29**(6): 789-791;
42. Mac Gabhann F and Popel AS. Systems biology of vascular endothelial growth factors. 2008 Microcirculation **15**(8): 715-738;
43. Carmeliet P. VEGF as a key mediator of angiogenesis in cancer. 2005 Oncology **69**(Suppl 3): 4-10;
44. Baeriswyl V and Christofori G. The angiogenic switch in carcinogenesis. 2009 Semin Cancer Biol **19**(5): 329-337;
45. Kazerounian S, Yee KO and Lawler J. Thrombospondins in cancer. 2008 Cell Mol Life Sci **65**(5): 700-712;
46. Singh RK, Gutman M, Bucana CD, Sanchez R, Llansa N and Fidler IJ. Interferons alpha and beta down-regulate the expression of basic fibroblasts growth factor in human carcinomas. 1995 Proc Natl Acad Sci USA **92**(10): 4562-4566;
47. Volpert OV, Dameron KM and Bouck N. Sequential development of an angiogenic phenotype by human fibroblasts progressing to tumorigenicity. 1997 Oncogene **14**(12): 1495-1502;
48. Nagy JA, Chang SH, Shih SC, Dvorak AM and Dvorak HF. Heterogeneity of the tumor vasculature. 2010 Semin Thromb Hemost **36**(3): 321-331;
49. Baluk P, Hashizume H and McDonald DM. Cellular abnormalities of blood vessels as targets in cancer. 2005 Curr Opin Genet Dev **15**(1): 102-111;
50. Talmadge JE and Fidler IJ. AARC centennial series: the biology of cancer metastasis: historical perspective. 2010 Cancer Res **70**(14): 5649-5669;
51. Fidler IJ. The pathogenesis of cancer metastasis: the 'seed and soil' hypothesis revisited. 2003 Nat Rev Cancer **3**(6): 453-458;
52. Sporn MB. The war on cancer. 1996 Lancet **347**(9012): 1377-1381;
53. Christofori G and Semb H. The role of the cell-adhesion molecule E-cadherin as a tumor-suppressor gene. 1999 Trends Biochem Sci **24**(2): 73-76;
54. Berx G and van Roy F. Involvement of members of the cadherin superfamily in cancer. 2009 Cold Spring Harb Perspect Biol **1**(6): a003129;
55. Cavallaro U and Christofori G. Cell adhesion and signalling by cadherin and Ig-CAMs in cancer. 2004 Nat Rev Cancer **4**(2): 118-132;
56. Klymkowsky MW and Savagner P. Epithelial-mesenchymal transition: a cancer researcher's conceptual friend and foe. 2009 Am J Pathol **174**(5): 1588-1593;
57. Polyak K and Weinberg RA. Transitions between epithelial and mesenchymal states: acquisition of malignant and stem cells traits. 2009 Nat Rev Cancer **9**(4): 265-273;
58. Thiery JP, Acloque H, Huang RY and Nieto MA. Epithelial-mesenchymal transitions in development and disease. 2009 Cell **139**(5): 871-890;
59. Yilmaz M and Christofori G. EMT, the cytoskeleton, and cancer cell invasion. 2009 Cancer Metastasis Rev **28**(1-2): 15-33;
60. Barrallo-Gimeno A and Nieto MA. The Snail genes as inducers of cell movement and survival: implications in development and cancer. 2005 Development **132**(14): 3151-3161;
61. Brabletz T, Jung A, Spaderna S, Hlubek F and Kirchner T. Opinion: migrating stem cells – an integrated concept of malignant tumor progression. 2005 Nat Rev Cancer **5**(9): 744-749;
62. Watnick RS. The role of the tumor microenvironment in regulating angiogenesis. 2012 Cold Spring Harb Perspect Med **2**(12): a006676;

63. Sounni NE and Noel A. Targeting the tumor microenvironment for cancer therapy. 2013 Clin Chem **59**(1):85-93;
64. Ansell SM and Vonderheide RH. Cellular composition of the tumor microenvironment. 2013 Am Soc Clin Oncol Educ Book **2013**: 91-97;
65. Hu M and Polyak K. Molecular characterization of the tumour microenvironment in breast cancer. 2008 Eur J Cancer **44**(18): 2760-2765;
66. De Wever O, Demetter P, Mareel M and Bracke M. Stromal myofibroblasts are drivers of invasive cancer growth. 2008 Int J Cancer **123**(10): 2229-2238;
67. Gangadhara S, Barrett-Lee P, Nicholson RI and Hiscox S. Pro-metastatic tumor-stroma interactions in breast cancer. 2012 Future Oncol **8**(11): 1427-1442;
68. Quail DF and Joyce JA. Microenvironment regulation of tumor progression and metastasis. 2013 Nat Med **19**(11): 1423-1437
69. Tarin D and Croft CB. Ultrastructure features of wound healing in mouse skin. 1969 J Anat **105**(Pt 1): 189-190;
70. Tomasek JJ, Gabbiani G, Hinz B, Chaponnier C and Brown RA. Myofibroblasts and mechano-regulation of connective tissue remodelling. 2002 Nat Rev Mol Cell Biol **3**(5): 349-363;
71. Rodemann HP and Müller GA. Characterization of human renal fibroblasts in health and disease: II. *In vitro* growth, differentiation, and collagen synthesis of fibroblasts from kidneys with interstitial fibrosis. 1991 Am J Kidney Dis **17**(6): 684-686;
72. Chang HY, Chi JT, Dudoit S, Bondre C, van de Rijn M, Botstein D and Brown PO. Diversity, topographic differentiation, and positional memory in human fibroblasts. 2002 Proc Natl Acad Sci USA **99**(20): 12877-12882;
73. Simian M, Hirai Y, Navre M, Werb Z, Lochter A and Bissell MJ. The interplay of matrix metalloproteinases, morphogenesis and growth factor is necessary for branching of mammary epithelial cells. 2001 Development **128**(16): 3117-3131;
74. Wiseman BS and Werb Z. Stromal effects on mammary gland development and breast cancer. 2002 Science **296**(5570): 1046-1049;
75. Personage G, Filer AD, Haworth O, Nash GB, Rainger GE, Salmon M and Buckley CD. A stromal address code defined by fibroblast. 2005 Trends Immunol **26**(3): 150-156;
76. Provenzano PP, Heisey D, Hayashi K, Lakes R and Vanderby R Jr. Subfailure damage in ligament: a structural and cellular evaluation. 2002 J Appl Physiol **92**(1): 362-371;
77. Gabbiani G. The myofibroblast in wound healing and fibrocontractive disease. 2003 J Pathol **200**(4): 500-503;
78. Gabbiani G, Ryan GB and Majne G. Presence of modified fibroblasts in granulation tissue and their possible role in wound contraction. 1971 Experientia **27**(5): 549-550;
79. Castor CW, Wilson SM, Heiss PR and Seidman JC. Activation of lung connective tissue cells in vitro. 1979 Am Rev Respir Dis **120**(1): 101-106;
80. Zeisberg M, Strutz F and Müller GA. Role of fibroblast activation in inducing interstitial fibrosis. 2000 J Nephrol **13** (Supp 3), S111-120;
81. Clayton A, Evans RA, Pettit E, Hallett M, Williams JD and Steadman R. Cellular activation through the ligation of intercellular adhesion molecules-1. 1998 J Cell Sci **111**(Pt 4): 443-453;
82. Kalluri R and Zeisberg M. Fibroblasts in cancer. 2006 Nat Rev Cancer **6**(5): 392-401;
83. Pietras K and Ostman A. Hallmarks of cancer: interactions with the tumor stroma. 2010 Exp Cell Res **316**(8): 1324-1331;
84. Mueller MM and Fusenig NE. Friends or foes – bipolar effects of the tumour stroma in cancer. 2004 Nat Rev Cancer **4**(11): 839-849;
85. Barsky SH, Green WR, Grotendorst GR and Liotta LA. Desmoplastic breast carcinoma as a source of human myofibroblasts. 1984 Am J Pathol **115**(3): 329-333;
86. Dvorak HF. Tumors: wounds that do not heal. Similarities between tumor stroma generation and wound healing. 1986 N Engl J Med **315**(26): 1650-1659;
87. Sugimoto H, Mundel TM, Kieran MW and Kalluri R. Identification of fibroblasts heterogeneity in the tumor microenvironment. 2006 Cancer Biol Ther **5**(12): 1640-1646;
88. Anderberg C, Li H, Fredriksson L, Andrae J, Betsholtz C, Li X, Eriksson U and Pietras K. Paracrine signaling by platelet-derived growth factor-CC promotes tumor growth by recruitment of cancer-associated fibroblasts. 2009 Cancer Res **69**(1): 369-378;
89. Mueller L, Goumas FA, Affeldt M, Sandtner S, Gehling UM, Brilloff S, Walter J, Karnatz N, Lamszus K, Rogiers X and Broering DC. Stromal fibroblasts in colorectal liver metastases originate from resident fibroblasts and generate an inflammatory microenvironment. 2007 Am J Pathol **171**(5): 1608-1618;
90. Gallagher PG, Bao Y, Prorock A, Zigrino P, Nischt R, Politi V, Mauch C, Dragulev B and Fox JW. Gene expression profiling reveals cross-talk between melanoma and fibroblasts: implications for host-tumor interactions in metastasis. 2005 Cancer Res **65**(10): 4134-4146;
91. Buess M, Nuyten DS, Hastie T, Nielsen T, Pesich R and Brown PO. Characterization of heterotypic interaction effects in vitro to deconvolute global gene expression profiles in cancer. 2007 Genome Biol **8**(9): R191;

92. Pittenger MF, Mackay AM, Beck SC, Jaiswal RK, Douglas R, Mosca JD, Moorman MA, Simonetti DW, Craig S and Marshak DR. Multilineage potential of adult human mesenchymal stem cells. 1999 Science **284**(5411): 143-147;
93. Ziegelhoeffer T, Fernandez B, Kostin S, Heil M, Voswinckel R, Helisch A and Schaper W. Bone marrow-derived cells do not incorporate into the adult growing vasculature. 2004 Circ Res **94**(2): 230-238;
94. Hung SC, Deng WP, Yang WK, Liu RS, Lee CC, Su TC, Lin RJ, Yang DM, Chang CW, Chen WH, Wei HJ and Gelovani JG. Mesenchymal stem cells targeting of microscopic tumors and tumor stroma development monitored by noninvasive in vivo positron emission tomography imaging. 2005 Clin Cancer Res **11**(21): 7749-7756;
95. Kidd S, Spaeth E, Dembinski JL, Dietrich M, Watson K, Klopp A, Battula VL, Weil M, Andreeff M and Marini FC. Direct evidence of mesenchymal stem cell tropism for tumor and wounding microenvironments using in vivo bioluminescent imaging. 2009 Stem Cells **27**(10): 2614-2623;
96. Hall B, Andreeff M and Marini F. The participation of mesenchymal stem cells in tumor stroma formation and their application as targeted-gene delivery vehicles. 2007 Handb Exp Pharmacol **180**: 263-283;
97. Mishra PJ, Humeniuk R, Medina DJ, Alexe G, Mesirov JP, Ganesan S, Glod JW and Banerjee D. Carcinoma-associated fibroblast-like differentiation of human mesenchymal stem cells. 2008 Cancer Res **68**(11): 4331-4339;
98. Spaeth EL, Dembinski JL, Sasser AK, Watson K, Klopp A, Hall B, Andreff M and Marini F. Mesenchymal stem cells transition to tumor-associated fibroblasts contributes to fibrovascular network expansion and tumor progression. 2009 PloS One **4**(4): e4992;
99. Dwyer RM, Potter-Beirne SM, Harrington KA, Lowery AJ, Hennessy E, Murphy JM, Barry FP, O'Brien T and Kerin MJ. Monocyte chemotactic protein-1 secreted by primary breast tumors stimulates migration of mesenchymal stem cells. 2007 Clin Cancer Res **13**(17): 5020-5027;
100. Spaeth E, Klopp A, Dembinski J, Andreeff M and Marini F. Inflammation and tumor microenvironments: defining the migratory itinerary of mesenchymal stem cells. 2008 Gene Ther **15**(10): 730-738;
101. Feng B and Chen L. Review of mesenchymal stem cells and tumors: executioner or coconspirator? 2009 Cancer Biother Radiopharm **24**(6): 717-721;
102. Ishii G, Sangai T, Oda T, Aoyagi Y, Hasebe T, Kanomata N, Endoh Y, Okumura C, Okuhara Y, Magae J, Emura M, Ochiya T and Ochiai A. Bone-marrow-derived myofibroblasts contribute to the cancer-induced stromal reaction. 2003 Biochem Biophys Res Commun **309**(1): 232-240;
103. Abangan RS Jr, Williams CR, Mehrotra M, Duncan JD and Larue AC. MCP1 directs trafficking of hematopoietic stem cell-derived fibroblast precursors in solid tumor. 2010 Am J Pathol **176**(4): 1914-1926;
104. Rønnov-Jessen L and Petersen OW. Induction of alpha-smooth muscle actin by transforming growth factor-beta 1 in quiescent human breast gland fibroblasts. Implications for myofibroblast generation in breast neoplasia. 1993 Lab Invest **68**(6): 696-707;
105. Hong KM, Belperio JA, Keane MP, Burdick MD and Strieter RM. Differentiation of human circulating fibrocytes as mediated by transforming growth factor-beta and peroxisome proliferator-activated receptor gamma. 2007 J Biol Chem **282**(31): 22910-22920;
106. Abe R, Donnelly SC, Peng T, Bucala R and Metz CN. Peripheral blood fibrocytes: differentiation pathway and migration to wound sites. 2001 J Immunol **166**(12): 7556-7562;
107. Jotzu C, Alt E, Welte G, Li J, Hennessy BT, Devarajan E, Krishnappa S, Pinilla S, Droll L and Song YH. Adipose tissue-derived stem cells differentiate into carcinoma-associated fibroblast-like cells under the influence of tumor-derived factors. 2010 Anal Cell Pathol (Amst) **33**(2): 61-79;
108. Radisky DC, Kenny PA and Bissell MJ. Fibrosis and cancer: do myofibroblasts come also from epithelial cells via EMT? 2007 J Cell Biochem **101**(4): 830-839;
109. Zeisberg EM, Potenta S, Xie L, Zeisberg M and Kalluri R. Discovery of endothelial to mesenchymal transition as a source for carcinoma-associated fibroblasts. 2007 Cancer Res 67(21): 10123-10128;
110. Petersen OW, Nielsen HL, Gudjonsson T, Villadsen R, Rank F, Niebuhr E, Bissell MJ and Rønnov-Jessen L. Epithelial to mesenchymal transition in human breast cancer can provide a nonmalignant stroma. 2003 Am J Pathol **162**(2): 391-402;
111. Kalluri R and Weinberg RA. The basics of epithelial-mesenchymal transition. 2009 J Clin Invest **119**(6): 1420-1428;
112. Göritz C, Dias DO, Tomilin N, Barbacid M, Shupliakov O and Frisén J. A pericytes origin of spinal cord scar tissue. 2011 Science **333**(6039): 238-242;
113. Dulauroy S, Di Carlo SE, Langa F, Eberl G and Peduto L. Lineage tracing and genetic ablation of ADAM12(+) perivascular cells identify a major source of profibrotic cells during acute tissue injury. 2012 Nat Med **18**(8): 1262-1270;
114. Madar S, Goldstein I and Rotter V. "Cancer associated fibroblasts" – more than meets the eye. 2013 Trends Mol Med **19**(8): 447-453;
115. McDonald LT and LaRue AC. Hematopoietic stem cell derived carcinoma-associated fibroblasts: a novel origin. 2012 Int J Clin Exp Pathol **5**(9): 863-873;

116. Cirri P and Chiarugi P. Cancer-associated fibroblasts: the dark side of the coin. 2011 Am J Cancer Res **1**(4): 482-497;
117. Löhr M, Schmidt C, Ringel J, Kluth M, Müller P, Nizze H and Jesnowski R. Transforming growth factor-beta 1induces desmoplasia in an experimental model of human pancreatic carcinoma. 2001 Cancer Res **61**(2): 550-555;
118. Bronzert DA, Pantazis P, Antoniades HN, Kasid A, Davidson N, Dickson RB and Lippman ME. Synthesis and secretion of platelet-derived growth factor by human breast cancer cell lines. 1987 Proc Natl Acad Sci USA **84**(16): 5763-5767;
119. Shao ZM, Nguyen M and Barsky SH. Human breast carcinoma desmoplasia is PDGF initiated. 2000 Oncogene **19**(38): 4337-4345;
120. Strutz F, Zeisberg M, Hemmerlein B, Sattler B, Hummel K, Becker V and Müller GA. Basic fibroblasts growth factor expression is increased in human renal fibrogenesis and may mediate autocrine fibroblast proliferation. 2000 Kidney Int **57**(4): 1521-1538;
121. Giannoni E, Bianchini F, Masieri L, Serni S, Torre E, Calorini L, and Chiarugi P. Reciprocal activation of prostate cancer cells and cancer-associated fibroblasts stimulates epithelial-mesenchymal transition and cancer stemness. 2010 Cancer Res **70**(17): 6945-6956;
122. Olumi AF, Grossfeld GD, Hayward SW, Carroll PR, Tlsty TD and Cunha GR. Carcinoma-associated fibroblasts direct tumor progression of initiated human prostatic epithelium. 1999 Cancer Res **59**(19): 5002-5011;
123. Bhowmick NA, Neilson EG and Moses HL. Stromal fibroblasts in cancer initiation and progression. 2004 Nature **432**(7015): 332-337;
124. Strnad H, Lacina L, Kolár M, Cada Z, Vleck C, Dvoránková B, Betka J, Plzák J, Chovanec M, Sáchová J, Valach J, Urbanová M and Smetana K Jr. Head and neck squamous cancer stromal fibroblasts produce growth factors influencing phenotype of normal human keratinocytes. 2010 Histochem Cell Biol **133**(2): 201-211;
125. LeBedis C, Chen K, Fallavollita L, Boutros T, Brodt P. Peripheral lymph node stromal cells can promote growth and tumorigeniciy of breast carcinoma cells through the release of IGF-1 and EGF. 2002 Int J Cancer **100**(1): 2-8;
126. Levental KR, Yu H, Kass L, Lakins JN, Egeblad M, Erler JT, Fong SF, Csiszar K, Giaccia A, Weninger W, Yamauchi M, Gasser DL and Weaver VM. Matrix crosslinking forces tumor progression by enhancing integrin signaling. 2009 Cell **139**(5): 891-906;
127. Chun TH, Hotary KB, Sabeh F, Saltiel AR, Allen ED and Weiss SJ. A pericellular collagenase directs the 3-dimensional development of white adipose tissue. 2006 Cell **125**(3): 577- 591;
128. Paszek MJ, Zahir N, Johnson KR, Lakins JN, Rozenberg GI, Gefen A, Reinhart-King CA, Margulies SS, Dembo M, Boettiger D, Hammer DA and Weaver VM. Tensional homeostasis and the malignant phenotype. 2005 Cancer Cell **8**(3): 241-254;
129. Santhanam AN, Baker AR, Hegamyer G, Kirschmann DA, and Colburn NH. Pdcd4 repression of lysyl oxidase inhibits hypoxia-induced breast cancer cell invasion. 2010 Oncogene **29**(27): 3921-3932;
130. Egeblad M, Rasch MG and Weaver VM. Dynamic interplay between the collagen scaffold and tumor evolution. 2010 Curr Opin Cell Biol **22**(5): 697-706;
131. Sidenius N and Blasi F. The urokinase plasminogen activator system in cancer: recent advances and implication for prognosis and therapy. 2003 Cancer Metastasis Rev **22**(2-3): 205-222;
132. Hynes RO. The extracellular matrix: not just pretty fibrils. Science 2009 **326**(5957): 1216-1219;
133. Roy R, Yang J, and Moses MA. Matrix metalloproteinases as novel biomarkers and potential therapeutic targets in human cancer. 2009 J Clin Oncol **27**(31): 5287-5297;
134. Boire A, Covic L, Agarwal A, Jacques S, Sherifi S and Kuliopulos A. PAR1 ia a matrix metalloprotease-1 receptor that promotes invasion and tumorigenesis of breast cancer cells. 2005 Cell **120**(3): 303-313;
135. Lochter A, Galosy S, Muschler J, Freedman N, Werb Z and Bissell MJ. Matrix metalloproteinase stromelysin-1 triggers a cascade of molecular alterations that leads to stable epithelial-to-mesenchymal conversion and a premalignant phenotype in mammary epithelial cells. 1997 J Cell Biol **139**(7): 1861-1872;
136. Lederle W, Hartenstein B, Meides A, Kunzelmann H, Werb Z, Angel P and Mueller MM. MMP13 as a stromal mediator in controlling persistent angiogenesis in skin carcinoma. 2010 Carcinogenesis **31**(7): 1175-1184;
137. Smith HW and Marshall CJ. Regulation of cell signalling by uPAR. 2010 Nat Rev Mol Cell Biol **11**(1): 23-36;
138. Carmeliet P, Moons L, Lijnen R, Baes M, LemaÎtre V, Tipping P, Drew A, Eeckhout Y, Shapiro S, Lupu F and Collen D. Urokinase-generated plasmin activates matrix metalloproteinases during aneurysm formation. 1997 Nat Genet **17**(4): 439-444;
139. Zhou HM, Nichols A, Meda P and Vassalli JD. Urokinase-type plasminogen activator and its receptor synergize to promote pathogenic proteolysis. 2000 EMBO J **19**(17): 4817-4826;
140. Joyce JA and Pollard JW. Microenvironmental regulation of metastasis. 2009 Nat Rev Cancer **9**(4): 239-252;

141. Luga V, Zhang L, Viloria-Petit AM, Ogunjimi AA, Inanlou MR, Chiu E, Buchanan M, Hosein AN, Basik M and Wrana JL. Exosomes mediate stromal mobilization of autocrine Wnt–PCP signaling in breast cancer cell migration. 2012 Cell **151**(7): 1542-1556;
142. Kaplan RN, Riba RD, Zacharoulis S, Bramley AH, Vincent L, Costa C, MacDonald DD, Jin DK, Shido K, Kerns SA, Zhu Z, Hicklin D, Wu Y, Port JL, Altorki N, Port ER, Ruggero D, Shmelkov SV, Jensen KK, Rafii S and Lyden D. VEGFR1-positive haematopoietic bone marrow progenitors initiate the pre-metastatic niche. 2005 Nature **438**(7069): 820-827;
143. Erler JT, Bennewith KL, Cox TR, Lang G, Bird D, Koong A, Le QT and Giaccia AJ. Hypoxia-induced lysyl oxidase is a critical mediator of bone marrow-derived cell recruitment to form the premetastatic niche. 2008 Cancer Cell **15**(1): 35-44;
144. van Deventer HW, Wu QP, Bergstralh DT, Davis BK, O'Connor BP, Ting JP and Serody JS. C-C chemokine receptor 5 on pulmonary fibrocytes facilitates migration and promotes metastasis via matrix metalloproteinase 9. 2008 Am J Pathol **173**(1): 253-264;
145. Kaplan RN, Rafii S and Lyden D. Preparing the "soil": the premetastatic niche. 2006 Cancer Res **66**(23): 11089-11093;
146. Psaila B and Lyden D. The metastatic niche: adapting the foreign soil. 2009 Nat Rev Cancer **9**(4): 285-293;
147. Duda DG, Duyverman AM, Kohno M, Snuderl M, Steller EJ, Fukumura D and Jain RK. Malignant cells facilitate lung metastasis by bringing their own soil. 2010 Proc Natl Acad Sci U S A **107**(50): 21677-21682;
148. Sung SY, Hsieh CL, Law A, Zhau HE, Pathak S, Multani AS, Lim S, Coleman IM, Wu LC, Figg WD, Dahut WL, Nelson P, Lee JK, Amin MB, Lyles R, Johnstone PA, Marshall FF and Chung LW. Coevolution of prostate cancer and bone stroma in three-dimensional coculture: implications for cancer growth and metastasis. 2008 Cancer Res **68**(23): 9996-10003;
149. Räsänen K and Vaheri A. Activation of fibroblasts in cancer stroma. 2010 Exp Cell Res **316**(17): 2713-2722;
150. Gerber PA, Hippe A, Buhren BA, Müller A and Homey B. Chemokines in tumor-associated angiogenesis. 2009 Biol Chem **390**(12): 1213-1223;
151. Erez N, Truitt M, Olson P and Hanahan D. Cancer-associated fibroblasts are activated in incipient neoplasia to orchestrate tumor-promoting inflammation in an NF-kappaB-dependent manner. 2010 Cancer Cell **17**(2): 135-147;
152. Orimo A, Gupta PB, Sgroi DC, Arenzana-Seisdedos F, Delaunay T, Naeem R, Carey VJ, Richardson AL and Weinberg RA. Stromal fibroblasts present in invasive human breast carcinomas promote tumor growth and angiogenesis through elevated SDF-1/CXCL12 secretion. 2005 Cell **121**(3): 335-348;
153. Matsuo Y, Ochi N, Sawai H, Yasuda A, Takahashi H, Funahashi H, Takeyama H, Tong Z and Guha S. CXCL8/IL-8 and CXCL12/SDF-1alpha cooperatively promote invasiveness and angiogenesis in pancreatic cancer. 2009 Int J Cancer **124**(4): 853-861;
154. Augsten M, Hägglöf C, Olsson E, Stolz C, Tsagozis P, Levchenko T, Frederick MJ, Borg A, Micke P, Egevad L and Ostman A. CXCL14 is an autocrine growth factor for fibroblasts and acts as a multi-modal stimulator of prostate tumor growth. 2009 Proc Natl Acad Sci USA **106**(9): 3414-3419;
155. Jung DW, Che ZM, Kim J, Kim K, Kim KY, Williams D and Kim J. Tumor-stromal crosstalk in invasion of oral squamous cell carcinoma: a pivotal role of CCL7. 2010 Int J Cancer **127**(2): 332-344;
156. Koukourakis MI, Giatromanolaki A, Harris AL and Sivridis E. Comparison of metabolic pathways between cancer cells and stromal cells in colorectal carcinomas: a metabolic survival role for tumor-associated stroma. 2006 Cancer Res **66**(2): 632-637;
157. Warburg O. On the origin of cancer cells. 1956 Science **123**(3191): 309-314;
158. Warburg O. On respiratory impairment in cancer cells. 1956 Science **124**(3215): 269-270;
159. Warburg OH. The Metabolism of Tumours: Investigations from the Kaiser Wilhelm Institute for Biology, Berlin-Dahlem (London, UK: Arnold Constable) 1930;
160. Jones RG and Thompson CB. Tumor suppressors and cell metabolism: a recipe for cancer growth. 2009 Genes Dev **23**(5): 537-548;
161. DeBerardinis RJ, Lum JJ, Hatzivassiliou G and Thompson CB. The biology of cancer: metabolic reprogramming fuels cell growth and proliferation. 2008 Cell Metab **7**(1): 11-20;
162. Hsu PP and Sabatini DM. Cancer cell metabolism: Warburg and beyond. 2008 Cell **134**(5): 703-707;
163. Potter VR. The biochemical approach to the cancer problem. 1958 Fed Proc **17**(2): 691-697;
164. Vander Heiden MG, Cantley LC and Thompson CB. Understanding the Warburg effect: the metabolic requirements of cell proliferation. 2009 Science **324**(5930): 1029-1033;
165. Pavlides S, Whitaker-Menezes D, Castello-Cros R, Flomenberg N, Witkiewicz AK, Frank PG, Casimiro MC, Wang C, Fortina P, Addya S, Pestell RG, Martinez-Outschoorn UE, Sotgia F and Lisanti MP. The reverse Warburg effect: aerobic glycolysis in cancer associated fibroblasts and the tumor stroma. 2009 Cell Cycle **8**(23): 3984-4001;
166. Folkman J. Role of angiogenesis in tumor growth and metastasis. 2002 Semin Oncol **29**(6 Suppl 16): 15-18;

167. Sparmann A and Bar-Sagi D. Ras-induced interleukin-8 expression plays a critical role in tumor growth and angiogenesis. 2004 Cancer Cell **6**(5): 447-458;
168. Asahara T, Kalka C and Isner JM. Stem cell therapy and gene transfer for regeneration. 2000 Gene Ther **7**(6): 451-457;
169. Rafii S. Circulating endothelial precursors: mystery, reality, and promise. 2000 J Clin Invest **105**(1): 17-19;
170. Patan S, Munn LL and Jain RK. Intussusceptive microvascular growth in a human colon adenocarcinoma xenograft: a novel mechanism of tumor angiogenesis. 1996 Microvasc Res **51**(2): 260-272;
171. Patan S. Vasculogenesis and angiogenesis as mechanisms of vascular network formation, growth and remodeling. 2000 J Neurooncol **50**(1-2): 1-15;
172. Singh S and Kaur H. Tumor microenvironment: a review. 2013 J Oral Maxillofac Surg Med Pathol http://dx.doi.org/10.1016/j.ajoms.2012.12.011;
173. Raza A, Franklin MJ and Dudek AZ. Pericytes and vessels maturation during tumor angiogenesis and metastasis. 2010 Am J Hematol **85**(8): 593-598;
174. Bergers G and Song S. The role of pericytes in blood-vessels formation and maintenance. 2005 Neuro Oncol **7**(4): 452-464;
175. Hall AP. Review of the pericyte during angiogenesis and its role in cancer and diabetic retinopathy. 2006 Toxicol Pathol **34**(6): 763-775;
176. Abramsson A, Lindblom P and Betsholtz C. Endothelial and nonendothelial sources of PDGF-B regulate pericyte recruitment and influence vascular pattern formation in tumors. 2003 J Clin Invest **112**(8): 1142-1151;
177. Gerhardt H and Semb H. Pericytes: gatekeepers in tumor cell metastasis? 2008 J Mol Med (Berl) **86**(2): 135-144;
178. Sadler TE, Jones DE and Castro JE. The effects of altered phagocytic activity on growth of primary and metastatic tumor. 1977 In James K, McBride JB and Stuart A (Eds.), The macrophage and cancer (pp. 155-163). Edinburgh: Econoprint;
179. Mantovani A, Giavazzi R, Polentarutti N, Spreafico F and Garattini S. Divergent effects of macrophage toxins on growth of primary tumors and lung metastases in mice. 1980 Int J Cancer **25**(5): 617-620;
180. Ross J and Auger M. The biology of the macrophage. 2002 In Burke B and Lewis C (Eds.), The macrophage (2nd ed.). Oxford: Oxford University Press;
181. Mantovani A, Sica A and Locati M. New vistas on macrophage differentiation and activation. 2007 Eur J Immunol **37**(1): 14-16;
182. Ghassabeh GH, De Baetselier P, Brys L, Nöel W, Van Ginderachter JA, Meerschaut S, Beschin A, Brombacher F and Raes G. Identification of a common gene signature for type II cytokine-associated myeloid cells elicited in vivo in different pathologic conditions. 2006 Blood **108**(2): 575-583;
183. Mantovani A, Sica A, Sozzani S, Allavena P, Vecchi A and Locati M. The chemokine system in diverse forms of macrophage activation and polarization. 2004 Trends Immunol **25**(12): 677-686;
184. Talmadge JE, Donkor M and Scholar E. Inflammatory cell infiltration of tumors: Jekyll or Hyde. 2007 Cancer Metastasis Rev **26**(3-4): 373-400;
185. Mantovani A. The chemokine system: redundancy for robust outputs. 1999 Immunol Today **20**(6): 254-257;
186. Mantovani A. Effects on in vitro tumor growth of murine macrophages isolated from sarcoma lines differing in immunogenicity and metastasizing capacity. 1978 Int J Cancer **22**(6): 741-746;
187. Hagemann T, Wilson J, Burke F, Kulbe H, Li NF, Plüddemann A, Charles K, Gordon S and Balkwill FR. Ovarian cancer cells polarize macrophages toward a tumor-associated phenotype. 2006 J Immunol **176**(8): 5023-5032;
188. Hagemann T, Wilson J, Kulbe H, Li NF, Leinster DA, Charles K, Klemm F, Pukrop T, Binder C and Balkwill FR. Macrophages induce invasiveness of epithelial cancer cells via NF-kappa B and JNK. 2005 J Immunol **175**(2): 1197-1205;
189. Grouard G, Rissoan MC, Filgueira L, Durand I, Banchereau J and Liu YJ. The enigmatic plasmacytoid T cells develop into dendritic cells with interleukin (IL)-3 and CD40-ligand. 1997 J Exp Med **185**(6): 1101-1111;
190. Inaba K, Inaba M, Deguchi M, Hagi K, Yasumizu R, Ikehara S, Muramatsu S and Steinman RM. Granulocytes, macrophages, and dendritic cells arise from a common major histocompatibility complex class II-negative progenitor in mouse bone marrow. 1993 Proc Natl Acad Sci USA **90**(7): 3038-3042;
191. Curiel TJ, Cheng P, Mottram P, Alvarez X, Moons L, Evdemon-Hogan M, Wei S, Zou L, Kryczek I, Hoyle G, Lackner A, Carmeliet P and Zou W. Dendritic cell subsets differentially regulate angiogenesis in human ovarian cancer. 2004 Cancer Res **64**(16): 5535-5538;
192. Conejo-Garcia JR, Benencia F, Courreges MC, Kang E, Mohamed-Hadley A, Buckanovich RJ, Holtz DO, Jenkins A, Na H, Zhang L, Wagner DS, Katsaros D, Caroll R and Coukos G. Tumor-

infiltrating dendritic cells precursors recruited by a beta-defensin contribute to vasculogenesis under the influence of Vegf-A. 2004 Nat Med **10**(9): 950-958;
193. de Visser KE, Eichten A and Coussens LM. Paradoxical roles of the immune system during cancer development. 2006 Nat Rev Cancer **6**(1): 24-37;
194. Kessenbrock K, Plaks V and Werb Z. Matrix metalloproteinases: regulators of the tumour microenvironment. 2010 Cell **141**(1): 52-67;
195. Almand B, Clark JI, Nikitina E, van Beynen J, English NR, Knight SC, Carbone DP and Gabrilovich DI. Increased production of immature myeloid cells in cancer patients: a mechanism of immunosuppression in cancer. 2001 J Immunol **166**(1): 678-689;
196. Diaz-Montero CM, Salem ML, Nishimura MI, Garrett-Mayer E, Cole DJ and Montero AJ. Increased circulating myeloid-derived suppressor cells correlate with clinical cancer stage, metastatic tumor burden, and doxorubicin-cyclophosphamide chemotherapy. 2009 Cancer Immunol Immunother **58**(1): 49-59;
197. Gabrilovich D. Mechanisms and functional significance of tumour-induced dendritic-cell defects. 2004 Nat Rev Immunol **4**(12): 941-952;
198. Marigo I, Dolcetti L, Serafini P, Zanovello P and Bronte V. Tumor-induced tolerance and immune suppression by myeloid derived suppressor cells. 2008 Immunol Rev **222**: 162-179;
199. Marx J. Cancer immunology. Cancer's bulwark against immune attack: MDS cells. 2008 Science **319**(5860): 154-156;
200. Nielsen BS, Timshel S, Kjeldsen L, Sehested M, Pyke C, Borregaard N and Danø K. 92 kDa type IV collagenase (MMP-9) is expressed in neutrophils and macrophages but not in malignant epithelial cells in human colon cancer. 1996 Int J Cancer **65**(1): 57-62;
201. Bellocq A, Antoine M, Flahault A, Philippe C, Crestani B, Bernaudin JF, Mayaud C, Milleron B, Baud L and Cadranel J. Neutrophil alveolitis in bronchioloalveolar carcinoma: induction by tumor-derived interleukin-8 and relation to clinical outcome. 1998 Am J Pathol **152**(1): 83-92;
202. Mentzel T, Brown LF, Dvorak HF, Kuhnen C, Stiller KJ, Katenkamp D and Fletcher CD. The association between tumour progression and vascularity in myxofibrosarcoma and myxoid/round cell liposarcoma. 2001 Virchows Arch **438**(1): 13-22;
203. Mhawech-Fauceglia P, Kaya G, Sauter G, McKee T, Donze O, Schwaller J and Huard B. The source of APRIL up-regulation in human solid tumors lesions. 2006 J Leukoc Biol **80**(4): 697-704;
204. Xie K. Interleukin-8 and human cancer biology. 2001 Cytokine Growth Factor Rev **12**(4): 375-391;
205. Coussens LM and Werb Z. Matrix metalloproteinases and the development of cancer. 1996 Chem Biol **3**(11): 895-904;
206. Gaudry M, Brégerie O, Andrieu V, El Benna J, Pocidalo MA and Hakim J. Intracellular pool of vascular endothelial growth factor in human neutrophils. 1997 Blood **90**(10): 4153-4161;
207. Di Carlo E, Forni G, Lollini P, Colombo MP, Modesti A and Musiani P. The intriguing role of polymorphonuclear neutrophils in antitumor reactions. 2001 Blood **97**(2): 339-345;
208. Ai S, Cheng XW, Inoue A, Nakamura K, Okumura K, Iguchi A, Murohara T and Kuzuya M. Angiogenic activity of bFGF and VEGF suppressed by proteolytic cleavage by neutrophil elastase. 2007 Biochem Biophys Res Commun **364**(2): 395-401;
209. Scapini P, Nesi L, Morini M, Tanghetti E, Belleri M, Noonan D, Presta M, Albini A and Cassatella MA. Generation of biologically active angiostatin kringle 1-3 by activated human neutrophils. 2002 J Immunol **168**(11): 5798-5804;
210. West JB. Pulmonary physiology and pathophysiology: an integrated, case-based approach. 2007 Lippincott Williams & Wilkins pp. 16;
211. Vaupel P and Harrison L. Tumor hypoxia: causative factors, compensatory mechanisms, and cellular response. 2004 Oncologist **9**(Suppl 5): 4-9;
212. Vaupel P, Kallinowski F and Okunieff P. Blood flow, oxygen and nutrient supply, and metabolic microenvironment of human tumors: a review. 1989 Cancer Res **49**(23): 6649-6665;
213. Vaupel P, Kelleher DK, editors. Tumor hypoxia: pathophysiology, clinical significance and therapeutic perspectives. Stuttgart (Germany): Wissenschaftliche Verlagsgesellschaft, 1999;
214. Vaupel P, Fortmeyer HP, Runkel S and Kallinowski F. Blood flow, oxygen consumption, and tissue oxygenation of human breast cancer xenografts in nude rats. 1987 Cancer Res **47**(13): 3496-3503;
215. Kallinowski F, Schlenger KH, Runkel S, Kloes M, Stohrer M, Okunieff P and Vaupel P. Blood flow, metabolism, cellular microenvironment, and growth rate of human tumor xenografts. 1989 Cancer Res **49**(14): 3759-3764;
216. Honig CR. Modern cardiovascular physiology. 2nd ed. Boston (MA) and Toronto (ON, Canada): Little and Brown, 1988;
217. Wilson DF, Rumsey WL, Green TJ and Vanderkooi JM. The oxygen dependence of mitochondrial oxidative phosphorylation measured by a new optical method for measuring oxygen concentration. 1988 J Biol Chem **263**(6): 2712-2718;
218. Chance B, Oshino N, Sugano T and Mayevsky A. Basic principles of tissue oxygen determination from mitochondrial signals. 1973 Adv Exp Med Biol **37A**: 277-292;

219. Giaccia AJ. Hypoxic Stress Proteins: survival of the fittest. 1996 Semin Radiat Oncol **6**(1): 46-58;
220. Durand RE. Keynote address: the influence of microenvironmental factors on the activity of radiation and drugs. 1991 Int J Radiat Oncol Biol Phys **20**(2): 253-258;
221. Moulder JE and Rockwell S. Tumor hypoxia: its impact on cancer therapy. 1987 Cancer Metastasis Rev **5**(4): 313-341;
222. Haroon ZA, Raleigh JA, Greenberg CS and Dewhirst MW. Early wound healing exhibits cytokine surge without evidence of hypoxia. 2000 Ann Surg **231**(1): 137-147;
223. Riva C, Chauvin C, Pison C and Leverve X. Cellular physiology and molecular events in hypoxia-induced apoptosis. 1998 Anticancer Res **18**(6B): 4729-4736;
224. Amellem O, Löffler M and Pettersen EO. Regulation of cell proliferation under extreme and moderate hypoxia: the role of pyrimidine (deoxy)nucleotides. 1994 Br J Cancer **70**(5): 857-866;
225. Koch CJ, Kruuv J and Frey HE. The effect of hypoxia on the generation time of mammalian cells. 1973 Radiat Res **53**(1): 43-48;
226. Pettersen EO and Lindmo T. Inhibition of cell-cycle progression by acute treatment with various degrees of hypoxia: modifications induced by low concentrations of misonidazole present during hypoxia. 1983 Br J Cancer **48**(6): 809-817;
227. Holmgren L, O'Reilly MS and Folkman J. Dormancy of micrometastases: balanced proliferation and apoptosis in the presence of angiogenesis suppression. 1995 Nat Med **1**(2): 149-153;
228. Demicheli R, Terenziani M, Valagussa P, Moliterni A, Zambetti M and Bonadonna G. Local recurrences following mastectomy: support for the concept of tumor dormancy. 1994 J Natl Cancer Inst **86**(1): 45-48;
229. Prehn RT. The inhibition of tumor growth by tumor mass. 1991 Cancer Res **51**(1): 2-4;
230. Semenza GL. Hypoxia, clonal selection, and the role of HIF-1 in tumor progression. 2000 Crit Rev Biochem Mol Biol **35**(2): 71-103;
231. Graham CH, Forsdike J, Fitzgerald CJ and Macdonald-Goodfellow S. Hypoxia-mediated stimulation of carcinoma cell invasiveness via upregulation of urokinase receptor expression. 1999 Int J Cancer **80**(4): 617-623;
232. Rice GC, Hoy C and Schimke RT. Transient hypoxia enhances the frequency of dihydrofolate reductase gene amplification in Chinese hamster ovary cells. 1986 Proc Natl Acad Sci U S A **83**(16): 5978-5982;
233. Dang CV and Semenza GL. Oncogenic alterations of metabolism. 1999 Trends Biochem Sci **24**(2): 68-72;
234. Jiang BH, Semenza GL, Bauer C and Marti HH. Hypoxia-inducible factor 1 levels vary exponentially over a physiologically relevant range of O_2 tension. 1996 Am J Physiol **271**(4 Pt 1): C1172-1180;
235. Mattern J, Kallinowski F, Herfarth C and Volm M. Association of resistance-related protein expression with poor vascularization and low levels of oxygen in human rectal cancer. 1996 Int J Cancer **67**(1): 20-23;
236. Sanna K and Rofstad EK. Hypoxia-induced resistance to doxorubicin and methotrexate in human melanoma cell lines in vitro. 1994 Int J Cancer **58**(2): 258-262;
237. Ausserer WA, Bourrat-Floeck B, Green CJ, Laderoute KR and Sutherland RM. Regulation of c-jun expression during hypoxic and low-glucose stress. 1994 Mol Cell Biol **14**(8): 5032-5042;
238. Graeber TG, Peterson JF, Tsai M, Monica K, Fornace AJ Jr and Giaccia AJ. Hypoxia induces accumulation of p53 protein, but activation of a G_1-phase checkpoint by low-oxygen conditions is independent of p53 status. 1994 Mol Cell Biol **14**(9): 6264-6277;
239. Laderoute KR, Grant TD, Murphy BJ and Sutherland RM. Enhanced epidermal growth factor receptor synthesis in human squamous carcinoma cells exposed to low levels of oxygen. 1992 Int J Cancer **52**(3): 428-432;
240. Shweiki D, Itin A, Soffer D and Keshet E. Vascular endothelial growth factor induced by hypoxia may mediate hypoxia-initiated angiogenesis. 1992 Nature **359**(6398): 843-845;
241. Wilson RE, Keng PC and Sutherland RM. Drug resistance in Chinese hamster ovary cells during recovery from severe hypoxia. 1989 J Natl Cancer Inst **81**(16): 1235-1240;
242. Hartmann A, Kunz M, Köstlin S, Gillitzer R, Toksoy A, Bröker EB and Klein CE. Hypoxia-induced up-regulation of angiogenin in human malignant melanoma. 1999 Cancer Res **59**(7): 1578-1583;
243. Koch AE, Polverini PJ, Kunkel SL, Harlow LA, DiPietro LA, Elner VM, Elner SG and Strieter RM. Interleukin-8 as a macrophage-derived mediator of angiogenesis. 1992 Science **258**(5089): 1798-1801;
244. O'Brien TP, Yang GP, Sanders L and Lau LF. Expression of cyr61, a growth factor-inducible immediate-early gene. 1990 Mol Cell Biol **10**(7): 3569-3577;
245. Hasan NM, Adams GE, Joiner MC, Marshall JF and Hart IR. Hypoxia facilitates tumour cell detachment by reducing expression of surface adhesion molecules and adhesion to extracellular matrices without loss of cell viability. 1998 Br J Cancer **77**(11): 1799-1805;
246. An WG, Kanekal M, Simon MC, Maltepe E, Blagosklonny MV and Neckers LM. Stabilization of wild-type p53 by hypoxia-inducible factor 1alpha. 1998 Nature **392**(6674): 405-408;

247. Höckel M, Schlenger K, Höckel S and Vaupel P. Hypoxic cervical cancers with low apoptotic index are highly aggressive. 1999 Cancer Res **59**(18): 4525-4528;
248. Young SD, Marshall RS and Hill RP. Hypoxia induces DNA overreplication and enhances metastatic potential of murine tumor cells. 1988 Proc Natl Acad Sci U S A **85**(24): 9533-9537;
249. Reynolds TY, Rockwell S and Glazer PM. Genetic instability induced by the tumor microenvironment. 1996 Cancer Res **56**(24): 5754-575;
250. Stoler DL, Anderson GR, Russo CA, Spina AM and Beerman TA. Anoxia-inducible endonuclease activity as a potential basis of the genomic instability of cancer cells. 1992 Cancer Res **52**(16): 4372-4378;
251. Cheng KC and Loeb LA. Genomic instability and tumor progression: mechanistic considerations. 1993 Adv Cancer Res **60**: 121-156;
252. Russo CA, Weber TK, Volpe CM, Stoler DL, Petrelli NJ, Rodriguez-Bigas M, Burhans WC and Anderson GR. An anoxia inducible endonuclease and enhanced DNA breakage as contributors to genomic instability in cancer. 1995 Cancer Res **55**(5): 1122-1128;
253. Höckel M and Vaupel P. Tumor hypoxia: definitions and current clinical, biologic and molecular aspects. 2001 J Natl Cancer Inst **93**(4): 266-276;
254. Gatenby RA and Gillies RJ. Why do cancers have high aerobic glycolysis? 2004 Nat Rev Cancer **4**(11): 891-899;
255. Neri D and Supuran CT. Interfering with pH regulation in tumours as a therapeutic strategy. 2011 Nat Rev Drug Discov **10**(10): 767-777;
256. Sonveaux P, Végran F, Schroeder T, Wergin MC, Verrax J, Rabbani ZN, De Saedeleer CJ, Kennedy KM, Diepart C, Jordan BF, Kelley MJ, Gallez B, Wahl ML, Feron O and Dewhirst MW. Targeting lactate-fueled respiration selectively kills hypoxic tumor cells in mice. 2008 J Clin Invest **118**(12): 3930-3942;
257. Parks SK, Chiche J and Pouyssegur J. pH control mechanisms of tumor survival and growth. 2011 J Cell Physiol **226**(2): 299-308;
258. Brahimi-Horn MC, Chiche J and Pouysségur J. Hypoxia and cancer. 2007 J Mol Med (Berl) **85**(12): 1301-1307;
259. Brahimi-Horn MC, Chiche J and Pouysségur J. Hypoxia signalling controls metabolic demand. 2007 Curr Opin Cell Biol **19**(2): 223-229;
260. Brahimi-Horn MC and Pouysségur J. Oxygen, a source of life and stress. 2007 FEBS Lett **581**(19): 3582-3591;
261. Fang JS, Gillies RJ and Gatenby RA. Adaptation to hypoxia and acidosis in carcinogenesis and tumor progression. 2008 Semin Cancer Biol **18**(5): 330-337;
262. Chambard JC and Pouyssegur J. Intracellular pH controls growth factor-induced ribosomal protein S6 phosphorylation and protein synthesis in the G_0----G_1 transition of fibroblasts. 1986 Exp Cell Res **164**(2): 282-294;
263. Pouysségur J, Sardet C, Franchi A, L'Allemain G and Paris S. A specific mutation abolishing Na^+/H^+ antiport activity in hamster fibroblasts precludes growth at neutral and acidic pH. 1984 Proc Natl Acad Sci U S A **81**(15): 4833-4837;
264. Roos A and Boron WF. Intracellular pH. 1981 Physiol Rev **61**(2): 296-434;
265. Ebbesen P, Pettersen EO, Gorr TA, Jobst G, Williams K, Kieninger J, Wenger RH, Pastorekova S, Dubois L, Lambin P, Wouters BG, Van Den Beucken T, Supuran CT, Poellinger L, Ratcliffe P, Kanopka A, Görlach A, Gasmann M, Harris AL, Maxwell P and Scozzafava A. Taking advantage of tumor cell adaptations to hypoxia for developing new tumor markers and treatment strategies. 2009 J Enzyme Inhib Med Chem **24**(Suppl 1): 1-39;
266. Huber V, De Milito A, Harguindey S, Reshkin SJ, Wahl ML, Rauch C, Chiesi A, Pouysségur J, Gatenby RA, Rivoltini L and Fais S. Proton dynamics in cancer. 2010 J Transl Med **8**: 57;
267. Swietach P, Wigfield S, Supuran CT, Harris AL and Vaughan-Jones RD. Cancer-associated, hypoxia-inducible carbonic anhydrase IX facilitates CO_2 diffusion. 2008 BJU Int **101**(Suppl 4): 22-24;
268. Swietach P, Wigfield S, Cobden P, Supuran CT, Harris AL and Vaughan-Jones RD. Tumor-associated carbonic anhydrase 9 spatially coordinates intracellular pH in three-dimensional multicellular growth. 2008 J Biol Chem **283**(29): 20473-20483;
269. Supuran CT. Carbonic anhydrases: novel therapeutic applications for inhibitors and activators. 2008 Nat Rev Drug Discov **7**(2): 168-181;
270. Supuran CT. Carbonic anhydrase inhibitors. 2010 Bioorg Med Chem Lett **20**(12): 3467-3474;
271. Pastorek J, Pastoreková S, Callebaut I, Mornon JP, Zelník V, Opavský R, Zat'ovicová M, Liao S, Portetelle D, Stanbridge EJ, Zavada J, Burny A, Kettmann R *et al.* Cloning and characterization of MN, a human tumor-associated protein with a domain homologous to carbonic anhydrase and putative helix–loop–helix DNA binding segment. 1994 Oncogene **9**(10): 2877-2888;
272. Pérez-Sayáns M, Somoza-Martín JM, Barros-Anqueira F, Rey JM and García-García A. V-ATPase inhibitors and implication in cancer treatment. 2009 Cancer Treat Rev **35**(8): 707-713;
273. Sterling D, Brown NJ, Supuran CT and Casey JR. The functional and physical relationship between the DRA bicarbonate transporter and carbonic anhydrase II. 2002 Am J Physiol Cell Physiol **283**(5): C1522-1529;

274. Morgan PE, Supuran CT and Casey JR. Carbonic anhydrase inhibitors that directly inhibit anion transport by the human Cl^-/HCO_3^- exchanger, AE1. 2004 Mol Membr Biol **21**(6): 423-433;
275. Pouysségur J, Dayan F, and Mazure NM. Hypoxia signalling in cancer and approaches to enforce tumour regression. 2006 Nature **441**(7092): 437-443;
276. Halestrap AP and Price NT. The proton-linked mono-carboxylate transporter (MCT) family: structure, function and regulation. 1999 Biochem J **343**(Pt 2): 281-299;
277. Enerson BE and Drewes LR. Molecular features, regulation, and function of monocarboxylate transporters: implications for drug delivery. 2003 J Pharm Sci **92**(8): 1531-1544;
278. McDonald PC, Winum JY, Supuran CT and Dedhar S. Recent developments in targeting carbonic anhydrase IX for cancer therapeutics. 2012 Oncotarget **3**(1): 84-97;
279. Supuran CT and Scozzafava A. Applications of carbonic anhydrase inhibitors and activators in therapy. 2002 Exp Opin Ther Patents **12**: 217-242;
280. Supuran CT and Scozzafava A. Carbonic anhydrase inhibitors and their therapeutic potential. 2000 Exp Opin Ther Patents **10**: 575-600;
281. Hewett-Emmett D. Evolution and distribution of the carbonic anhydrase gene families. In: Chegwidden WR, Edwards Y, Carter N, editors. The carbonic anhydrases—New horizons. Basel: Birkhauser Verlag; 2000. pp 29-78;
282. Xu Y, Feng L, Jeffrey PD, Shi Y and Morel FM. Structure and metal exchange in the cadmium carbonic anhydrase of marine diatoms. 2008 Nature **452**(7183): 56-61;
283. Scozzafava A, Mastrolorenzo A and Supuran CT. Modulation of carbonic anhydrase activity and its applications in therapy. 2004 Expert Opin Ther Pat **14**: 667-702;
284. Scozzafava A, Mastrolorenzo A and Supuran CT. Carbonic anhydrase inhibitors and activators and their use in therapy. 2006 Expert Opin Ther Pat **16**: 627-1664;
285. Türeci O, Sahin U, Vollmar E, Siemer S, Göttert E, Seitz G, Parkkila AK, Shah GN, Grubb JH, Pfreundschuh M and Sly WS. Human carbonic anhydrase XII: cDNA cloning, expression, and chromosomal localization of a carbonic anhydrase gene that is overexpressed in some renal cell cancers. 1998 Proc Natl Acad Sci USA **95**(13): 7608-7613;
286. Svastová E, Hulíková A, Rafajová M, Zat'ovicová M, Gibadulinová A, Casini A, Cecchi A, Scozzafava A, Supuran CT, Pastorek J and Pastoreková S. Hypoxia activates the capacity of tumor-associated carbonic anhydrase IX to acidify extracellular pH. 2004 FEBS Lett **577**(3): 439-445;
287. Závada J, Závadová Z, Pastoreková S, Ciampor F, Pastorek J and Zelník V. Expression of MaTu-MN protein in human tumor cultures and in clinical specimens. 1993 Int J Cancer **54**(2): 268-274;
288. Pastoreková S, Závadová Z, Kostál M, Babusíková O and Závada J. A novel quasi-viral agent, MaTu, is a two-component system. 1992 Virology **187**(2): 620-626;
289. Opavský R, Pastoreková S, Zelník V, Gibadulinová A, Stanbridge EJ, Závada J, Kettmann R and Pastorek J. Human MN/CA9 gene, a novel member of the carbonic anhydrase family: structure and exon to protein domain relationships. 1996 Genomics **33**(3): 480-487;
290. Hilvo M, Baranauskiene L, Salzano AM, Scaloni A, Matulis D, Innocenti A, Scozzafava A, Monti SM, Di Fiore A, De Simone G, Lindfors M, Jänis J, Valjakka J, Pastoreková S, Pastorek J, Kulomaa MS, Nordlund HR, Supuran CT and Parkkila S. Biochemical characterization of CA IX, one of the most active carbonic anhydrase isozymes. 2008 J Biol Chem **283**(41): 27799-27809;
291. Alterio V, Hilvo M, Di Fiore A, Supuran CT, Pan P, Parkkila S, Scaloni A, Pastorek J, Pastorekova S, Pedone C, Scozzafava A, Monti SM, and De Simone G. Crystal structure of the catalytic domain of the tumor-associated human carbonic anhydrase IX. 2009 Proc Natl Acad Sci USA **106**(38):16233-16238;
292. De Simone G and Supuran CT. Carbonic anhydrase IX: biochemical and crystallographic characterization of a novel antitumor target. 2010 Biochim Biophys Acta **1804**(2): 404-409;
293. Innocenti A, Pastorekova S, Pastorek J, Scozzafava A, De Simone G and Supuran CT. The proteoglycan region of the tumor-associated carbonic anhydrase isoform IX acts as anintrinsic buffer optimizing CO_2 hydration at acidic pH values characteristic of solid tumors. 2009 Bioorg Med Chem Lett **19**(20): 5825-5828;
294. Hulikova A, Zatovicova M, Svastova E, Ditte P, Brasseur R, Kettmann R, Supuran CT, Kopacek J, Pastorek J and Pastorekova S. Intact intracellular tail is critical for proper functioning of the tumor-associated, hypoxia-regulated carbonic anhydrase IX. 2009 FEBS Lett **583**(22): 3563-3568;
295. Zatovicova M, Jelenska L, Hulikova A, Csaderova L, Ditte Z, Ditte P, Goliasova T, Pastorek J and Pastorekova S. Carbonic anhydrase IX as an anticancer therapy target: preclinical evaluation of internalizing monoclonal antibody directed to catalytic domain. 2010 Curr Pharm Des **16**(29): 3255-3263;
296. Dorai T, Sawczuk IS, Pastorek J, Wiernik PH and Dutcher JP. The role of carbonic anhydrase IX overexpression in kidney cancer. 2005 Eur J Cancer **41**(18): 2935-2947;
297. Ditte P, Dequiedt F, Svastova E, Hulikova A, Ohradanova-Repic A, Zatovicova M, Csaderova L, Kopacek J, Supuran CT, Pastorekova S and Pastorek J. Phosphorylation of carbonic

anhydrase IX controls its ability to mediate extracellular acidification in hypoxic tumors. 2011 Cancer Res **71**(24): 7558-7567;
298. Vullo D, Franchi M, Gallori E, Pastorek J, Scozzafava A, Pastorekova S and Supuran CT. Carbonic anhydrase inhibitors: inhibition of the tumor-associated isozyme IX with aromatic and heterocyclic sulfonamides. 2003 Bioorg Med Chem Lett **13**(6): 1005-1009;
299. Vullo D, Franchi M, Gallori E, Pastorek J, Scozzafava A, Pastorekova S and Supuran CT. Carbonic anhydrase inhibitors. Inhibition of cytosolic isozymes I and II and transmembrane, cancer-associated isozyme IX with anions. 2003 J Enzyme Inhib Med Chem **18(5)**: 403-406;
300. Saarnio J, Parkkila S, Parkkila AK, Waheed A, Casey MC, Zhou XY, Pastorekova S, Pastorek J, Karttunen T, Haukipuro K, Kairaluoma MI and Sly WS. Immunohistochemistry of carbonic anhydrase isozyme IX (MN/CA IX) in human gut reveals polarized expression in the epithelial cells with the highest proliferative capacity. 1998 J Histochem Cytochem **46**(4): 497-504;
301. Karhumaa P, Kaunisto K, Parkkila S, Waheed A, Pastoreková S, Pastorek J, Sly WS and Rajaniemi H. Expression of the transmembrane carbonic anhydrases, CA IX and CA XII, in the human male excurrent ducts. 2001 Mol Hum Reprod **7**(7): 611-616;
302. Potter CP and Harris AL. Diagnostic, prognostic and therapeutic implications of carbonic anhydrases in cancer. 2003 Br J Cancer **89**(1): 2-7;
303. Pastoreková S, Parkkila S, Parkkila AK , Opavský R, Zelník V, Saarnio J and Pastorek J. Carbonic anhydrase IX, MN/CA IX: analysis of stomach complementary DNA sequence and expression in human and rat alimentary tracts. 1997 Gastroenterology **112**(2): 398-408;
304. Wykoff CC, Beasley NJ, Watson PH, Turner KJ, Pastorek J, Sibtain A, Wilson GD, Turley H, Talks KL, Maxwell PH, Pugh CW, Ratcliffe PJ and Harris AL. Hypoxia-inducible expression of tumor-associated carbonic anhydrases. 2000 Cancer Res **60**(24): 7075-7083;
305. Ihnatko R, Kubes M, Takacova M, Sedlakova O, Sedlak J, Pastorek J, Kopacek J and Pastorekova S. Extracellular acidosis elevates carbonic anhydrase IX in human glioblastoma cells via transcriptional modulation that does not depend on hypoxia. 2006 Int J Oncol **29**(4): 1025-1033;
306. Rafajová M, Zatovicová M, Kettmann R, Pastorek J and Pastoreková S. Induction by hypoxia combined with low glucose or low bicarbonate and high posttranslational stability upon reoxygenation contribute to carbonic anhydrase IX expression in cancer cells. 2004 Int J Oncol **24**(4): 995-1004;
307. Vordermark D, Kaffer A, Riedl S, Katzer A and Flentje M. Characterization of carbonic anhydrase IX (CA IX) as an endogenous marker of chronic hypoxia in live human tumor cells. 2005 Int J Radiat Oncol Biol Phys **61**(4): 1197-1207;
308. Stillebroer AB, Mulders PF, Boerman OC, Oyen WJ and Oosterwijk E. Carbonic anhydrase IX in renal cell carcinoma: implications for prognosis, diagnosis, and therapy. 2010 Eur Urol **58**(1): 75-83;
309. Swinson DE, Jones JL, Richardson D, Wykoff C, Turley H, Pastorek J, Taub N, Harris AL and O'Byrne KJ. Carbonic anhydrase IX expression, a novel surrogate marker of tumor hypoxia, is associated with a poor prognosis in non-small-cell lung cancer. 2003 J Clin Oncol **21**(3): 473-482;
310. Korkeila E, Talvinen K, Jaakkola PM, Minn H, Syrjänen K, Sundström J and Pyrhönen S. Expression of carbonic anhydrase IX suggests poor outcome in rectal cancer. 2009 Br J Cancer **100**(6): 874-880;
311. Chia SK, Wykoff CC, Watson PH, Han C, Leek RD, Pastorek J, Gatter KC, Ratcliffe P and Harris AL. Prognostic significance of a novel hypoxia-regulated marker, carbonic anhydrase IX, in invasive breast carcinoma. 2001 J Clin Oncol **19**(16): 3660-3668;
312. Loncaster JA, Harris AL, Davidson SE, Logue JP, Hunter RD, Wycoff CC, Pastorek J, Ratcliffe PJ, Stratford IJ and West CM. Carbonic anhydrase (CA IX) expression, a potential new intrinsic marker of hypoxia: correlations with tumor oxygen measurements and prognosis in locally advanced carcinoma of the cervix. 2001 Cancer Res **61**(17): 6394-6399;
313. Innocenti A, Vullo D, Scozzafava A, Casey JR and Supuran CT. Carbonic anhydrase inhibitors. Interaction of isozymes I, II, IV, V, and IX with carboxylates. 2005 Bioorg Med Chem Lett **15**(3): 573-578;
314. Swietach P, Vaughan-Jones RD and Harris AL. Regulation of tumor pH and the role of carbonic anhydrase 9. 2007 Cancer Metastasis Rev **26**(2): 299-310;
315. Swietach P, Hulikova A, Vaughan-Jones RD and Harris AL. New insights into the physiological role of carbonic anhydrase IX in tumour pH regulation. 2010 Oncogene **29**(50): 6509-6521;
316. Swietach P, Patiar S, Supuran CT, Harris AL and Vaughan-Jones RD. The role of carbonic anhydrase 9 in regulating extracellular and intracellular ph in three-dimensional tumor cell growths. 2009 J Biol Chem **284**(30): 20299-20310;
317. Raghunand N, Gatenby RA and Gillies RJ. Microenvironmental and cellular consequences of altered blood flow in tumours. 2003 Br J Radiol **76** Spec No 1: S11-22;
318. Vince JW and Reithmeier RAF. Carbonic anhydrase II binds to the carboxyl terminus of human band 3, the erythrocyte Cl^-/HCO_3^- exchanger. 1998 J Biol Chem **273**(43): 28430-28437;

319. McMurtrie HL, Cleary HJ, Alvarez BV, Loiselle FB, Sterling D, Morgan PE, Johnson DE and Casey JR. The bicarbonate transport metabolon. 2004 J Enzyme Inhib Med Chem **19**(3): 231-236;
320. Chiche J, Ilc K, Laferrière J, Trottier E, Dayan F, Mazure NM, Brahimi-Horn MC, Pouysségur J. Hypoxia-inducible carbonic anhydrase IX and XII promote tumor cell growth by counteracting acidosis through the regulation of the intracellular pH. 2009 Cancer Res **69**(1): 358-368;
321. Závada J, Závadová Z, Pastorek J, Biesová Z, Jezek K and Velek J. Human tumour-associated cell adhesion protein MN/CA IX: identification of M75 epitope and of the region mediating cell adhesion. 2000 Br J Cancer **82**(11): 1808-1813;
322. Svastová E, Zilka N, Zat'ovicová M, Gibadulinová A, Ciampor F, Pastorek J and Pastoreková S. Carbonic anhydrase IX reduces E-cadherin-mediated adhesion of MDCK cells via interaction with beta-catenin. 2003 Exp Cell Res **290**(2): 332-345;
323. Csaderova L, Debreova M, Radvak P, Stano M, Vrestiakova M, Kopacev J, Pastorekova S and Svastova E. The effect of carbonic anhydrase IX on focal contacts during cell spreading and migration. 2013 Front Physiol **4**: 271;
324. Ivanov SV, Kuzmin I, Wei MH, Pack S, Geil L, Johnson BE, Stanbridge EJ and Lerman MI. Down-regulation of transmembrane carbonic anhydrases in renal cell carcinoma cell lines by wild-type von Hippel–Lindau transgenes. 1998 Proc Natl Acad Sci USA **95**(21): 12596-12601;
325. Ivanov S, Liao SY, Ivanova A, Danilkovitch-Miagkova A, Tarasova N, Weirich G, Merrill MJ, Proescholdt MA, Oldfield EH, Lee J, Zavada J, Waheed A, SlyW, Lerman MI and Stanbridge EJ. Expression of hypoxia-inducible cell-surface transmembrane carbonic anhydrases in human cancer. 2001 Am J Pathol **158**(3): 905-919;
326. Chiche J, Brahimi-Horn MC, Pouysségur J. Tumour hypoxia induces a metabolic shift causing acidosis: a common feature in cancer. 2010 J Cell Mol Med **14**(4): 771-794;
327. Watson PH, Chia SK, Wykoff CC, Han C, Leek RD, Sly WS, Gatter KC, Ratcliffe P and Harris AL. Carbonic anhydrase XII is a marker of good prognosis in invasive breast carcinoma. 2003 Br J Cancer **88**(7): 1065-1070;
328. Haapasalo J, Hilvo M, Nordfors K, Haapasalo H, Parkkila S, Hyrskyluoto A, Rantala I, Waheed A, Sly WS, Pastorekova S, Pastorek J and Parkkila AK. Identification of an alternatively spliced isoform of carbonic anhydrase XII in diffusely infiltrating astrocytic gliomas. 2008 Neuro Oncol **10**(2): 131-138;
329. Parkkila S, Lasota J, Fletcher JA, Ou WB, Kivelä AJ, Nuorva K, Parkkila AK, Ollikainen J, Sly WS, Waheed A, Pastorekova S, Pastorek J, Isola J and Miettinen M. Carbonic anhydrase II. A novel biomarker for gastrointestinal stromal tumors. 2010 Mod Pathol **23**(5): 743-750;
330. Yoshiura K, Nakaoka T, Nishishita T, Sato K, Yamamoto A, Shimada S, Saida T, Kawakami Y, Takahashi TA, Fukuda H, Imajoh-Ohmi S, Oyaizu N and Yamashita N. Carbonic anhydrase II is a tumor vessel endothelium-associated antigen targeted by dendritic cell therapy. 2005 Clin Cancer Res **11**(22): 8201-8207;
331. Pan P, Leppilampi M, Pastorekova S, Pastorek J, Waheed A, Sly WS and Parkkila S. Carbonic anhydrase gene expression in CA II-deficient (Car2-/-) and CA IX-deficient (Car9-/-) mice. 2006 J Physiol **571**(Pt 2): 319-327;
332. Wakabayashi S, Shigekawa M and Pouyssegur J. Molecular physiology of vertebrate Na^+/H^+ exchangers. 1997 Physiol Rev **77**(1): 51-74;
333. Counillon L and Pouysségur J. The expanding family of eucaryotic Na(+)/H(+) exchangers. 2000 J Biol Chem **275**(1): 1-4;
334. Alper SL. Molecular physiology and genetics of Na^+-independent SLC4 anion exchangers. 2009 J Exp Biol **212**(Pt 11): 1672-1683;
335. Boron WF, Chen L and Parker MD. Modular structure of sodium-coupled bicarbonate transporters. 2009 J Exp Biol **212**(Pt 11): 1697-1706;
336. Casey JR, Grinstein S and Orlowski J. Sensors and regulators of intracellular pH. 2010 Nat Rev Mol Cell Biol **11**(1): 50-61;
337. Karumanchi SA, Jiang L, Knebelmann B, Stuart-Tilley AK, Alper SL and Sukhatme VP. VHL tumor suppressor regulates Cl^-/HCO_3^- exchange and Na^+/H^+ exchange activities in renal carcinoma cells. 2001 Physiol Genomics **5**(3): 119-128;
338. Ullah MS, Davies AJ and Halestrap AP. The plasma membrane lactate transporter MCT4, but not MCT1, is up-regulated by hypoxia through a HIF-1alpha-dependent mechanism. 2006 J Biol Chem **281**(14): 9030-9037;
339. Cardone RA, Casavola V and Reshkin SJ. The role of disturbed pH dynamics and the Na^+/H^+ exchanger in metastasis. 2005 Nat Rev Cancer **5**(10): 786-795;
340. Sardet C, Franchi A and Pouysségur J. Molecular cloning, primary structure, and expression of the human growth factor-activatable Na^+/H^+ antiporter. 1989 Cell **56**(2): 271-280;
341. Shimoda LA, Fallon M, Pisarcik S, Wang J and Semenza GL. HIF-1 regulates hypoxic induction of NHE1 expression and alkalinization of intracellular pH in pulmonary arterial myocytes. 2006 Am J Physiol Lung Cell Mol Physiol **291**(5): L941-999;
342. Condeelis J and Segall JE. Intravital imaging of cell movement in tumours. 2003 Nat Rev Cancer **3**(12): 921-930;

343. Cardone RA, Bagorda A, Bellizzi A, Busco G, Guerra L, Paradiso A, Casavola V, Zaccolo M and Reshkin SJ. Protein kinase A gating of a pseudopodial-located RhoA/ROCK/p38/NHE1 signal module regulates invasion in breast cancer cell lines. 2005 Mol Biol Cell **16**(7): 3117-3127;
344. Lagana A, Vadnais J, Le PU, Nguyen TN, Laprade R, Nabi IR and Noël J. Regulation of the formation of tumor cell pseudopodia by the Na(+)/H(+) exchanger NHE1. 2000 J Cell Sci **113**(Pt 20): 3649-3662;
345. Paradiso A, Cardone RA, Bellizzi A, Bagorda A, Guerra L, Tommasino M, Casavola V and Reshkin SJ. The Na^+-H^+ exchanger-1 induces cytoskeletal changes involving reciprocal RhoA and Rac1 signaling, resulting in motility and invasion in MDA-MB-435 cells. 2004 Breast Cancer Res **6**(6): R616-628;
346. Orlowski J and Grinstein S. Diversity of the mammalian sodium/proton exchanger SLC9 gene family. 2004 Pflugers Arch **447**(5): 549-565;
347. Stock C, Cardone RA, Busco G, Krähling H, Schwab A and Reshkin SJ. Protons extruded by NHE1: digestive or glue? 2008 Eur J Cell Biol **87**(8-9): 591-599;
348. Stock C, Mueller M, Kraehling H, Mally S, Noël J, Eder C and Schwab A. pH nanoenvironment at the surface of single melanoma cells. 2007 Cell Physiol Biochem **20**(5): 679-686;
349. Stüwe L, Muller M, Fabian A, Waning J, Mally S, Noël J, Schwab A and Stock C. pH dependence of melanoma cell migration: protons extruded by NHE1 dominate protons of the bulk solution. 2007 J Physiol **585**(Pt 2): 351-360;
350. Grinstein S, Woodside M, Waddell TK, Downey GP, Orlowski J, Pouyssegur J, Wong DC and Foskett JK. Focal localization of the NHE-1 isoform of the Na^+/H^+ antiport: assessment of effects on intracellular pH. 1993 EMBO J **12**(13): 5209-5218;
351. Klein M, Seeger P, Schuricht B, Alper SL and Schwab A. Polarization of Na(+)/H(+) and Cl(−)/HCO(3)(−) exchangers in migrating renal epithelial cells. 2000 J Gen Physiol **115**(5): 599-608;
352. Schwab A. Function and spatial distribution of ion channels and transporters in cell migration. 2001 Am J Physiol Renal Physiol **280**(5): F739-747;
353. Schwab A. Ion channels and transporters on the move. 2001 News Physiol Sci **16**: 29-33;
354. Papadopoulos MC, Saadoun S and Verkman AS. Aquaporins and cell migration. 2008 Pflugers Arch **456**(4): 693-700;
355. Frantz C, Barreiro G, Dominguez L, Chen X, Eddy R, Condeelis J, Kelly MJ, Jacobson MP and Barber DL. Cofilin is a pH sensor for actin free barbed end formation: role of phosphoinositide binding. 2008 J Cell Biol **183**(5): 865-879;
356. Wang W, Eddy R and Condeelis J. The cofilin pathway in breast cancer invasion and metastasis. 2007 Nat Rev Cancer **7**(6): 429-440;
357. Svastova E, Witarski W, Csaderova L, Kosik I, Skvarkova L, Hulikova A, Zatovicova M, Barathova M, Kopacek J, Pastorek J and Pastorekova S. Carbonic anhydrase IX interacts with bicarbonate transporters in lamellipodia and increases cell migration via its catalytic domain. 2012 J Biol Chem **287**(5): 3392-3402;
358. Morgan PE, Pastoreková S, Stuart-Tilley AK, Alper SL and Casey JR. Interactions of transmembrane carbonic anhydrase, CAIX, with bicarbonate transporters. 2007 Am J Physiol Cell Physiol **293**(2): C738-748;
359. Orlowski A, De Giusti VC, Morgan PE, Aiello EA and Alvarez BV. Binding of carbonic anhydrase IX to extracellular loop 4 of the NBCe1 Na^+/HCO_3^- cotransporter enhances NBCe1-mediated HCO_3^- influx in the rath eart. 2012 Am J Physiol Cell Physiol **303**(1): C69-80;
360. Sun HQ, Yamamoto M, Mejillano M and Yin HL. Gelsolin, a multifunctional actin regulatory protein. 1999 J Biol Chem **274**(47): 33179-33182;
361. Lueck A, Yin HL, Kwiatkowski DJ and Allen PG. Calcium regulation of gelsolin and adseverin: a natural test of the helix latch hypothesis. 2000 Biochemistry **39**(18): 5274-5279;
362. Azuma T, Witke W, Stossel TP, Hartwig JH and Kwiatkowski DJ. Gelsolin is a downstream effector of rac for fibroblast motility. 1998 EMBO J **17**(5): 1362-1370;
363. Stock C and Schwab A. Protons make tumor cells move like clockwork. 2009 Pflugers Arch **458**(5): 981-992;
364. Eble JA and Tuckwell DS. The alpha2beta1 integrin inhibitor rhodocetin binds to the A-domain of the integrin alpha2 subunit proximal to the collagen-binding site. 2003 Biochem J **376**(Pt 1): 77-85;
365. Lehenkari PP and Horton MA. Single integrin molecule adhesion forces in intact cells measured by atomic force microscopy. 1999 Biochem Biophys Res Commun **259**(3): 645-650;
366. Stock C, Gassner B, Hauck CR, Arnold H, Mally S, Eble JA, Dieterich P and Schwab A. Migration of human melanoma cells depends on extracellular pH and Na^+/H^+ exchange. 2005 J Physiol **567**(Pt 1): 225-238;
367. Holman CM, Kan CC, Gehring MR and Van Wart HE. Role of His-224 in the anomalous pH dependence of human stromelysin-1. 1999 Biochemistry **38**(2): 677-681;
368. Monaco S, Gioia M, Rodriguez J, Fasciglione GF, Di Pierro D, Lupidi G, Krippahl L, Marini S and Coletta M. Modulation of the proteolytic activity of matrix metalloproteinase-2 (gelatinase A) on fibrinogen. 2007 Biochem J **402**(3): 503-513;

369. Jiang J, Li M and Yue L. Potentiation of TRPM7 inward currents by protons. 2005 J Gen Physiol **126**(2): 137-150;
370. Gallagher SM, Castorino JJ and Philp NJ. Interaction of monocarboxylate transporter 4 with beta1-integrin and its role in cell migration. 2009 Am J Physiol Cell Physiol **296**(3): C414-421;
371. Trabold O, Wagner S, Wicke C, Scheuenstuhl H, Hussain MZ, Rosen N, Seremetiev A, Becker HD and Hunt TK. Lactate and oxygen constitute a fundamental regulatory mechanism in wound healing. 2003 Wound Repair Regen **11**(6): 504-509;
372. Tsuji T. Physiological and pathological roles of alpha3beta1 integrin. 2004 J Membr Biol **200**(3): 115-132;
373. Rotin D, Wan P, Grinstein S and Tannock I. Cytotoxicity of compounds that interfere with the regulation of intracellular pH: a potential new class of anticancer drugs. 1987 Cancer Res **47**(6): 1497-1504;
374. Newell K, Wood P, Stratford I and Tannock I. Effects of agents which inhibit the regulation of intracellular pH on murine solid tumours. 1992 Br J Cancer **66**(2): 311-317;
375. Luo J and Tannock IF. Inhibition of the regulation of intracellular pH: potential of 5-(N,N-hexamethylene) amiloride in tumour-selective therapy. 1994 Br J Cancer **70**(4): 617-624;
376. Lagarde AE, Franchi AJ, Paris S and Pouysségur J. Effect of mutations affecting Na^+/H^+ antiport activity on tumorigenic potential of hamster lung fibroblasts. 1988 J Cell Biochem **36**(3): 249-260;
377. Rotin D, Steele-Norwood D, Grinstein S and Tannock I. Requirement of the Na^+/H^+ exchanger for tumor growth. 1989 Cancer Res **49**(1): 205-211;
378. Théry C, Ostrowski M and Segura E. Membrane vesicles as conveyors of immune response. 2009 Nat Rev Immunol **9**(8): 581-593;
379. Vanherberghen B, Andersson K, Carlin LM, Nolte-'t Hoen EN, Williams GS, Höglund P and Davis DM. Human and murine inhibitory natural killer cell receptors transfer from natural killer cells to target cells. 2004 Proc Natl Acad Sci USA **101**(48): 16873-16878;
380. Joly E and Hudrisier D. What is trogocytosis and what is its purpose? 2003 Nat Immunol **4**(9): 815;
381. Xu H, Dhanireddy KK and Kirk AD. Human monocytes as intermediaries between allogeneic endothelial cells and allospecific T cells: a role for direct scavenger receptor-mediated endothelial membrane uptake in the initiation of alloimmunity. 2006 J Immunol **176**(2): 750-761;
382. Harshyne LA, Watkins SC, Gambotto A and Barratt-Boyes SM. Dendritic cells acquire antigens from live cells for cross-presentation to CTL. 2001 J Immunol **166**(6): 3717-3723;
383. Arnold PY, Davidian DK and Mannie MD. Antigen presentation by T cells: T cell receptor ligation promotes antigen acquisition from professional antigen-presenting cells. 1997 Eur J Immunol **27**(12): 3198-3205;
384. Hudrisier D, Riond J, Mazarguil H, Gairin JE and Joly E. Cutting edge: CTLs rapidly capture membrane fragments from target cells in a TCR signaling-dependent manner. 2001 J Immunol **166**(6): 3645-3649;
385. Stinchcombe JC, Bossi G, Booth S and Griffiths GM. The immunological synapse of CTL contains a secretory domain and membrane bridges. 2001 Immunity **15**(5): 751-761;
386. Puaux AL, Campanaud J, Salles A, Préville X, Timmerman B, Joly E and Hudrisier D. A very rapid and simple assay based on trogocytosis to detect and measure specific T and B cell reactivity by flow cytometry. 2006 Eur J Immunol **36**(3): 779-788;
387. Patel DM and Mannie MD. Intercellular exchange of class II major histocompatibility complex/peptide complexes is a conserved process that requires activation of T cells but is constitutive in other types of antigen presenting cell. 2001 Cell Immunol **214**(2): 165-172;
388. Patel D, Arnold PY, White GA, Nardella JP and Mannie MD. Class II MHC/peptide complexes are released from APC and are acquired by T cell responders during specific antigen recognition. 1999 J Immunol **163**(10): 5201-5210;
389. Davis DM. Intercellular transfer of cell-surface proteins is common and can affect many stages of an immune response. 2007 Nat Rev Immunol **7**(3): 238-243;
390. Rustom A, Saffrich R, Markovic I, Walther P and Gerdes HH. Nanotubular highways for intercellular organelle transport. 2004 Science **303**(5660): 1007-1010;
391. Onfelt B, Nedvetzki S, Yanagi K and Davis DM. Cutting edge: Membrane nanotubes connect immune cells. 2004 J Immunol **173**(3): 1511-1513;
392. Eriksson M, Leitz G, Fällman E, Axner O, Ryan JC, Nakamura MC and Sentman CL. Inhibitory receptors alter natural killer cell interactions with target cells yet allow simultaneous killing of susceptible targets. 1999 J Exp Med **190**(7): 1005-1012;
393. Watkins SC and Salter RD. Functional connectivity between immune cells mediated by tunneling nanotubules. 2005 Immunity **23**(3): 309-318;
394. Pasquier J, Guerrouahen BS, Al Thawadi H, Ghiabi P, Maleki M, Abu-Kaoud N, Jacob A, Mirshahi M, Galas L, Rafii S, Le Foll F and Rafii A. Preferential transfer of mitochondria from endothelial to cancer cells through tunneling nanotubes modulates chemoresistance. 2013 J Transl Med **11**: 94;

395. Gurke S, Barroso JF and Gerdes HH. The art of cellular communication: tunneling nanotubes bridge the divide. 2008 Histochem Cell Biol **129**(5): 539-550;
396. Gerdes HH, Bukoreshtliev NV and Barroso JF. Tunneling nanotubes: a new route for the exchange of components between animal cells. 2007 FEBS Lett **581**(11): 2194-2201;
397. Koyanagi M, Brandes RP, Haendeler J, Zeiher AM and Dimmeler S. Cell-to-cell connection of endothelial progenitor cells with cardiac myocytes by nanotubes: a novel mechanism for cell fate changes? 2005 Circ Res **96**(10): 1039-1041;
398. Gurke S, Barroso JF, Hodneland E, Bukoreshtliev NV, Schlicker O and Gerdes HH. Tunneling nanotube (TNT)-like structures facilitate a constitutive, actomyosin-dependent exchange of endocytic organelles between normal rat kidney cells. 2008 Exp Cell Res **314**(20): 3669-3683;
399. Eugenin EA, Gaskill PJ and Berman JW. Tunneling nanotubes (TNT) are induced by HIV-infection of macrophages: a potential mechanism for intercellular HIV trafficking. 2009 Cell Immunol **254**(2): 142-148;
400. Gerdes HH. Prions tunnel between cells. 2009 Nat Cell Biol **11**(3): 235-236;
401. Pasquier J, Galas L, Boulangé-Lecomte C, Rioult D, Bultelle F, Magal P, Webb G and Le Foll F. Different modalities of intercellular membrane exchanges mediate cell-to-cell p-glycoprotein transfers in MCF-7 breast cancer cells. 2012 J Biol Chem **287**(10): 7374-7387;
402. Klueg KM and Muskavitch MA. Ligand–receptor interactions and trans-endocytosis of Delta, Serrate and Notch: members of the Notch signalling pathway in Drosophila. 1999 J Cell Sci **112**(Pt 19): 3289-3297;
403. Parks AL, Klueg KM, Stout JR and Muskavitch MA. Ligand endocytosis drives receptor dissociation and activation in the Notch pathway. 2000 Development **127**(7): 1373-1385;
404. Le Borgne R and Schweisguth F. Notch signaling: endocytosis makes delta signal better. 2003 Curr Biol **13**(7): R273-275;
405. Krämer H. RIPping notch apart: a new role for endocytosis in signal transduction? 2000 Sci STKE **2000**(29): pe1;
406. Nichols JT, Miyamoto A, Olsen SL, D'Souza B, Yao C and Weinmaster G. DSL ligand endocytosis physically dissociates Notch1 heterodimers before activating proteolysis can occur. 2007 J Cell Biol **176**(4): 445-458;
407. Cocucci E, Racchetti G and Meldolesi J. Shedding microvesicles: artefacts no more. 2009 Trends Cell Biol **19**(2): 43-51;
408. Ratajczak J, Wysoczynski M, Hayek F, Janowska-Wieczorek A and Ratajczak MZ. Membrane-derived microvesicles: important and underappreciated mediators of cell-to-cell communication. 2006 Leukemia **20**(9): 1487-1495;
409. Belting M and Wittrup A. Nanotubes, exosomes, and nucleic acid-binding peptides provide novel mechanisms of intercellular communication in eukaryotic cells: implications in health and disease. 2008 J Cell Biol **183**(7): 1187-1191;
410. Valadi H, Ekström K, Bossios A, Sjöstrand M, Lee JJ and Lötvall JO. Exosome-mediated transfer of mRNAs and microRNAs is a novel mechanism of genetic exchange between cells. 2007 Nat Cell Biol **9**(6): 654-659;
411. Balaj L, Lessard R, Dai L, Cho YJ, Pomeroy SL, Breakefield XO and Skog J. Tumour microvesicles contain retrotransposon elements and amplified oncogene sequences. 2011 Nat Commun **2**: 180;
412. Spees JL, Olson SD, Whitney MJ and Prockop DJ. Mitochondrial transfer between cells can rescue aerobic respiration. 2006 Proc Natl Acad Sci USA **103**(5): 1283-1288;
413. Friend C, Marovitz W, Henie G, Henie W, Tsuei D, Hirschhorn K, Holland JG and Cuttner J. Observations on cell lines derived from a patient with Hodgkin's disease. 1978 Cancer Res **38**(8): 2581-2591;
414. Poste G and Nicolson GL. Arrest and metastasis of blood-borne tumor cells are modified by fusion of plasma membrane vesicles from highly metastatic cells. 1980 Proc Natl Acad Sci USA **77**(1): 399-403;
415. Raposo G, Nijman, HW, Stoorvogel W, Liejendekker R, Harding CV, Melief CJ and Geuze HJ. B lymphocytes secrete antigen-presenting vesicles. 1996 J Exp Med **183**(3): 1161-1172;
416. Zitvogel L, Regnault A, Lozier A, Wolfers J, Flament C, Tenza D, Ricciardi-Castagnoli P, Raposo G and Amigorena S. Eradication of established murine tumors using a novel cell-free vaccine: dendritic cell-derived exosomes. 1998 Nat Med **4**(5): 594-600;
417. Obregon C, Rothen-Rutishauser B, Gitahi SK, Gehr P and Nicod LP. Exovesicles from human activated dendritic cells fuse with resting dendritic cells, allowing them to present alloantigens. 2006 Am J Pathol **169**(6): 2127-2136;
418. Raposo G, Tenza D, Mecheri S, Peronet R, Bonnerot C and Desaymard C. Accumulation of major histocompatibility complex class II molecules in mast cell scretory granules and their release upon degranulation. 1997 Mol Biol Cell **8**(12): 2631-2645;
419. Blanchard N, Lankar D, Faure F, Regnault A, Dumont C, Raposo G and Hivroz C. TCR activation of human T cells induces the production of exosomes bearing the TCR/CD3/zeta complex. 2002 J Immunol **168**(7): 3235-3241;
420. Zöller M. Tetraspanins: push and pull in suppressing and promoting metastasis. 2009 Nat Rev Cancer **9**(1): 40-55;

421. Heijnen HF, Schiel AE, Fijnheer R, Geuze HJ and Sixma JJ. Activated platelets release two types of membrane vesicles: microvesicles by surface shedding and exosomes derived from exocytosis of multivesicular bodies and alpha-granules. 1999 Blood **94**(11): 3791-3799;
422. George JN, Thoi LL, McManus LM and Reimann TA. Isolation of human platelet membrane microparticles from plasma and serum. 1982 Blood **60**(4): 834-840;
423. van Niel G, Raposo G, Candalh C, Boussac M, Hershberg R, Cerf-Bensussan N and Heyman M. Intestinal epithelial cells secrete exosome-like vesicles. 2001 Gastroenterology **121**(2): 337-349;
424. Wolfers J, Lozier A, Raposo G, Regnault A, Théry C, Masurier C, Flament C, Pouzieux S, Faure F, Tursz T, Angevin E, Amigorena S and Zitvogel L. Tumor derived exosomes are a source of shared tumor rejection antigens for CTL cross-priming. 2001 Nat Med **7**(3): 297-303;
425. Muralidharan-Chari V, Clancy J, Plou C, Romao M, Chavrier P, Raposo G and D'Souza-Schorey C. ARF6-regulated shedding of tumor cell derived plasma membrane microvesicles. 2009 Curr Biol **19**(22): 1875-1885;
426. Fevrier B,Vilette D, Archer F, Loew D, Faigle W, Vidal M, Laude H and Raposo G. Cells release prions in association with exosomes. 2004 Proc Natl Acad Sci USA **101**(26): 9683-9688;
427. Fauré J, Lachenal G, Court M, Hirrlinger J, Chatellard-Causse C, Blot B, Grange J, Schoehn G, Goldberg Y, Boyer V, Kirchhoff F, Raposo G, Garin J and Sadoul R. Exosomes are released by cultured cortical neurones. 2006 Mol Cell Neurosci **31**(4): 642-648;
428. Schiera G, Proia P, Alberti C, Mineo M, Savettieri G and Di Liegro I. Neurons produce FGF2 and VEGF and secrete them at least in part by shedding extracellular vesicles. 2007 J Cell Mol Med **11**(6): 1384-1394;
429. Proia P, Schiera G, Mineo M, Ingrassia AM, Santoro G, Savettieri G and Di Liegro I. Astrocytes shed extracellular vesicles that contain fibroblast growth factor-2 and vascular endothelial growth factor. 2008 Int J Mol Med **21**(1): 63-67;
430. Deregibus MC, Cantaluppi V, Calogero R, Lo Iacono M, Tetta C, Biancone L, Bruno S, Bussolati B and Camussi G. Endothelial progenitor cell derived microvesicles activate an angiogenic program in endothelial cells by a horizontal transfer of mRNA. 2007 Blood **110**(7): 2440-2448;
431. Piccin A, Murphy WG and Smith OP. Circulating microparticles: pathophysiology and clinical implications. 2007 Blood Rev **21**(3): 157-171;
432. Ronquist G and Brody I. The prostasome: its secretion and function in man. 1985 Biochim Biophys Acta **822**(2): 203-218;
433. Park KH, Kim BJ, Kang J, Nam TS, Lim JM, Kim HT, Park JK, Kim YG, Chae SW and Kim UH. Ca^{2+} signaling tools acquired from prostasomes are required for progesterone-induced sperm motility. 2011 Sci Signal **4**(173): ra31;
434. Aalberts M, van Dissel-Emiliani FM, van Adrichem NP, van Wijnen M, Wauben MH, Stout TA and Stoorvogel W. Identification of distinct populations of prostasomes that differentially express prostate stem cell antigen, annexin A1, and GLIPR2 in humans. 2012 Biol Reprod **86**(3): 82;
435. Caby MP, Lankar D, Vincendeau-Scherrer C, Raposo G and Bonnerot C. Exosomal-like vesicles are present in human blood plasma. 2005 Int Immunol **17**(7): 879-887;
436. Pisitkun T, Shen RF and Knepper MA. Identification and proteomic profiling of exosomes in human urine. 2004 Proc Natl Acad Sci USA **101**(36): 13368-13373;
437. Smalley DM, Sheman NE, Nelson K and Theodorescu D. Isolation and identification of potential urinary microparticle biomarkers of bladder cancer. 2008 J Proteome Res **7**(5): 2088-2096;
438. Ogawa Y, Miura Y, Harazono A, Kanai-Azuma M, Akimoto Y, Kawakami H, Yamaguchi T, Toda T, Endo T, Tsubuki M and Yanoshita R. Proteomic analysis of two types of exosomes in human whole saliva. 2011 Biol Pharm Bull **34**(1): 13-23;
439. Admyre C, Johansson SM, Qazi KR, Filén JJ, Lahesmaa R, Norman M, Neve EP, Scheynius A and Gabrielsson S. Exosomes with immune modulatory features are present in human breast milk. 2007 J Immunol **179**(3): 1969-1978;
440. Asea A, Jean-Pierre C, Kaur P, Rao P, Linhares IM, Skupski D and Witkin SS. Heat shock protein-containing exosomes in mid-trimester amniotic fluids. 2008 J Reprod Immunol **79**(1): 12-17;
441. Andre F, Schartz NE, Movassagh M, Flament C, Pautier P, Morice P, Pomel C, Lhomme C, Escudier B, Le Chevalier T, Tursz T, Amirogena S, Raposo G, Angevin E and Zitvogel L. Malignant effusions and immunogenic tumour-derived exosomes. 2002 Lancet **360**(9329): 295-305;
442. Graves LE, Ariztia EV, Navari JR, Matzel HJ, Stack MS and Fishman DA. Proinvasive properties of ovarian cancer ascites-derived membrane vesicles. 2004 Cancer Res **64**(19): 7045-7049;
443. Choi DS, Park JO, Jang SC, Yoon YJ, Jung JW, Choi DY, Kim JW, Kang JS, Park J, Hwang D, Lee KH, Park SH, Kim YK, Desiderio DM, Kim KP and Gho YS. Proteomic analysis of microvesicles derived from human colorectal cancer ascites. 2011 Proteomics **11**(13): 2745-2751;

444. Vella LJ, Sharples RA, Lawson VA, Masters CL, Cappai R and Hill AF. Packaging of prions into exosomes is associated with a novel pathway of PrP processing. 2007 J Pathol **211**(5): 582-590;
445. Masyuk AI, Huang BQ, Ward CJ, Gradilone SA, Banales JM, Masyuk TV, Radtke B, Splinter PL and LaRusso NF. Biliary exosomes influence cholangiocyte regulatory mechanisms and proliferation through interaction with primary cilia. 2010 Am J Physiol Gastrointest Liver Physiol **299**(4): G990-999;
446. Smithers DW. No cell is an island. 1969 Br Med J **3**(5673): 778;
447. Simpson RJ, Jensen SS and Lim JW. Proteomic profiling of exosomes: current perspectives. 2008 Proteomics **8**(19): 4083-4099;
448. Denzer K, van Eijk M, Kleijmeer MJ, Jakobson E, de Groot C and Geuze HJ. Follicular dendritic cells carry MHC class II-expressing microvesicles at their surface. 2000 J Immunol **165**(3): 1259-1265;
449. Pan BT, Teng K, Wu C, Adam M and Johnstone RM. Electron microscopic evidence for externalization of the transferrin receptor in vesicular form in sheep reticulocytes. 1985 J Cell Biol **101**(3): 942-948;
450. Harding C, Heuser J and Stahl P. Receptor-mediated endocytosis of transferrin and recycling of the transferrin receptor in rat reticulocytes. 1983 J Cell Biol **97**(2): 329-339;
451. van Niel G, Porto-Carreiro I, Simoes S and Raposo G. Exosomes: a common pathway for a specialized function. 2006 J Biochem **140**(1): 13-21;
452. Rieu S, Géminard C, Rabesandratana H, Sainte-Marie J and Vidal M. Exosomes released during reticulocyte maturation bind to fibronectin via integrin alpha4beta1. 2000 Eur J Biochem **267**(2): 583-590;
453. Février B and Raposo G. Exosomes: endosomal-derived vesicles shipping extracellular messages. 2004 Curr Opin Cell Biol **16**(4): 415-421;
454. Chaput N, Flament C, Viaud S, Taieb J, Roux S, Spatz A, André F, LePecq JB, Boussac M, Garin J, Amigorena S, Théry C and Zitvogel L. Dendritic cell derived-exosomes: biology and clinical implementations. 2006 J leukoc Biol **80**(3): 471-478;
455. Théry C, Zitvogel L and Amigorena S. Exosomes: composition, biogenesis and function. 2002 Nat Rev Immunol **2**(8): 569-579;
456. Raiborg C and Stenmark H. The ESCRT machinery in endosomal sorting of ubiquitylated membrane proteins. 2009 Nature **458**(7237): 445-452;
457. Hurley JH. The ESCRT complexes. 2010 Crit Rev Biochem Mol Biol **45**(6): 463-487;
458. Géminard C, De Gassart A, Blanc L and Vidal M. Degradation of AP2 during reticulocyte maturation enhances binding of hsc70 and Alix to a common site on TFR for sorting into exosomes. 2004 Traffic **5**(3): 181-193;
459. Trajkovic K, Hsu C, Chiantia S, Rajendran L, Wenzel D, Wieland F, Schwille P, Brügger B and Simons M. Ceramide triggers budding of exosome vesicles into multivesicular endosomes. 2008 Science **319**(5867): 1244-1247;
460. Hemler ME. Tetraspanin proteins mediate cellular penetration, invasion, and fusion events and define a novel type of membrane microdomain. 2003 Annu Rev Cell Dev Biol **19**: 397-422;
461. de Gassart A, Geminard C, Fevrier B, Raposo G and Vidal M. Lipid raft-associated protein sorting in exosomes. 2003 Blood **102**(13): 4336-4344;
462. Chaput N and Théry C. Exosomes: immune properties and potential clinical implementations. 2011 Semin Immunopathol **33**(5): 419-440;
463. Wubbolts R, Leckie RS, Veenhuizen PT, Schwarzmann G, Möbius W, Hoernschemeyer J, Slot JW, Geuze HJ and Stoorvogel W. Proteomic and biochemical analyses of human B cell-derived exosomes. Potential implications for their function and multivesicular body formation. 2003 J Biol Chem **278**(13): 10963-10972;
464. Laulagnier K, Motta C, Hamdi S, Roy S, Fauvelle F, Pageaux JF, Kobayashi T, Salles JP, Perret B, Bonnerot C and Record M. Mast cell- and dendritic cell-derived exosomes display a specific lipid composition and an unusual membrane organization. 2004 Biochem J **380**(Pt 1): 161-171;
465. Subra C, Laulagnier K, Perret B and Record M. Exosome lipidomics unravels lipid sorting at the level of multivesicular bodies. 2007 Biochimie **89**(2): 205-212;
466. Brouwers JF, Aalberts M, Jansen JW, van Niel G, Wauben MH, Stout TA, Helms JB and Stoorvogel W. Distinct lipid compositions of two types of human prostasomes. 2012 Proteomics **13**(10-11):1660-1666;
467. Möbius W, Ohno-Iwashita Y, van Donselaar EG, Oorschot VM, Shimada Y, Fujimoto T, Heijnen HF, Geuze HJ and Slot JW. Immunoelectron microscopic localization of cholesterol using biotinylated and non-cytolytic perfringolysin O. 2002 J Histochem Cytochem **50**(1): 43-55;
468. Guescini M, Genedani S, Stocchi V and Agnati LF. Astrocytes and Glioblastoma cells release exosomes carrying mtDNA. 2010 J Neural Transm **117**(1): 1-4;
469. Skog J, Würdinger T, van Rijn S, Meijer DH, Gainche L, Sena-Esteves M, Curry WT Jr, Carter BS, Krichevsky AM and Breakefield XO. Glioblastoma microvesicles transport RNA and

proteins that promote tumour growth and provide diagnostic biomarkers. 2008 Nat Cell Biol **10**(12): 1470-1476;
470. Pegtel DM, Cosmopoulos K, Thorley-Lawson DA, van Eijndhoven MA, Hopmans ES, Lindenberg JL, de Gruijl TD, Würdinger T and Middeldorp JM. Functional delivery of viral miRNAs via exosomes. 2010 Proc Natl Acad Sci USA **107**(14): 6328-6333;
471. Irion U and St Johnston D. bicoid RNA localization requires specific binding of an endosomal sorting complex. 2007 Nature **445**(7127): 554-558;
472. Gibbings DJ, Ciaudo C, Erhardt M and Voinnet O. Multivesicular bodies associate with components of miRNA effector complexes and modulate miRNA activity. 2009 Nat Cell Biol **11**(9): 1143-1149;
473. Cai H, Reinisch K and Ferro-Novick S. Coats, tethers, Rabs, and SNAREs work together to mediate the intracellular destination of a transport vesicle. 2007 Dev Cell **12**(5): 671-682;
474. Savina A, Fader CM, Damiani MT and Colombo MI. Rab11 promotes docking and fusion of multivesicular bodies in a calcium-dependent manner. 2005 Traffic **6**(2): 131-143;
475. Hsu C, Morohashi Y, Yoshimura S, Manrique-Hoyos N, Jung S, Lauterbach MA, Bakhti M, Gronborg M, Möbius W, Rhee J, Barr FA and Simons M. Regulation of exosome secretion by Rab35 and its GTPase-activating proteins TBC1D10A-C. 2010 J Cell Biol **189**(2): 223-232;
476. Ostrowski M, Carmo NB, Krumeich S, Fanget I, Raposo G, Savina A, Moita CF, Schauer K, Hume AN, Freitas RP, Goud B, Benaroch P, Hacohen N, Fukuda M, Desnos C Seabra MC, Darchen F, Amigorena S, Moita LF and Thery C. Rab27a and Rab27b control different steps of the exosome secretion pathway. 2010 Nat Cell Biol **12**(1): 19-30;
477. Bobrie A, Colombo M, Krumeich S, Raposo G and Théry C. Diverse subpopulations of vesicles secrted by different intracellular mechanisms are present in exosome preparations obtained by differential ultracentrifugation. 2012 J Extracell Vesicles **1**: 18397;
478. Pelham HR. SNAREs and the specificity of membrane fusion. 2001 Trends Cell Biol **11**(3): 99-101;
479. Rao SK, Huynh C, Proux-Gillardeaux V, Galli T and Andrews NW. Identification of SNAREs involved in synaptotagmin VII-regulated lysosomal exocytosis. 2004 J Biol Chem **279**(19): 20471-20479;
480. Buschow SI, Nolte-'t Hoen EN, van Niel G, Pols MS, ten Broeke T, Lauwen M, Ossendorp F, Melief CJ, Raposo G, Wubbolts R, Wauben MH and Stoorvogel W. MHC II in dendritic cells is targeted to lysosomes or T cell-induced exosomes via distinct multivesicular body pathways. 2009 Traffic; **10**(10): 1528-1542;
481. Lachenal G, Pernet-Gallay K, Chivet M, Hemming FJ, Belly A, Bodon G, Blot B, Haase G, Goldberg Y and Sadoul R. Release of exosomes from differentiated neurons and its regulation by synaptic glutamatergic activity. 2011 Mol Cell Neurosci **46**(2): 409-418;
482. Pilzer D, Gasser O, Moskovich O, Schifferli JA and Fishelson Z. Emission of membrane vesicles: roles in complement resistance, immunity and cancer. 2005 Springer Semin Immunopathol **27**(3): 375-387;
483. van Dommelen SM, Vader P, Lakhal S, Kooijmans SA, vanSolinge WW, Wood MJ and Schiffelers RM. Microvesicles and exosomes: opportunities for cell-derived membrane vesicles in drug delivery. 2011 J Control Release **161**(2): 635-644;
484. Nickel W. Unconventional secretory routes: direct protein export across the plasma membrane of mammalian cells. 2005 Traffic **6**(8): 607-614;
485. Kobayashi T, Okamoto H, Yamada J, Setaka M and Kwan T. Vesiculation of platelet plasma membranes. Dilauroylglycerophosphocholine-induced shedding of a platelet plasma membrane fraction enriched in acetylcholinesterase activity. 1984 Biochim Biophys Acta **778**(1): 210-218;
486. Dolo V, Li R, Dillinger M, Flati S, Manela J, Taylor BJ, Pavan A and Ladisch S. Enrichment and localization of ganglioside G(D3) and caveolin-1 in shed tumor cell membrane vesicles. 2000 Biochim Biophys Acta **1486**(2-3): 265-274;
487. Cocucci E, Racchetti G , Podini P and Meldolesi J. Enlargeosome traffic: exocytosis triggered by various signals is followed by endocytosis, membrane shedding or both. 2007 Traffic **8**(6): 742-757;
488. Farsad K and De Camilli P. Mechanisms of membrane deformation. 2003 Curr Opin Cell Biol **15**(4): 372-381;
489. Boulbitch AA. Deflection of a cell membrane under application of a local force. 1998 Phys Rev E **57**: 2123-2128;
490. Kadota K and Kadota T. Isolation of coated vesicles, plain synaptic vesicles, and flocculent material from a crude synaptosome fraction of guinea pig whole brain. 1973 J Cell Biol **58**(1): 135-151;
491. Heuser JE and Keen J. Deep-etch visualization of proteins involved in clathrin assembly. 1988 J Cell Biol **107**(3): 877-886;
492. Rothman JE. Mechanisms of intracellular protein transport. 1994 Nature **372**(6501): 55-63.
493. Corbeil D, Röper K, Fargeas CA, Joester A and Huttner WB. Prominin: a story of cholesterol, plasma membrane protrusions and human pathology. 2001 Traffic **2**(2): 82-91.

494. Sheetz MP and Singer SJ. Biological membranes as bilayer couples. A molecular mechanism of drug-erythrocyte interactions. 1974 Proc Natl Acad Sci USA **71**(11): 4457-4461;
495. Sheetz MP, Painter RG and Singer SJ. Biological membranes as bilayer couples. III. Compensatory shape changes induced in membranes. 1976 J Cell Biol **70**(1): 193-203;
496. Nossal R and Zimmerberg J. Endocytosis: curvature to the ENTH degree. 2002 Curr Biol **12**(22): R770-772;
497. Miao L, Seifert U, Wortis M and Döebereiner HG. Budding transitions of fluid-bilayer vesicles: the effect of area-difference elasticity. 1994 Phys Rev E Stat Phys Plasmas Fluids Relat Interdiscip Topics **49**(6): 5389-5407;
498. Daleke DL. Regulation of transbilayer plasma membrane phospholipid asymmetry. 2003 J Lipid Res **44**(2): 233-242;
499. Bell RM, Ballas LM and Coleman RA. Lipid topogenesis. 1981 J Lipid Res **22**(3): 391-403;
500. Seigneuret M and Devaux PF. ATP-dependent asymmetric distribution of spin-labeled phospholipids in the erythrocyte membrane: relation to shape changes. 1987 Proc Natl Acad Sci USA **81**(12): 3751-3755;
501. Martin OC and Pagano RE. Transbilayer movement of fluorescent analogs of phosphatidylserine and phosphatidylethanolamine at the plasma membrane of cultured cells. Evidence for a protein-mediated and ATP-dependent process(es). 1987 J Biol Chem **262**(12): 5890-5898;
502. Sune A, Bette-Bobillo P, Bienvenüe A, Fellmann P and Devaux PF. Selective outside-inside translocation of aminophospholipids in human platelets. 1987 Biochemistry **26**(11): 2972-2978.
503. Zwaal RF and Schroit AJ. Pathophysiologic implications of membrane phospholipid asymmetry in blood cells. 1997 Blood **89**(4): 1121-1132;
504. Hugel B, Martínez MC, Kunzelmann C and Freyssinet JM. Membrane microparticles: two sides of the coin. 2005 Physiology (Bethesda) **20**: 22-27;
505. Brown MF, Thurmond RL, Dodd SW, Otten D and Beyer K. Elastic deformation of membrane bilayers probed by deuterium NMR relaxation. 2002 J Am Chem Soc **124**(28): 8471-8484;
506. Brown MF, Thurmond RL, Dodd SW, Otten D and Beyer K. Composite membrane deformation on the mesoscopic length scale. 2001 Phys Rev E Stat Nonlin Soft Matter Phys **64**(1 Pt 1): 010901.
507. Baba T, Rauch C, Xue M, Terada N, Fujii Y, Ueda H, Takayama I, Ohno S, Farge E and Sato SB. Clathrin-dependent and clathrin-independent endocytosis are differentially sensitive to insertion of poly (ethylene glycol)-derivatized cholesterol in the plasma membrane. 2001 Traffic **2**(7): 501-512.
508. Muralidharan-Chari V, Clancy JW, Sedgwick A and D'Souza-Schorey C. Microvesicles: mediators of extracellular communication during cancer progression. 2010 J Cell Sci **123**(Pt 10): 1603-1611;
509. Huttner WB and Zimmerberg J. Implications of lipid microdomains for membrane curvature, budding and fission. 2001 Curr Opin Cell Biol **13**(4): 478-484;
510. McConnell RE, Higginbotham JN, Shifrin DA Jr, Tabb DL, Coffey RJ and Tyska MJ. The enterocyte microvillus is a vesicle-generating organelle. 2009 J Cell Biol **185**(7): 1285-1298;
511. Salzer U, Hinterdorfer P, Hunger U, Borken C and Prohaska R. Ca(++)-dependent vesicle release from erythrocytes involves stomatin-specific lipid rafts, synexin (annexinVII), and sorcin. 2002 Blood **99**(7): 2569-2577;
512. Shedden K, Xie XT, Chandaroy P, Chang YT and Rosania GR. Expulsion of small molecules in vesicles shed by cancer cells: association with gene expression and chemosen- sitivity profiles. 2003 Cancer Res **63**(15): 4331-4337;
513. Yu X, Harris SL and Levine AJ. The regulation of exosome secretion: a novel function o fthe p53 protein. 2006 Cancer Res **66**(9): 4795-4801;
514. Lehmann B, Paine MS, Brooks AM, McCubrey JA, Renegar RH, Wang R and Terrian DM. Senescence-associated exosome release from human prostate cancer cells. 2008 Cancer Res **68**(19): 7864-7871;
515. Bianco F, Perrotta C, Novellino L, Francolini M, Riganti L, Menna E, Saglietti L, Schuchman EH, Furlan R, Clementi E, Matteoli M and Verderio C. Acid sphingomyelinase activity triggers microparticle release from glial cells. 2009 EMBO J **28**(8): 1043-1054;
516. Nolte-'t Hoen EN, van der Vlist EJ, de Boer-Brouwer M, Arkesteijn GJ, Stoorvogel W and Wauben MH. Dynamics of dendritic cell-derived vesicles: high-resolution flow cytometric analysis of extracellular vesicle quantity and quality. 2012 J Leukoc Biol **93**(3): 395-402;
517. Morris CE and Homann U. Cell surface area regulation and membrane tension. 2001 J Membr Biol **179**(2): 79-102;
518. Chieregatti E and Meldolesi J. Regulated exocytosis: new organelles for non-secretory purposes. 2005 Nat Rev Mol Cell Biol **6**(2): 181-187;
519. Ratajczak J, Miekus K, Kucia M, Zhang J, Reca R, Dvorak P and Ratajczak MZ. Embryonic stem cell-derived microvesicles reprogram hematopoietic progenitors: evidence for horizontal transfer of mRNA and protein delivery. 2006 Leukemia **20**(5): 847-856;

520. Baj-Krzyworzeka M, Szatanek R, Weglarczyk K, Baran J, Urbanowicz B, Brański P, Ratajczak MZ and Zembala M. Tumour-derived microvesicles carry several surface determinants and mRNA of tumour cells and transfer some of these determinants to monocytes. 2006 Cancer Immunol Immunother **55**(7): 808-818;
521. McDaniel K, Correa R, Zhou T, Johnson C, Francis H, Glaser S, Venter J, Alpini G and Meng F. Functional role of microvesicles in gastrointestinal malignancies. 2013 Ann Transl Med **1**(1): 4;
522. Pelchen-Matthews A, Raposo G and Marsh M. Endosomes, exosomes and Trojan viruses. 2004 Trends Microbiol **12**(7): 310-316;
523. Février B, Vilette D, Laude H and Raposo G. Exosomes: a bubble ride for prions? 2005 Traffic **6**(1): 10-17;
524. Robertson C, Booth SA, Beniac DR, Coulthart MB, Booth TF and McNicol A. Cellular prion protein is released on exosomes from activated platelets. 2006 Blood 107(10): 3907-3911;
525. Rozmyslowicz T, Majka M, Kijowski J, Murphy SL, Conover DO, Poncz M, Ratajczak J, Gaulton GN and Ratajczak MZ. Platelet- and megakaryocyte-derived microparticles transfer CXCR4 receptor to CXCR4-null cells and make them susceptible to infection by X4-HIV. 2003 AIDS **17**(1): 33-42;
526. Donaldson JG. Multiple roles for Arf6: sorting, structuring, and signaling at the plasma membrane. 2003 J Biol Chem **278**(43): 41573-41576;
527. D'Souza-Schorey C and Chavrier P. ARF proteins: roles in membrane traffic and beyond. 2006 Nat Rev Mol Cell Biol **7**(5): 347-358;
528. Booth AM, Fang Y, Fallon JK, Yang JM, Hildreth JE and Gould SJ. Exosomes and HIV Gag bud from endosome-like domains of the T cell plasma membrane. 2006 J Cell Biol **172**(6): 923-935;
529. Akers JC, Gonda D, Kim R, Carter BS and Chen CC. Biogenesis of extracellular vesicles (EV): exosomes, microvesicles, retrovirus-like vesicles, and apoptotic bodies. 2013 J Neurooncol **113**(1): 1-11;
530. Bobrie A, Colombo M, Raposo G and Théry C. Exosomes secretion: molecular mechanisms and roles in immune responses. 2011 Traffic **12**(12): 1659-1668;
531. Théry C, Boussac M, Véron P, Ricciardi-Castagnoli P, Raposo G, Garin J and Amigorena S. Proteomic analysis of dendritic cell-derived exosomes: a secreted subcellular compartment distinct from apoptotic vesicles. 2001 J Immunol **166**(12): 7309-7318;
532. Théry C, Regnault A, Garin J, Wolfers J, Zitvogel L, Ricciardi-Castagnoli P, Raposo G and Amigorena S. Molecular characterization of dendritic cell-derived exosomes. Selective accumulation of the heat shock protein hsc73. 1999 J Cell Biol **147**(3): 599-610;
533. Mathivanan S and Simpson RJ. ExoCarta: A compendium of exosomal proteins and RNA. 2009 Proteomics **9**(21): 4997-5000;
534. Beaudoin AR and Grondin G. Shedding of vesicular material from the cell surface of eukaryotic cells: different cellular phenomena. 1991 Biochim Biophys Acta **1071**(3): 203-219;
535. Lakkaraju A and Rodriguez-Boulan E. Itinerant exosomes: emerging roles in cell and tissue polarity. 2008 Trends Cell Biol **18**(5) 199-209;
536. Raposo G and Stoorvogel W. Extracellular vesicles: exosomes, microvesicles, and friends. 2013 J Cell Biol **200**(4): 373-383;
537. Gasser O and Schifferli JA. Activated polymorphonuclear neutrophils disseminate anti-inflammatory microparticles by ectocytosis. 2004 Blood **104**(8): 2543-2548;
538. Segura E, Guérin C, Hogg N, Amigorena S and Théry C. $CD8^+$ dendritic cells use LFA-1 to capture MHC-peptide complexes from exosomes in vivo. 2007 J Immunol **179**(3): 1489-1496;
539. Barrès C, Blanc L, Bette-Bobillo P, André S, Mamoun R, Gabius HJ and Vidal M. Galectin-5 is bound onto the surface of rat reticulocyte exosomes and modulates vesicle uptake by macrophages. 2010 Blood **115**(3): 696-705;
540. Müller I, Klocke A, Alex M, Kotzsch M, Luther T, Morgenstern E, Zieseniss S, Zahler S, Preissner K and Engelmann B. Intravascular tissue factor initiates coagulation via circulating microvesicles and platelets. 2003 FASEB J **17**(3): 476-478;
541. Del Conde I, Shrimpton CN, Thiagarajan P and López JA. Tissue-factor-bearing microvesicles arise from lipid rafts and fuse with activated platelets to initiate coagulation. 2005 Blood **106**(5): 1604-1611;
542. Köppler B, Cohen C, Schlöndorff D and Mack M. Differential mechanisms of microparticle transfer to B cells and monocytes: anti-inflammatory properties of microparticles. 2006 Eur J Immunol **36**(3): 648-660;
543. Dolo V, Ginestra A, Cassarà D, Violini S, Lucania G, Torrisi MR, Nagase H, Canevari S, Pavan A and Vittorelli ML. Selective localization of matrix metalloproteinase 9, beta1 integrins, and human lymphocyte antigen class I molecules on membrane vesicles shed by 8701-BC breast carcinoma cells. 1998 Cancer Res **58**(19): 4468-4474;
544. Sidhu SS, Mengistab AT, Tauscher AN, LaVail J and Basbaum C. The microvesicle as a vehicle for EMMPRIN in tumor-stromal interactions. 2004 Oncogene **23**(4): 956-963;
545. Mochizuki S and Okada Y. ADAMs in cancer cell proliferation and progression. 2007 Cancer Sci **98**(5): 621-628;

546. Taverna S, Rigogliuso S, Salamone M and Vittorelli ML. Intracellular trafficking of endogenous fibroblast growth factor-2. 2008 FEBS J **275**(7): 1579-1592;
547. Taraboletti G, D'Ascenzo S, Giusti I, Marchetti D, Borsotti P, Millimaggi D, Giavazzi R, Pavan A and Dolo V. Bioavailability of VEGF in tumor-shed vesicles depends on vesicle burst induced by acidic pH. 2006 Neoplasia **8**(2): 96-103;
548. Pan BT and Johnstone RM. Fate of the transferrin receptor during maturation of sheep reticulocytes *in vitro*: selective externalization of the receptor. 1983 Cell **33**(3): 967-978;
549. Lorger M. Tumor microenvironment in the brain. 2012 Cancers (Basel) **4**(1): 218-243;
550. Camussi G, Deregibus MC, Bruno S, Grange C, Fonsato V and Tetta C. Exosome/microvesicle-mediated epigenetic reprogramming of cells. 2011 Am J Cancer Res **1**(1): 98-110;
551. Rak J. Extracellular vesicles – biomarkers and effectors of the cellular interactome in cancer. 2013 Front Pharmacol **4**: 21;
552. Andre F, Escudier B, Angevin E, Tursz T and Zitvogel L. Exosomes for cancer immunotherapy. 2004 Ann Oncol **15**(Suppl 4): iv141- iv144 ;
553. Dolo V, D'Ascenzo S, Giusti I, Millimaggi D, Taraboletti G and Pavan A. Shedding of membrane vesicles by tumor and endothelial cells. 2005 Ital J Anat Embryol **110**(2 Suppl 1): 127-133;
554. Taylor DD and Gerçel-Taylor C. Tumour-derived exosomes and their role in cancer-associated T-cell signalling defects. 2005 Br J Cancer **92**(2): 305-311;
555. Gesierich S, Berezovskiy I, Ryschich E and Zöller M. Systemic induction of the angiogenesis switch by the tetraspanin D6.1A/CO-029. 2006 Cancer Res **66**(14): 7083-7094;
556. Bebawy M, Combes V, Lee E, Jaiswal R, Gong J, Bonhoure A and Grau GE. Membrane microparticles mediate transfer of P-glycoprotein to drug sensitive cancer cells. 2009 Leukemia **23**(9): 1643-1649;
557. Camussi G, Deregibus MC, Bruno S, Cantaluppi V and Biancone L. Exosomes/microvesicles as a mechanism of cell-to-cell communication. 2010 Kidney Int **78**(9): 838-848;
558. Hendrix A, Maynard D, Pauwels P, Braems G, Denys H, Van den Broecke R, Lambert J, Van Belle S, Cocquyt V, Gespach C, Bracke M, Seabra MC, Gahl WA, De Wever O and Westbroek W. Effect of the secretory small GTPase Rab27B on breast cancer growth, invasion, and metastasis. 2010 J Natl Cancer Inst **102**(12): 866-880;
559. Hood JL, San RS and Wickline SA. Exosomes released by melanoma cells prepare sentinel lymph nodes for tumor metastasis. 2011 Cancer Res **71**(11): 3792-3801;
560. Zwicker JI, Trenor CC 3rd, Furie BC and Furie B. Tissue factor-bearing microparticles and thrombus formation. 2011 Arterioscler Thromb Vasc Biol **31**(4): 728-733;
561. Peinado H, Alečković M, Lavotshkin S, Matei I, Costa-Silva B, Moreno-Bueno G, Hergueta-Redondo M, Williams C, García-Santos G, Ghajar C, Nitadori-Hoshino A, Hoffman C, Badal K, Garcia BA, Callahan MK, Yuan J, Martins VR, Skog J, Kaplan RN, Brady MS, Wolchok JD, Chapman PB, Kang Y, Bromberg J and Lyden D. Melanoma exosomes educate bone marrow progenitor cells toward a pro-metastatic phenotype through MET. 2012 Nat Med **18**(6): 833-891;
562. D'Souza-Schorey C and Clancy JW. Tumor-derived microvesicles: shedding light on novel microenvironment modulators and prospective cancer biomarkers. 2012 Genes Dev **26**(12): 1287-1299;
563. D'Asti E, Garnier D, Lee TH, Montermini L, Meehan B and Rak J. Oncogenic extracellular vesicles in brain tumor progression. 2012 Front Physiol **3**: 294;
564. Di Vizio D, Kim J, Hager MH, Morello M, Yang W, Lafargue CJ, True LD, Rubin MA, Adam RM, Beroukhim R, Demichelis F and Freeman MR. Oncosome formation in prostate cancer: association with a region of frequent chromosomal deletion in metastatic disease. 2009 Cancer Res **69**(13): 5601-5609;
565. Böing AN, Hau CM, Sturk A and Nieuwland R. Platelet microparticles contain active caspase 3. 2008 Platelets **19**(2): 96-103;
566. Sapet C, Simoncini S, Loriod B, Puthier D, Sampol J, Nguyen C, Dignat-George F and Anfosso F. Thrombin-induced endothelial microparticle generation: identification of a novel pathway involving ROCK-II activation by caspase-2. 2006 Blood **108**(6): 1868-1876;
567. Sims PJ, Faioni EM, Wiedmer T and Shattil SJ. Complement proteins C5b-9 cause release of membrane vesicles from the platelet surface that are enriched in the membrane receptor for coagulation factor Va and express prothrombinase activity. 1988 J Biol Chem **263**(34): 18205-18212;
568. Hakulinen J, Junnikkala S, Sorsa T and Meri S. Complement inhibitor membrane cofactor protein (MCP; CD46) is constitutively shed from cancer cell membranes in vesicles and converted by a metalloproteinase to a functionally active soluble form. 2004 Eur J Immunol **34**(9): 2620-2629;
569. Andreola G, Rivoltini L, Castelli C, Huber V, Perego P, Deho P, Squarcina P, Accornero P, Lozupone F, Lugini L, Stringaro A, Molinari A, Arancia G, Gentile M, Parmiani G and Fais S. Induction of lymphocyte apoptosis by tumor cell secretion of FasL-bearing microvesicles. 2002 J Exp Med **195**(10): 1303-1316;

570. Huber V, Fais S, Iero M, Lugini L, Canese P, Squarcina P, Zaccheddu A, Colone M, Arancia G, Gentile M, Seregni E, Valenti R, Ballabio G, Belli F, Leo E, Parmiani G and Rivoltini L. Human colorectal cancer cells induce T-cell death through release of proapoptotic microvesicles: role in immune escape. 2005 Gastroenterology **128**(7): 1796-1804;
571. Flanagan J, Middeldorp J and Sculley T. Localization of the Epstein-Barr virus protein LMP 1 to exosomes. 2003 J Gen Virol **84**(Pt 7): 1871-1879;
572. Valenti R, Huber V, Filipazzi P, Pilla L, Sovena G, Villa A, Corbelli A, Fais S, Parmiani G and Rivoltini L. Human tumor-released microvesicles promote the differentiation of myeloid cells with transforming growth factor-beta-mediated suppressive activity on T lymphocytes. 2006 Cancer Res **66**(18): 9290-9298;
573. Ginestra A, La Placa MD, Saladino F, Cassarà D, Nagase H and Vittorelli ML. The amount and proteolytic content of vesicles shed by human cancer cell lines correlates with their *in vitro* invasiveness. 1998 Anticancer Res **18**(5A): 3433-3437;
574. Angelucci A, D'Ascenzo S, Festuccia C, Gravina GL, Bologna M, Dolo V and Pavan A. Vesicle-associated urokinase plasminogen activator promotes invasion in prostate cancer cell lines. 2000 Clin Exp Metastasis **18**(2): 163-170;
575. Hakulinen J, Sankkila L, Sugiyama N, Lehti K and Keski-Oja J. Secretion of active membrane type 1 matrix metalloproteinase (MMP-14) into extracellular space in microvesicular exosomes. 2008 J Cell Biochem **105**(5): 1211-1218;
576. Dvorak HF, Van DeWater L, Bitzer AM, Dvorak AM, Anderson D, Harvey VS, Bach R, Davis GL, DeWolf W and Carvalho AC. Procoagulant activity associated with plasma membrane vesicles shed by cultured tumor cells. 1983 Cancer Res **43**(9): 4434-4442;
577. Mezzano D, Matus V, Sáez CG, Pereira J and Panes O. Tissue factor storage, synthesis and function in normal and activated human platelets. 2008 Thromb Res **122**(Suppl 1): S31-S36;
578. Edwards RL, Rickles FR and Bobrove AM. Mononuclear cell tissue factor: cell of origin and requirements for activation. 1979 Blood **54**(2): 359-370;
579. Berckmans RJ, Neiuwland R, Boing AN, Romijn FP, Hack CE and Sturk A. Cell-derived microparticles circulate in healthy humans and support low grade thrombin generation. 2001 Thromb Haemost **85**(4): 639-646;
580. Sinauridze EI, Kireev DA, Popenko NY, Pichugin AV, Panteleev MA, Krymskaya OV and Ataullakhanov FI. Platelet microparticle membranes have 50- to 100-fold higher specific procoagulant activity than activated platelets. 2007 Thromb Haemost **97**(3): 425-434;
581. Gilbert GE, Sims PJ, Wiedmer T, Furie B, Furie BC and Shattil SJ. Platelet-derived microparticles express high affinity receptors for factor VIII. 1991 J Biol Chem **266**(26): 17261-17268;
582. Svensson KJ, Kucharzewska P, Christianson HC, Sköld S, Löfstedt T, Johansson MC, Mörgelin M, Bengzon J, Ruf W and Belting M. Hypoxia triggers a proangiogenic pathway involving cancer cell microvesicles and PAR-2-mediated heparin-binding EGF signaling in endothelial cells. 2011 Proc Natl Acad Sci U S A **108**(32): 13147-13152;
583. Al-Nedawi K, Meehan B, Micallef J, Lhotak V, May L, Guha A and Rak J. Intercellular transfer of the oncogenic receptor EGFRvIII by microvesicles derived from tumour cells. 2008 Nat Cell Biol **10**(5): 619-624;
584. Rabinowits G, Gerçel-Taylor C, Day JM, Taylor DD and Kloecker GH. Exosomal microRNA: a diagnostic marker for lung cancer. 2009 Clin Lung Cancer **10**(1): 42-46;
585. Ohshima K, Inoue K, Fujiwara A, Hatakeyama K, Kanto K, Watanabe Y, Muramatsu K, Fukuda Y, Ogura S, Yamaguchi K and Mochizuki T. Let-7 microRNA family is selectively secreted into the extracellular environment via exosomes in a metastatic gastric cancer cell line. 2010 PLoS ONE **5**(10): e13247;
586. Grange C, Tapparo M, Collino F, Vitillo L, Damasco C, Deregibus MC, Tetta C, Bussolati B and Camussi G. Microvesicles released from human renal cancer stem cells stimulate angiogenesis and formation of lung premetastatic niche. 2011 Cancer Res **71**(15): 5346-5356;
587. Gibb EA, Brown CJ and Lam WL.. The functional role of long non-coding RNA in human carcinomas. 2011 Mol Cancer **10**: 38;
588. Cordaux R and Batzer MA. The impact of retrotransposons on human genome evolution. 2009 Nat Rev Genet **10**(10): 691-703;
589. Hong BS, Cho JH, Kim H, Choi EJ, Rho S, Kim J, Kim JH, Choi DS, Kim YK, Hwang D and Gho YS. Colorectal cancer cell-derived microvesicles are enriched in cell cycle-related mRNAs that promote proliferation of endothelial cells. 2009 BMC Genomics **10**: 556;
590. Baj-Krzyworzeka M, Szatanek R, Weglarczyk K, Baran J and Zembala M. Tumour-derived microvesicles modulate biological activity of human monocytes. 2007 Immunol Lett **113**(2): 76-82;
591. Wysoczynski M and Ratajczak MZ. Lung cancer secreted microvesicles: underappreciated modulators of microenvironment in expanding tumors. 2009 Int J Cancer **125**(7): 1595-1603;
592. Zhang HC, Liu XB, Huang S, Bi XY, Wang HX, Xie LX, Wang YQ, Cao XF, Lv J, Xiao FJ, Yang Y and Guo ZK. Microvesicles derived from human umbilical cord mesenchymal stem cells stimulated by hypoxia promote angiogenesis both *in vitro* and *in vivo*. 2012 Stem Cells Dev 21(18): 3289-3297;

593. King HW, Michael MZ and Gleadle JM. Hypoxic enhancement of exosome release by breast cancer cells. 2012 BMC Cancer **12**: 421;
594. Parolini I, Federici C, Raggi C, Lugini L, Palleschi S, De Milito A, Coscia C, Iessi E, Logozzi M, Molinari A, Colone M, Tatti M, Sargiacomo M and Fais S. Microenvironmental pH is a key factor for exosome traffic in tumor cells. 2009 J Biol Chem **284**(49): 34211-34222.
595. Eldh M, Ekström K, Valadi H, Sjöstrand M, Olsson B, Jernås M and Lötvall J. Exosomes communicate protective messages during oxidative stress; possible role of exosomal shuttle RNA. 2010 PloS One **5**(12): e15353;
596. Hedlund M, Nagaeva O, Kargl D, Baranov V and Mincheva-Nilsson L. Thermal- and oxidative stress causes enhanced release of NKG2D ligand-bearing immunosuppressive exosomes in leukemia/lymphoma T and B cells. 2011 PLoS One **6**(2): e16899;
597. Zhan R, Leng X, Liu X, Wang X, Gong J, Yan L, Wang Y, Wang X and Qian LJ. Heat shock protein 70 is secreted from endothelial cells by a nonclassical pathway involving exosomes. 2009 Biochem Biophys Res Commun **387**(2): 229-233;
598. Clayton A, Turkes A, Navabi H, Mason MD and Tabi Z. Induction of heat shock proteins in B-cell exosomes. 2005 J Cell Sci **118**(Pt 16): 3631-3638;
599. Chen T, Guo J, Yang M, Zhu X and Cao X. Chemokine-containing exosomes are released from heat-stressed tumor cells via lipid raft-dependent pathway and act as efficient tumor vaccine. 2011 J Immunol **186**(4): 2219-2228;
600. Miyazaki Y, Nomura S, Miyake T, Kagawa H, Kitada C, Taniguchi H, Komiyama Y, Fujimura Y, Ikeda Y and Fukuhara S. High shear stress can initiate both platelet aggregation and shedding of procoagulant containing microparticles. 1996 Blood **88**(9): 3456-3464;
601. Lv LH, Wan YL, Lin Y, Zhang W, Yang M, Li GL, Lin HM, Shang CZ, Chen YJ and Min J. Anticancer drugs cause release of exosomes with heat shock proteins from human hepatocellular carcinoma cells that elicit effective natural killer cell antitumor responses *in vitro*. 2012 J Biol Chem **287**(19): 15874-15885;
602. Aung T, Chapuy B, Vogel D, Wenzel D, Oppermann M, Lahmann M, Weinhage T, Menck K, Hupfeld T, Koch R, Trümper L and Wulf GG. Exosomal evasion of humoral immunotherapy in aggressive B-cell lymphoma modulated by ATP-binding cassette transporter A3. 2011 Proc Natl Acad Sci U S A **108**(37): 15336-15341;
603. Kucharzewska P and Belting M. Emerging roles of extracellular vesicles in the adaptive response of tumour cells to microenvironment stress. 2013 J Extracell Vesicles **2**: 20304;
604. Janowska-Wieczorek A, Wysoczynski M, Kijowski J, Marquez-Curtis L, Machalinski B, Ratajczak J and Ratajczak MZ. Microvesicles derived from activated platelets induce metastasis and angiogenesis in lung cancer. 2005 Int J Cancer **113**(5): 752-760;
605. Tesselaar ME, Romijn FP, van der Linden IK, Prins FA, Bertina RM and Osanto S. Microparticle-associated tissue factor activity: a link between cancer and thrombosis? 2007 J Thromb Haemost **5**(3): 520-527;
606. Helley D, Banu E, Bouziane A, Banu A, Scotte F, Fischer AM and Oudard S. Platelet microparticles: a potential predictive factor of survival in hormone-refractory prostate cancer patients treated with docetaxel-based chemotherapy. 2009 Eur Urol **56**(3): 479-484;
607. Kim HK, Song KS, Park YS, Kang YH, Lee YJ, Lee KR, Kim HK, Ryu KW, Bae JM and Kim S. Elevated levels of circulating platelet microparticles, VEGF, IL-6 and RANTES in patients with gastric cancer: possible role of a metastasis predictor. 2003 Eur J Cancer **39**(2): 184-191;
608. Ogorevc E, Kralj-Iglic V and Veranic P. The role of extracellular vesicles in phenotypic cancer transformation. 2013 Radiol Oncol **47**(3): 197-205;
609. Svensson KJ and Belting M. Role of extracellular membrane vesicles in intercellular communication of the tumour microenvirnoment. 2013 Biochem Soc Trans **41**(1): 273-276;
610. Chaput N, Schartz NE, André F, Taieb J, Novault S, Bonnaventure P, Aubert N, Bernard J, Lemonnier F, Merad M, Adema G, Adams M, Ferrantini M, Carpentier AF, Escudier B, Tursz T, Angevin E and Zitvogel L. Exosomes as potent cell-free peptide-based vaccine. II. Exosomes in CpG adjuvants efficiently prime naive Tc1 lymphocytes leading to tumor rejection. 2004 J Immunol **172**(4): 2137-2146;
611. Escudier B, Dorval T, Chaput N, André F, Caby MP, Novault S, Flament C, Leboulaire C, Borg C, Amigorena S, Boccaccio C, Bonnerot C, Dhellin O, Movassagh M, Piperno S, Robert C, Serra V, Valente N, Le Pecq JB, Spatz A, Lantz O, Tursz T, Angevin E and Zitvogel L. Vaccination of metastatic melanoma patients with autologous dendritic cell (DC) derived-exosomes: results of the first phase I clinical trial. 2005 J Transl Med **3**(1): 10;
612. Morse MA, Garst J, Osada T, Khan S, Hobeika A, Clay TM, Valente N, Shreeniwas R, Sutton MA, Delcayre A, Hsu DH, Le Pecq JB and Lyerly HK. A phase I study of dexosome immunotherapy in patients with advanced non-small cell lung cancer. 2005 J Transl Med **3**(1): 9;
613. Dai S, Wei D, Wu Z, Zhou X, Wei X, Huang H and Li G. Phase I clinical trial of autologous ascites-derived exosomes combined with GM-CSF for colorectal cancer. 2008 Mol Ther **16**(4): 782-790;
614. Delcayre A, Shu H and Le Pecq JB. Dendritic cell-derived exosomes in cancer immunotherapy: exploiting nature's antigen delivery pathway. 2005 Expert Rev Anticancer Ther **5**(3): 537-547;

615. van Doormaal FF, Kleinjan A, Di Nisio M, Büller HR and Nieuwland R. Cell-derived microvesicles and cancer. 2009 Neth J Med **67**(7): 266-273;
616. Admyre C, Johansson SM, Paulie S and Gabrielsson S. Direct exosome stimulation of peripheral human T cells detected by ELISPOT. 2006 Eur J Immunol **36**(7): 1772-1781;
617. Nolte-'t Hoen EN, Buschow SI, Anderton SM, Stoorvogel W and Wauben MH. Activated T cells recruit exosomes secreted by dendritic cells via LFA-1. 2009 Blood **113**(9): 1977-1981;
618. Muntasell A, Berger AC and Roche PA. T cell-induced secretion of MHC class II-peptide complexes on B cell exosomes. 2007 EMBO J **26**(19): 4263-4272;
619. Théry C, Duban L, Segura E, Véron P, Lantz O and Amigorena S. Indirect activation of naïve CD4+ T cells by dendritic cell-derived exosomes. 2002 Nat Immunol **3**(12): 1156-1162;
620. Clayton A, Turkes A, Dewitt S, Steadman R, Mason MD and Hallett MB. Adhesion and signaling by B cell-derived exosomes: the role of integrins. 2004 FASEB J **18**(9): 977-979;
621. Van Niel G, Mallegol J, Bevilacqua C, Candalh C, Brugière S, Tomaskovic-Crook E, Heath JK, Cerf-Bensussan N and Heyman M. Intestinal epithelial exosomes carry MHC class II/peptides able to inform the immune system in mice. 2003 Gut **52**(12): 1690-1697;
622. McKechnie NM, Copland D and Braun, G. Hr44 secreted with exosomes: loss from ciliary epithelium in response to inflammation. 2003 Invest Ophthalmol Vis Sci **44**(6): 2650-2656;
623. Gatti JL, Métayer S, Belghazi M, Dacheux F and Dacheux JL. Identification, proteomic profiling, and origin of ram epididymal fluid exosome-like vesicles. 2005 Biol Reprod **72**(6): 1452-1465;
624. Hergenreider E, Heydt S, Tréguer K, Boettger T, Horrevoets AJ, Zeiher AM, Scheffer MP, Frangakis AS, Yin X, Mayr M, Braun T, Urbich C, Boon RA and Dimmeler S. Atheroprotective communication between endothelial cells and smooth muscle cells through miRNAs. 2012 Nat Cell Biol **14**(3): 249-256;
625. Taylor DD, Akyol S and Gercel-Taylor C. Pregnancy-associated exosomes and their modulation of T cell signaling. 2006 J Immunol **176**(3): 1534-1542;
626. Wessel D and Flügge UI. A method for the quantitative recovery of protein in dilute solution in the presence of detergents and lipids. 1984 Anal Biochem **138**(1): 141-143;
627. Laemmli UK. Cleavage of structural proteins during the assembly of the head of bacteriophage T4. 1970 Nature **227**(5259): 680-685;
628. Shevchenko A, Wilm M, Vorm O and Mann M. Mass spectrometric sequencing of proteins silver-stained polyacrylamide gels. 1996 Anal Chem **68**(5): 850-858;
629. Lohr M, Schmidt C, Ringel J, Kluth M, Müller P, Nizze H and Jesnowski R. Transforming growth factor-beta1 induces desmoplasia in an experimental model of human pancreatic carcinoma. 2001 Cancer Res **61**(2): 550-555;
630. Shao ZM, Nguyen M and Barsky SH. Human breast carcinoma desmoplasia is PDGF initiated. 2000 Oncogene **19**(38): 4337-4345;
631. Giannoni E, Bianchini F, Masieri L, Serni S, Torre E, Calorini L and Chiarugi P. Reciprocal activation of prostate cancer cells and cancer-associated fibroblasts stimulates epithelial-mesenchymal transition and cancer stemness. 2010 Cancer Res **70**(17): 6945-6956;
632. Fiaschi T, Marini A, Giannoni E, Taddei ML, Gandellini P, De Donatis A, Lanciotti M, Serni S, Cirri P and Chiarugi P. Reciprocal metabolic reprogramming through lactate shuttle coordinately influences tumor-stroma interplay. 2012 Cancer Res **72**(19): 5130-5140;
633. Vaupel P. Tumor microenvironmental physiology and its implications for radiation oncology. 2004 Semin Radiat Oncol **14**(3): 198-206;
634. Lee S, Shin HJ, Han IO, Hong EK, Park SY, Roh JW, Shin KH, Kim TH and Kim JY. Tumor carbonic anhydrase 9 expression is associated with the presence of lymph node metastases in uterine cervical cancer. 2007 Cancer Sci **98**(3): 329-333;
635. Robertson N, Potter C and Harris AL. Role of carbonic anhydrase IX in human tumor cell growth, survival, and invasion. 2004 Cancer Res, **64**(17): 6160-6165;
636. Cirri P and Chiarugi P. Cancer-associated-fibroblasts and tumour cells: a diabolic liaison driving cancer progression. 2012 Cancer Metastasis Rev **31**(1-2): 195-208;
637. Chiche J, Ilc K, Brahimi-Horn MC and Pouysségur J. Membrane-bound carbonic anhydrases are key pH regulators controlling tumor growth and cell migration. 2010 Adv Enzyme Regul **50**(1): 20-33;
638. Pastorekova S, Ratcliffe PJ and Pastorek J. Molecular mechanisms of carbonic anhydrase IX-mediated pH regulation under hypoxia. 2008 BJU Int **101**(Suppl 4): 8-15;
639. Shin HJ, Rho SB, Jung DC, Han IO, Oh ES and Kim JY. Carbonic anhydrase IX (CA9) modulates tumor-associated cell migration and invasion. 2011 J Cell Sci **124**(Pt 7): 1077-1087;
640. Hlubek F, Brabletz T, Budczies J, Pfeiffer S, Jung A and Kirchner T. Heterogeneous expression of Wnt/beta-catenin target genes within colorectal cancer. 2007 Int J Cancer **121**(9): 1941-1948;
641. Buanne P, Renzone G, Monteleone F, Vitale M, Monti SM, Sandomenico A, Garbi C, Montanaro D, Accardo M, Troncone G, Zatovicova M, Csaderova L, Supuran CT, Pastorekova S, Scaloni A, De Simone G and Zambrano N. Characterization of carbonic anhydrase IX

interactome reveals proteins assisting its nuclear localization in hypoxic cells. 2013 J Proteome Res **12**(1): 282-292;
642. Hongisto H, Vuoristo S, Mikhailova A, Suuronen R, Virtanen I, Otonkoski T and Skottman H. Laminin-511 expression is associated with the functionality of feeder cells in human embryonic stem cell culture. 2012 Stem Cell Res **8**(1): 97-108;
643. Eiselleova L, Peterkova I, Neradil J, Slaninova I, Hampl A and Dvorak P. Comparative study of mouse and human feeder cells for human embryonic stem cells. 2008 Int J Dev Biol **52**(4): 353-363;
644. Zhang J and Liu J. Tumor stroma as targets for cancer therapy. 2013 Pharmacol Ther **137**(2): 200-215;
645. Karagiannis GS, Poutahidis T, Erdman SE, Kirsch R, Riddell RH and Diamandis EP. Cancer-associated fibroblasts drive the progression of metastasis through both paracrine and mechanical pressure on cancer tissue. 2012 Mol Cancer Res **10**(11): 1403-1418;
646. Santi A, Caselli A, Paoli P, Corti D, Camici G, Pieraccini G, Taddei ML, Serni S, Chiarugi P and Cirri P. The effect of CA IX catalysis products within tumor microenvironment. 2013 Cell Commun Signal 11: 81;
647. Tammela T and Alitalo K. Lymphangiogenesis: molecular mechanisms and future promise. 2010 Cell **140**(4): 460-476;
648. Angelucci C, Maulucci G, Lama G, Proietti G, Colabianchi A, Papi M, Maiorana A, De Spirito M, Micera A, Balzamino OB, Di Leone A, Masetti R and Sica G. Epithelial-stromal interactions in human breast cancer: effects on adhesion, plasma membrane fluidity and migration speed and directness. 2012 PLoS One **7**(12):e50804.